Y3 At 7:
36/12-1

REACTOR AND FUEL-PROCESSING TECHNOLOGY

A Quarterly Technical Progress Review

Prepared for DIVISION OF TECHNICAL INFORMATION, U. S. ATOMIC ENERGY COMMISSION

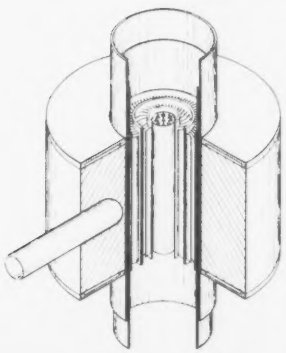

The HFIR Core—see the feature article.

ILLINOIS STATE LIBRARY
JUN 24 1969
U.S. Dept. of Interior

Winter 1968-1969

VOLUME 12

NUMBER 1

TECHNICAL PROGRESS REVIEWS

The United States Atomic Energy Commission publishes the Technical Progress Reviews to meet the needs of industry and government for concise summaries of current nuclear developments. Each journal digests and evaluates the latest findings in a specific area of nuclear technology and science. *Nuclear Safety* is a bimonthly journal; the other three are quarterly journals.

Isotopes and Radiation Technology
P. S. Baker, A. F. Rupp, and associates
Isotopes Information Center, Oak Ridge National Laboratory

Nuclear Safety
Wm. B. Cottrell, W. H. Jordan, J. P. Blakely, and associates
Nuclear Safety Information Center, Oak Ridge National Laboratory

Reactor and Fuel-Processing Technology

Reactor Materials
E. M. Simons and associates
Battelle Memorial Institute, Columbus Laboratories

All are available from the U. S. Government Printing Office. See the back cover for ordering instructions.

The views expressed in this publication do not necessarily represent those of the United States Atomic Energy Commission, its divisions or offices, or of any Commission advisory committee or contractor.

Availability of Reports Cited in This Review

United States Atomic Energy Commission (USAEC) reports are available at USAEC depository libraries and are sold by the Clearinghouse for Federal Scientific and Technical Information (CFSTI), National Bureau of Standards, U. S. Department of Commerce, Springfield, Va. 22151. All reports sold by CFSTI are $3.00 for printed copy and $0.65 for microfiche. Each separately bound part of a report is priced as a separate report. Some reports may not be available because of their preliminary nature; however, the information contained in them will generally be found in later progress or topical reports on the subject.

Other U. S. Government agency reports identified in this journal generally are available from CFSTI.

Private-organization reports should be requested from the originator.

United Kingdom Atomic Energy Authority (UKAEA) and Atomic Energy of Canada Limited (AECL) reports are available at USAEC depository libraries. UKAEA reports are sold by Her Majesty's Stationery Office, London; AECL reports are sold by the Scientific Document Distribution Office, Atomic Energy of Canada Limited, Chalk River, Ontario, Canada. UKAEA and AECL reports issued after March 1, 1967, are sold by CFSTI to purchasers in the United States and its territories.

Y 3.A+7:
36/12-1

REACTOR AND FUEL-PROCESSING TECHNOLOGY

Vol. 12, No. 1 Winter 1968–1969

Contents

FEATURE ARTICLE	**Test-Reactor Perspectives** **by James A. Lane**	1
REACTOR PHYSICS	**Xenon-Transient Calculations in Large Light-Water Reactors** *Patrick S. Lacy and E. D. Kendrick*	10
	Tritium in Power Reactors *Joseph W. Ray*	19
FUEL REPROCESSING	**The Impact of Large-Scale Plants on Fuel Reprocessing** *Walton A. Rodger and Stanton L. Reese*	27
	Book Review: Justin T. Long's *Engineering for Nuclear Fuel Reprocessing*	41
DESIGN AND CONSTRUCTION PRACTICE	**New-Form Technical Specifications as Applied to First-Generation Nuclear Power Plants** *P. Tuite, C. Anderson, and F. Lobbin*	43
	Reliability Techniques as Applied to Operating Systems and to Design Optimization *E. A. Saltarelli and D. G. Fitzgerald*	55
	Radiolytic Decomposition of Water in Water-Moderated Reactors Under Accident Conditions *Stanley E. Turner*	66
COMPONENTS	**Brine-Heater Leakage-Control Problems in Large Power–Desalting Plants** *W. H. Kelley, Jr.*	80
FLUID AND THERMAL TECHNOLOGY	**Thermal Bowing in Pin-Type Fuel Elements** *C. Anderson, R. Anderson, R. Baer, F. Lobbin, and R. Riggs*	88
	Higher Power Densities in Water Reactors—Economic and Technical Bases *W. J. Gallagher and N. Barrie McLeod*	98

Superintendent of Documents, U. S. Government Printing Office, Washington, D. C. 20402, $2.50 per year.

TECHNICAL PROGRESS REVIEWS

The United States Atomic Energy Commission publishes the Technical Progress Reviews to meet the needs of industry and government for concise summaries of current nuclear developments. Each journal digests and evaluates the latest findings in a specific area of nuclear technology and science. *Nuclear Safety* is a bimonthly journal; the other three are quarterly journals.

Isotopes and Radiation Technology
P. S. Baker, A. F. Rupp, and associates
Isotopes Information Center, Oak Ridge National Laboratory

Nuclear Safety
Wm. B. Cottrell, W. H. Jordan, J. P. Blakely, and associates
Nuclear Safety Information Center, Oak Ridge National Laboratory

Reactor and Fuel-Processing Technology

Reactor Materials
E. M. Simons and associates
Battelle Memorial Institute, Columbus Laboratories

All are available from the U. S. Government Printing Office. See the back cover for ordering instructions.

The views expressed in this publication do not necessarily represent those of the United States Atomic Energy Commission, its divisions or offices, or of any Commission advisory committee or contractor.

Availability of Reports Cited in This Review

United States Atomic Energy Commission (USAEC) reports are available at USAEC depository libraries and are sold by the Clearinghouse for Federal Scientific and Technical Information (CFSTI), National Bureau of Standards, U. S. Department of Commerce, Springfield, Va. 22151. All reports sold by CFSTI are $3.00 for printed copy and $0.65 for microfiche. Each separately bound part of a report is priced as a separate report. Some reports may not be available because of their preliminary nature; however, the information contained in them will generally be found in later progress or topical reports on the subject.

Other U. S. Government agency reports identified in this journal generally are available from CFSTI.

Private-organization reports should be requested from the originator.

United Kingdom Atomic Energy Authority (UKAEA) and Atomic Energy of Canada Limited (AECL) reports are available at USAEC depository libraries. UKAEA reports are sold by Her Majesty's Stationery Office, London; AECL reports are sold by the Scientific Document Distribution Office, Atomic Energy of Canada Limited, Chalk River, Ontario, Canada. UKAEA and AECL reports issued after March 1, 1967, are sold by CFSTI to purchasers in the United States and its territories.

Y 3.A 7:
36/12-1

REACTOR AND FUEL-PROCESSING TECHNOLOGY

Vol. 12, No. 1 Winter 1968–1969

Contents

FEATURE ARTICLE	**Test-Reactor Perspectives** **by James A. Lane**	1
REACTOR PHYSICS	**Xenon-Transient Calculations in Large Light-Water Reactors** *Patrick S. Lacy and E. D. Kendrick*	10
	Tritium in Power Reactors *Joseph W. Ray*	19
FUEL REPROCESSING	**The Impact of Large-Scale Plants on Fuel Reprocessing** *Walton A. Rodger and Stanton L. Reese*	27
	Book Review: Justin T. Long's *Engineering for Nuclear Fuel Reprocessing*	41
DESIGN AND CONSTRUCTION PRACTICE	**New-Form Technical Specifications as Applied to First-Generation Nuclear Power Plants** *P. Tuite, C. Anderson, and F. Lobbin*	43
	Reliability Techniques as Applied to Operating Systems and to Design Optimization *E. A. Saltarelli and D. G. Fitzgerald*	55
	Radiolytic Decomposition of Water in Water-Moderated Reactors Under Accident Conditions *Stanley E. Turner*	66
COMPONENTS	**Brine-Heater Leakage-Control Problems in Large Power–Desalting Plants** *W. H. Kelley, Jr.*	80
FLUID AND THERMAL TECHNOLOGY	**Thermal Bowing in Pin-Type Fuel Elements** *C. Anderson, R. Anderson, R. Baer, F. Lobbin, and R. Riggs*	88
	Higher Power Densities in Water Reactors—Economic and Technical Bases *W. J. Gallagher and N. Barrie McLeod*	98

Superintendent of Documents, U. S. Government Printing Office, Washington, D. C. 20402, $2.50 per year.

Reactor and Fuel-Processing Technology

is a quarterly review of developments in reactor and reactor-fuel technology. As such, this journal reports and interprets progress in the reactor field in terms of its significance to the reactor designer, operator, and fuel-cycle specialist. Articles either summarize and critically evaluate recently reported developments or review the "state of the art" of a particular topic. Both types of articles reference reports and publications that merit study; readers are urged to consult the references for additional information and the judgments of the original authors.

The scope of the journal encompasses:

CONCEPTS and APPLICATIONS: Progress in evaluating the applicability and economics of various reactor types and systems (including unconventional approaches), as well as of fuel resources and cycles, for utility central-station generation of electricity, auxiliary power, process radiation and heat, desalting, and propulsion—and for terrestrial, undersea, aerospace, and other advanced uses.

ANALYSIS and EXPERIMENTATION: Advancements in the techniques of reactor physics, fluid and thermal technology, energy conversion, fuel elements, materials, mechanics and control and dynamics.

SYSTEMS and COMPONENTS: Experience as reflected in design and construction practice, components, systems technology, and operating performance of various specific types of reactors—including pressurized- and boiling-water reactors, molten-salt, organic-, gas-, and liquid-metal-cooled reactors, as well as generally applicable aspects of research and test reactors.

FUEL PROCESSING: Recent research and development on fuel aqueous processing, nonaqueous processing, waste disposal, and processing safety.

Articles for this issue of *Reactor and Fuel-Processing Technology* have been assembled from several sources by the Division of Technical Information, USAEC, pending a decision on the future status of the journal. Contributors include NUS Corporation, Rockville, Md.; Nuclear Safety Associates, Rockville, Md.; Hittman Associates, Inc., Columbia, Md.; Southern Nuclear Engineering, Inc., Dunedin, Florida; Nuclear Associates International Corporation, Rockville, Md.; Battelle Memorial Institute, Columbus, Ohio; and Oak Ridge National Laboratory.

We welcome comments on this issue.

U. S. Atomic Energy Commission
Division of Technical Information
Washington, D. C. 20545

Issued quarterly by the U. S. Atomic Energy Commission. Use of funds for printing this publication approved by the Director of the Bureau of the Budget on July 8, 1966.

FEATURE ARTICLE

Test-Reactor Perspectives*

By James A. Lane

James A. Lane, graduate of Worcester Polytechnic Institute, received the B.S. in chemistry in 1936 and the M.S. in chemical engineering in 1938. As W.P.I.'s first exchange fellow, in 1938–1939 he attended the University of Goettingen, Germany, specializing in physical chemistry. From 1939–1942 he worked at the E. I. du Pont Company in Wilmington, Del., in the fields of physical-property measurements, dialysis technology, and diffusional operations. His work in atomic energy started in 1942 at the Metallurgical Laboratory, University of Chicago. Since that time he has held posts of Assistant Director, Technical Division, Clinton Laboratories; Chief of the Evaluation Branch, AEC, Washington, D. C.; Director, Reactor Engineering Division, Oak Ridge National Laboratory (ORNL); Director of the Thorium Utilization Program, ORNL; and Director of Studies and Evaluations, ORNL. At the present time Mr. Lane is Director of the Middle East Study Group, ORNL.

Abstract: *A review of the historical evolution of research and test reactors during the last two decades indicates a distinct trend toward higher and higher neutron-flux levels despite associated increases in both investment and operating costs. It appears, however, that, for cross-section measurements, neutron-diffraction work, solid-state physics, and other nuclear research programs, the end point in test-reactor development has been reached. Other approaches such as pulsed-accelerator sources or improved measuring techniques offer more for such programs than higher reactor fluxes. On this basis the only justification for building a test reactor with fluxes above 10^{16} neutrons/(cm^2)(sec) is the investigation of the effect of fast-neutron bombardment on metals and other reactor materials at high fluences. Although a fast reactor is generally believed to be the best means of obtaining such data, the possibility also exists of using a high-power-density thermal high-flux reactor for fast-neutron damage experiments. It is the opinion of some experts in the field that this latter approach may provide more immediate answers to some of the problems confronting fast breeder development.*

*Presented at the American Nuclear Society Winter Meeting, Washington, D. C., Nov. 10–15, 1968.

Historical Background of Test Reactors

The test-reactor program in the United States originated as sort of an afterthought on the tail end of a series of research-reactor conceptual designs. In August 1944 the chemists at Oak Ridge requested that the laboratory construct a reactor that would produce[1] radioactive isotopes and ^{233}U. The first design of such a reactor involved a 50-kw aqueous homogeneous reactor. Later, the power level was increased to 10 Mw(t) in order to achieve a thermal-flux level of 2×10^{14} neutrons/(cm^2)(sec) necessary for breeding at short doubling times.[2] The radiation-induced decomposition of the heavy water at these flux levels, however, created a nuclear instability problem. This problem was solved by replacing the uranium fuel solution with solid plate-type elements[3] (Fig. 1). The D_2O cooling system was switched to an H_2O cooling system for reasons of economy. Then the laboratory became more ambitious and increased[4] the power to

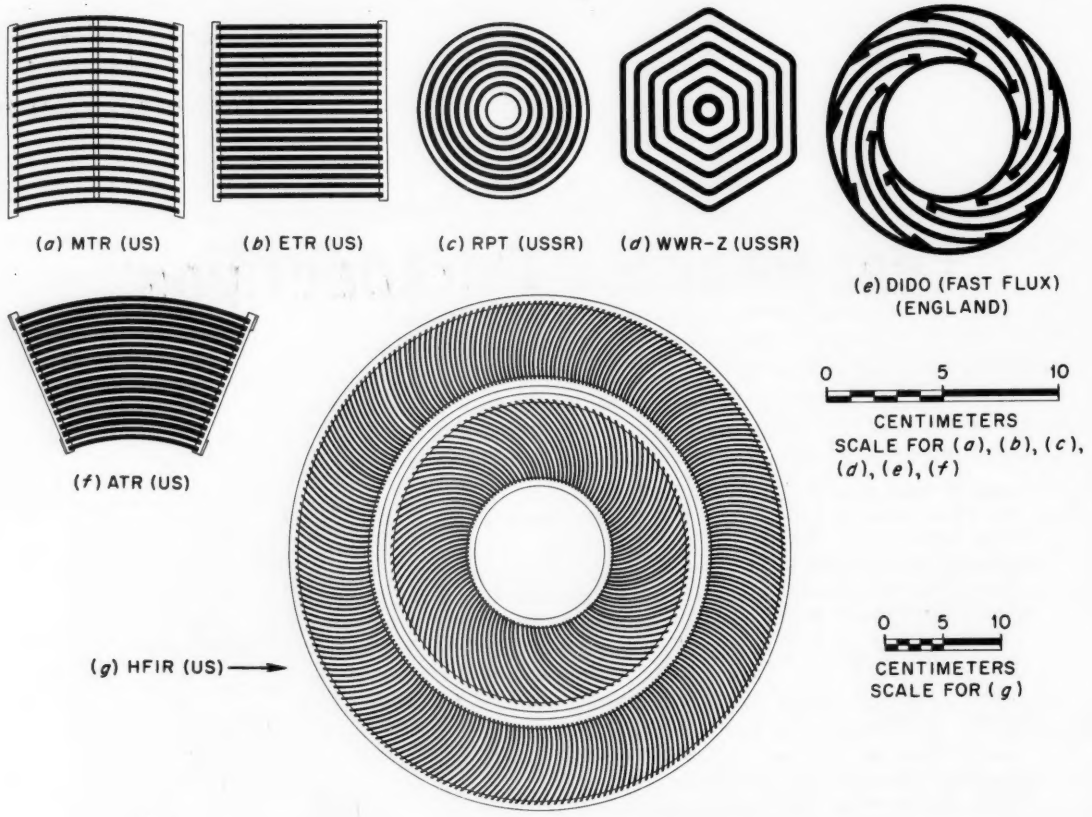

Fig. 1 Cross sections of plate-type fuel elements.

30 Mw. Thus by May 1946 the stage was set for the construction of the first high-flux reactor in the world.

The entire project involved the construction of not only the reactor but also a fuel-fabrication facility, a ^{235}U reprocessing plant, a ^{233}U reprocessing plant, a metal-recovery plant, and numerous associated facilities. In all, 40 new buildings were to be constructed. The planned schedule called for start of construction July 1, 1946, and completion July 1, 1947, at a cost of $15 million. What a bargain that would have been! However, at this point Dr. Wigner suggested the use of an H_2O moderator instead of the D_2O moderator as a means of obtaining high fast fluxes as well as high thermal fluxes. The decision to proceed[5] with this design was agreed to in September 1946. So everyone went back to the drawing boards and started over. In November 1947 the design of a 30-Mw H_2O-cooled and -moderated reactor was completed.[6] By this time the estimated cost of the project increased to $27 million, and the construction schedule increased to 2 years.

Important aspects of that early program were the changes in objectives for the reactor which took place along with the design changes. Whereas the first designs were aimed primarily at isotope production, the later designs reflected an awareness of the need for testing the behavior of materials at fluxes that might be encountered in breeders. In the high-flux-pile design report,[6] the following statement was made as justification for constructing the reactor: "The effect of high fluxes, particularly of fast neutrons, on the properties of structural materials is not well known." Twenty-one years later we can say the same thing!

Despite its worthy objectives, the high-flux pile failed to materialize. In December 1947 the AEC reactor-development program was centralized at Argonne National Laboratory (ANL), and the decision was made to terminate the Oak Ridge project. A

lengthy review by the AEC of the need for and the costs of a high-flux reactor revealed that such a reactor was indeed needed for radiation-damage experiments on reactor materials. Thus the Materials Testing Reactor (MTR) project was initiated as a joint effort of ORNL and ANL. The high-flux-pile design was modified to emphasize radiation-damage experiments by taking out the thorium blanket rods and changing a thermal column to a shielding facility. Construction of the MTR was started in May 1950; full-power operation was achieved on schedule 2 years later.[7]

But the MTR was not the first test reactor to go into operation. As part of ORNL's responsibility for designing and testing the reactor core, a mockup of the reactor was constructed at Oak Ridge in 1948. After the ORNL tests on the core were completed, the mockup was used for critical experiments, and criticality was achieved in February 1950. It was then converted into a training reactor for MTR operators and was called the Low-Intensity Training Reactor. In 1951 the name was changed to Low-Intensity Testing Reactor, and the power was increased to 1 Mw. Two years later the power was further increased to 3 Mw, and the reactor was operated as a test reactor in support of ORNL's reactor-development programs until it was shut down[8] in October 1968. Little did those who first built that hydraulic mockup suspect that it would be the prototype of the light-water enriched-uranium class of research-and-test reactors, of which there are now more than 100 in the United States and abroad.

Trends in Research-Reactor Development

Although there have been noticeable trends in the development of research reactors during the last two decades, the objectives in building such reactors have remained the same. These objectives are neutron research, isotope production, and radiation-damage studies. Since all of these things can be done better at higher neutron fluxes than at lower fluxes, there has been a constant striving to get as high a neutron flux as possible in any given reactor. But high fluxes require high power levels and associated increases in costs.[9] Reactors in the 1-watt to 100-kw range designed primarily for teaching and training purposes can be bought for about $200,000. Reactors in the 1- to 5-Mw range designed for graduate research programs are available for $500,000 to $1 million. A 40-Mw research-and-test reactor, however, would cost about $15 million if built today, and at the upper end of the scale, the 400-Mw Fast Flux Test Facility (FFTF), scheduled for startup in 1974, is estimated to cost about $100 million. In addition to these high investment costs, reactors with very high fluxes have high power densities and associated high operating costs. The High Flux Isotope Reactor (HFIR) (Fig. 2), for example, with an average power density of 2000 kw/liter has an annual operating cost of $3.8 million exclusive of the ^{235}U consumed.[10] So the desire for high fluxes is in many cases tempered by the availability of adequate funding. This is the reason that only 10 of the more than 300 research-and-test reactors in existence today are of the so-called very-high-flux type with usable neutron fluxes above 5×10^{14} neutrons/(cm^2)(sec).

The Need for Ultrahigh-Flux Reactors

Recognizing that the achievement of even higher fluxes than are obtainable in present-day reactors will lead to very expensive facilities, planners have given considerable thought to whether or not such ultrahigh fluxes [i.e., $> 10^{16}$ neutrons/(cm^2)(sec)] are in fact needed.[10,11]

The main conclusions of the experts in the field are as follows:

1. The best justification for building a 10^{16} flux reactor is the investigation of the effect of fast-neutron bombardment on metals and on other reactor materials at high fluences.

2. Thermal and fast fluxes available from the very-high-flux reactors now in existence are, in general, adequate for cross-section measurements, neutron-diffraction work, solid-state physics, and other nuclear research programs.

3. Except for the nuclear explosion with its extremely high instantaneous intensity, fission sources are inferior to pulsed-accelerator sources for high-resolution neutron cross-section measurements.

4. The development of experimental techniques leading to increased counting rates is likely to offer more for neutron-diffraction experiments than are increases in flux levels.

5. Increasing the specific activity of isotopes by increasing the neutron flux requires more than a corresponding increase in power level. As an alternative, one should consider isotope-separation methods that require proportionally lower power increases.

From the foregoing, it is apparent that the primary objective of building an ultrahigh-flux reactor is to provide a means of carrying out fast-neutron radiation-damage experiments up to high fluences (i.e., $> 10^{23}$

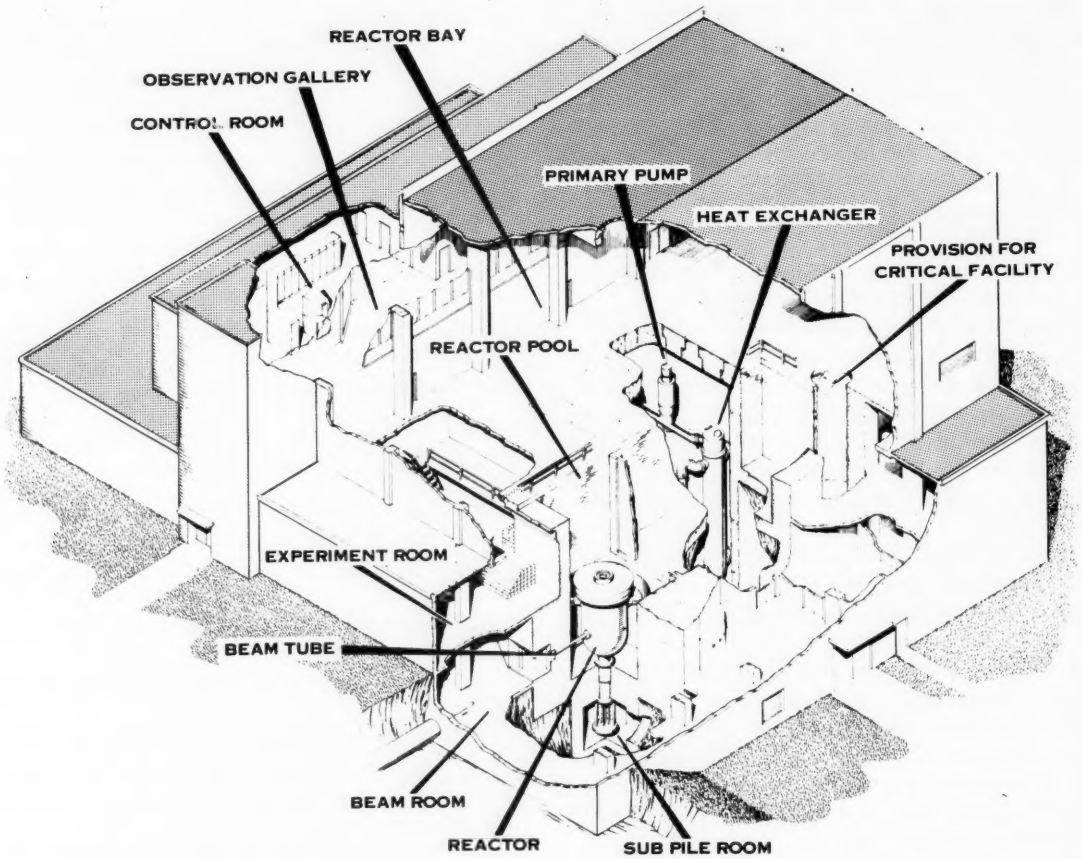

Fig. 2 The HFIR is housed in a building that is 128 ft wide, 160 ft long, and 86 ft high. It has five working levels.

neutrons/cm^2). The question now becomes "What is the best way to provide such a facility?"

Fast-Flux Test Reactors

The three possible approaches to a fast-flux materials-testing facility are (1) a fast test reactor such as the FFTF, (2) an experimental fast reactor such as the Fermi, EBR-II (Experimental Breeder Reactor II), or Dounreay, and (3) a high-power-density high-flux thermal reactor such as the ETR (Engineering Test Reactor) or HFIR with appropriate fast-flux irradiation facilities. The pros and cons of these alternatives are reviewed in the following paragraphs.[1,2]

FFTF. This reactor will be a major facility in the AEC's fast breeder development program, occupying a role analogous to that of the MTR, ETR, or other thermal test reactor in the development of water reactors. The FFTF will permit controlled testing of fuel elements, structural materials, control materials, and instrumentation under the environmental conditions of fast reactor designs of the future.

Before it was changed in October 1968, the core configuration of the FFTF involved a split conical array of 150 fuel, test, control, and reflector assemblies with accommodations for five vertical, closed test loops in the center. The main parameters of the selected configuration are summarized in Table 1.

Unfortunately, the gap in the center of the split-core configuration caused an unsatisfactory flux depression, making it difficult to achieve the target flux requirements. For this reason, alternative designs were evaluated on the basis of more tightly packed cores with the test holes located in an annular region rather than in the core center. As a result of this evaluation, a vertical-core concept with provision for

Table 1 Characteristics of the Split-Core FFTF

Peak flux (typical LMFBR* spectrum), neutrons/(cm^2)(sec)	0.6 to 1.3 X 10^{16}
Fuel composition (PuO_2/UO_2), %	20.5/79.5
Peak fuel-pin linear heat rating, kw/ft	15.6
Average burnup (first core), Mwd/kg	45
Power level, Mw(t)	400
Core volume (adjustable), liters	400 to 1000

*Liquid-metal-cooled fast breeder reactor.

six closed test loops and for individual instrumentation of each subassembly has been chosen for the final design.[13] The compactness of the vertical core and the corresponding lack of room for test loops have been overcome by the design of the closed loops on a Y configuration that splits the core into three sectors. Required instrumentation is mounted on plates above each sector. The core will generate 400 Mw(t), will operate at a bulk reactor outlet temperature of 800 to 900°F, and will produce a fast flux of at least 7 x 10^{15} neutrons/(cm^2)(sec).

As an alternative to the FFTF, some consideration has been given at Oak Ridge to the possibility of using a molten-salt reactor as a fast-flux test facility.[14] The primary virtue of this approach includes the ability to achieve very high power densities and at the same time eliminate the downtime associated with refueling the reactor. A fast-spectrum molten-salt reactor, however, requires a high fissile concentration (i.e., 300 to 500 g ^{235}U/liter) in order to get mean fission energies in the range of 10 to 50 kev. Switching from an NaF–UF_4-salt (on which the energy range just mentioned is based) to a chloride-salt reactor would permit a higher mean energy for the same fuel concentration but would require the development of new technology associated with the use of chlorides.

Since the fast-flux level is largely determined by the power density, a flux of the order of 10^{16} or more corresponds to a peak power density in the fuel salt in the range of 5 to 10 Mw/liter and to a power level of about 1000 Mw(t). This means that there will be only 100 to 200 liters in the core; however, the external volume would be about 10,000 liters. On this basis, ^{235}U inventory requirements would be about 45 kg in the core and 3600 kg in the external system. Interest charges on the fuel would amount to $4.4 million per year, and fuel-processing costs would be an additional $1 million per year. Although use of such a molten-salt fast test reactor would give considerable flexibility with regard to testing capabilities, the economics, safety, and technical feasibility all appear to be somewhat questionable.

Fermi, EBR-II, and Dounreay. Fast test reactors such as the FFTF or molten-salt test reactors are not particularly suitable for obtaining statistical data on fuel behavior, for defining problems of systems and component interactions, or for yielding data that would permit refined economic projections. Such information can be obtained from prototype fast reactors like Fermi, EBR-II, and Dounreay. Although these reactors were not designed as test reactors, the requirements of the various reactor programs have led to their use for testing fuels and materials as well as providing the data mentioned above.

The significant features of the three plants are shown in Table 2. The peak total flux in all three reactors is about 2.5 x 10^{15} neutrons/(cm^2)(sec). This is a factor of 2 to 3 below the flux anticipated for the LMFBR. Therefore the burnup rates are increased in experimental fuels by enriching in ^{235}U and maintain-

Table 2 Some Important Features of Existing Fast Reactors

Feature	Fermi	EBR-II	Dounreay
Thermal power, Mw	110	45	60
Average neutron flux, neutron/(cm^2)(sec)	1.6 X 10^{15}	1.7 X 10^{15}	2 X 10^{15}
Peak neutron flux, neutrons/(cm^2)(sec)	2.6 X 10^{15}	2.6 X 10^{15}	2.5 X 10^{15}
Fuel heating rate at reactor center, watts/g Pu	355	420	390
Burnup per full-power month at core center in 15% PuO_2–85% $^{235}UO_2$, Mwd/metric ton	8100	9400	8900
Core height, in.	30.5	14.2	21
Available test height, in.	50	37	28
Test volume, cu ft	6	3	1

ing the uranium-to-plutonium ratio in the fuel composition at U/Pu ~ 5.

Several subassembly designs exist for each reactor. The designs are intended to allow special irradiations of fuel and structural materials under temperature and flow conditions different from the reactor ambient.

In view of the fact that there is no instrumentation available for experiments in EBR-II and Fermi, it is necessary to use the nuclear heating and gas gaps to attain temperatures above the ambient coolant temperature. The inlet and mixed-mean outlet temperatures, respectively, are 450 and 560°F for Fermi and 700 and 850°F for EBR-II. Currently, complicated experiments such as in-pile mechanical-properties or fission-gas-release experiments cannot be performed because of the lack of experimentation access. Design work is under way for both reactors to allow instrumentation to one subassembly through a control-rod-drive access.

Problem areas common to all three fast reactors when they are considered as testing facilities are as follows:

1. The flux is too low. This results in the inability to match fuel-burnup rate with cladding-damage rate, in the long times required to obtain fluences desired in materials irradiations, and in a restricted volume over which the fuel-burnup rate can be maintained at values of interest even when fully enriched fuel is used.
2. Instrumentation for experiments is absent, and the plans for reactor modification will result in only one instrumented subassembly each in EBR-II and Fermi.
3. There generally is pressure to keep parasitic materials out of the high-worth (center) regions of the cores. This is because there is insufficient fuel available to make up reactivity lost by replacing fuel in the high-flux regions.
4. The reactors were designed for only small temperature differences between adjacent fuel elements. This complicates the design and places limitations on the types of experiments possible.
5. The double-containment requirement for fuel further limits the volume (number of pins) available and forces the use of a stagnant, noncorrosive, and unpredictable sodium jacket around fuel pins.
6. Basic experiments requiring irradiation temperatures below the reactor ambient are not possible. There are no beam holes or "poolsides" in which such experiments may be conducted.

The advantages of these reactors are that they exist and are operating and that the operators are quite cooperative in assisting experimenters in every way they can.

In addition, the use of a fast reactor for irradiation testing avoids some of the problems associated with the use of a thermal high-flux reactor to test fast reactor fuels.[15] For example, the extreme ratings in some fast reactor projects involve melting of the central zone in the fuel pins, and the way the central zone melts, or remains melted, depends very much on the flux distribution inside the pin. A very absorbent pin placed in a thermal reactor would reach the same power density as in a fast reactor. The resulting very important flux depression inside the pin would give a distribution of temperature, melted zone, and fission products quite different from what would be expected in the actual fast reactor.

Also, the problems of gamma heating and xenon and samarium buildup are less significant in a fast reactor than in a thermal reactor.

High-Flux Thermal Reactors. A high-flux thermal reactor such as the ORR (Oak Ridge Research Reactor) or HFIR can be used for fast-neutron irradiations. Although the ORR is not a fast-flux reactor, fast-neutron doses over most of the energy spectrum can be obtained approaching those available in fast reactors like EBR-II, Dounreay, and Fermi. Fig. 3 shows the fluxes available in the ORR, EBR-II, Fermi, HFIR, Dounreay, and the Savannah River High Flux Demonstration Reactors. Although the ORR does not have as high a flux as most of the other reactors, its fast-neutron fluence (above 1 Mev) is actually about equal to that available elsewhere (except for the HFIR), as shown in Fig. 4. This comes about because the plant factor, or operating time, at the ORR is higher than that of the others. Since most experiments depend upon fluences rather than fluxes, it is seen that except for the HFIR the ORR is competitive with other reactors.

Higher-flux research-and-test reactors such as the ETR, HFBR (High Flux Beam Reactor), ATR (Advanced Test Reactor), and HFIR could be used to even better advantage in support of the fast-flux irradiation program. Some of the characteristics of these reactors are summarized in Table 3. It is seen that all four of these very-high-thermal-flux reactors also have non-thermal fluxes of the order of 10^{15} neutrons/(cm^2)(sec) or higher. The highest-performance reactor, measured in terms of power density and flux, is the HFIR, which is already being used to determine the effect of fast-neutron bombardment on small samples of metals and graphite placed in the central target

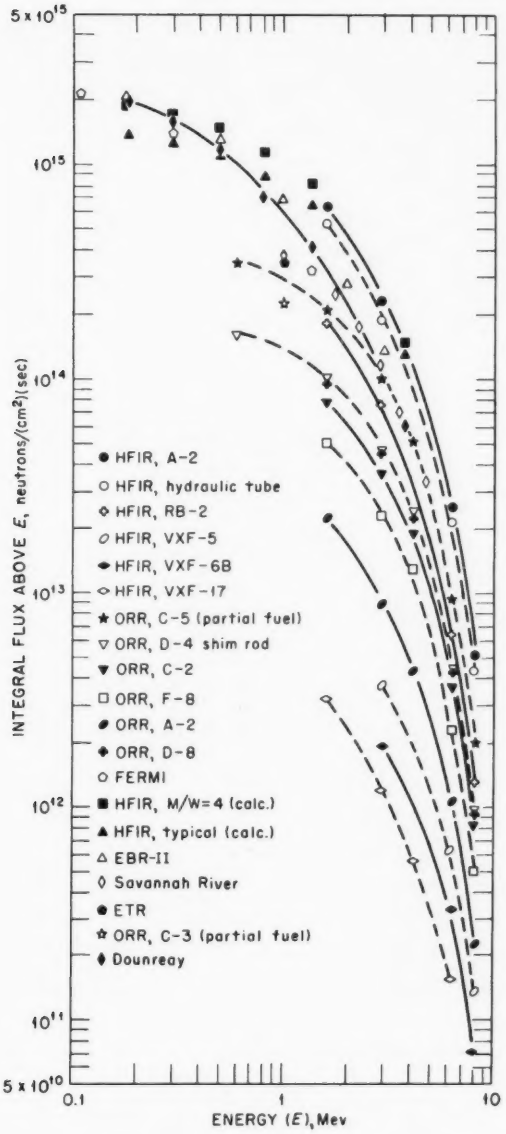

Fig. 3 Fluxes available in some fast reactors.

region (Fig. 5.) Flux levels, however, are still below those necessary for the proper testing of fast reactor materials. For this reason ORNL has carried out preliminary studies to assess the possibility of achieving fluxes significantly higher than 10^{16} neutrons/(cm^2)(sec) in an HFIR-type core.

By drawing on the experience in the design of the original HFIR and on measurements of burnout heat flux by W. R. Gambill of ORNL, R. D. Cheverton of ORNL was able to show that a fivefold increase in power density to an average of 10 Mw/liter of core is possible. Because of the required coolant velocity of 120 ft/sec, the aluminum fuel plates in this case would have to be nickel plated to minimize corrosion. The use of D_2O as coolant would yield approximately a 15% increase in maximum flux, and increasing the core volume from 50 to 75 liters would produce a further 25% increase. On this basis a thermal flux of 3×10^{16} neutrons/(cm^2)(sec) in the central flux trap of an HFIR-type core could be achieved at a reactor power of 750 Mw. Both the capital and operating costs of such a reactor would, of course, be very high. For this reason, more recent considerations have centered on a scaled-down version of the above "ultimate" reactor optimized for fast-flux materials testing. A description of this concept follows:

First, the modified HFIR would have double the power density of the present design and half the core volume. The flux-trap region would be enlarged and most of the water in the trap replaced with beryllium, nickel, or aluminum. The control rods would be located in this region rather than in between the core and the side reflector.

Such a reactor, operating at about 100 Mw, might have a single annular fuel element with 40-mil involute-shaped aluminum fuel plates and 60-mil coolant channels; the channels could contain wire spacers to help support the plates. The side reflector could be of one of several materials, but nickel plus H_2O coolant appears to have several advantages.

The primary irradiation facilities consist of as many as fifteen 3-in.-diameter holes adjacent to the outer surface of the fuel element and several small sample-irradiation spaces in the flux-trap region. The outer test holes could be individually piped and accessible from outside the vessel.

The achievable fast-neutron fluxes (>0.8 Mev) in such a system would be approximately 2×10^{15} in the flux trap, 3×10^{15} in the fuel region, and 8×10^{14} in the side-reflector test holes. In other words, fast fluxes would be comparable to those in the FFTF. Thermal-neutron fluxes in the main experimental facilities would be lower than the fast fluxes by a factor of about 40. A compilation of core characteristics is given in Table 4.

The capital cost for a reactor of this type, excluding the cost of experimental loops and associated equipment, has been estimated at $\$25 \times 10^6$. On the basis of present HFIR fuel-element costs and

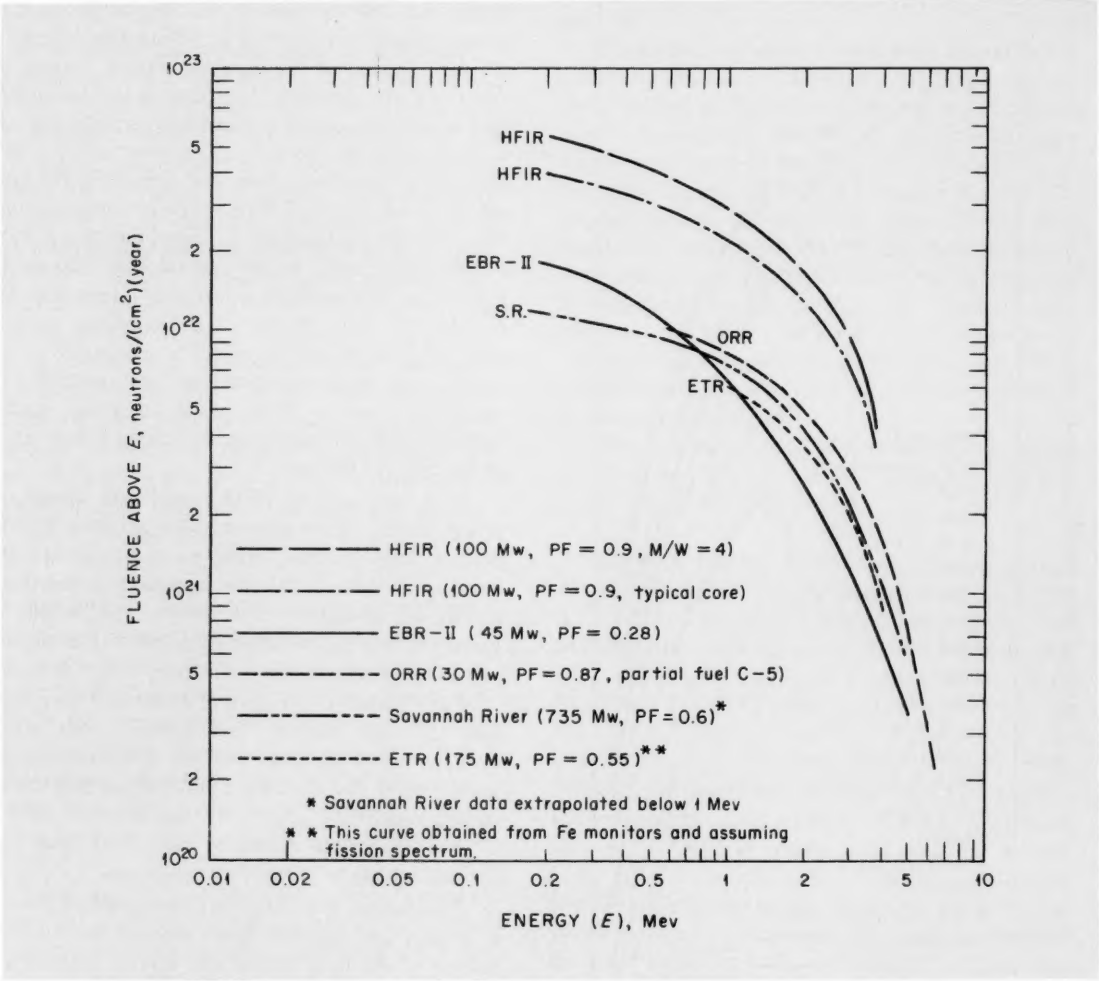
FLUENCE ABOVE E, neutrons/(cm²)(year)
ENERGY (E), Mev
HFIR
HFIR
EBR-II
S.R.
ORR
ETR
HFIR (100 Mw, PF = 0.9, M/W = 4)
HFIR (100 Mw, PF = 0.9, typical core)
EBR-II (45 Mw, PF = 0.28)
ORR (30 Mw, PF = 0.87, partial fuel C-5)
Savannah River (735 Mw, PF = 0.6)*
ETR (175 Mw, PF = 0.55)**
* Savannah River data extrapolated below 1 Mev
** This curve obtained from Fe monitors and assuming fission spectrum.

Fig. 4 Fast-neutron fluences for some fast reactors.

Table 3 Characteristics of Selected High-Flux Research Reactors

	ETR	HFBR	ATR	HFIR
Power level, Mw	175	40	250	100
Maximum neutron flux, neutrons/(cm^2)(sec)				
Thermal (X 10^{14})	5	7*	25	55
Nonthermal (X 10^{14})	8	16	23	40†
Fuel-region volume, liters	318	38	262	51
Core-power density, maximum, kw/liter	1280	1480	2520	4380
Fuel-cycle time, days	42	38	17	22

*Reflector positions.
†Fuel positions.

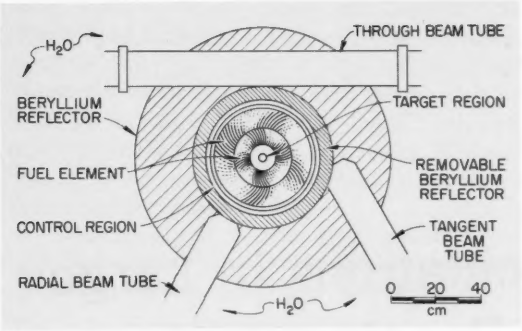

Fig. 5 The HFIR core region.

Table 4 Characteristics of Modified HFIR for Fast-Flux Irradiations

Power, Mw(t)	100
Core volume, liters	25
Core height, in.	12
Flux-trap diameter, in.	7.1
Outside diameter of fuel region, in.	14.6
Number of fuel plates per element	223
Number of fuel elements	1
Coolant velocity, ft/sec	~70
Fuel loading (93% ^{235}U), kg	25
Fuel-cycle time, days	20

considering the similarity between the HFIR and the proposed modified HFIR element, it is estimated that the latter element will cost $50,000.

Future Outlook for Test Reactors

The present generation of very-high-flux research-and-test reactors based on light- or heavy-water-moderated enriched cores and capable of producing beam and irradiation fluxes of 1 to 5 x 10^{15} neutrons/(cm^2)(sec) probably represents the final step in the evolution of these reactors. Design changes necessary to achieve neutron fluxes above 10^{16} appear to be technically feasible; however, the cost of building and operating such an ultrahigh-flux reactor may be considerably higher than can be justified for neutron research. As a result, nuclear scientists are looking more toward improvements in measuring techniques as a means of refining experiments with neutrons than they are toward improvements in flux levels.

The availability of ultrahigh fast fluxes for testing the effect of high-energy-neutron fluences on the properties of structural materials, however, appears to be an essential key to the development of an economically competitive fast breeder. Although the present AEC program includes the construction of the Fast Test Reactor to provide such fluxes, many experts in the field believe that alternative approaches such as a very small high-power-density fast reactor or a modified high-thermal-flux test reactor may provide more immediate answers to the problem. Beyond this, the outlook for future developments in test reactors appears small.

References

1. C. D. Coryell and A. Turkevich, Clinton Laboratories, unpublished memorandum, August 1944.
2. L. W. Nordheim, Clinton Laboratories, unpublished, 1944.
3. M. C. Leverett et al., Technical Division Report for Month Ending Dec. 20, 1945, USAEC Report MonN-43, Clinton Laboratories.
4. M. C. Leverett and J. R. Huffman, Preliminary Process Design Report—1000 Project, USAEC Report MonN-108, Clinton Laboratories, May 15, 1946.
5. M. C. Leverett and W. P. Bigler, Technical Division Report for Month Ending Sept. 20, 1946, USAEC Report MonN-175, Clinton Laboratories.
6. J. R. Huffman, M. C. Leverett, H. W. Newson, and A. M. Weinberg, Feasibility Report of Clinton High Flux Pile, USAEC Report MonT-433, Clinton Laboratories, Dec. 1, 1947.
7. R. L. Doan and J. R. Huffman, Materials Testing Reactor, Experimental Program and Reactor Operation, in *Proceedings of the International Conference on the Peaceful Uses of Atomic Energy, Geneva, 1955,* Vol. 2, p. 270, United Nations, New York, 1956.
8. Oak Ridge National Laboratory, Press Release, NR-ORNL-388, Oct. 11, 1968.
9. T. E. Cole and A. M. Weinberg, Technology of Research Reactors, *Annu. Rev. Nucl. Sci.*, **12**: (1962).
10. T. E. Cole, The Oak Ridge High Flux Isotope Reactor Design and Initial Operation, in *Proceedings of the USAEC–ENEA Seminar on Intense Neutron Sources,* USAEC Report CONF-660925, p. 183, September 1966.
11. W. K. Ergen, Oak Ridge National Laboratory, to J. A. Lane, personal communication, 1968.
12. E. R. Astley, The Conceptual Evaluation of a Fast Flux Test Facility, presented at the National Topical Meeting on Fast Reactors, USAEC Report BNWL-SA-978, Pacific Northwest Laboratory, April 1967. See also *Nucleonics Week,* 8(15): 1-2 (Apr. 13, 1967), and 9(46): (Nov. 14, 1968).
13. *Nucleonics Week,* **10**(1): 1 (Jan. 2, 1969).
14. P. R. Kasten, Oak Ridge National Laboratory, Molten Salt Reactors for Generation of High Fluxes, unpublished, Aug. 21, 1968.
15. Irradiation Techniques at Very High Flux Reactors, in *Research Reactor Utilization,* Summary of Study Group Meeting, Istanbul, Nov. 15–19, 1965, Technical Reports Series, No. 71, p. 33, International Atomic Energy Agency, Vienna, 1967 (STI/DOC/10/71).
16. J. A. Cox et al., Oak Ridge National Laboratory, unpublished, Aug. 27, 1968.

Xenon-Transient Calculations in Large Light-Water Reactors

By P. S. Lacy and E. D. Kendrick*

Transients in the spatial distribution of xenon within a reactor core can be excited by changes in core power level, control-rod configuration, coolant density distribution, or any combination of these three. Two examples of these are: for a boiling-water reactor (BWR), a change in coolant flow combined with repositioning of control rods to maintain core power, and for a pressurized-water reactor (PWR), a change in control-rod position to change core power.

The core power distribution in current BWR or PWR cores rated at more than 1500 Mw(t) can be significantly affected by transients in the spatial distribution of xenon. The power distribution in most cases will respond to transients in the xenon distribution by changing in time to a power distribution with a higher peak-to-average ratio. This is possible because during a transient the actual power distribution is a mixture of a fundamental flux mode and the higher flux modes that have been excited by the xenon redistribution. The variation with space of these higher modes is inherently more rapid than is the fundamental-mode variation with space. This effect is compounded in reactors that are designed to low peak-to-average power ratios (flat fundamental mode). The nearer the core is to the xenon-stability threshold, the greater will be the fraction of power generated in the higher flux modes and hence the greater the increase in peak-to-average ratio as a result of xenon transients.

The trends of current design, furthermore, are in the direction to make easier the initiation of higher flux modes. These design trends which have tended to lower the xenon-stability threshold relative to actual operating conditions are as follows:

1. Increase in the physical size of the core.
2. Increase in the thermal power level of the core.
3. Decrease in the core peak-to-average power ratio.
4. Decrease (i.e., less negative) in local power coefficients.
5. Decrease, in some cases, in neutron-migration area.

To provide guidance in the design and operation of large water reactors, it is highly desirable to be able to compute xenon transients in three dimensions with fuel and coolant thermal and coolant hydraulic feedbacks. Only in this way can the effects of control-rod positioning, coolant density and temperature distribution, fuel burnup, and neutron coupling between core regions be accurately represented. The objective of this article is to review the programs that have reports available for analysis of the phenomena discussed above. The article is written from the point of view of the nuclear engineer who wants to make power-distribution calculations including xenon-transient spatial effects in current-generation light-water reactors and therefore wants a review of what tools are in use with a brief discussion of these tools. Analyses for divergent as well as convergent spatial redistributions in power due to xenon transients are included in this review.

Background

The theory of spatial neutron-flux-distribution stability associated with xenon (^{135}Xe) redistribution within a core has been presented for some time. The

*Nuclear Associates International Corporation, Rockville, Md.

early work by Ward,[1] Henry and Germann,[2] and Randall and St. John[3] considered the xenon-transient problem from the point of view of determining whether or not a core is inherently stable and, if not, what the threshold power level for instability is with a given power coefficient. The formulation of Randall and St. John to establish the stability characteristics of a core has been used extensively.

The Randall and St. John basic equation is given and discussed here to provide insight for the remainder of this article. The stability of the jth flux mode is related to the core conditions by:

$$\frac{(M^2 B_g^2)}{\alpha_{Xe}}\Lambda_j - \frac{\alpha_T}{\alpha_{Xe}}\phi_{TH} = f(\phi) \qquad (1)$$

where $f(\phi) = \dfrac{\dfrac{1}{1+\lambda_{Xe}/\sigma_{Xe}\phi}}{1+\dfrac{\lambda_{Xe}+\lambda_I}{\sigma_{Xe}\phi}} - \gamma_{Xe}$

$\Lambda_j = (B_j^2 - B_g^2)/B_g^2$

B_g^2 = geometric buckling, cm^{-2}

M^2 = neutron-migration area, cm^2

α_{Xe} = reactivity in equilibrium xenon, $\triangle k/k$

Λ_j = buckling fractional change between the fundamental mode and the jth mode

α_T = power coefficient in units of reactivity per unit flux, $\triangle k/k/\phi$

ϕ_{TH} = threshold flux

ϕ = core average thermal flux, neutrons/(cm^2)(sec)

λ_{Xe}, λ_I = ^{135}Xe and ^{135}I decay constants, sec^{-1}

σ_{Xe} = ^{135}Xe microscopic absorption cross section, cm^2

γ_{Xe} = ^{135}Xe direct-yield fraction from fissions

The function $f(\phi)$ can be computed as a function of ϕ for a core average value of σ_{Xe}. If the core average flux is inserted in Eq. 1 for $f(\phi)$ and for ϕ_{TH} and both sides are equal, the core is at the threshold. If the left side is greater than the right side, the core is stable, and if less than the right side the core is unstable, to xenon-induced oscillations in the spatial power distribution.

Equation 1 requires inputs of

1. Core dimensions.
2. Core power coefficient.
3. Core average power level.
4. Neutron-migration area.
5. Core reactivity in equilibrium xenon.
6. Degree of flux flattening.

The core dimensions yield the geometric buckling that is identified with the fundamental flux mode and also bucklings of the higher flux modes that are identified with a particular dimension, e.g., axial, radial, and azimuthal. The closer a higher mode is to the fundamental mode, as measured by the smaller buckling change between fundamental and higher mode, the closer the core is to the instability threshold for that mode.

The less negative the power coefficient, the closer the core will be to instability. The core flux level corresponds directly to the core power level; however, the flux level is the independent variable of interest. The higher the core average thermal flux, the less stable is the core. A smaller neutron-migration area gives weaker neutronic coupling among core regions which results in a less stable core. Large equilibrium-xenon reactivity results in greater reactivity available to feed the growth of a higher flux mode and thus lessens core stability. The greater the degree of fundamental-mode flux flattening, the smaller is the reactivity required to excite a higher flux mode, and the core is less stable. Randall and St. John[4] analyzed the effects of flux flattening in the radial and axial directions for cylindrical reactors to show that a flat flux over 40% of the radial or axial dimension will reduce the instability threshold by 40% in the core average flux.

The usefulness of Eq. 1 for cores with control rods, distributed voids, and fuel zones is limited to qualitative analysis of stability characteristics. From a design and operation point of view, threshold analysis to determine whether or not a core is inherently stable is of secondary interest. Of prime interest is the effect of spatial redistribution of xenon on power distribution and the methods for detection and control of spatially dependent transients in the power distribution. This is the case whether or not the core is operated above and below the xenon-instability threshold. However, the spatial redistributions would be more pronounced in cores above or close to the instability threshold than in cores well below the threshold.

The half-lives of the ^{135}Xe and ^{135}I isotopes which cause xenon transients are long, relative to detection, operator-reaction, and control-mechanism times. Randall and St. John[4] show oscillation periods as a function of the threshold value of the neutron flux to be approximately 25 hr for flux levels typical of current light-water reactors. Thus, provided adequate core instrumentation is used, the detection and control of power redistributions due to xenon should not present operational problems. This was shown by the first light-water reactor experience with xenon oscilla-

tions in the Shippingport first core and was reported by Simpson and Rickover.[5] (Shippingport was the first light-water reactor to exhibit xenon oscillations.) Such oscillations are slightly divergent and nicely illustrate the 24-hr period characteristic of xenon power transients.

For design and operation the need is to be able to perform a detailed analysis of the spatial characteristics of xenon and neutron-flux redistributions during a transient. Calculational methods to satisfy this need for current-generation light-water reactors must be multidimensional and multiregional in nature. These methods must include hydraulic, heat-transfer, and neutronic phenomena in the core as well as in the primary system. In summary the calculational methods must include:

1. Multidimensional geometries.
2. Fuel zones.
3. Control-rod positioning and movement.
4. Xenon and iodine inventories.
5. Core coolant density and temperature distribution.
6. Fuel-temperature distribution.
7. Core coolant-flow changes.

Methods of converting calculated core power distributions to in-core neutron-detector and thermocouple readings and to out-of-core neutron-detector readings should be included as well.

Effects such as delayed neutrons, heat transfer from the fuel to the coolant, and coolant-loop times, as shown by Chernick, Lellouche, and Wollman[6] and again by Lellouche,[7] are short-term relative to the xenon and iodine half-lives and need not be considered. Fuel-burnup effects are long-term and need not be considered during a given transient. However, transient analysis of partially depleted cores is necessary because the power coefficient changes with burnup, and hence the core response to xenon changes.

Current Programs

The previous paragraphs began with a discussion of the effect of xenon transients on the core peak-to-average power ratio and ended with the xenon spatial-stability problem. The remaining paragraphs will review current programs that aim to solve the problem from a design and operation point of view. This problem is not one of determining the core xenon stability but rather of detecting and controlling with acceptable peak-to-average power ratios the power redistributions caused by xenon.

BWR Cores

Programs for BWR's are described briefly by Crowther, Fischer, Niemi, and Wood[8] and by Crowther.[9] Calculations and operating data show that power redistributions due to xenon spatial transients in BWR's are well damped by the strong negative power coefficients. The Randall and St. John formulation assumes the reactor as a uniform core with a uniform power coefficient and predicts that the calculated power coefficient is approximately twice as strong as that needed to prevent instability. Crowther and his associates[8] state that this general conclusion is confirmed by more-detailed numerical calculations that include the significant nonuniformities in a boiling-water reactor core. They also state that in a BWR the changes in power distribution due to changes in power level are much greater than are the changes in power distribution caused by xenon effects. This is demonstrated by measurements using axial strings of in-core flux monitors in the Dresden 1 plant of Commonwealth Edison. These measurements show that changes in core power level produce changes in the coolant-density distribution which in turn shift the axial power distribution much more than the resultant xenon spatial transient.

PWR Cores—Diffusion Theory and Modal Analysis

Calculations of xenon transients in PWR cores have been discussed more extensively in the open literature than have BWR-core xenon calculations. Poncelet and Christie[10] have calculated the spatial xenon problem extensively in two-dimensional geometry in the plane perpendicular to the direction of coolant flow. The model included fuel-temperature and coolant-enthalpy feedback. The restriction is imposed, however, that only the core is considered; that is, inlet conditions to the core are taken to be constant in time. The use of digital simulation made it possible to represent core configurations with several fuel zones in multidimensional geometry with realistic control action and the inclusion of nonlinearities in the equations including nonlinear feedback effects. The numerical calculations reported showed, for the most part, free-running xenon-induced spatial power oscillations that were strongly divergent or mildly convergent since most calculations were done without temperature feedback. Also, control actions were not taken to squelch an oscillation once initiated. The effect of temperature feedback was excluded to reduce computer time, which was extensive for this program. The

lack of temperature feedback and control actions lessened the practical information gained relative to the problem of power redistribution caused by xenon; however, a large amount of information pertinent to calculational techniques was developed. Many figures are given in the reference to illustrate free-running power oscillations in both one and two dimensions.

The use of digital-computer programs permitted calculation of two-dimensional power distributions; such programs, however, required analysis to determine the errors introduced by the use of discrete mesh-spacing in both space and time approximations in the numerical treatment. The effects of mesh size in both space and time and the tightness of the convergence criterion for the flux distribution were studied to determine the size of these errors. Also studied were the physical effects of nonlinearities in the thermal feedbacks and the effects of the following: delayed neutrons, number of energy groups, initial power distribution, core diameter, power tilt in core, power density, equilibrium power distribution, ^{135}Xe absorption cross section, ^{135}I yield, and ^{135}Xe direct yield.

The spatial mesh size was found not to be a sensitive parameter; however, the increment between time steps was found to be a highly significant one. Both the time dependence and the magnitude of the oscillations were found to depend on time-step length. Figure 1 is reproduced here from Ref. 10 to illustrate this dependence on time step for time-step lengths of 1, 2, and 4 hr for a 12-ft-slab core with uniform fuel and no temperature feedbacks. In other calculations a 4-hr time step predicted stability, whereas the use of a 2-hr time-step length showed the core to be spatially unstable to xenon. Figure 2, also from Poncelet and Christie,[10] shows results from two-dimensional calculations for an 11-ft core with flattened power distribution and no temperature feedback. The calculations show that the less stable a core is, the greater will be the sensitivity to time-step length. A time-step length ≤ 1 hr is required for accurate results.

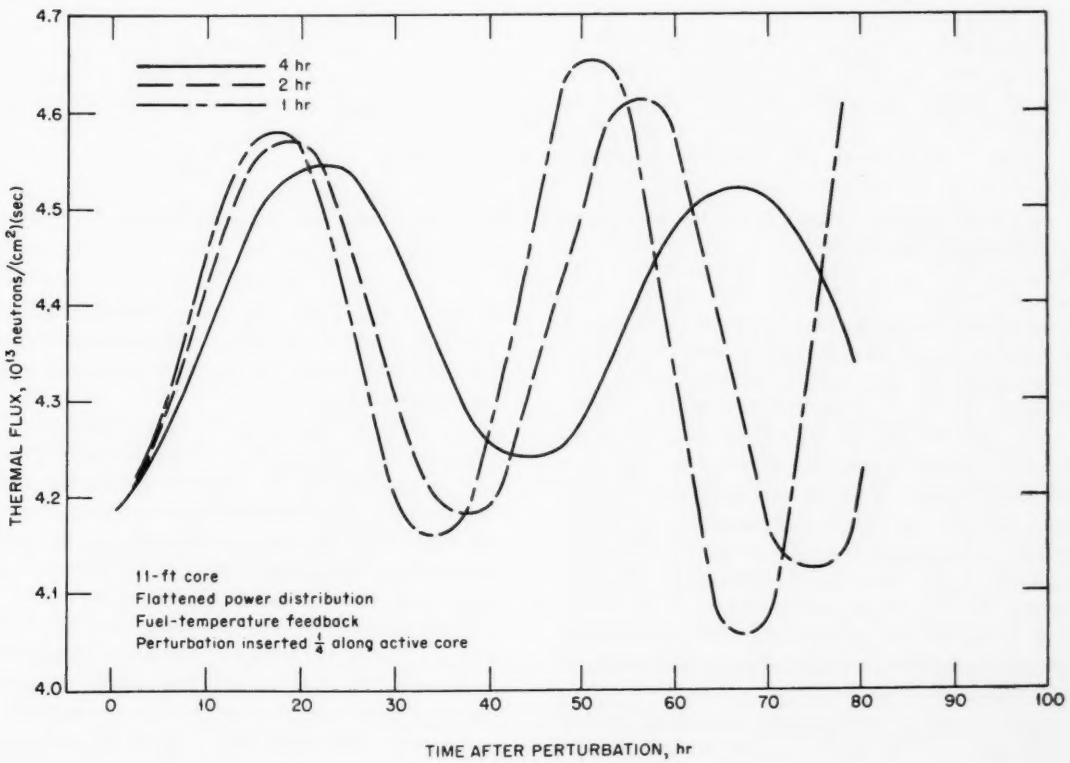

Fig. 1 Variation of xenon-induced spatial stability characteristics with time-step length in digital calculations (11-ft core, 1-dimensional calculation).[10]

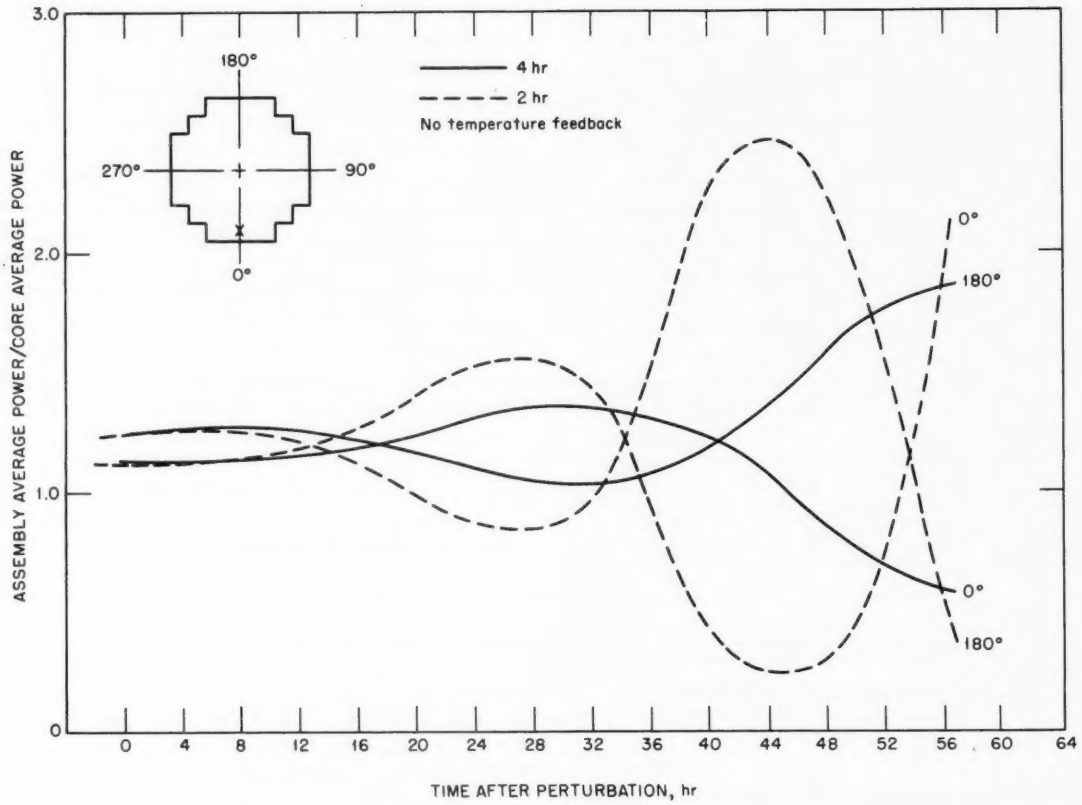

Fig. 2 Variation of xenon-induced spatial stability characteristics with time-step length in digital calculations (11-ft core, 2-dimensional calculation).[10]

A detailed analysis was performed to develop a correlation to correct the stability index from finite time-step results to a zero time-step result. The stability index is the multiple of time in the exponential for the envelope of the oscillations—a positive index for divergent power oscillations. An expression was developed to compute an average flux between time steps for use in the calculation of iodine and xenon number densities at the next time step rather than use of the flux at each time step to calculate number densities at the next time step. It was found that a convergence criterion of 10^{-5} in pointwise source is required for accuracy in calculations of xenon-transient characteristics.

The number of energy groups was found not to be significant; even one group was adequate provided that the neutron-removal-coefficient dependence on fuel and coolant temperatures was included in the neutron group formulation. It was concluded that the digital results are insensitive to the nonlinear characteristics of the Doppler effect but that it is important to account for the nonlinear properties of heat transfer from the fuel to the coolant.

The initial unperturbed power distribution was found to be very significant. Calculations were done with cosine, flat, dished, and severely dished fundamental flux modes to simulate power distributions for different PWR fuel-management schemes. The same core size, average power level, and fuel enrichment were used for these calculations, so that only the neutron coupling between regions changed from case to case. This of course affected the ease with which the first-higher flux mode could be excited, and significantly different stability indices were computed for these cases. Thus it was stated that stability characteristics should be expected to vary with core life. A variation will also occur owing to the power-coefficient dependence on core burnup. Two-dimensional calcula-

tions were also done to excite oscillations which precessed around the core by using a sequence of azimuthally asymmetric local-reactivity perturbations.

An analysis of PWR cores using Eq. 1 of Randall and St. John (nodal analysis) was done to determine the dependence of stability index on ^{235}U enrichment, core diameter, power density, power distribution, power coefficient, ^{135}I fission yield, ^{135}Xe absorption, and ^{135}Xe direct-fission yield. Some direct comparisons were performed between modal theory and digital-simulation results; the agreement was satisfactory, giving confidence in the use of modal theory for stability characteristics studies.

The work of Pearce[11] on the effect of neutron leakage out of finite slabs was not used to relate the extensive slab work reported by Poncelet and Christie to multidimensional core sizes. Thus, for example, 10-ft-long slab cores were used to represent 10-ft-diameter cores, whereas the effective neutron size of a 10-ft-diameter core must be greater than the physical diameter owing to circumferential neutron migration. The reference consistently refers to diametral oscillations, which more properly should be called azimuthal. Also, in the many figures showing power oscillations, the period is between 35 and 40 hr, whereas modal analysis gives periods between 25 and 30 hr for these cores. Shippingport experience shows a measured period of approximately 24 hr.

Other work using modal, analog, and digital techniques, with results compared one with another and with measured data from Shippingport, has been done by England,[12] England, Deremer, and Hartfield,[13-15] Stacey,[16-18] and Hooper, Rydin, and Stacey.[19]

England, Hartfield, and Deremer analyzed extensively the Shippingport PWR-1 reactor using modal, diffusion-theory, and analog models. The same methods were extended to the large seed-blanket reactor. The analysis accounted for the factors of size, thermal-flux distribution, geometric heterogeneities, and thermal feedbacks which affect k_∞. The work reported shows that the model successfully predicts the observed stability of the Shippingport cores. Similar work had been done earlier by Harris and Lacy[20] using diffusion-theory and modal techniques applied to Shippingport.

Stacey[16] reports a linear analysis of the Xe–I flux equations with power feedback which includes the detailed spatial distribution of the fundamental and first-higher flux modes. These are called λ modes with the eigenvalues of k_0 and k_1 (fundamental and first harmonic) and the corresponding neutron fluxes and adjoints computed using standard diffusion-theory codes. A suspected first harmonic is selected, digital diffusion-theory calculations are done, modal parameters are calculated from the output, and then the stability threshold in power level or power coefficient is determined. Good agreement was obtained with Shippingport data.

PWR Cores—Nodal Analysis

Calculations using a nodal core model have been done for PWR reactors by Stacey[17,18] and by Valerino and Kern.[21] Both approaches use a digital program to represent the core in three dimensions with many nodes coupled using modified one-group diffusion theory. Each node is represented by its k_∞ (infinite multiplication factor) and M^2 (neutron-migration area) properties. These are made to depend on xenon concentrations, control-rod presence, and temperature feedbacks. Stacey includes only coolant-enthalpy feedback; Kern includes fuel-temperature feedback as well.

Stacey in Ref. 17 reports calculations done to follow a xenon transient with control rods maintaining core criticality at a predetermined power level. Two xenon transients were studied, and for one the coolant-temperature coefficient was varied. The need to maintain core criticality using explicit control-rod representation is illustrated if meaningful power distributions are to be calculated. The destabilizing effect of a negative coolant-temperature coefficient is discussed and illustrated by showing axial peak-to-average power ratios as a function of time following a change in core power level. The axial power-distribution oscillation is convergent with a positive coefficient and divergent with a negative coefficient large in magnitude. A nominal negative coefficient gives neutral oscillations. A significant increase in axial peak-to-average ratio is calculated at the first oscillation in all cases. Some of Stacey's results are illustrated in Figs. 3 and 4. The results discussed above are from the 12-hr transient. Region XX is high in the core and region YY low in the core. The coolant coefficient is αk. These calculations point up the need to actually compute in multidimensions the detailed behavior of the power distribution, even though a modal analysis indicates core stability to xenon spatial oscillations. Calculations comparing nodal results with a modal analysis were not reported.

Stacey[17,22,23] also reports a formulation developed to provide the digital calculations with automatic programming of the control rods to meet

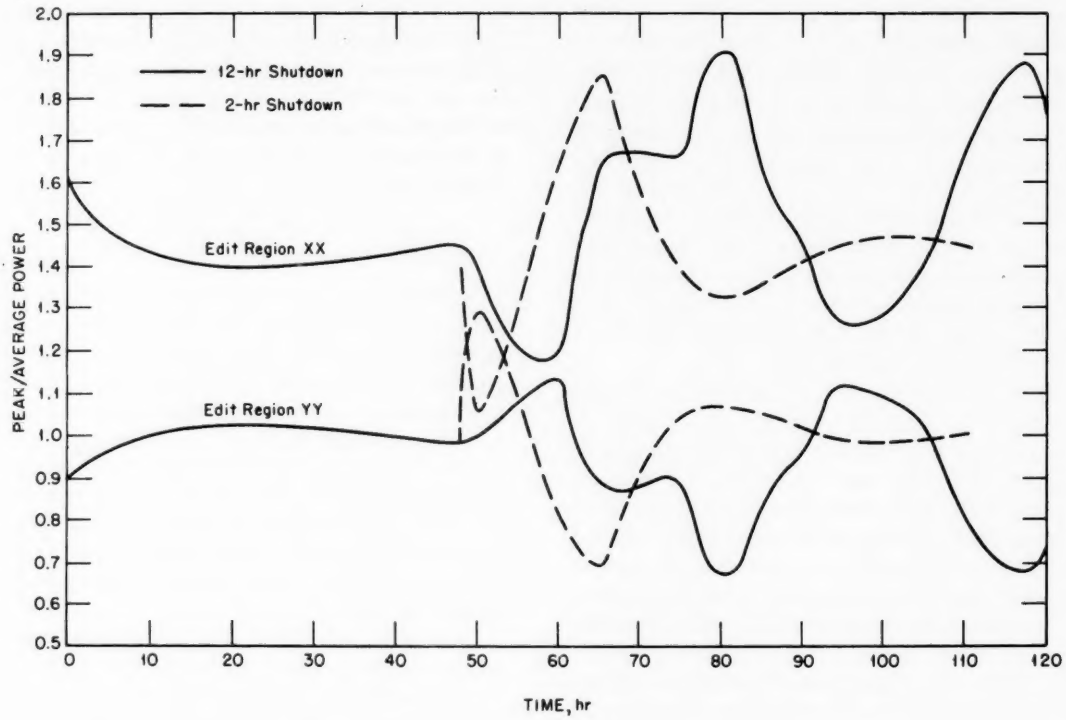

Fig. 3 Effect of initiating perturbation upon xenon transient.[17]

optimal requirements. The computer program used for these studies is the 3DXT code in FORTRAN IV for a 144K CDC-6600 computer. A xenon transient in a 777 node core followed for 110 hr with optimal control-rod motion required 1½ hr of 6600 machine time vs. 3 hr without optimal control. This is the 2-hr transient of Fig. 3.

Currently options are being added to the program to include both in-core and out-of-core instrumentation response and nonsymmetric coolant-enthalpy input into the core. A report on this work is planned for mid-1969.

Valerino and Kern have developed the XENCON nodal program in FORTRAN IV for the IBM 360/65 system. They have compared nodal and diffusion-theory results in one and two dimensions and have found good agreement in the stability index. All necessary feedback equations are incorporated including fuel-temperature effects and xenon microscopic cross-section dependence on coolant temperature.

A control-rod-search option to optimize the power distribution is being programmed. The effects of time-step length and convergence criterion, investigated in three dimensions, substantiate the conclusions stated above. The theoretical kernel used, the node size, and the acceleration techniques have been studied. The investigators have observed that, if fewer than three dimensions are used, it is necessary to represent accurately, by flux weighting, the core parameters in lines or planes normal to the plane or line of calculation, otherwise significant error will be introduced into the calculations of the stability index.

Calculations were done for cores using up to 2640 nodes with reasonable computing times. Typical cases require approximately 5 sec per source iteration with a maximum of 150 source iterations per time step to give the desired convergence.

The model is presently being applied to analysis of the Pickering D_2O-moderated and -cooled reactor. One initiating perturbation being investigated consists of the on-line refueling of three-fifths of one fuel channel, and the resulting oscillation is followed for up to 100 hr with 4-hr time steps. Various control schemes for damping the oscillations are being investigated. A final report is planned for mid-1969.

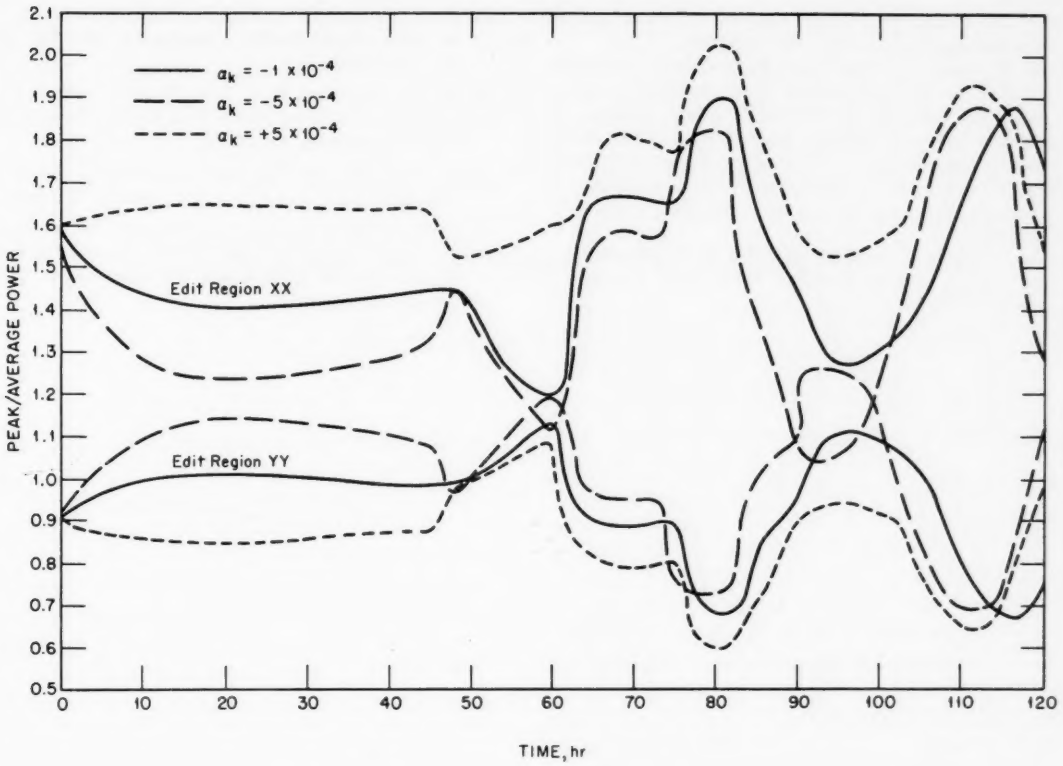

Fig. 4 Effect of thermal feedback upon xenon transient.[17]

References

1. A. G. Ward, The Problem of Flux Instability in Large Power Reactors, Canadian Report AECL-345, July 1956.
2. A. F. Henry and J. D. Germann, Oscillations in the Power Distribution Within a Reactor, *Nucl. Sci. Eng.*, **2**: 469 (1957).
3. D. Randall and D. S. St. John, Xenon Spatial Oscillations, *Nucleonics*, **16**(3): 82 (1958).
4. D. Randall and D. S. St. John, Xenon Spatial Oscillations, *Nucl. Sci. Eng.*, **14**: 204 (1962).
5. J. W. Simpson and H. G. Rickover, Shippingport Atomic Power Station (PWR), in *Proceedings of the Second United Nations International Conference on the Peaceful Uses of Atomic Energy, Geneva, 1958*, United Nations, New York, 1958.
6. J. Chernick, G. Lellouche, and W. Wollman, The Effect of Temperature on Xenon Instability, *Nucl. Sci. Eng.*, **10**: 120 (1961).
7. G. S. Lellouche, Control of Xenon Spatial Oscillations, USAEC Report BNL-6330, Brookhaven National Laboratory, August 1962.
8. R. L. Crowther, D. L. Fischer, R. O. Niemi, and J. E. Wood, Reactor Kinetics Effects of Significance to Large Boiling Water Reactor Design and Operation, in Proceedings of the Brookhaven Conference on Industrial Needs and Academic Research in Reactor Kinetics, USAEC Report BNL-50117(T-497), pp. 1-36, Brookhaven National Laboratory, July 1968.
9. R. L. Crowther, Xenon Considerations in the Design of Large Boiling Water Reactors, Report APED-5640, General Electric Company, June 1968.
10. C. G. Poncelet and A. M. Christie, Xenon-Induced Spatial Instabilities in Large Pressurized Water Reactors, USAEC Report WCAP-3680-20, Westinghouse Electric Corporation, Atomic Power Division, March 1968.
11. R. M. Pearce, Xenon Oscillations in Finite Reactors, *Nucl. Sci. Eng.*, **16**: 336 (1963).
12. T. R. England, Xenon-Power Oscillations in PWR-1-Analysis and Observations, *Trans. Amer. Nucl. Soc.*, **7**(2): 220 (1964).
13. T. R. England, R. K. Deremer, and G. L. Hartfield, Practical Model for Analysis of Reactor Xenon Stability Including Plant and Temperature Feedback, *Trans. Amer. Nucl. Soc.*, **10**(1): 255 (1967).
14. G. L. Hartfield, R. K. Deremer, and T. R. England, Stability Characteristics of Large Seed-Blanket Reactors, *Trans. Amer. Nucl. Soc.*, **10**(1): 255 (1967).
15. T. R. England, G. L. Hartfield, and R. K. Deremer, Xenon Spatial Stability in Large Seed-Blanket Reactors, USAEC Report WAPD-TM-606, Westinghouse Electric Corporation, Bettis Plant, April 1967.

16. W. M. Stacey, Jr., Linear Analysis of Xenon Spatial Oscillations, *Nucl. Sci. Eng.*, **30**: 453 (1967).
17. W. M. Stacey, Jr., Space–Time Reactor Kinetics Development at KAPL, in Proceedings of the Brookhaven Conference on Industrial Needs and Academic Research in Reactor Kinetics, USAEC Report BNL-50117(T-497), pp. 380-405, Brookhaven National Laboratory, July 1968.
18. W. M. Stacey, Jr., A Numerical Study of Xenon-Power Spatial Oscillations, *Trans. Amer. Nucl. Soc.*, **11**(1): 226 (1968).
19. R. J. Hooper, R. A. Rydin, and W. M. Stacey, Verification of a Xenon Stability Criterion, *Trans. Amer. Nucl. Soc.*, **11**(1): 227 (1968).
20. D. R. Harris and P. S. Lacy, A Simple Approximate Test for Spatial Xenon Stability, *Trans. Amer. Nucl. Soc.*, **3**(2): 437-438 (1960).
21. M. F. Valerino and R. C. Kern, Monthly Progress Letter Nos. 1–12, Optimum Spatial Flux Control Project, Combustion Engineering, Inc., 1968.
22. W. M. Stacey, Jr., Optimal Control of Spatial Xenon Transients, *Trans. Amer. Nucl. Soc.*, **10**(2): 572 (1967).
23. W. M. Stacey, Jr., Application of Dynamic Programming to the Optimal Control of Xenon-Power Spatial Transients, USAEC Report KAPL-M-6725, Knolls Atomic Power Laboratory, July 1967.

Tritium in Power Reactors

By Joseph W. Ray*

Tritium is a radioactive isotope of hydrogen which decays to stable ^{3}He by emission of a soft beta particle (18-kev end-point energy, 5.7-kev average energy) with no attendant gamma emission. The half-life for tritium decay is a relatively long 12.3 years. Tritium buildup in heavy-water reactors has been of concern for many years, with the tritium production being attributed to neutron capture in the deuterium isotope. However, it has been only in the last several years that the problem of tritium buildup in light-water reactors has been recognized.

The first indication that tritium might be generated in significant quantities in light-water reactors was the discovery that tritium was produced[1,2] as a fission product in the ternary fission of ^{235}U at the rate of approximately 8.7×10^{-5} triton† per fission. With such a low energy for the emitted beta particle and no attendant gamma emission, it is reasonable to question the significance of tritium generation in power reactors. The answer is related principally to the chemical and atomic similarity between tritium and hydrogen. Tritium, like hydrogen, will diffuse very rapidly through most materials, will replace hydrogen in water molecules, and will behave as hydrogen chemically in the human body.

Health-Physics Aspects of Tritium

Tritium decays by emission of a soft beta particle with no attendant gamma radiation. Consequently it presents no radiological health hazard if it is prevented from entering the body. However, introduction of tritium into the body in any form does constitute a potential hazard.

Tritium gas enters the body primarily by inhalation. Retention of this form of tritium is quite low[3] (less than 0.1%), and this is reflected in the high concentration limit for exposure to air containing tritium gas. The hazard present in exposure to elemental tritium appears to arise from oxidation of a small amount of the inhaled gas in the lungs.[4]

Exposure to the oxide of tritium, either liquid or vapor, presents a more serious hazard because of the rapid uptake of this material and retention of it in the body. Tritium oxide may enter the body by inhalation, ingestion, or absorption through the skin. From the respiratory standpoint, over 90% of the tritium activity inhaled as tritiated water vapor is absorbed through the respiratory system. In addition, absorption of this form of tritium through the total skin area occurs at a rate comparable to that through the lungs.[4] For short exposures, absorption through the skin is reduced by about 50% by wearing coveralls. However, for exposure times in excess of 30 min, the coveralls do not reduce skin absorption.[1,7] From the digestive standpoint, essentially all ingested tritium oxide is assumed to be completely absorbed and to metabolize in the same manner as water.

The maximum permissible concentrations of environmental tritium as given in Title 10, *Code of Federal Regulations*, Part 20, are presented in Table 1 for reference.

Generation of Tritium in Power Reactors

Appreciable quantities of tritium are generated in light-water-cooled power reactors. The principal sources are ternary fission and, in pressurized-water reactors employing boron shim control, neutron-

*Battelle Memorial Institute, Columbus Laboratories, Columbus, Ohio.

†A triton is the tritium nucleus without an orbiting electron; i.e., a positively charged tritium ion.

Table 1 Maximum Permissible Concentration of Tritium as Given in 10 CFR 20

	Maximum permissible concentration, μc/ml			
	Restricted area (40-hr week)		Unrestricted area (168-hr week)	
Tritium form	Air	Water	Air	Water
Water (liquid or vapor)	5×10^{-6}	1×10^{-1}	2×10^{-7}	3×10^{-3}
Gas	2×10^{-3}		4×10^{-5}	

absorption reactions in boron. There are several other potential tritium sources such as neutron absorption in carbon, deuterium, and beryllium (in startup neutron sources), as well as photonuclear reactions in core materials; but, in typical light-water power reactors, these are negligible. Evaluations of these various sources of tritium are discussed below.

Ternary Fission

Tritium is produced in the fission process at the rate of 8.7×10^{-5} triton per fission. This rate is equivalent to 1.23×10^{-2} curie of tritium per day per thermal megawatt of reactor power, or about 40 curies/day for a typical 1000-Mw(e) reactor.

Boron Reactions

The boron present as chemical shim in the coolant of pressurized-water reactors is another source of tritium. Neutron reactions or reaction chains which yield tritium from boron are

$$^{10}\mathrm{B}(n,2\alpha)\mathrm{T}$$

$$^{10}\mathrm{B}(n,\alpha)^{7}\mathrm{Li}(n,n\alpha)\mathrm{T}$$

$$^{10}\mathrm{B}(n,d)^{9}\mathrm{Be}^{*}(n,\alpha)^{6}\mathrm{Li}(n,\alpha)\mathrm{T}$$

$$^{10}\mathrm{B}(n,d)^{9}\mathrm{Be}(n,\alpha)^{6}\mathrm{Li}(n,\alpha)\mathrm{T}$$

$$^{11}\mathrm{B}(n,\mathrm{T})^{9}\mathrm{Be}$$

The $^{11}\mathrm{B}(n,\mathrm{T})^{9}\mathrm{Be}$ reaction is a threshold reaction with a threshold neutron energy above 10 Mev and can therefore be ignored. The reaction chain $^{10}\mathrm{B}(n,d)^{9}\mathrm{Be}^{*}(n,\alpha)^{6}\mathrm{Li}(n,\alpha)\mathrm{T}$ is unlikely to lead to tritium production because the $^{9}\mathrm{Be}^{*}$ is unstable and decays instantaneously to a neutron and two alpha particles. The reaction chain $^{10}\mathrm{B}(n,d)^{9}\mathrm{Be}$ has a threshold neutron energy of 4.35 Mev. The only cross-section information found[16] indicates a cross section of 21 mb for 14-Mev neutrons. Because of the relatively low neutron flux above 14.5 Mev, the small cross section for the reaction, and the necessity to undergo two additional neutron captures before producing tritium, it is presumed that the $^{10}\mathrm{B}(n,d)^{9}\mathrm{Be}(n,\alpha)^{6}\mathrm{Li}(n,\alpha)\mathrm{T}$ is negligible. The $^{10}\mathrm{B}(n,2\alpha)\mathrm{T}$ reaction is a threshold reaction with a threshold energy of 1 Mev. The reaction cross section may be considered to increase linearly from 15 mb at 1 Mev to 75 mb at 5 Mev and remain constant at 75 mb from 5 to 10 Mev. The tritium-generation rate from this reaction may be calculated from

$$\dot{\mathrm{T}}(t) = 2.36 \times 10^{-11} N_{\mathrm{B}}(t) V \times \int_{1}^{10\ \mathrm{Mev}} \sigma_1(E)\phi(E)\,dE \ \text{curies/day} \qquad (1)$$

where $\dot{\mathrm{T}}(t)$ = time-dependent tritium-generation rate, curies/day

$N_{\mathrm{B}}(t)$ = natural boron concentration in coolant, atoms/cm^3

V = coolant volume in core, cu ft

$\sigma_1(E)$ = energy-dependent reaction cross section, cm^2

$\phi(E)\,dE$ = energy-dependent neutron flux, neutrons/(cm^2)(sec)

The calculated tritium-generation rate from this reaction in a typical 1000-Mw(e) pressurized-water reactor is shown in the lower curve in Fig. 1. In this calculation a fission-neutron-energy spectrum was used for $\phi(E)$. This spectrum was normalized to a total flux above 1 Mev of 6×10^{13} neutrons/(cm^2)(sec). The linear decrease in tritium-generation rate with time is due to the assumed linear decrease in the concentration of boron shim from an initial value of 1500 ppm to a level of 400 ppm after 350 days. The volume of coolant in the core was assumed to be 650 cu ft.

Considering the $^{10}\mathrm{B}(n,\alpha)^{7}\mathrm{Li}(n,n\alpha)\mathrm{T}$ reaction chain, the (n,α) reaction in $^{10}\mathrm{B}$ is a thermal-neutron reaction. The $(n,n\alpha)$ reaction in $^{7}\mathrm{Li}$ is a threshold reaction with a threshold neutron energy of 3 Mev. The reaction cross section increases linearly from zero at 3 Mev to 400 mb at 6 Mev and remains constant at 400 mb between 6 and 10 Mev. The tritium-generation rate from this reaction may be calculated from

$$\dot{\mathrm{T}}(t) = \frac{9.85 \times 10^{5} \sigma_{\mathrm{B10}} \phi_{\mathrm{th}} V}{F} \times \left[\left(a - \frac{b}{F}\right)(1 - e^{-Ft}) + bt\right] \int_{1}^{10} \sigma_2(E)\phi(E)\,dE \qquad (2)$$

where $T(t)$ = time-dependent tritium-generation rate, curies/day
σ_{B10} = cross section for $^{10}B(n,\alpha)^{7}Li$ reaction, cm^2
ϕ_{th} = thermal-neutron flux, neutrons/(cm^2)(sec)
F = fraction of primary-coolant-volume turnover daily, day^{-1}
$\sigma_2(E)$ = cross section for the $^{7}Li(n,\alpha n)T$ reaction, cm^2
a and b = constants in the equation for ppm boron in coolant, ppm = $a + bt$, with a in ppm and b in ppm/day

and the other symbols were defined earlier. The calculated tritium-generation rate from this reaction in a typical 1000-Mw(e) pressurized-water reactor is shown in the middle curve in Fig. 1. The values used for boron concentration, core coolant volume, and fast-neutron flux were the same as those used for the $^{10}B(n,2\alpha)T$ reaction. For the $^{10}B(n,\alpha)^{7}Li$ reaction, a Maxwellian average cross section (σ_{B10}) of 2600 barns was used with a thermal flux of 4×10^{13} neutrons/(cm^2)(sec). A primary-coolant turnover rate of 0.12%/day was used, corresponding to a leakage rate of 240 lb/day for a primary-coolant mass of 200,000 lb. The slope of the curve decreases with time owing to the assumed linear reduction of boron concentration with time.

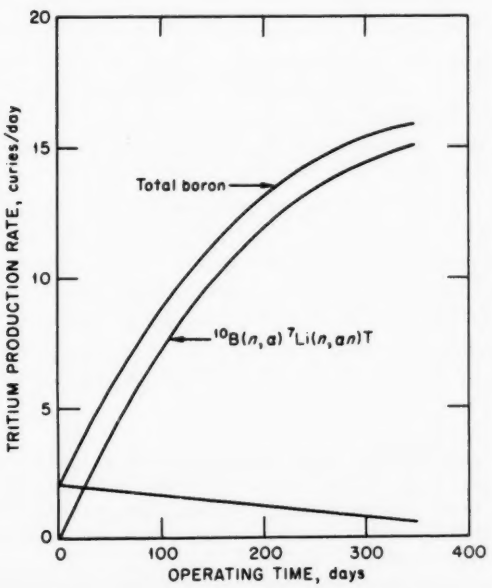

Fig. 1 Calculated production rate of tritium from boron shim in coolant of a typical 1000-Mw(e) pressurized-water reactor.

The upper curve of Fig. 1 is the sum of the other two curves and represents the total tritium-generation rate from boron shim in the coolant of a typical 1000-Mw(e) pressurized-water reactor. It is seen that this increases with time to a level of about 16 curies/day after 350 days of operation.

These calculations neglect any reactor-shutdown operations, such as refueling, which would cause the primary coolant to be diluted with large amounts of makeup water and result in significant changes in the concentration of ^{7}Li built up in the coolant from the $^{10}B(n,\alpha)^{7}Li$ reaction. More exact studies for specific reactors can be made using the actual reactor operating history. The values of boron concentration, neutron flux, core coolant volume, and primary-coolant-water turnover rate in specific reactors will also differ from those used in these calculations; however, the calculated tritium-generation rates are directly proportional to fast-neutron flux,* thermal-neutron flux, boron concentration, and core coolant volume; therefore the tritium-generation rates of Fig. 1 can be easily corrected to the conditions in a similar reactor system. The primary-coolant turnover rate, F, enters into the exponential term in Eq. 2, and corrections for differences in this parameter must be handled accordingly.

Migration of Tritium

Tritium generated from boron in the coolant of pressurized-water reactors is likely to remain in the coolant as tritiated-water molecules and will migrate in the reactor system by those paths available for primary-coolant migration. Tritium generated in the fission process, however, must first escape from the fuel pins before it can migrate to other plant locations. Prior to discussing the question of tritium migration, it is important to point out two aspects of tritium which are of significance: (1) energy and range of fission-product tritons and (2) affinity of the water molecule for tritium.

Energy and Range of Fission-Product Tritons

Little experimental effort has been devoted to the determination of the energy spectrum of tritons in

*Proportionality to the total flux above 1 Mev relies on the assumption that the neutron-energy spectrum in this range is represented by a fission spectrum. In this case the energy-dependent fast-neutron flux may be written as the product of a constant times an energy-dependent term, where the constant is proportional to total flux above 1 Mev and the energy-dependent term is the same for all reactors of interest.

product tritium escapes from Zircaloy-clad UO_2 fuel pins. On the basis of measured tritium levels in water from a reactor with Zircaloy-clad fuel, Smith[13] concludes that only approximately 0.1% of fission-product tritium escaped from the pins. Investigations of tritium buildup in the primary coolant of a Zircaloy-clad boiling-water reactor showed no detectable tritium buildup.[9] This indirect evidence, together with the considerations presented in the previous paragraph, suggests strongly that essentially all fission-product tritium may be considered to remain in Zircaloy-clad UO_2 fuel pins and not escape to the reactor coolant water.

It is possible to establish a crude estimate of the fraction of fission-product tritium escaping from reactor fuel pins by developing a simple tritium balance on the primary coolant system and comparing the tritium concentration predicted by this balance with measured concentrations in samples of primary-coolant-system water. The rate of change of tritium concentration in the primary coolant may be written as

$$\frac{dA_{sp}}{dt} = \frac{1}{M_p}(\dot{P}_c + \dot{R}_{fp} - \dot{L}_c) \qquad (3)$$

where A_{sp} = specific activity of tritium in coolant samples, μc/g
M_p = mass of water in primary coolant system, g
$\dot{P}_c$ = rate of production of tritium primary coolant, μc/day
$\dot{R}_{fp}$ = rate of release of fission-product tritium from fuel pins, μc/day
$\dot{L}_c$ = rate of loss of tritium due to primary-coolant leakage, μc/day

Assuming that tritium generated in the primary coolant is due to neutron absorption in boron, $\dot{P}_c$ may be written as

$$\dot{P}_c = \frac{9.85 \times 10^{11}\sigma_{B10}\phi_{th}V}{F}\left[\left(a - \frac{b}{F}\right)(1 - e^{-Ft}) + bt\right] \times \int_1^{10\ \text{Mev}} \sigma_2(E)\phi(E)\,dE + 2.0 \times 10^{11} V(a + bt) \int_1^{10\ \text{Mev}} \sigma_1(E)\phi(E)\,dE$$

where $\dot{P}_c$ is in microcuries per day and the other terms have been defined earlier.

The rate of release of fission-product tritium from fuel pins can be written as

$$\dot{R}_{fp} = 1.236 \times 10^4\, P f_R\ \mu\text{c/day}$$

where f_R is the fraction of fission-product tritium escaping from fuel pins and P is the core thermal power in megawatts. The rate of loss of tritium due to primary-coolant leakage* may be expressed as

$$\dot{L}_c = 454\, A_{sp}\, L_R$$

where L_R is the primary-coolant leakage rate in pounds per day. If the reactor power and primary-coolant leakage rate are assumed to be independent of time, Eq. 3 can be integrated readily to yield an expression for tritium specific activity in the primary coolant as a function of operating time. Comparison of predicted and measured specific activities permits estimation of the fraction of fission-product tritium which escapes from the fuel pins.

Migration of Tritium in Reactor Plant

Migration of tritium within the nuclear power station will occur as tritiated water originating in the primary coolant system. Any path available for leakage or other removal of water from the primary coolant system is, accordingly, a path for tritium migration. This could include such items as pump leakage, pressurizer venting, primary-coolant sampling, and removal through injection and purification systems. The principal path for release of tritium from the plant would be effluents from the liquid-waste-disposal system.

It is difficult to determine the magnitude of tritium migration and accumulation in various plant systems for a particular nuclear power station without details on the specific design and operating procedures of that plant. However, it is possible to develop mathematical models describing tritium-generation rates and the interactions between appropriate power-plant water streams as was done for the PM-3A nuclear power plant.[9] These models can then be used to predict tritium concentrations at various plant locations.

Tritium in Fuel-Reprocessing Plants

The principal source of tritium in light-water reactors is ternary fission, and there is strong evidence that virtually all of this tritium is retained in zirconium-clad UO_2 fuel pins. Accordingly, this tritium will be delivered to the fuel-reprocessing plant as part of the spent fuel. Assuming an average fuel burnup of

*Leakage is interpreted here as all water losses from the primary coolant system.

25,000 Mwd/metric ton of uranium, this will amount to approximately 270 curies of tritium/metric ton of UO_2. Measurements of tritium release during reprocessing of stainless-steel-clad UO_2–ThO_2 fuel specimens[14] indicated that 0.2% of the fission-product tritium was released during the shearing operation. During dissolution of the fuel, another 0.2% of the tritium was released as gas, and the remaining 99.6% remained in the fuel solution. In other tests with zirconium-clad UO_2 pins, the same investigators found approximately 9% of the fission-product tritium present as gas when the pins where sheared. Although these investigations do not provide totally conclusive evidence concerning the distribution of fission-product tritium within zirconium-clad UO_2 fuel pins, they do suggest that a large fraction of it will be tied up in the fuel and/or cladding and will be retained in the liquid streams in reprocessing plants.

Tritium Control and Disposal

Control of tritium generated in nuclear power plants involves primarily the control of potentially tritiated water originating in the primary coolant system. Water leaving the primary coolant system due to leakage, routine sampling, pressurizer venting, startup coolant expansion, or other causes is likely to contain tritium as tritiated water. The specific activity of tritium in this water, and hence the procedures necessary to prevent unacceptable personnel exposures, depends upon several factors, including reactor type (BWR or PWR), recent operating history (power and primary-coolant leakage rate, core average neutron flux), volume of water in the core, and mass of water in the primary coolant system. This in turn will determine the procedures that must be employed in handling and disposing of water emanating from the primary coolant system.

The difficulty in handling and disposing of tritiated waste is that the tritium will generally be tied up in water molecules and therefore cannot be separated by normal radioactive-waste-treatment techniques (e.g., precipitation or evaporation). Isotopic enrichment is too expensive for consideration in most cases. Therefore the alternatives are retention of tritiated water for use as primary-coolant makeup or dilution for release as liquid or vapor.

Release as Liquid

The volume of diluent water required for off-site release of tritiated water may be computed from

$$V_D \geqslant {}^{330}V_W(A_{sp} - 0.003)$$

where V_D is the volume of diluent in gallons, V_W is the volume of tritiated water in gallons, and A_{sp} is the specific activity of tritiated water in microcuries per milliliter. As an example, a nuclear power plant discharging 100 gal/day of tritiated water with a specific activity of 3 μc/ml would require 1 Mgd of diluent water. This amount of water would certainly be readily available at any power-reactor site.

The problem is more severe for fuel-reprocessing plants. For example, a reprocessing plant with a capacity of 5 metric tons/day will handle approximately 1350 curies/day of tritium. Dilution of this for off-site release would require approximately 120 Mgd of diluent water. This would require a reasonably good size stream, but it is not prohibitive.

Release as Vapor

An alternative disposal technique is controlled evaporation of tritium into a flowing air stream and release of the air stream through a stack. It is difficult to estimate the required air flow for disposal of tritiated water by this technique without information concerning air temperature, humidity, wind velocity, stack height, and site boundaries. The analytical method of Sutton and Roy[15] can be used to find ground-level dilution factors. These ground-level dilution factors, together with the quantity and specific activity to be released and information on air temperature and humidity, can be used to calculate required air flow rates. Rough calculations indicate that a continuous flow of 1000 to 10,000 cfm of air can handle 100 gal/day of tritiated water containing 3 μc/ml of tritium, assuming that the water-evaporation rate is not controlling.

References

1. E. L. Albenesius and R. S. Ondrejcin, Nuclear Fission Product Tritium, *Nucleonics*, **18**(9): 100 (1960).
2. E. N. Sloth et al., Tritium in Thermal Neutron Fission of Uranium-235, *J. Inorg. Nucl. Chem.*, **24**: 337 (1962).
3. H. L. Butler, Tritium Hazards in Heavy-Water-Moderated Reactors, *Nucl. Safety*, **4**(3): 77-82 (1963).
4. E. A. Pinson and W. H. Langhan, Physiology and Toxicology of Tritium in Man, *J. Appl. Physiol.*, **10**(1): 108-126 (1957).
5. H. E. Wegner, Additional Long-Range Particles from the Spontaneous Fission of Cf^{252}, paper presented at the American Physical Society Meeting, Washington, April 24–27, 1961, *Bull. Amer. Phys. Soc.*, **6**: 307 (1961).
6. R. A. Nobles, Long-Range Particles from Nuclear Fission, *Phys. Rev.*, **126**(4): 1508-1513 (1962).

7. J. C. Watson, High-Energy Alpha Particles and Tritons from the Spontaneous Fission of Californium-252, *Phys. Rev.*, **121**(1): 230-231 (1961).
8. C. B. Fulmer and B. L. Cohen, Magnetic Analysis of the Long-Range Particles from Fission of U^{235}, *Phys. Rev.*, **108**(2): 370-372 (1957).
9. J. W. Ray, R. O. Wooton, and R. H. Barnes, Investigation of Tritium Generation and Release in PM Nuclear Power Plants, USAEC Report BMI-1787, Battelle Memorial Institute, Oct. 31, 1966.
10. J. B. Marion, 1960 Nuclear Data Tables, Part 3, Nuclear Reaction Graphs, USAEC Report ACCESS-64, National Research Council, August 1960.
11. W. H. Barkas and M. J. Berger, Tables of Energy Loss and Ranges of Heavy Charged Particles, in Studies in Penetration of Charged Particles in Matter, Report NAS-NRC-PUB-1133, pp. 103-172, National Research Council, 1964.
12. A. O. Allen, Mechanism of the Radiolysis of Water by Gamma Rays or Electrons, *The Chemical and Biological Actions of Radiations*, Academic Press Inc., New York, 1961.
13. J. M. Smith, Jr., Significance of Tritium in Water Reactors, General Electric Company, unpublished.
14. J. H. Goode, Hot-Cell Evaluation of the Release of Tritium and ^{85}Kr During Processing of ThO_2–UO_2 Fuels, USAEC Report ORNL-3956, Oak Ridge National Laboratory, June 1966.
15. O. G. Sutton and Q. J. Roy, The Theoretical Distribution of Airborne Pollution from Factory Chimneys, *Meteorol. Soc.*, **73**: 257, 426 (1947).
16. F. L. Ribe and J. D. Seagrave, The Pickup Reactions $^{10}B(n,d)^{9}Be$ for 14-Mev Neutrons, *Phys. Rev.*, **94**: 934-940 (May 15, 1954).
17. R. V. Osborne, Absorption of Tritiated Water Vapor by People, *Health Phys.*, **12**: 1527 (1966).

Impact of Large-Scale Plants on Fuel Reprocessing

By Walton A. Rodger and Stanton L. Reese*

The reprocessing of spent nuclear fuel has gone through two rather different phases in the past. It appears that a new third phase is about to begin.

The first phase, which encompasses the processing of fuel in government-owned plants to provide material for military purposes, began in 1944 with the commissioning of the original Bismuth Phosphate Plant at Hanford (Fig. 1). This phase is, of course, not over. The plants at Hanford, Savannah River, and Idaho are still in operation and are likely to remain so for a long time. Most reprocessing technology is a product of this phase.

The second phase, which encompasses the first generation of commercial reprocessing plants, began in 1956 when the AEC encouraged industry to enter the field of reprocessing to provide a commercial service for the fuel that would be coming out of central power-station reactors.[1] This encouragement took the form of the offer of a near-term "base load" of fuel, to be provided from AEC-production fuels.

The AEC offer led to the construction and operation of the West Valley plant of Nuclear Fuel Services, Inc. (NFS), a 1 metric ton/day plant that went into commercial operation in April 1966 (Fig. 2). This plant employs a conventional Purex-type solvent extraction process for the separation and purification of its products. But it introduced into full-scale operation for the first time a mechanical head end generally referred to as "chop–leach."

More recently the General Electric Company (GE) has begun the construction of the second commercial reprocessing plant. This too is a 1 metric ton/day plant. It also employs a mechanical head end, but it is introducing a combination of solvent extraction and fluoride-volatility techniques for the separation and purification of the products.[2]

With the promise of sizable quantities of spent fuel to be discharged in the mid-1970's, the third phase of reprocessing, that of the scale-up second-generation plant, has been threatening to come on the scene for some time. In November 1968 the Allied Chemical Corp. filed with the AEC Division of Materials Licensing a preliminary safety-analysis report (PSAR) seeking a construction permit to build at Barnwell, S. C., adjacent to the Savannah River Plant, a 5 metric ton/day reprocessing plant.[3] At the same time the trade press has been carrying a succession of items[4-6] indicating that two other companies, Atlantic Richfield Company and National Lead Company, also are interested in building a similar plant. Atlantic Richfield has indicated an interest in a site near Leeds, S. C., and has an agreement with Duke Power Company for processing the fuel from the Oconee reactors.[4] The plans of the National Lead Company are less clear.[4]

With two major companies clearly stating their intention to do so, it seems certain that the mid-1970's will find at least one plant of about 5 metric ton/day nominal capacity in operation and that plant in all probability will be located in the southeast.

It is the purpose of this paper to consider the impact of this new generation of larger reprocessing plants on fuel-cycle costs, their radiological impact on the environment, and the technical, engineering, and operational problems associated with this scale-up.

*Nuclear Safety Associates, Rockville, Md.

Fig. 1 Bismuth Phosphate Plant at Hanford.

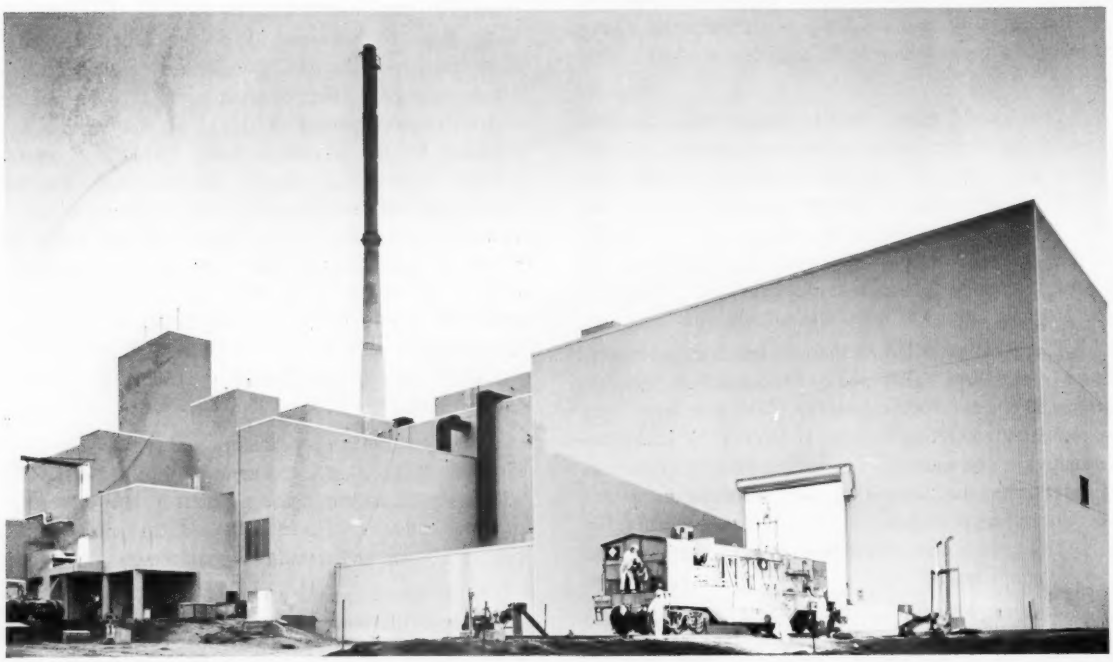

Fig. 2 West Valley plant of Nuclear Fuel Services, Inc.

Plants of the 1970's

Description

With the filing of the Allied PSAR, the shape of the larger facilities that will be constructed in the next generation of plants has become a good deal clearer. In its PSAR, Allied describes a plant that, although it has some specific design differences, is similar in most respects to the process used at West Valley. That Allied should have chosen to go this route is quite significant. Allied has the greatest amount of industrial experience with the handling of fluorine of any of the companies who have so far expressed any interest in reprocessing. They have the experience of building and operating the Metropolis, Ill., plant, which converts U_3O_8 to UF_6. They were originally partners with GE in the development of the mixed aqueous–fluoride volatility process. Yet they have chosen to stay with chop–leach solvent extraction. So far as is known, this is also the route being considered by other entrants in the race to build the next plant. It is the opinion of the authors that at least the next two or three plants of this third generation will be of this type. In fact, it is not at all clear that any competing new technology will ever be able to compete successfully with the solvent extraction plants for the processing of light-water reactor fuel.

The block flow diagram of the Allied plant is shown in Fig. 3 (Ref. 3). Irradiated fuel assemblies will be received in shielded, water-filled shipping casks by truck or rail. Road dirt is removed at an outdoor washdown station. After such decontamination as is necessary, the cask is placed in an unloading pool where the cover is removed underwater, and the fuel elements are removed individually into a multiple-element storage canister that is stored in a fuel-storage pool. Fuel will normally be received after 120 days' cooling at the reactor and will be cooled a minimum of 160 days prior to processing. The empty cask is removed from the water, decontaminated, and replaced on the carrier.

When the fuel elements are ready to be processed, the desired fuel-storage canisters will be moved to an unloading station from which the fuel assemblies will be lifted individually into the mechanical processing area. Allied does not plan to remove end hardware; rather, they propose to chop the entire fuel element. Capability is being provided to handle assemblies up to 20 ft long and 12 by 12 in. in cross section.

The shear will cut the fuel-containing part of the elements into 1- to 3-in. lengths, which will fall by gravity into one of two dissolver barrels through one leg of a two-legged diverter. Each leg of the diverter will contain two seal gates. The seals in the operating legs will be synchronized with the stroke of the shear blade so that one seal will always be closed between the shear and the dissolver to prevent the entry of dissolver off-gases into the shear internals while feeding the dissolver continuously. The rate of feeding the chopped fuel into the dissolver will be determined by the gross rate of the dissolution.

One of two dissolvers will be charged at a time with chopped fuel elements. The dissolver will be filled with nitric acid containing neutron-absorbing poison before charging is started. The dissolver will be cooled and heated with poisoned water circulated in a jacket. The dissolution will be carried out at about 90°C and at a pressure slightly below cell pressure.

The dissolver solution will first pass through a cooler in which some solids are expected to precipitate out. These solids are to be removed by batch centrifugation. The solids retained by the centrifuge will be transferred as a slurry, after rinsing and sampling, to waste-storage tanks. The clarified solution is transferred to an accountability tank, sized to contain a complete dissolver batch including hull and centrifuge rinses, where accountability samples will be taken. Rinsed hulls will be removed from the dissolver by basket for disposal.

Separation and purification of uranium and plutonium will be carried out by conventional Purex-type solvent extraction. In the first contactor the uranium and plutonium will be separated from fission products and from neptunium. (Thus any neptunium recovery practiced in this plant will be done upon the full-activity first-cycle aqueous waste stream.) The extracted uranium and plutonium will then be partitioned from one another. It is of interest to note that Allied proposes to use a centrifugal contactor for the initial extraction step and for the plutonium-partition step. Thereafter pulse columns will be used. Another difference (from U. S. practice at least) is that U^{4+} will be used as the reductant in plutonium partition, rather than ferrous iron.

The uranium product will be further decontaminated in a second uranium solvent extraction cycle and then by a silica-gel treatment. It is noteworthy here that this is one full cycle of solvent extraction cleanup less than that used at West Valley. It is questionable that full decontamination of the uranium product can be achieved with this abbreviated treatment.

The plutonium product will be given two additional solvent extraction cycles followed by concentra-

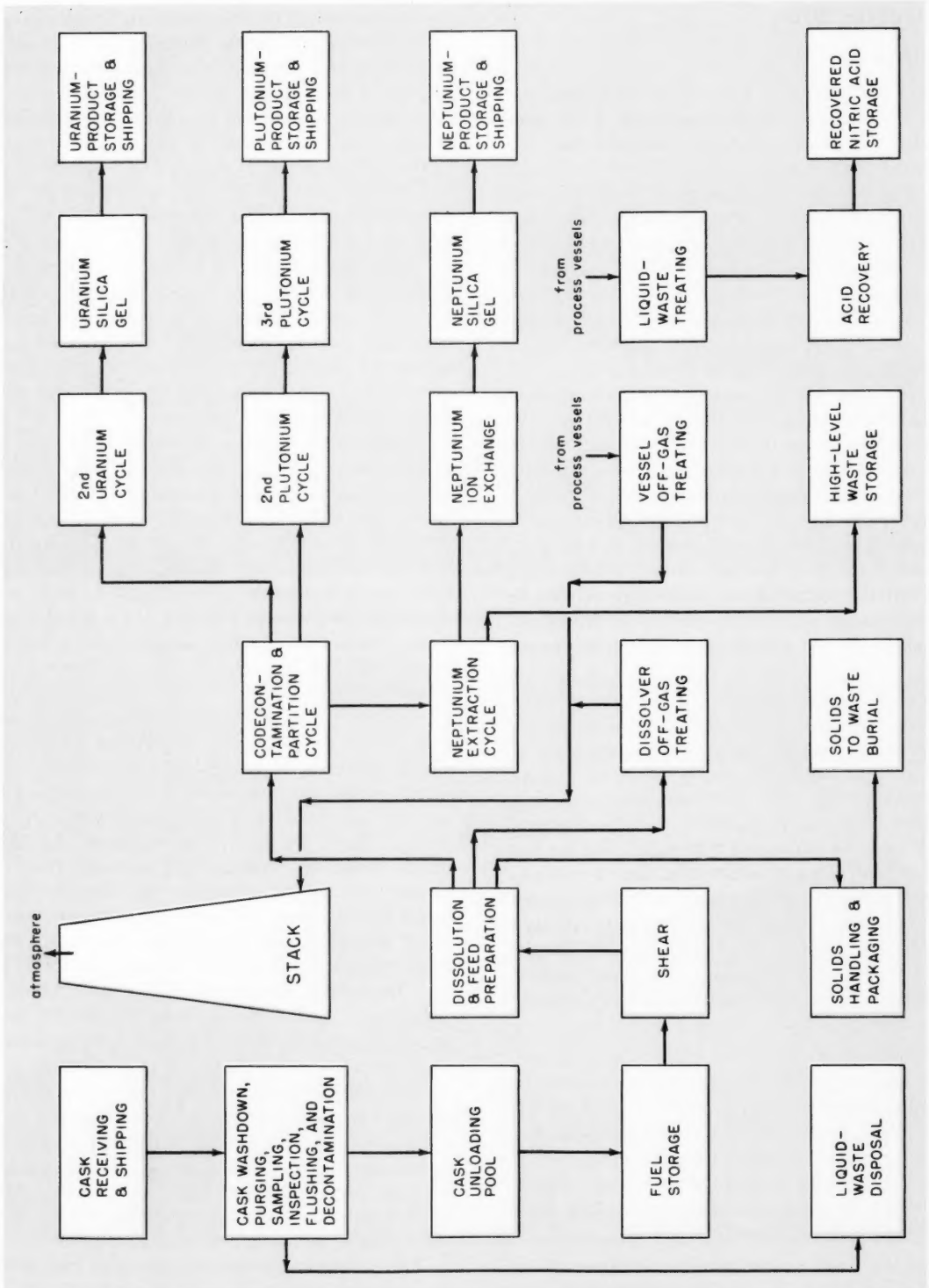

Fig. 3 Simplified flow diagram of Allied Chemical Corp. plant at Barnwell, S. C.

tion. In this instance Allied is replacing the final ion-exchange cycle that has been used in the past with an additional solvent extraction cycle.

Allied treats as confidential its neptunium extraction system from the high-level waste stream. The conventional processes for this step are solvent extraction (as used at Hanford) or a stirred ion-exchange step (the Savannah River approach). The initial extraction is followed by an ion-exchange cleanup step and final purification with silica gel.

Allied also treats its handling of high-level waste as confidential. They do say, however, that the concentrated waste will be centrifuged to remove precipitated solids and that the acid solution will be stored in cooled, stainless-steel storage tanks. The separated solids are treated as intermediate-level wastes. Lower-level wastes are to be concentrated, and the decontaminated overheads are to be vaporized up the stack so that the tritium is discarded to the atmosphere rather than into a watercourse.

Solvent treatment proposed is the conventional condenser, a vapor–liquid phase separator, a mercurous/mercuric nitrate–nitric acid scrubber, an absorption column for oxides of nitrogen, activated-charcoal beds, a second scrubber, a heater, and a pair of high-efficiency filters. The vessel off-gas system will consist of a condenser, a vapor–liquid phase separator, a high-pressure steam heater, two parallel silver nitrate reactors, a cooler, and a pair of high-efficiency filters. The treated effluents from each of these systems, together with the cell ventilation air, will be discharged to the atmosphere through a 100-m stack.

Impact of West Valley on Its Successor Plants

During the past 3 years, the startup problems of the West Valley plant have received a good deal of formal[7] and informal comment in the industry. Fundamentally the problems that West Valley has had fall into the following categories:

1. Discharge of particulate activity.
2. Discharge of low-level liquid wastes into watercourses.
3. Acid recovery.
4. Inadequacy of mechanical aids.
5. Contamination control.

It seems clear that Allied has been influenced in its design by the lessons learned at West Valley.

In the first place the difficulty experienced at West Valley in meeting continuously the very low (perhaps unduly low) standards required for particulate emission strongly suggests the desirability of providing dual (series) filtration of process off-gases with high-efficiency filters.

The matter of discharge of low-level wastes to watercourses would appear to have received a great deal of attention in the Allied design. They are planning to discharge tritium to the atmosphere, so that it will no longer be the controlling isotope in liquid discharge. It would seem that they have added considerably to the amount of low-level waste treatment equipment used at West Valley. These two steps may have been dictated by the fact that the stream into which they must discharge has an average flow only one-third of that of Cattaraugus Creek (the West Valley discharge point), which could hardly accommodate the tritium output of a 5 metric ton/day plant.

The acid-recovery system at West Valley has never worked as well as was expected in design. Thus additional steps may be required, and certainly the equipment should be provided with more shielding than was provided at West Valley. Since Allied has treated this entire subject as proprietary, it is not possible to assess the changes they have made in this regard.

The same thing is true of the mechanical-handling portion of the Allied plant. No details are given. Any new plant would do well to take into consideration the very definite West Valley experience that none of the mechanical-handling aids on the market today are capable of handling the heavy-duty production demands required of them in a plant of this type.

Contamination control is another area that has been troublesome at West Valley. Here it would seem that Allied has profited by West Valley experience and taken steps to provide additional ventilation, control zones, interlocks, and the like.

The authors find it noteworthy that, although Allied has clearly been influenced in its design by the startup problems of West Valley, they, nonetheless, have designed a plant very similar to West Valley.

Size

Determining the size of a highly capital-intensive plant to fit a growing market in a highly competitive field is a difficult task. Such a determination can be made by management from a relatively simple analysis of load projections or from a highly sophisticated analysis of the parameters with computer programs. Oak Ridge National Laboratory (ORNL) has recently done a great deal of work using the latter technique.[8] In either case the answer arrived at is very markedly

influenced by the assumptions made and the ground rules adopted.

One of the most important ingredients for making a decision as to plant size is the projection of load for the plant. There is a surprising amount of disagreement on even this fundamental figure. Table 1 gives the load-projection estimates from three sources, ORNL,[9] AEC Division of Industrial Participation,[10] and NFS.[10] It can be seen that these estimates differ by as much as a factor of 2, particularly in the early years, and they never agree within 30%. These estimates are made up for the early years by combining known reactor projects, the output therefrom, and the date at which said output is likely to become available for processing. Since there is little disagreement about the first two of these factors, it follows that the differences in these load estimates come about due to differences in the estimate of time at which the fuel will become available for processing. In view of the experience to date on project timing, the more pessimistic of the estimates are likely to turn out to be the more nearly correct. It is clear, however, that the growing quantity of fuel to be processed in the middle and late 1970's warrants the construction of larger plants, such as the 1500 metric ton/year size selected by Allied.

Table 1 Estimates of Fuel Availability for Reprocessing

	Metric tons of uranium		
Year	ORNL* estimate	NFS† estimate	AEC† estimate
1973	782	338	350
1974	1,078	843	580
1975	1,351	1,288	870
1976	1,711	1,852	1,100
1977	2,042	2,068	1,600
1978	2,556	2,446	2,100
1979	2,950	3,013	2,500
1980	4,001	3,551	3,000
1981	5,807		
1982	7,365		
1983	9,914		
1984	13,544		
1985	17,697		
1986	20,907		
1987	24,571		
1988	28,623		

*D. E. Ferguson et al., Chemical Technology Division Annual Progress Report for the Period Ending May 31, 1968, USAEC Report ORNL-4272, page 233, Oak Ridge National Laboratory, September 1968.

†E. B. Tremmel, The Nuclear Industry, 1968, presented at Atomic Industrial Forum International Conference, Washington, D. C., November 1968.

Table 2 Estimated Distribution of Available Load

	Metric tons of uranium			
		Assigned to†		
Year	Total available*	NFS	GE	Available for new plants
1973	340	240	100	0
1974	840	300	250	290
1975	1,290	350	250	690
1976	1,850	400	250	1,200
1977	2,070	500	250	1,320
1978	2,450	500	250	1,700
1979	3,000	500	250	2,250
1980	3,550	500	250	2,800
1981	5,800	500	250	5,050
1982	7,350	500	250	6,600
1983	9,900	500	250	9,150
1984	13,500	500	250	12,750
1985	17,700	500	250	16,950
1986	20,900	500	250	20,150
1987	24,500	500	250	23,750
1988	28,500	500	250	27,750

*The NFS estimate for 1973–1980; the ORNL estimate thereafter.

†The authors' assessment of NFS and GE capability.

Table 2 gives an estimate of the fuel available from 1973 through 1988, together with the authors' independent (and perhaps arbitrary) assignment of load to the NFS and GE plants and the residue that would be available to a new plant. This table suggests very strongly that a 1500 metric ton/year plant coming on-line before 1975 is going to have very little load available to it and that it is not likely to be fully loaded before 1976. We shall try to show later the effect of the lack of load in early years on the cost of the service. But strictly from a load standpoint it can be seen that it is hard to justify a startup date for a larger plant until 1975, and 1976 might be better. Allied proposes to complete construction of its plant in late 1972, which would place startup in the latter part of 1973.

It is even more clear that the construction of two 1500 metric ton/year plants as early as 1975 would be ruinous to the economic health of all four of the plants

that would then exist. The personal opinions of the authors coincide with that of the distinguished AEC chairman.[11]

It has been the experience of the authors that boards of directors of U. S. corporations of substance are manned by individuals with business sense and that, furthermore, they are normally somewhat conservative fiscally. If this is true, it should be axiomatic that two 1500 metric ton/year plants will not be built before 1975.

Location

Essentially all of the discussion about the next new plant has centered about one to be built in the southeast portion of the United States. That this is so is no accident. The cost of shipping fuel from a reactor to a reprocessing plant is not insignificant. Therefore the utilities would like to have reprocessing facilities located reasonably proximate to them. The West Valley plant serves one of the load centers—the northeast. There are two other growing centers of load, the midwest and the southeast. Although the GE plant would seem to be smaller than economically desirable, it is, nonetheless, located in the midwest and tends to have an advantage in that area for a few years. The largest available load for a new plant will then be forthcoming largely from the southeast during the next few years; thus it is only logical that all of the contenders have centered their attention in this area. It seems certain that the next plant will be built there.

The location of the next plant to follow is not quite so certain. It will depend, in all probability, upon the relative rates of growth of load in the midwest and the far west. It seems likely that the fourth plant will be constructed in the west, and the fifth, in the midwest. If the third, fourth, and fifth plants each have a capacity of 1500 metric tons/year, the combined capability of all five plants would then be about 5300 metric tons/year, which is sufficient to handle the entire United States load up through about 1981. Thereafter reprocessing plants will have to come on-stream at a fairly rapid rate, but it would be gazing into a clouded crystal ball to try to size or locate those plants at this time.

Radiological Impact of Larger Plants

As the throughput of chemical reprocessing plants grows larger, it follows directly that the potential contamination of the plant environment also increases. Either the environment must be shown able to accept increased releases or the removal factors now experienced in the smaller plants must be increased.

The radionuclides of most importance in the routine atmospheric discharge from reprocessing plants are ^{85}Kr, ^{3}H, ^{131}I, and ^{129}I. The quantities of each of these per metric ton of uranium processed are shown in Table 3. The data presented are those reported by Allied[3] with some ORNL data[12] for comparison. Oak Ridge National Laboratory has concluded that worldwide pollution hazards from release of radionuclides at these concentrations are avoided and that plant personnel are protected by the necessary requirement of ensuring appropriately low exposures of the public near the site boundary.[13]

Table 3 Concentrations of Volatile Fission Products in Spent Reactor Fuel

	Allied*	ORNL†	Authors' assumptions‡
Fuel			
Burnup, Mwd/metric ton	35,000	33,000	35,000
Specific power, Mw/metric ton	40	24.5	35
Decay, days	160	150	150
Concentration, curies/metric ton			
^{85}Kr	8,000§	10,600	11,200
^{3}H	400	680¶	400
^{131}I	1.41	1.95	2.6
^{129}I		0.032	0.03

*Allied Chemical Nuclear Products, Inc., Preliminary Safety-Analysis Report, Docket 50-332, filed with the AEC Division of Materials Licensing, November 1968.

†D. E. Ferguson and R. E. Blanco, General Survey of Reprocessing of Thermal Reactor Fuels, paper presented at American Nuclear Society International Meeting, Washington, D. C., November 10–15, 1968.

‡Used in calculations in this review.

§Value appears to be low.

¶ORNL uses some recent Argonne data on the ^{3}H fission yield from ^{239}Pu, and this results in their higher value (N. D. Dudey, Review of Low-Mass Atom Production in Fast Reactors, USAEC Report ANL-7434, Argonne National Laboratory, April 1968).

The maximum acceptable annual concentrations in air for the four isotopes listed above are shown in column 2 of Table 4. These values are one-third of the limit prescribed in Appendix B, Table II, of 10 CFR

Part 20 as required by paragraph 20, 106(e), of 10 CFR except for ^{131}I. In this case the concentration is reduced by a factor of 700, as a simplified method of accounting for reconcentration in the grass–cow–milk pathway to the thyroids of small children.

Allied predicts a maximum off-site annual relative ground concentration of 5.7×10^{-8} sec/m^3. This value agrees within 10% with the values we have found for similar sites and meteorology, and we believe that it is an appropriate value to use in determining the impact upon the environment of the processing of 1500 metric tons of fuel per year. The maximum average ground concentrations (in the most unfavorable direction from the stack) for these four isotopes are shown in column 4 of Table 4. The percent of the maximum acceptable concentration is also shown in the table. Finally, to emphasize these figures, the annual metric tons of fuel which could be processed while still meeting the maximum acceptable concentration limits are shown. It can be seen that the limiting isotope is ^{131}I, which will require about one-half of the environmental dilution power at 150 days' cooling. The next most restrictive isotope is ^{85}Kr, which requires about 30% of the environmental dilution. The ^{131}I limitation can be brought below that of the ^{85}Kr by allowing about 1 week's additional cooling.

If it is assumed that prudent plant-operating management will dictate that the actual discharges from a plant be kept at some reasonable percentage of the maximum acceptable concentration, in order to assure that they stay within that maximum, then a 1500 metric ton/year plant is approaching the largest-sized plant that can be built in many locations without adding facilities for controlling the release of ^{85}Kr in some way. Essentially the same conclusion can be drawn concerning ^{131}I. These calculations have assumed a 99% removal of iodine. This represents about the best that can be expected on a yearly average using present technology. If larger plants are going to be built, it would seem likely that either the cooling time will have to be increased to allow for additional decay of the ^{131}I or the plants will have to be built essentially completely contained, as in the case of the Experimental Breeder Reactor II (EBR-II) Fuel Cycle Facility.

For these larger plants the Allied proposal to discharge the tritium into the atmosphere, rather than into a watercourse, is highly desirable and in most cases may well be required. If the tritium were to be discharged to a watercourse, the required dilution would amount to an average flow of 700 cfs for 1500 metric tons/year. This would use up completely the dilution power of the stream; therefore nothing would be left for the other isotopes. Thus a usable site in which tritium were to be discharged to a stream would require a river with no less than 1000-cfs average flow. If the tritium is sent to the atmosphere, the other nongaseous isotopes can be removed to the degree desired or required, and plant siting need not be limited by water availability.

Another aspect of these larger plants which, when combined with the high burnup projected, presents a problem is the handling of the high-level waste stream. In a very real sense, this becomes strictly a problem of handling under all conditions the heat produced by the radioactive decay. If the wastes are stored in acid solution in cooled stainless-steel tanks (as suggested by Allied) and if the tanks are sized to hold about 1 year's output of waste, the heat load at the conclusion of the filling period will be about 60 million Btu/hr. This is a considerably larger heat load for a tank than has been experienced to date. It is clear that continuous cooling must be guaranteed because the tanks would reach boiling in about 1 hr after loss of cooling. Thereafter steam would be produced at a rate of about 60,000 lb/hr.

If the 1500 metric ton/year plant size were doubled and tanks were still sized to handle the output of waste from 1 year's operation, the heat load per tank would simply double to 120 million Btu/hr. If the size of tank were kept constant (filled in 6 months), the heat load at the point of filling would then be about 80 million Btu/hr. In other words the heat problem becomes increasingly more difficult as the size of the plant increases.

On both counts, the effect of these plants on their immediate environment and the problem of handling the waste heat, it would seem prudent to obtain some operating experience with 5 metric ton/day plants before considering anything larger.

Effect of Plant Scale on Costs

The most sensitive area of confidential information about these plants is that of costs. Allied has not made public any of their capital- or operating-cost estimates in the filing of their PSAR; nor should they be expected to do so.

It is of interest, however, to speculate on the effect of this increase in plant size on the cost of reprocessing. Oak Ridge National Laboratory has done some speculation[14] of this type, and they have suggested that rather significant cost reductions from present levels can be achieved by permitting reprocessing plants

Table 4 Limiting Values for Discharge of Gaseous Radioisotopes

Isotope	Max. acceptable concentration,* $\mu c/cm^3$	Release rate,† curies/sec	Highest environmental concentration,‡ $\mu c/cm^3$	Percent of max. acceptable concentration	Quantity of fuel to reach max. acceptable, metric tons/year
^{85}Kr	1×10^{-7}	0.53	3.0×10^{-8}	30	5,000
^{3}H	0.7×10^{-7}	0.019	1.1×10^{-9}	1.5	97,000
^{131}I	1.4×10^{-13}	1.23×10^{-6} §	7.10^{-14}	50	3,000
^{129}I	6.7×10^{-12}	1.42×10^{-8} §	8.1×10^{-16}	0.012¶	¶

*One-third of the 10 CFR Part 20 limits for the isotope in air in unrestricted areas except for ^{131}I, in which case the limit is reduced by a factor of 700.

†The quantities in the last column of Table 3 for 1500 metric tons released over 1 year, 3.16×10^7 sec, annual average.

‡At a value of X/Q of 5.7×10^{-8} sec/m^3.

§At 99% removal.

¶Reconcentration was ignored.

to increase in size several times that suggested by Allied. We propose to apply the ORNL cost-estimation method to the proposed Allied plant in order to arrive at both capital and operating costs. In doing so, however, we will apply a few modifications that we believe are required by commercial practice and present conditions.

The cost-estimation method used at ORNL involves the following three equations:

$$CI = A(S)^{0.35} \tag{1}$$

$$AOC = 0.084(CI) + (0.13 \times 10^6)(S^*) \tag{2}$$

$$WC = 1.46 \times 10^6 (T \times B \times 10^{-7})^{0.844} \tag{3}$$

where CI = total capital investment, \$
AOC = annual operating cost, \$/year
WC = waste cost, \$/year
S = nominal plant capacity, metric tons/day
S^* = actual average production rate, metric tons/day
$= \frac{\text{actual metric tons/year}}{260}$
A = capital-cost estimate for a 1 metric ton/day plant
T = actual throughput, metric tons/year
B = average burnup, Mwd/metric ton

Thus all the ORNL estimates relate back to the capital cost of a 1 ton/day plant. This basic capital cost is shown in Table 5, together with the cost for a 5 ton/day plant computed by direct application of Eq. 1. The capital cost shown in Table 5 for a 1 ton/day plant of \$29 million is the entire project cost without the waste-disposal facilities (which are handled separately by Eq. 3). This value is in 1966 dollars and can be compared with the reported project cost of the West Valley plant[15] of \$32 million, which is in 1964 dollars. About \$2 million may be subtracted from the West Valley cost for the waste facilities. Thus the ORNL base line of \$29 million in 1966 dollars compares to a West Valley cost of \$30 million in 1964 dollars, a fairly reasonable agreement. The 0.35-power scaling factor used in Eq. 1 reasonably represents the increase in cost due to increase in size; however, it does

Table 5 ORNL Capital-Cost Estimates for 1 and 5 Metric Ton/Day Plants*

	1 metric ton/day plant, $10^6†	5 metric ton/day plant, $10^6†
Construction of facilities, including field engineering and construction interest but *not* including waste-storage facilities	23.0	40.4
Plant site, working capital, and pre-operational testing	3.0	5.3
Contingency	3.0	5.3
Total	29.0	51.0

*D. E. Ferguson et al., Chemical Technology Division Annual Progress Report for the Period Ending May 31, 1968, USAEC Report ORNL-4272, page 230, Oak Ridge National Laboratory, September 1968.

†1966 dollars.

not take into account the escalation in construction costs which has already taken place, let alone that which may be expected to occur between now and when the larger plant will actually be built. The difference is far from negligible.

Figure 4 shows the change in the *Engineering News Record (ENR)* Building Cost Index (based on skilled labor) which has taken place from 1964 to date, the estimated increase for 1969, and a spread of increases for 1970 through 1972 based on varying assumptions. If we use the intermediate of these and assume that the median year for project expenditures for the larger plant is 1972, the *ENR* ratio is 935/610 = 1.53. Thus, although Eq. 1 gives a value of $51 million in constant dollars for the capital investment (*CI*), we estimate that the total project cost in 1972 dollars will be about $78 million.

Next, ORNL calculates a fixed charge rate (*FCR*) to be taken against the total capital employed (*CI*); this amounts to 24%. The derivation of this value is given in Table 6. Equation 3 is used to calculate waste costs assuming the burnup to be 35,000 Mwd/metric ton.

Table 7 shows the calculation of the price per metric ton for reprocessing which would be predicted by the use of the unmodified ORNL equations. The resulting average, $16.85/kg, is in constant 1966 dollars. It should be noted that the required selling price in the first year of $61.25/kg is unrealistically high and could not be obtained in practice.

We believe that a number of modifications to the ORNL calculation are required to bring the results into line with commercial practice. In the first place, a 5% charge against debt capital is not realistic in today's market. We propose to use instead 7%. More important is the fact that any commercial organization will take cognizance of the fact that this project requires the expenditure of large amounts of equity capital several years before any return is realized. They will expect then to make a sufficiently larger amount on the equity capital during the profitable years to provide the normal rate of return on their money during the entire period for which it is employed. Furthermore, they will expect to compound these amounts; that is, they will year-by-year add the unrealized return to the equity debt and the following year will require the normal return on the total.

There are a number of ways used by industry to account for the timing involved in the expenditure of capital. One, which is useful not only in illustrating the effect of early capital expenditures but which also handles the problem of losses or reduced return during early years of operation, is a method called "interest

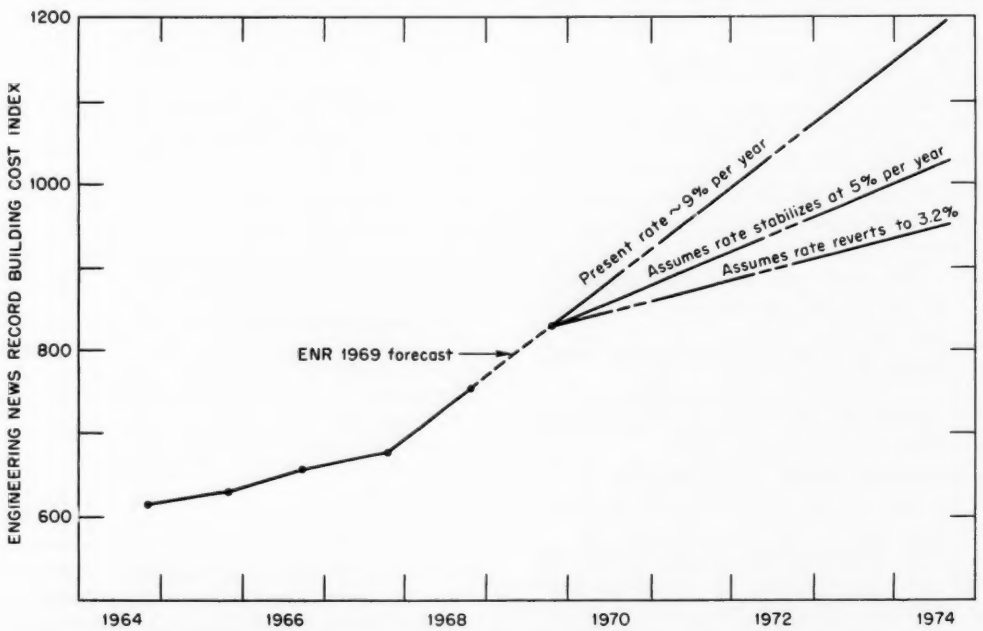

Fig. 4 Projections of *ENR* Building Cost Index.

Table 6 Derivation of Fixed Charge Rate*

	Percent
Cost of money	
70% equity at 16%/year	11.2
30% debt at 5%/year	1.5
Subtotal	12.7
Other charges	
Depreciation	2.54
Federal income tax	5.69
State and local taxes	2.51
Interim replacement	0.35
Property insurance	0.25
Total	24.04

*D. E. Ferguson et al., Chemical Technology Division Annual Progress Report for the Period Ending May 31, 1968, USAEC Report ORNL-4272, page 229, Oak Ridge National Laboratory, September 1968.

rate of return." This method is described in some detail by Weaver and Reilly.[16]

We have applied this method to the Oak Ridge case with the same modifications:

Equity	70% at 16% after tax return
Debt	30% at 7%
Operating cost	Equation 2
Waste cost	Equation 3 at 35,000 Mwd/metric ton
Total capital	Equation 1 multiplied by construction-cost index ratio of 1.53
Plant on stream	1974
Plant load	As in Table 2

The resulting calculation is detailed in Table 8. It can be seen that the resulting levelized price for reprocessing is $27.50/kg, compared to the unmodified ORNL estimate (in constant dollars) of $16.85. We believe that the $27.50/kg value is far more representative of a real commercial price.

In a business as highly capital intensive as fuel reprocessing, the cost of the service is very much dependent upon the debt/equity ratio. To illustrate this, we have repeated the calculation with the same conditions as those shown above except that 100% equity capital is used. This calculation, shown in Table 9, results in a levelized price of just over $37.00/kg.

As pointed out earlier, the load projections do not justify a plant coming on-line as early as 1974. It is quite possible that competitive pressures, or the pressures of utility customers who want adequate capacity available to them just as soon as it is needed, will force the commissioning of a new plant as early as 1974. It should be recognized, however, that there is a significant penalty that will be paid for starting a plant too early. This penalty will be paid in the form of either higher prices for the service or lower return on investment to the processor. A third calculation is detailed in Table 10 to illustrate the order of magnitude of the penalty. In this case we have used the same assumptions employed in the calculation of Table 8, except that the plant is assumed to come on-stream in 1976 and to be fully loaded from the start. In this case we have extrapolated the construction-cost index two more years to give a ratio of 1.67 and a total capital cost of $85 million for the plant. The resulting levelized cost for processing is then $22.80/kg.

It is to be noted that the reprocessing charges presented do not reflect escalation in the cost of operating labor and materials which will most certainly take place. It is assumed that the reprocessing contracts will include suitable escalation clauses such that the return on investment will remain constant. The net result is that the relation between charges under various conditions remains valid, but the actual charges in the mid-1970's will be higher than shown.

In their cost studies, ORNL have suggested that extremely large plants be built in the future and have predicted very low reprocessing costs for them. We have not attempted to compare costs for plants larger than this 5 metric ton/day size for the following reasons:

1. In view of the load-sensitive nature of reprocessing plants, it would be difficult to justify a plant significantly larger than 1500 metric tons/year until into the 1980's.

2. At that distance in time, the effect of escalation in building costs, if present trends continue, will so overshadow any other cost element that meaningful extrapolations are almost impossible.

3. We do not believe that the 0.35 scaling factor should be used over a much larger range than the factor of 5 used here. Our reasoning is that, as the size increases, duplicate facilities may have to be built for criticality reasons or simply for logistic reasons (as, for instance, with multiple cask unloading facilities and duplicate mechanical head ends). Further, in the larger plants some additional facilities will be required to handle radioactivity releases, which at the 5 metric

Table 7 Estimates of Reprocessing Price in 5 Metric Ton/Day Plant

(Unmodified ORNL Equations—Results Are in Millions of Constant 1966 Dollars)

Year	1	2	3	4	5	6	7	8	9	10	11	12	13	14	15	Total	Average
Load availabie, metric tons/year	290	690	1,200	1,320	1,500	1,500	1,500	1,500	1,500	1,500	1,500	1,500	1,500	1,500	1,500	20,000	1,333
Estimate with Unmodified ORNL equations																	
Annual operating charge, *AOC*	4,425	4,625	4,880	4,940	5,034	5,034	5,034	5,034	5,034	5,034	5,034	5,034	5,034	5,034	5,034	74,244	4,950
Waste charge, *WC*	1,013	3,080	4,920	5,310	5,913	5,913	5,913	5,913	5,913	5,913	5,913	5,913	5,913	5,913	5,913	79,366	5,290
Capital charge	12,240	12,240	12,240	12,240	12,240	12,240	12,240	12,240	12,240	12,240	12,240	12,240	12,240	12,240	12,240	183,600	12,240
Total	17,678	19,945	22,040	22,490	23,187	23,187	23,187	23,187	23,187	23,187	23,187	23,187	23,187	23,187	23,187	337,210	22,480
Required selling price, $/kg	61.25	28.90	18.40	17.05	15.45	15.45	15.45	15.45	15.45	15.45	15.45	15.45	15.45	15.45	15.45	16.85	16.85

Table 8 Calculation of Levelized Selling Price—Basic Conditions*

(Note That "000" Is Omitted from All Money Values)

Year		Fuel processed, metric tons/year	Operating costs†	Debt service	Depreciation	Other fixed costs§	Total costs	Gross receipts at $27.50/kg	Before-tax income	Federal tax¶	Cash flow	Obligation
1971	−2										(18,200)	−19,660
1972	−1										(18,200)	−42,470
1973	0										(18,200)	−68,870
1974	1	290	7,708	2,567	9,750	2,430	22,455	7,975	(14,480)		(4,730)	−85,370
1975	2	690	9,975	2,567	9,130	2,430	24,102	19,000	(5,120)		4,028	−94,342
1976	3	1,200	12,070	2,567	8,420	2,430	25,487	33,000	7,513		15,933	−90,939
1977	4	1,320	12,520	2,567	7,800	2,430	25,317	36,300	10,983		18,783	−83,686
1978	5	1,500	13,215	2,567	7,170	2,430	25,382	41,250	15,868	7,090	15,948	−78,568
1979	6	1,500	13,215	2,567	6,500	2,430	24,712	41,250	16,538	7,940	15,098	−73,590
1980	7	1,500	13,215	2,567	5,840	2,430	24,052	41,250	17,198	8,250	14,788	−68,202
1981	8	1,500	13,215	2,567	5,220	2,430	23,432	41,250	17,818	8,560	14,478	−62,324
1982	9	1,500	13,215	2,567	4,550	2,430	22,762	41,250	18,468	8,860	14,158	−55,856
1983	10	1,500	13,215	2,567	3,500	2,430	22,112	41,250	19,138	9,200	13,838	−48,748
1984	11	1,500	13,215	2,567	3,270	2,430	21,482	41,250	19,768	9,480	13,558	−40,820
1985	12	1,500	13,215	2,567	2,570	2,430	20,782	41,250	20,468	9,820	13,218	−32,022
1986	13	1,500	13,215	2,567	1,950	2,430	20,162	41,250	21,088	10,100	12,938	−22,134
1987	14	1,500	13,215	2,567	1,330	2,430	19,542	41,250	21,708	10,400	12,638	−11,016
1988	15	1,500	13,215	2,567	620	2,430	18,832	41,250	22,418	10,780	12,258	+1,242

*70% equity at 16%; 30% debt at 7%.
†*AOC* from Eq. 2 plus *WC* from Eq. 3.
‡Sum-of-year digits.
§State and local taxes, insurance, and interim replacement from Table 6.
¶At 48%.

Table 9 Calculation of Levelized Selling Price—100% Equity

(Note That "000" Is Omitted from All Money Values)

Year		Fuel processed, metric tons/year	Operating costs*	Depreciation†	Other fixed costs‡	Total costs	Gross receipts at $37.00/kg	Before-tax income	Federal tax§	Cash flow	Obligation
1971	−2									(26,000)	−28,800
1972	−1									(26,000)	−62,210
1973	0									(26,000)	−100,960
1974	1	290	7,708	9,750	2,430	19,888	10,720	(9,168)		582	−116,378
1975	2	690	9,975	9,130	2,430	21,535	25,500	3,965		13,095	−121,883
1976	3	1,200	12,070	8,420	2,430	22,920	44,400	21,480	7,680	22,220	−119,163
1977	4	1,320	12,520	7,800	2,430	22,570	48,800	26,230	12,600	21,430	−116,833
1978	5	1,500	13,215	7,170	2,430	22,815	55,500	32,685	15,700	24,155	−111,328
1979	6	1,500	13,215	6,500	2,430	22,145	55,500	33,355	16,100	23,755	−105,373
1980	7	1,500	13,215	5,840	2,430	21,485	55,500	34,015	16,300	23,555	−98,688
1981	8	1,500	13,215	5,220	2,430	20,865	55,500	34,635	16,600	23,255	−91,193
1982	9	1,500	13,215	4,550	2,430	20,195	55,500	35,305	16,950	22,905	−82,888
1983	10	1,500	13,215	3,500	2,430	19,545	55,500	35,955	17,200	22,255	−73,883
1984	11	1,500	13,215	3,270	2,430	18,915	55,500	36,585	17,550	22,305	−63,378
1985	12	1,500	13,215	2,570	2,430	18,215	55,500	37,285	17,900	21,955	−51,553
1986	13	1,500	13,215	1,950	2,430	17,595	55,500	37,905	18,200	21,655	−38,148
1987	14	1,500	13,215	1,330	2,430	16,975	55,500	38,525	18,500	21,355	−22,893
1988	15	1,500	13,215	620	2,430	16,265	55,500	39,235	18,800	21,055	−5,508

*AOC from Eq. 2 plus WC from Eq. 3.
†Sum-of-year digits.
‡State and local taxes, insurance, and interim replacement from Table 6.
§At 48%.

Table 10 Calculation of Levelized Selling Price—Fully Loaded Plant*

(Note That "000" Is Omitted from All Money Values)

Year		Fuel processed, metric tons/year	Operating costs†	Debt service	Depreciation‡	Other fixed costs§	Total costs	Gross receipts at $22.80/kg	Before-tax income	Federal tax	Cash flow	Obligation
1973	−2										(20,000)	−21,600
1974	−1										(20,000)	−46,665
1975	0										(20,000)	−75,725
1976	1	1,500	13,215	2,745	10,620	2,643	29,223	34,200	4,977	2,485	13,112	−72,613
1977	2	1,500	13,215	2,745	9,940	2,643	28,543	34,200	5,657	2,715	12,882	−69,291
1978	3	1,500	13,215	2,745	9,180	2,643	27,783	34,200	6,417	3,080	12,517	−65,854
1979	4	1,500	13,215	2,745	8,500	2,643	27,103	34,200	7,097	3,400	12,197	−62,247
1980	5	1,500	13,215	2,745	7,820	2,643	26,423	34,200	7,777	3,730	11,867	−58,430
1981	6	1,500	13,215	2,745	7,080	2,643	25,683	34,200	8,517	4,080	11,517	−54,423
1982	7	1,500	13,215	2,745	6,370	2,643	24,973	34,200	9,227	4,330	11,267	−50,056
1983	8	1,500	13,215	2,745	5,690	2,643	24,293	34,200	9,907	4,760	10,837	−45,499
1984	9	1,500	13,215	2,745	4,950	2,643	23,553	34,200	10,647	5,110	10,487	−40,612
1985	10	1,500	13,215	2,745	4,250	2,643	22,853	34,200	11,347	5,440	10,157	−35,325
1986	11	1,500	13,215	2.745	3,570	2,643	22,173	34,200	12,027	5,780	9,817	−29,588
1987	12	1,500	13,215	2.745	2,810	2,643	21,413	34,200	12,787	6,130	9,467	−23,341
1988	13	1,500	13,215	2,745	2,120	2,643	20,723	34,200	13,477	6,470	9,127	−16,489
1989	14	1,500	13,215	2,745	1,440	2,643	20,043	34,200	14,157	6,790	8,807	−8,912
1990	15	1,500	13,215	2,745	670	2,643	19,273	34,200	14,927	7,170	8,427	−563

*70% equity at 16%; 30% debt at 7% interest.
†AOC from Eq. 2 plus WC from Eq. 3.
‡Sum-of-years digits on $85 million.
§State and local taxes, insurance, and interim replacement from Table 6.
¶At 48%.

ton/day level are already reaching toward acceptable limits with no treatment. The 0.35 factor does not allow for these additional facilities.

Summary and Conclusions

1. A new phase of chemical reprocessing of spent nuclear fuel will begin sometime in the mid-1970's with the introduction of the 5 metric ton/day plant.

2. This larger plant will in most respects be similar to the West Valley plant.

3. None of the competing technologies is likely to dislodge the chop–leach, solvent extraction technology in the 1970's. It is not clear that they ever will.

4. Although two companies definitely state that they will build a 5 metric ton/day plant before 1975, any rational review of the available load picture suggests clearly that there is sufficient load for only one before the very late 1970's. Because of this, it is highly unlikely that two plants will be built before then.

5. The next plant will be built in the southeast, probably in South Carolina.

6. A 1500 metric ton/year plant can be built with the technology available today and still stay within the presently established standards for the discharge of radioactivity into the atmosphere. However, these discharges are beginning to approach prudent operating limits. If plants are to get much larger, additional facilities will have to be provided to handle ^{85}Kr and ^{131}I. The latter problem can be handled, if desired, by cooling longer than 150 days.

7. There are no engineering scale-up problems that should make it impossible to go to a 1500 metric ton/year size. One of the most difficult problems which will have to be handled in this scale-up is the increased amount of heat that will emanate from the high-level waste.

8. We estimate the capital cost (total project) for a 1500 metric ton plant built to the Allied schedule to be $78 million.

9. Increasing the size of a reprocessing plant without question decreases the unit cost of reprocessing service. Working against any reduction of today's costs, however, is the steadily escalating cost of construction. A second factor that will reduce cost savings realized from scale-up is the fact that, to load a larger plant, fuel must be drawn from a larger area. Therefore the average shipping cost must be lightened. Still a third factor that will cut very heavily into cost savings is the penalty paid by the plant if it comes on-line much before it can be fully loaded. We estimate that, if the Allied plant is constructed and put on-stream when they say, in 1973, they will be hard pressed to realize a reasonable return on invested capital at a selling price of much less than $27.50/kg. The magnitude of the penalty for haste is indicated by our estimate that, if the plant were to come on-stream at the beginning of 1976, the selling price could drop to about $23/kg.

References

1. AEC Press Release, Statement of W. K. Davis at Second Power Reactor Fuel Reprocessing Symposium, Idaho Falls, Idaho, Jan. 18, 1956.
2. General Electric Company, Preliminary Safety-Analysis Report, Midwest Fuel Reprocessing Plant, Docket 50-268, filed Nov. 22, 1966.
3. Allied Chemical Nuclear Products, Inc., Preliminary Safety-Analysis Report, Barnwell Nuclear Fuel Plant, Docket 50-332, filed Nov. 6, 1968.
4. *Nucl. Industry*, **15**(10): 23-24 (October 1968).
5. *Nucleonics Week*, **9**(33): 1 (Aug. 15, 1968).
6. *Nucleonics Week*, **9**(46): 3 (Nov. 15, 1968).
7. Letter, Harold Price to T. C. Runion, Docket 50-201.
8. O. L. Culberson and J. T. Roberts, Oak Ridge National Laboratory, in preparation.
9. D. E. Ferguson et al., Chemical Technology Division Annual Report for the Period Ending May 31, 1968, USAEC Report ORNL-4272, page 233, Oak Ridge National Laboratory, September 1968.
10. E. B. Tremmel, The Nuclear Industry, 1968, presented at Atomic Industrial Forum International Conference, Washington, D. C., November 1968.
11. *Nucl. News*, **12**(1): 28 (January 1969).
12. D. E. Ferguson and R. E. Blanco, General Survey of Reprocessing of Thermal Reactor Fuels, page 30, paper presented at American Nuclear Society International Meeting, Washington, D. C., November 10–15, 1968.
13. *Ibid*, page 27.
14. D. E. Ferguson et al., Chemical Technology Division Annual Report for the Period Ending May 31, 1968, USAEC Report ORNL-4272, page 230, Oak Ridge National Laboratory, September 1968.
15. T. C. Runion and W. H. Lewis, Construction and Operation of the West Valley Reprocessing Plant, paper presented at meeting of American Institute of Chemical Engineers, New York City, November 1967.
16. J. B. Weaver and R. J. Reilly, Interest Rate of Return for Capital Expenditure Evaluation, *Chem. Eng. Progr.*, **52**(10): 405-412 (October 1956).

Engineering for Nuclear Fuel Reprocessing

By Justin T. Long. Prepared under the auspices of Division of Technical Information, United States Atomic Energy Commission. Gordon and Breach Science Publishers, Inc., New York, London, and Paris (1967). 1023 pp. $51.50 Library/Reference edition; $25.75 Student/Professional edition. (Reviewed here by Albert A. Kishbaugh.)

Justin Long has been responsibly involved in supervising research and development in chemical reprocessing of nuclear fuels at the Oak Ridge National Laboratory since 1953. He is, therefore, well qualified to write an authoritative book summarizing the processing of spent nuclear reactor fuel elements to recover the still valuable unburned fuel safely and economically. The field is covered in great detail, and to achieve this the author has obtained and evaluated technology from engineers throughout the United States. As a result the authoritative references in the book are numerous, up to date, and invaluable to anyone associated with the processing of nuclear fuels.

The first two chapters are mainly devoted to a discussion on the history and importance of nuclear fuel processing and on the problems associated with this industry. The concepts of shielding, criticality, buildup and decay of radioactive nuclides, maintenance in a remotely operated plant, and management of radioactive waste are carefully reviewed.

Chapter 3 describes the various separation processes previously and currently used to separate and recover fissionable material from spent reactor fuel with emphasis placed on the important solvent extraction processes. Head-end and tail-end chemical treatments used to complement solvent extraction are also presented in detail.

Chapter 4 presents a very good, detailed discussion of the many dissolving schemes required to process the variety of materials used in reactor fuels. The very latest electrolytic dissolution technique is included, which illustrates the completeness and currentness of the text.

Chapters 5 to 9 describe in detail mechanical operations, fluid flow, heat-transfer operations, solvent extraction, and other mass-transfer operations. Emphasis is placed on special problems brought about by radioactivity. Agitation, centrifugation, filtration of liquids, filtration of gaseous streams, gas–solids fluidization, and mechanical separations are included under mechanical operations. The section on fluid flow concentrates on piping, pumps, and valves with respect to the necessity for shielding, remote operation, and remote maintenance and replacement. Since normal heat-transfer operations are complicated by the necessity of avoiding contamination and radioactivity, Chap. 7 describes in detail unconventional heat-transfer equipment items and their design bases. Solvent extraction equipment pertaining to radiochemical processing is described at length in Chap. 8 with emphasis on packed columns, pulse columns, mixer–settlers, and centrifugal contactors. Other mass-transfer operations described in detail include distillation and rectification, absorption, ion exchange, and foam separation.

The instrumentation required for a nuclear fuel-reprocessing plant is discussed in Chap. 10 and includes radiochemical instrumentation design considerations, instrumentation for process information, continuous analytical instruments, and instrumentation for radiation protection. Chapter 11 describes various viewing devices, manipulators, casks, and samplers required for carrying out essential auxiliary operations. The last three chapters deal with the problems of radiochemical plant design, plant management and operation, and radiochemical processing costs.

For those working in the field of nuclear fuel reprocessing, it is inevitable that this large book will be a valuable and authoritative source of technology and data. The many tables, charts, and photographs are presented in excellent, useful fashion. The appendixes consist of "Properties of Nuclides in Fission-Product Mixtures," "Properties of Some Heavy Nuclides," "Data for Shielding Calculations," "Typical Procedure for Changing Oxygen Filters," "Compositions of Some Alloys of Importance in Fuel Reprocessing," "Solvent-Extraction-Column Startup and Operation Run Sheet," and "Availability of Engineering Design Information."

All topics covered in the book are treated expertly and are well written. The book contains important and pertinent information in the literature up to about 1965 and can be regarded as up to date. The author achieved his goal of writing *Engineering for Nuclear*

Fuel Reprocessing for a wide audience: an excellent source for the specialist in the field, provides the nonspecialist in conventional engineering with an overall perspective of the field along with an orientation in various scientific and engineering disciplines on radiochemical processing, and will give insight into plant design, costs, and operating complexity to any member of a company planning on getting into the nuclear fuel-processing business. Perhaps another group to whom this book should appeal is that comprised of bright, curious students, from high-school seniors on up.

About the Reviewer: Albert A. Kishbaugh is a senior research supervisor for E. I. du Pont de Nemours & Company in the Separations Engineering group of the Savannah River Laboratory. Since receiving his B.S. degree in Chemical Engineering from Pennsylvania State University in 1952, he has been active in the field of nuclear fuel reprocessing.

New-Form Technical Specifications as Applied to First-Generation Nuclear Power Plants

By P. Tuite, F. Lobbin, and C. Anderson*

(Editor's Note: The following article represents only the authors' opinions and views of the new Technical Specifications system. It has not had the review or concurrence of the AEC Regulatory Staff.)

In 1962 the Atomic Energy Commission first provided licensees with specific guidelines with respect to the content of Technical Specifications.[1] Recently, those provisions in 10CFR50 which relate to the content of Technical Specifications were revised.[2]

These revisions were first published for comment in August 1966, and since that time both industry and the Commission have worked together to ensure that the requirements which became effective in January 1969 were consistent with public safety. In general, the latest revisions represent a considerable improvement over those in effect since 1962. They define the underlying philosophy to be used with regard to safety as well as the approach to be used by the licensee in applying this philosophy to preparation of the specifications. As with all such regulations, problems will arise with regard to interpretation of various provisions. However, since the philosophy that underlies the content of the new-form Technical Specifications is consistent with second- and third-generation plant technology and design criteria, these problems of interpretation should be readily resolved. Two second-generation central-station plants, San Onofre and Connecticut Yankee, are presently operating with these new-form specifications, and several more plants are presently awaiting operating authorizations which will include these new-form specifications. Thus, by the time the large number of central-station plants, scheduled for early 1970 operation, apply for operating authorizations, the content of Technical Specifications should be well defined.

What about first-generation plants—designed in accordance with the criteria and technology that existed in the late 1950's? How do these new regulations and guidelines compare to those used to prepare these first-generation plant Technical Specifications? What are the major problems confronting a first-generation plant licensee who undertakes a Technical Specifications revision, and how might some of these problems be resolved?

This article addresses itself to these questions and attempts to answer them based on the conduct of one such first-generation plant Technical Specifications revision effort.

Regulations Governing Technical Specifications

Historically, the federal regulations governing the construction and operation of nuclear power plants have required that the licensee submit two major documents to the Commission for approval. The first document, submitted prior to construction and amended throughout plant construction, essentially describes the facility and analyzes the plant's response to abnormal and accident situations. This document forms the basis for issuance of a construction permit and was originally known as a Hazards Summary

*Hittman Associates, Inc., Columbia, Md.

Report (HSR). Today it is called a Safety Analysis Report (SAR). The other document that forms the basis for issuance of an operating authorization is submitted prior to plant operation. It essentially describes the conditions under which the plant will be operated by the licensee and is called Technical Specifications. These documents represent the basis for continuing dialogue between the Commission and the plant operator and form the foundation for ensuring that nuclear power plants are designed, constructed, and operated in a manner consistent with public safety.

As the complexion of the nuclear power industry has changed, the regulations set forth in 10CFR50 have been changed to be consistent with the state of the industry. In the late 1950's the regulations governing the design, construction, and operation of nuclear power plants were quite straightforward.[3] The licensee was required to prepare and submit a Hazards Summary Report for approval prior to construction, and, prior to plant operation, the Commission would designate to the applicant those portions of the Hazards Summary Report it considered to be Technical Specifications. Alternatively, the applicant could propose what portions he thought should be Technical Specifications. Regardless of who did the designating, the philosophy was the same, i.e., Technical Specifications were looked upon as condensed versions of the Hazards Summary Report. This system, which did not provide the applicant with specific guidelines, was successful while the only plants under consideration for receipt of operating authorizations were research and test reactors.

Sometime in 1960 the Vallecitos Boiling Water Reactor came under consideration for an operating authorization. Here was a plant considerably different from its predecessors, and the old system of Technical Specifications was put to a test. Apparently the system yielded, and in 1962 the regulations governing the content of Technical Specifications were revised by the Commission. A change in philosophy concerning the role of Technical Specifications is evident from the following excerpt from the Statements of Consideration:[4]

> Certain significant design and operating limitations and procedures will be designated as technical specifications which must be adhered to in the absence of specific authorization from the Commission. The technical specifications will reflect in such form limits in design and procedures approved by the Commission. They will represent in essence those parameters which define the boundaries of licensed activity which the Commission has evaluated and approved from a safety standpoint.

The 1962 regulations provide that the applicant for an operating authorization must designate portions of the Hazards Summary Report for incorporation in the license as Technical Specifications. They also provide some guidance to the applicant in terms of content: "Technical Specifications . . . will be designed to include those significant design features, operating procedures, and operating limitations which are considered important in providing reasonable assurance that the facility will be constructed and operated without undue hazard to public health and safety. . . ."[5] The Commission also provided the applicant with a rather detailed guide to the contents of Technical Specifications included in 10CFR50 as Appendix A.

Appendix A lists the subject matter to be included in Technical Specifications and bears a close resemblance to the Commission's guide[6] to the contents of Hazards Summary Reports published in draft form about the same time.

The 1962 regulations adhered to the original philosophy that some relation should exist between the content of Hazards Summary Reports and Technical Specifications and described the contents of both these documents in detail in Appendix A and the draft guide. These regulations also gave the licensee some flexibility in that changes could be made in design features and/or procedures described in the Hazards Summary Report, provided these changes did not involve an "unreviewed safety question" or a change in Technical Specifications. The above changes were primarily directed toward providing the licensee with guidelines, but, more significantly, these revisions recognized that Technical Specifications requirements should be couched in terms of operating limitations as well as design features and operating procedures. Technical Specifications subsequently prepared in accordance with these regulations placed equal emphasis on design and operating limitations.[7]

As experience was gained by all parties concerned with the licensing of nuclear power plants, it became apparent that Technical Specifications prepared in accordance with the 1962 regulations contained much extraneous material unrelated to plant safety. Furthermore, despite all the detailed information contained in these Technical Specifications, the question of why a particular requirement was included went unanswered in the document itself.

These inadequacies prompted the Commission's Director of Regulation to appoint a special task force to evaluate the 1962 regulations and recommend improvements compatible with public safety and consistent with the emergence of commercial central-

station nuclear power. This task force, composed of key personnel from government and industry, developed the new system for preparation of Technical Specifications published by the Commission for comment[8] on Aug. 16, 1966. Prior to this, in June 1966, the Commission published a Guide to the Contents of Safety Analysis Reports (formerly the Hazards Summary Report).[9]

The published revisions pertaining to Technical Specifications were reviewed for some time by both industry and government and were published in final form in December 1968 and became effective in January 1969. Basically, these latest provisions required that Technical Specifications address themselves to five major areas: (1) Safety Limits and Limiting Safety System Settings, (2) Limiting Conditions of Operation, (3) Surveillance Requirements, (4) Design Features, and (5) Administrative Controls. Additionally, for items 1 through 4, the specification must include a Design Basis that essentially tells why each requirement is included.

These five major areas of interest are specifically defined in 10CFR50:36 as follows:[10]

> (1) *Safety limits and limiting safety system settings.* (i) Safety limits are limits upon important process variables which are found to be necessary to reasonably protect the integrity of certain of the physical barriers which guard against the uncontrolled release of radioactivity . . . .
>
> (ii) Limiting safety system settings are settings for automatic protective devices related to those variables having significant safety functions. Where a limiting safety system setting is specified for a variable on which a safety limit has been placed, the setting shall be so chosen that automatic protective action will correct the most severe abnormal situation anticipated before a safety limit is exceeded . . . .
>
> (2) *Limiting conditions for operation.* Limiting conditions for operation are the lowest functional capability or performance levels of equipment required for safe operation of the facility . . . .
>
> (3) *Surveillance requirements.* Surveillance requirements are requirements relating to test, calibration, or inspection to assure that the necessary quality of systems and components is maintained, that facility operation will be within the safety limits, and that the limiting conditions of operation will be met.
>
> (4) *Design features.* Design features to be included are those features of the facility such as materials of construction and geometric arrangements, which, if altered or modified, would have a significant effect on safety and are not covered in categories described in subparagraphs (1), (2), and (3) . . . .
>
> (5) *Administrative controls.* Administrative controls are the provisions relating to organization and management, procedures, recordkeeping, review and audit, and reporting necessary to assure operation of the facility in a safe manner.

These types of guidelines, coupled with other revisions to 10CFR50 (Ref. 11), will serve to eliminate much of the extraneous material included in old-form Technical Specifications and at the same time let the operator know why certain limitations in the form of Technical Specifications are included in the plant operating authorization. Furthermore, although the historic relation between the content of Safety Analysis Reports and Technical Specifications is retained, now the Final Safety Analysis Reports will specifically address themselves to those matters associated with Technical Specifications bases. Hence, as opposed to including design, procedural, and operating limitations covering all aspects of the plant, the content of new-form Technical Specifications will include performance limitations insofar as these limitations relate to areas directly affecting public safety.

Revising Old-Form Technical Specifications

Basic to the underlying philosophy and methodology involved in preparing Technical Specifications in accordance with the new regulations is the symmetry that exists between the contents of the Preliminary Safety Analysis Report, the Final Safety Analysis Report, and the new-form Technical Specifications. This symmetry greatly facilitates the second- or third-generation plant licensee's effort in preparing Technical Specifications. On the other hand, the lack of such symmetry among documents prepared for earlier plants represents one of the major problems confronting licensees who must revise old-form Technical Specifications to conform to the new regulations. An equally significant problem is the locating of design criteria and/or supporting analyses both of which aid in developing the basis for the new-form Technical Specifications.

The Commission has published a guide[12] for the preparation of new-form Technical Specifications, and this guide greatly facilitates the preparation of Technical Specifications for new plants. This guide does not, however, address itself to the problems that will be encountered in connection with revising old-form Technical Specifications, nor does it discuss how such a revision effort might be conducted. The following discussion addresses itself to both these matters and, although in some cases it repeats what is emphasized in the guide, it should provide some meaningful guidance

to those undertaking Technical Specifications revisions. Since the changes affecting administrative controls and design features are not that significant from a revision point of view, these sections are not considered in the following discussion.

Safety Limits

Since the determination of Safety Limits involves the analysis of those parameters which affect the barriers within a given plant, one must first look at the plant-design characteristics and identify these barriers. Most plants have a minimum of three such barriers, namely, the fuel cladding, the primary-coolant-system boundary, and some form of containment. However, since the containment vessel is typically the last line of defense in an accident situation, the barriers that are typically considered for the purposes of determining Safety Limits are the fuel cladding and the primary-coolant-system boundary. The process variables that affect these barriers are then identified and typically include as a minimum: pressure, flow rate, temperature, and power level. The existing Technical Specifications include requirements for each of these process parameters; however, in most instances the limits specified are set points as opposed to Safety Limits. At this juncture the licensee encounters the first obstacle, that of determining just what the Safety Limits for the cladding and primary system are.

The information concerning Safety Limits for the primary vessel and coolant-system boundary can usually be found in the Hazards Summary Report. These limits can be specified in terms of maximum allowable pressure and their basis developed in terms of the maximum allowable stress as per the code requirements to which the system was designed.

Determination of the Safety Limits for the core is another matter. The definition of fuel-cladding Safety Limits is based on the core's susceptibility to burnout, and the core characteristics described in the Hazards Summary Report are probably no longer applicable. Later analyses, conducted in support of operation with replacement cores, will usually contain the required information. Thus it would seem that defining Safety Limits and the basis for fuel-cladding Safety Limits is a simple task. This is not the case, for the new regulations recognize that susceptibility to burnout will vary with the principal process parameters mentioned above, and hence the licensee must treat the problem of burnout parametrically. This parametric thermal-hydraulic analysis has probably never been performed for the core in question since worst-case situations were the only ones typically analyzed. Further, the licensee may well find that the analytical techniques previously used for thermal studies have to be updated. Therefore establishing core safety limits represents a major portion of the effort associated with revising old-form Technical Specifications.

Limiting Safety System Settings

Under the new regulations a Limiting Safety System Setting must be established for each of the process parameters having a Safety Limit on the premise that the automatic trip settings used as Limiting Safety System Settings will preclude infringement of the Safety Limit under all abnormal modes of operation. To establish these Limiting Safety System Settings, one must analyze all of the transient conditions which have an effect on the principal process parameters.

The establishment of Limiting Safety System Settings must also take into account the measurement and instrument uncertainties associated with principal process-parameter instrumentation. The margin that exists between Safety Limits and Limiting Safety Systems Settings so established is considered the safety margin. These Limiting Safety System Settings need not correspond to the trip settings used for operation of the plant.

The general philosophy used to establish reactor trip settings for earlier plants was to analyze plant transients, evaluate the results in terms of effect on the core and system, and then establish trip settings that prevent the occurrence of unacceptable conditions with reactor trip. The trip settings so established were then adjusted to account for instrument errors and uncertainties. Thus, although the criteria used to establish unacceptable conditions resulting from transient conditions were similar to Safety Limit criteria, there were no analyses that defined Safety Limits per se, particularly from a parametric viewpoint.

Because of this difference in approach, the first-generation plant licensee has two alternatives available to him with regard to establishing Limiting Safety System Settings. The first alternative is to use existing trip settings as Limiting Safety System Settings and, after accounting for both transients and instrument uncertainties, establish in the basis that these trip settings will not result in infringement of the newly established Safety Limits. The second alternative is to disregard existing trip settings and establish Limiting

Safety System Settings based on the newly established Safety Limits.

The choice of alternatives is dependent on the type and applicability of transient-analysis data which are available and which the licensee desires in terms of operating flexibility. If the transients analyzed in the Hazards Summary Report have been modified or updated to account for replacement cores, then little or no transient-reanalysis effort is required to develop the basis for Limiting Safety System Settings. Under these conditions, and the further stipulation that the operator wishes to increase the plant's operating flexibility, the second alternative of selecting new Limiting Safety System Settings is the most practicable, since the licensee can readily justify the Limiting Safety System Settings chosen and eliminate undue conservatism in the safety margin.

If, on the other hand, the transient analyses contained in the Hazards Summary Report have not been modified except on a comparative basis, the licensee is hard pressed to justify new Limiting Safety System Settings and at the same time eliminate undue conservatism in establishing the safety margin. Hence the first alternative of adhering to existing trip settings as Limiting Safety System Settings becomes most practicable.

Unfortunately the licensee will find that the information available on transients will fall into neither of the categories described above. Thus the actual task of revision will involve weighing the costs of reanalyzing transients against the benefits associated with increased operating flexibility due to the elimination of undue conservatism in safety margins. Therefore, owing to practical considerations, some existing trip settings will be retained as Limiting Safety System Settings, whereas others will be changed based on a transient reanalysis to enhance operating flexibility.

Thus, before selecting Limiting Safety System Settings for a first-generation plant, the licensee must thoroughly review the transient data in the Hazards Summary Report and its amendments to determine if (1) the analyses can be applied to the core in question and (2) the results of these analyses are compatible with the previously established Safety Limits. The degree to which both these questions can be answered positively determines how the licensee should proceed with the revision effort.

This type of situation does not exist for later-generation plants because of the similarity of content required between Final Safety Analysis Reports and new-form Technical Specifications. However, later-generation plants will be confronted with analogous situations in connection with the use of replacement cores albeit to a lesser extent.

In the area of determining the instrument and measurement uncertainties associated with principal process instrumentation, the first-generation plant licensees have a slight advantage. These plants have been operated for relatively long periods of time, and the operators know the characteristics of the plant instrumentation. Because of this, undue conservatism in that portion of the safety margin which accounts for these uncertainties can be eliminated.

Limiting Conditions of Operation

That section of the new-form Technical Specifications which addresses itself to Limiting Conditions of Operation is the only section that includes requirements similar to those included in the old-form Technical Specifications. Therefore the effort involved in identifying requirements and developing bases is not so extensive as that mentioned above to establish Safety Limits and Limiting Safety System Settings. The format used to date for this section of the Technical Specifications is system oriented, and the first task involved in preparing this section is identifying those systems within the plant which for reasons of safety should have Limiting Conditions of Operation. The systems typically included are as follows: coolant, containment, instrumentation and control, control rods, emergency power, and engineered safeguards such as core spray and emergency cooling. Limiting Conditions of Operation are also established for gaseous- and liquid-waste systems and refueling operations.

Having identified the systems involved, the next task is to determine the kinds of requirements to be included as Limiting Conditions of Operation for each system. These requirements can be categorized as equipment limitations, process limitations, procedural limitations, and, in the case of control rods and soluble poison systems, reactivity limitations. Equipment limitations are usually couched in terms of what equipment must be operating (performing its design function), what equipment must be operable (capable of performing its design function upon activation), and the characteristics indicative of equipment or system operability. Process limitations usually address themselves to primary-coolant and plant-effluent activity, whereas procedural limitations are couched in terms of what the operator can or cannot do under certain prescribed conditions. The specifications for each

system will invariably include a combination of the types of limitations described above.

Generally speaking, the first-generation plant operator has an advantage over new plant operators when it comes to establishing plant Limiting Conditions of Operation. The first-generation plant has been operated for relatively long periods of time, operating manuals and procedures have been updated to reflect true plant characteristics, and equipment needs and limitations have been determined from experience. Since the kinds of requirements includable in new-form Technical Specifications as Limiting Conditions of Operation will not be found in their entirety in the old-form Technical Specifications, this experience coupled with the information contained in the other documents used for normal operation of the plant becomes the primary source for preparation of the Limiting Conditions of Operation section of the Technical Specifications.

The new aspect of this section of the Technical Specifications is the development of a basis for each requirement included in the specification. Where the specification addresses itself to equipment being operable or operating, and/or process or procedural limitations, the basis can readily be developed by virtue of the operator's past experience. Where the specification addresses itself to equipment design characteristics such as relief-valve capacity, pressure-vessel heatup and cooldown rate limitations, or containment-vessel leak rates, the task of developing the basis is somewhat more extensive and involves a review of the Hazards Summary Report and other available documentation which usually contains the analyses used to support the design characteristic. Again though, because of the lack of planned consistency between the content of the Hazards Summary Report and old-form Technical Specifications, the licensee will find that some original analyses will have to be performed to justify some of these requirements.

In the area of reactivity limitations, the first-generation plant licensee is in the same position as the new plant licensee since these limitations are so dependent on the core characteristics. Both new and replacement cores are analyzed in depth regardless of the plant involved. Once the first-generation plant licensee develops an appreciation for those requirements includable as Limiting Conditions of Operation, the identification of reactivity-type limitations and the development of the basis for these limitations become relatively simple. In most instances the licensee will find that the specifications involving reactivity limitations in the new-form Technical Specifications are less exhaustive than those contained in existing-plant Technical Specifications.

Surveillance Requirements

Specifications includable in the Surveillance Requirement section of new-form Technical Specifications are those related to the tests and inspections which will be conducted to ensure that the plant will be operated within the Safety Limits and that the Limiting Conditions of Operation will be met. Thus, whereas previous sections of the Technical Specifications specify requirements in terms of limitations, this section specifies what the licensee will do to ensure that these requirements are being satisfied. Because of the interrelation between this section of the Technical Specifications and the Safety Limit and Limiting Conditions of Operation section, there must be a one-to-one correspondence between specifications cited in the Limiting Conditions of Operation section and those included in the Surveillance Requirement section. This is one of the basic premises of the new-form Technical Specifications approach.

From the viewpoint of conducting the actual revision, this section should be prepared in parallel with or after the Limiting Conditions of Operation section to ensure this one-to-one correspondence. Because of the nature of the requirements that are includable in this section, the format need not be completely system oriented as is the case for the Limiting Conditions of Operation section.

For the most part, requirements in the Limiting Conditions of Operation section deal with systems and components used continuously and those which would be used periodically, if at all. From an operational reliability viewpoint, the measures taken by the licensee to ensure that the latter type of systems and/or components are functioning properly represent the most critical area. This functional distinction provides the rationale for dividing surveillance requirements into two categories, namely, those required for operational safety and those required for safety under abnormal or emergency conditions.

Specifying surveillance requirements dealing with operational safety should present little or no problems to the first-generation plant licensee undertaking a Technical Specifications revision. Requirements includable in this category typically include process and nuclear instrumentation tests, checks and calibrations, radioactive-waste sampling, relief-valve tests, and other surveillance measures normally conducted by the oper-

ator. These requirements can readily be specified based on information contained in existing Technical Specifications and plant test procedures. Developing the basis for these requirements is also straightforward, and the licensee's experience with the plant is the primary source of information presented in the basis, particularly where the matter of test frequency is considered.

Surveillance Requirements for systems and for components required for abnormal or emergency situations and hence not continuously operating, are usually specified by system. These requirements can be readily specified by virtue of the licensee's previous experience. The only significant difference with regard to preparing these system-oriented Surveillance Requirements is in the development of the basis, since the basis must address itself to how the system must perform under abnormal conditions and why the tests specified ensure this ability to perform. Again though, the experienced licensee will find that he is in a better position to develop the basis for these specifications because of experience with the plant.

Definitions

Although the definition of certain terms is not specifically required by the new regulations, it behooves the licensee to define those terms which are used repeatedly throughout an individual section of the Technical Specifications. Terms that do require definition, in addition to those cited in 10CFR50, are those concerned with modes of reactor operation, such as *startup* and *shutdown*; those concerned with modes of equipment operation, such as *operating* and *operable*; and those concerned with testing, such as *check, test,* and *calibration*. These definitions greatly facilitate any subsequent discussions with the Commission.

In conclusion, once the licensee develops an appreciation for the approach set forth in the guide,[12] the actual task of revising old-form Technical Specifications is not as ominous as it may seem. Specifications and bases can usually be developed by virtue of only the licensee's experience and the exercise of engineering judgment in all areas except core Safety Limits. Thus the development of core Safety Limits and their basis will represent the major portion of any such revision effort. This in turn primarily involves the parametric analysis of the core thermal-hydraulic characteristics and to a lesser extent an evaluation of plant transient analyses. Because of the significance of the thermal aspect of any revision effort, the following portions of this article address themselves to core thermal-hydraulic design criteria, the changes these criteria have undergone, and the effect of these changes on developing Safety Limits and Limiting Safety System Settings.

Core Thermal Characteristics

Since both thermal-design criteria and analytical techniques have undergone considerable change in the 1960's, the implications of these changes and how they affect the establishment of both Safety Limits and Limiting Safety System Settings are examined.

The primary cause for evolution in reactor design criteria is increased confidence in methods and results. For example, the improvements in boiling-water-reactor (BWR) design characteristics result principally from better optimization of core power distributions, design innovations, improvements in anticipated heat-transfer characteristics, and application of internal steam separation. This increased confidence has been obtained from accumulated operating experience and continuous experimentation. Similarly, pressurized-water-reactor (PWR) designs have improved performance characteristics that include important advances in core design, incorporation of chemical shim and rod cluster control, and optimization of fuel-management programs. Again, greater confidence in the design is a direct result of operating experience and experimentation.

The major considerations related to first-generation PWR core thermal design were:

1. Departure from nucleate boiling (DNB).
2. Bulk boiling in the outlet of the hot channel.
3. Centerline fuel melting.

The analysis of core thermal characteristics in light of these considerations is largely dependent on core power distribution and the values of design peaking factors used. Analytical design procedures presently available are quite adequate for the confident prediction of the core power distribution over the lifetime of the core. However, the major uncertainty in such calculations is whether or not the design rod patterns, power levels, fuel-management procedures, etc., will be followed throughout the core life. Because of this, usual practice is to base both design peaking factors and design power distributions on calculations pertaining to worst core configurations. These factors are then increased by some margin of safety.

There are two types of design peaking factors presently incorporated in the conduct of thermal-hydraulic analysis. The first, the local hot-spot peaking factor, is used to determine the highest fuel operating

temperature. The second, the enthalpy factor, is employed to establish the proximity to the boiling crises.

Each peaking factor may be divided into its engineering and nuclear subfactors. For example, the engineering components of the enthalpy peaking factor may be deviations in fuel pellet diameter, density, and enrichment. The nuclear subfactors are typically the local power peaking and the overall maximum-to-average flux ratio in the core.

First-generation core analysis assumed that the overall factor (enthalpy or hot spot) was equal to the product of the individual subfactors. Thus every deviation from nominal design values was given equal weight. This method assumed that there was at least one channel in which all possible adverse deviations occur simultaneously.

Later-generation designs have found that the probability of all events occurring simultaneously is extremely small. As a result, the trend in design criteria has been to make use of statistical considerations to determine the probability of the occurrence of various deviations and to design the heat-removal system accordingly. This approach is based on the assumption that the significant hot-channel factors arise from variables which are statistical in nature. Applications of this method and the techniques for calculating the factors in later-generation plants have significantly reduced the magnitude of the enthalpy and hot-spot factors and have thus resulted in a corresponding increase in power output from a reactor of a given size.

Table 1 shows the trend in improvements in the peaking factors for a typical PWR. As shown, significant reductions have accrued through the discriminate application of statistics and increased confidence.

Another important change in design philosophy is related to fuel centerline melting. First-generation design criteria made no allowance for some initial melting, and, as a result, this restriction became an operating limitation. Now the emphasis is directed toward burnout and hence maximum allowable cladding-surface temperatures. Experience has shown that some central fuel melting can be tolerated during transients, although there is still no proof that this condition can be allowed to exist in the core over long periods of time. This increase in the maximum allowable centerline temperature has resulted in increased allowable linear heat rates. First-generation design criteria typically were based on maximum linear heat rates of 12 to 14 kw/ft. Later-generation design philosophy allows for maximum linear heat rates between 18 and 20 kw/ft. Since centerline melting is presently considered to take place at about 23 kw/ft, a value closer to 21 or 22 kw/ft is considered prudent for design purposes. Later-generation designs are also based on a more sophisticated analysis of the fuel rods, which account for the effects of gap conductance and fission-gas plenum volume effects on the design rating at which centerline fuel melting will occur.

Table 1 Power Peaking Factors Used for the PWR

	Early 1960's	Late 1960's
Nuclear (or Nominal)		
Local peaking factor	1.08	1.08
Radial (bundle) peaking factor	1.60	1.46
Enthalpy peaking factor, $F^N_{\Delta H}$	1.73	1.58
Axial peaking factor		
Value	1.80	1.72
Position of peak	$\frac{1}{3}$ down from top of core	$\frac{1}{3}$ down from top of core
Overall peaking factor, F^N_q	3.11	2.71
Engineering		
Enthalpy, $F^E_{\Delta H}$	1.22	1.075
Overall, $F^E_{\Delta q}$	1.045	1.04
Design		
Enthalpy	2.11	1.70
Overall	3.25	2.82
Overpower allowance	1.18	1.12

There has been a significant change in philosophy with respect to bulk boiling in PWR cores. First-generation designs did not permit bulk boiling under any conditions. The reason for this was the uncertainty of the effect of bulk boiling upon DNB. Through increased experimentation in this area, the effects of limited bulk boiling in a coolant channel upon DNB were studied and then incorporated into the critical heat-flux correlations. As a result, later-generation design criteria allow bulk boiling during transients so long as a minimum DNB ratio (DNBR) is maintained. In addition, steady-state design criteria have made provisions for a limited allowable void fraction at the core exit. For example, Technical Specifications for the Connecticut Yankee power plant[13] limit the core exit void fraction to less than 32%.

Correlations that attempt to predict the onset of DNB in the subcooled and low-quality region and dry out in the high-quality region have reflected the changing design philosophy of power reactors. New correlations, based on recent data, have resulted in a more knowledgeable approach to the problem of burnout. For example, investigators have examined the effect of a DNB rod in a rod bundle and have found

the condition to be less detrimental than previously thought. In addition, they have found that the presence of properly designed spacers has the effect of increasing the heat flux at which DNB occurs[14] by as much as 10%.

The most important change in burnout philosophy between first- and later-generation designs has been the lowering of the minumum value for the DNBR. In the period of the last 10 years, the minimum DNBR has been decreased from about 2.0 to a value of 1.3 which is presently used with the W-3 burnout correlation. This is primarily a reflection of increased knowledge of the effects of rod bundles, mixing, and the statistical applicability of the experimental data upon which the correlations are based.

Each of the improvements in analytical techniques and changes in design philosophy discussed above has a marked effect on determining the thermal limitations imposed on operation.

Parametric Thermal Studies for the N.S. *Savannah*[15]

Before conducting a parametric thermal analysis to establish Safety Limits, the licensee must consider:

- The parameters to be studied.
- The use of existing set points as boundary conditions relative to operating flexibility.
- The interrelation between the chosen parameters that can conceivably reduce the magnitude of the effort without compromising operational flexibility.

Each of these areas was considered prior to initiating a parametric thermal study for the N.S. *Savannah*. The objective of this study was to determine the effects of variations in core flow, system pressure, core lifetime, and core mean coolant temperature on the burnout power level. For any particular set of the above parameters, DNBR's were calculated and plotted as a function of steady-state power. From the curves generated in this manner, the burnout powers corresponding to the critical DNBR's were determined.

The range of any variable was chosen such that the nominal and worst values of that parameter were considered in the calculations. For example, the nominal core mean coolant temperature is 508°F, corresponding to the normal operating pressure at 1750 psia. Under some conditions it is possible for the mean coolant temperature to reach 525°F, which initiates a reactor trip due to high reactor outlet temperature. Therefore the total range of coolant mean temperature that might exist during reactor operation is provided for in the parametric analysis. In the same way a primary-coolant pressure of 1500 psia represents the minimum attainable pressure without reactor scram due to the low-pressure trip setting.

The axial power distributions corresponding to 2000 effective full-power hours (EFPH) and 8500 EFPH were previously determined from a FLARE depletion study.[16] The 2000 EFPH represents the time in core life when steady-state fuel temperature peaks, and 8500 EFPH represents the projected end of core 1A lifetime when the axial and radial power distribution were determined to be worst with respect to burnout.

Attempts were made to minimize the number of values treated for each parameter since each additional value doubles the total number of cases. A preliminary analysis was performed to assure that inflection points within the final analysis would not be overlooked. In this manner the values decided upon (shown in Table 2) assured that the analysis would consider the worst combination of parameters that could be expected during steady-state operation.

The system variables used in the steady-state parametric analysis of the N.S. *Savannah* core 1A are presented in Table 2.

Table 2 System Variables

Core flow, % full flow	System pressure, psia	Core lifetime, EFPH	Core mean coolant temp., °F
100	1750	2000	508
80	1500*	8500	525*
60			
40			
20			

*Boundary conditions corresponding to existing set points.

Since the thermal limitations in the existing Technical Specifications were based on a minimum DNBR of 1.8 using the WAPD-188 (Ref. 17) correlation, DNB was calculated using the WAPD-188 correlation and the more recent W-3 (Ref. 18) correlation. Additionally, the minimum design values chosen for DNBR to establish Safety Limits were reduced to values used for later-generation plants. The results of these analyses for what were determined to be the limiting conditions of all conditions analyzed are shown in Fig. 1. For example, the results shown in

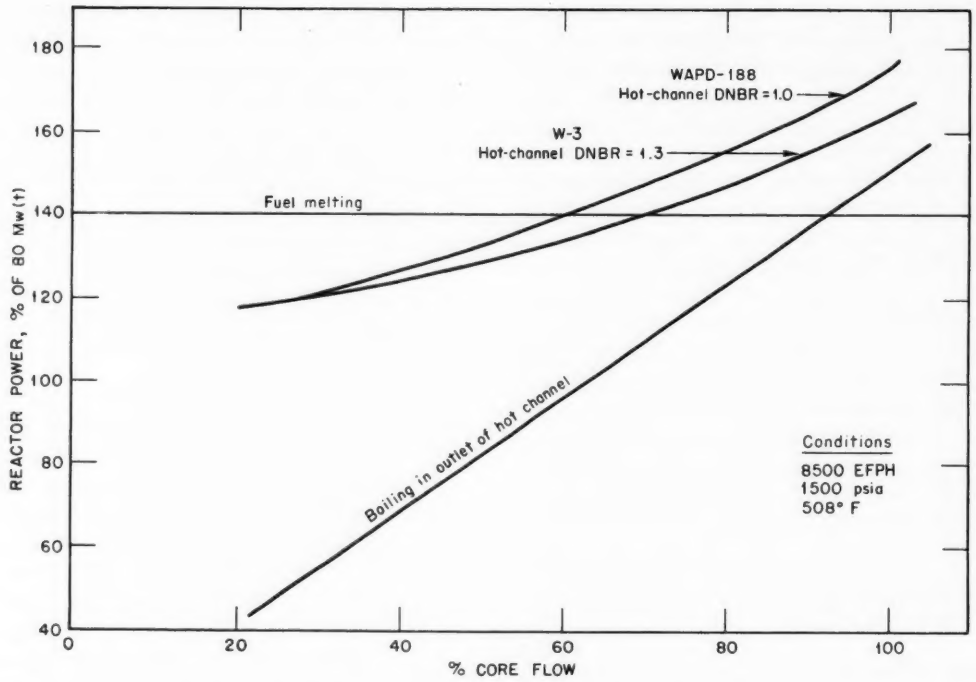

Fig. 1 Reactor core Safety Limits.

Fig. 1 were compared to the results calculated for a mean coolant temperature of 525°F and a primary pressure of 1750 psia at 8500 EFPH. Since it is not feasible that the transient which increases mean coolant temperature from the nominal value of 508°F to the maximum value before scram of 525°F can occur simultaneously with the transient that decreases pressure from the nominal 1750 to 1500 psia, the conditions represented by Fig. 1 with a mean coolant temperature of 508°F were determined to be the most limiting from the viewpoint of DNB.

Since one of the original criteria for the N.S. *Savannah* core was that there would be no bulk boiling in the outlet of the hot channel under steady-state conditions, initiation of bulk boiling was also considered. These results are also shown in Fig. 1.

Earlier methods used to determine first-generation PWR core thermal characteristics treated bulk boiling and DNB separately because of the uncertainties that existed with regard to the effect of boiling on burnout. The burnout correlations used for this analysis provide for bulk boiling, and experience has indicated that some degree of bulk boiling in the hot channel can be tolerated from the viewpoint of burnout. For example, up to 5% quality is acceptable in the hot channel during normal transients. Since the bulk-boiling limitations shown in Fig. 1 were based on initiation of bulk boiling in the outlet of the hot channel, a very conservative treatment relative to more recent criteria, the bulk-boiling limitations shown were not used to establish Safety Limits. This change in approach results in an overall increase in the Safety Limits and hence a greater operating flexibility of the reactor plant. It should be noted, however, that this difference in philosophy is not arbitrary, but is a direct result of increased knowledge in the thermal hydraulics of the system which has come about through operating experience and experimentation.

Another thermal criterion for the N.S. *Savannah* core was fuel melting. Previous work[19] established that fuel melting occurs at 140% of rated power. This power was based on the worst time in life with respect to the peak steady-state fuel temperature in core 1A which occurs at 2000 EFPH. The maximum steady-state pellet centerline temperature at this time in life is 3700°F. The power-level limitation resulting from adherence to this criterion is also shown in Fig. 1. Again though, because of changes in the state of the

art, this criterion was not used to establish Safety Limits in the N.S. *Savannah* new-form Technical Specifications.

The DNB results were next examined to determine which correlation would form the basis for establishing Safety Limits. The design DNBR used with the WAPD-188 correlation was unity, whereas that used with the W-3 correlation was 1.3, and, on this basis alone, one would expect the WAPD-188 results to be less conservative. However, on further examination of the WAPD-188 correlation and considering the 0.65 design reduction factor typically used when working with this correlation, the design DNBR of unity is effectively a DNBR of 1.54 for the purposes of comparing results from the two correlations. Thus the use of the earlier WAPD-188 correlation would seem to increase operating flexibility rather than reduce it. However, this is not the case because, even though a design DNBR of 1.3 using the W-3 correlation is consistent with later-generation plant burnout criteria, the use of a design DNBR of 1.0 using the WAPD-188 correlation is not. This is primarily due to the greater confidence that exists with regard to the W-3 correlation's ability to estimate critical heat flux. Hence using design DNBR's with the WAPD-188 correlation of 1.8 which was previously used for the N.S. *Savannah* does, in fact, result in a decrease in operating flexibility. Therefore the W-3 correlation results were used to establish Safety Limits.

To determine appropriate Limiting Safety System Settings, the Safety Limits represented by Fig. 1 were adjusted to account for effects of instrument and measurement uncertainties. To facilitate this analysis, the most adverse combination of these uncertainties was considered, and these results are shown in Fig. 2. The loci of acceptable power-level set points are about 10% below the previously established Safety Limits. The power-level Limiting Safety System Settings shown in Fig. 2 were then established based on consideration of transients and power overshoot, and the margin that exists between these set points and the adjusted Safety Limits represents the Safety Margin. For comparison purposes the Safety Limits resulting from using a combination of bulk boiling and fuel melting as the limiting criteria are also shown in Fig. 2. As illustrated, these criteria greatly reduce the allowable Limiting Safety System Settings.

The N.S. *Savannah* is unique when its operating criteria are compared to other first-generation plants because of its need and ability to operate under less

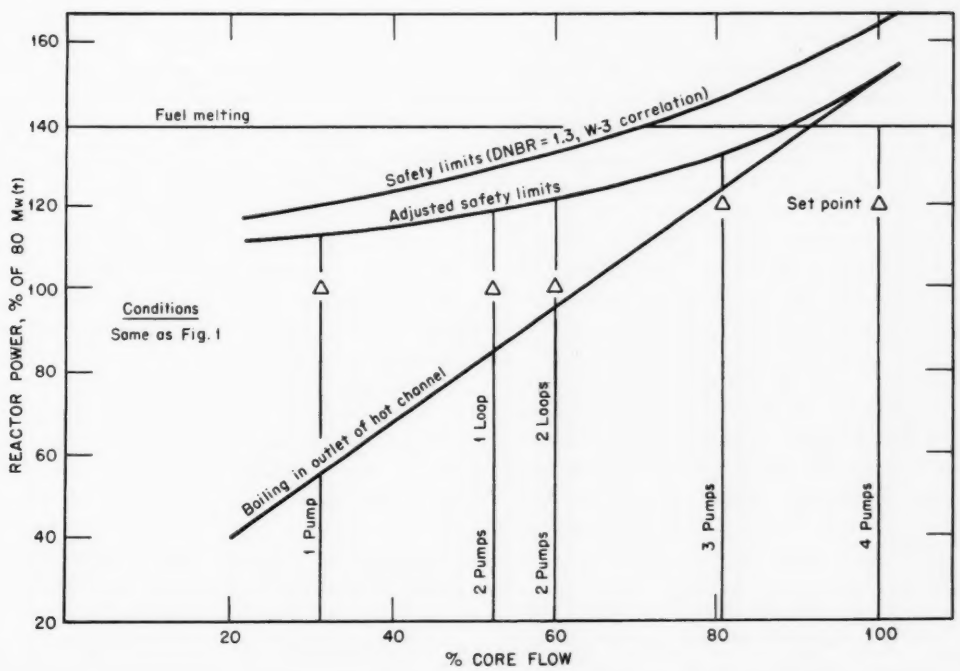

Fig. 2 Basis for Limiting Safety System Settings.

than the 80 to 90% of full-flow conditions typical of other plants. However, the value of analyzing core thermal limitations parametrically as required for new-form Technical Specifications should be apparent from the above results.

Acknowledgment

The authors wish to thank J. Thorpe of FAST Inc. for the assistance he provided during the N.S. *Savannah* Technical Specifications revision effort which led to the preparation of this article.

References

1. 10CFR50:36, 27 FR 5491.
2. 33 FR 18610-18613, Dec. 17, 1968.
3. 10CFR50:36, 21 FR 355.
4. 27 FR 5491, June 9, 1962.
5. 10CFR50:36 (*b*), 27 FR 5491.
6. Purpose, Organization, and Contents of Hazards Summary Reports for Power Reactors, U. S. Atomic Energy Commission, Division of Licensing and Regulation, Aug. 28, 1962, Draft.
7. Technical Specifications for the La Crosse Boiling Water Reactor (LACBWR), Exhibit D, DPRA-5.
8. 31 FR 10891-10894, Aug. 16, 1966.
9. A Guide to the Organization and Contents of Safety Analysis Reports, June 30, 1966.
10. 33 FR 18612, 50:36 (*c*), Dec. 17, 1968.
11. *Ibid.*, pp. 18610-18612.
12. Guide to the Content of Technical Specifications for Nuclear Reactors, November 1968.
13. Connecticut Yankee Atomic Power Company Nuclear Power Plant—Haddam Neck Plant, Haddam, Conn., Technical Specifications and Bases, May 1967.
14. Jackson and Moreland and S. M. Stoller Associates, Current Status and Future Technical and Economic Potential of Light Water Reactors, USAEC Report WASH-1082, March 1968.
15. Hittman Associates, Inc., Parametric Thermal Analysis of N.S. *Savannah* Core 1A, USAEC Report HIT-372, February 1969.
16. Y. S. Kim and T. R. Robbins, N.S. *Savannah* Shuffled Core I Nuclear Characteristics, Revision I, Report NUS-389, NUS Corporation, November 1967.
17. N.S. *Savannah* Technical Specifications and Postoperation Criteria, First Atomic Ship Transport Inc. (FAST), February 1967.
18. L. S. Tong, An Evaluation of the Departure from Nucleate Boiling in Bundles of Reactor Fuel Rods, *Nucl. Sci. Eng.*, **33:** 7-15 (1968).
19. NUS Corporation, N.S. *Savannah* Shuffled Core I Thermal Characteristics, Report NUS-460, April 1968.

Reliability Techniques as Applied to Operating Systems and to Design Optimization

By E. A. Saltarelli and D. G. Fitzgerald*

Every land-based nuclear power plant incorporates systems and equipment designed wholly or partly to limit the release of radioactive material to the environment in the event of any of a variety of highly abnormal occurrences. A considerable fraction of the cost of a nuclear power plant, although it does not contribute to the efficient production of electrical energy, is incurred for these systems and equipment. The importance of these protection systems, essential to public health and safety, needs no further emphasis.

Those parts of the protection system which have an active function, such as to scram the reactor, cool the core, or cool the containment, are designed to assure that they will perform if they are ever called upon to do so. At the same time no mechanical or electrical device is so nearly perfect that it will never fail. As a result, a few rules and criteria have evolved which are intended to yield designs tolerable of some failures. That is, the safety function may still proceed even though some element of the system does not perform. Despite the application of these single-failure criteria and functional redundancy, system failures can occur.

The objective of the protection-system designer, then, is to maximize the probability of the system's functioning when called upon and to minimize cost and complexity.

The protection-system designer must consider several factors when working toward his objective. He must do his best to assure that his design is capable of performing its intended function, that the component parts are appropriate for the intended service, that the equipment is of the required quality, and that the total system design represents the optimum application of equipment to achieve maximum probability to function when called upon to perform. The last factor, probably the least understood and the most inconsistently applied, is the subject of this paper.

The design tool used to maximize performance probability is called reliability engineering. The theory and practice of reliability engineering analysis are well established. Concepts and methods have been continually developed and refined over the past decade, and reliability is an integral and important factor in the design of many systems such as aircraft, ships and their electronic systems, missiles, and spacecraft. These systems are characterized by requirements for safety, predictable mission success, and minimum maintenance per operating hour—three attributes that apply strongly to nuclear power plant systems.

Reliability methodology offers a tool by which nuclear power-plant protection systems may be designed and optimized to achieve, within the limits of engineering capabilities, the dual requirements for maximum safety and plant availability and minimum cost and complexity.

Status of Applied Reliability in the Nuclear Power Industry

With one or two exceptions, reliability methodology has not been applied in the U. S. nuclear

*NUS Corporation, Rockville, Md.

power industry in any deliberate way. The exceptions are internally sponsored work at General Electric Company's Atomic Power Equipment Department and government-sponsored work by Holmes and Narver, Inc.

Results of General Electric's reliability work have supported operating-license applications and technical specifications (e.g., Jersey Central Power & Light Co. and Oyster Creek Unit 1). Two General Electric-sponsored publications[1,2] indicate the extent and depth of this work. Greatest attention has been directed toward the reactor scram system. General Electric has also effectively used reliability techniques to evaluate and optimize the design of engineered safeguards systems, although results of this work are not yet public.

The Atomic Energy Commission, through Holmes and Narver,[3] has sponsored the application of computer-aided reliability analysis. One program, ARMM (Automatic Reliability Mathematical Model), is a general-purpose computer program for deriving and solving a mathematical model of the reliability of a complex system. North American Aviation, Inc., originally developed the ARMM program under a U. S. Air Force contract. Holmes and Narver and General Electric have applied it to nuclear reactor systems.

Another computer program, called SAFTE-1 (Systems Analysis by Fault Tree Evaluation), uses a Monte Carlo technique to provide a concise and orderly qualitative description of various combinations of possible occurrences within a system that could result in a predefined undesired event. Bell Telephone Laboratories, Inc., developed the fault-tree analysis concept for the Minuteman program; the Boeing Co. refined and computerized it. Holmes and Narver further refined the methods for application to reactor safeguards systems.

Europeans are applying reliability engineering methods to nuclear reactor systems more than Americans are. A series of United Kingdom Atomic Energy Authority, Health and Safety Branch, publications[4-7] indicates the work going on in England alone. Other evidence of European activity is in three papers given at the second CREST meeting (Ispra, Italy, June 1968) of specialists on the reliability of electrical supply systems and related electromechanical components for nuclear reactor safety.[8-10]

Although the application of reliability engineering to nuclear power-plant design and analysis in the United States is lagging compared to activity in other countries, interest is growing. For example, the Institute of Electrical and Electronic Engineers, Nuclear Science Group, is actively preparing reliability standards and criteria for application to nuclear reactor protection systems. Technical personnel within the U. S. Atomic Energy Commission are actively developing reliability methods for license-application evaluations, and the Division of Reactor Development and Technology has included reliability in its standards program. The U. S. nuclear steam-supply-system manufacturers are also rapidly building reliability engineering capabilities.

The balance of this paper discusses a few of the many ways that reliability engineering is applicable to safety-system-design evaluation. The examples highlight its simplicity and utility.

Application of Reliability Techniques to Nuclear Safety Systems

Types of Analyses

The application of formal reliability evaluation methods to all nuclear plant systems will result in higher probability of systems functioning properly when they are called upon to operate. The greatest need today, however, is in the area of nuclear safety systems.

It must be emphasized that formal reliability methods do not evaluate a system's capability to meet the functional requirements for which it was designed. Rather, reliability analysis establishes the relative probability of the system performing adequately for the period intended under the operating conditions specified. The capability of the system to adequately meet the design function is not part of the reliability analysis. For example, the ability of a pump to deliver at a given flow rate is a measure of its capability. The probability of the pump's functioning when called upon to perform is its reliability.

An important element of a reliability-assurance program is the reliability analysis. The reliability analysis is performed to evaluate the potential reliability attributes of alternative designs. The reliability analysis usually takes two forms, quantitative and qualitative. The quantitative analysis uses probability theory to consider the contributions of the various components to the total system. The use of a block diagram and a series of statements that describe the allowable up-state configuration of the system permits the probability of system success to be calculated by means of relatively simple mathematical equations. The qualitative analysis points out limitations of the quantitative analysis, clarifies assumptions, and provides input for the quantitative analysis.

The quantitative analysis attempts to determine from design characteristics and data taken from past experience with similar components the probability that the system will not fail during a given period. In a very limited number of technological areas where there is an abundance of failure-rate data, a quantitative value for the reliability of a single configuration can be predicted with confidence. However, in the case of nuclear components, there is a paucity of data due to the relatively short operating history of commercial nuclear plants. Thus the benefit to be gained from the quantitative analysis is generally limited to a comparison of the relative reliability of different designs. The results of analysis of two or more designs can be compared to determine the relative advantages and disadvantages of each. Since the primary purpose of the reliability analysis is to help the design engineer choose among alternative designs, a meaningful analysis can be performed without establishing an absolute reliability number for a given design.

Quantitative Analysis. The purposes of the quantitative-analysis techniques are:

- To assist the design engineer in making an early relative estimate of the difference in the expected reliability of various design approaches.
- To assist the design engineer in identifying those aspects of the design which can be considered critical from the standpoint that they control reliability; that is, they pinpoint the most likely contributory factors of system unreliability. This allows concentration of reliability effort on the problem areas and refinement of the design to reduce their effect.
- To encourage the design engineer to look at his design from the standpoint of reliability as well as capability to meet the design requirements.
- To standardize critical evaluation criteria for review or certification.

Quantitative reliability analyses can be performed with computer codes or manual calculational techniques. When applying these techniques to nuclear safety systems, the entire evaluation can be done without a computer since the mathematical expressions usually are not complex. In those instances where equations are unwieldy, the use of nomographs is recommended. The additional advantage of using hand calculation vs. a computer code is that it enables the system designer to keep in touch with what the system is trying to do.

The classical approach to manual calculations assumes that catastrophic failures in the mature design are usually characterized by a constant failure rate (at the device level). The wear-out failure is handled separately. It further assumes that the probability of failure of a device that has not progressed to the point of wear-out does not change as a result of a repair or maintenance action. These assumptions enable the design engineer to predict the probability of success by means of relatively simple mathematical equations.

Computer-aided reliability analyses are most often applied to models that are very complex as a result of repair considerations or complex configurations. Where there is a large variation in the available failure-rate data, the computer also has advantages. There is a variety of computer-aided reliability techniques. As examples of the types available, three are summarized below.

The application to engineered safety systems of the Automatic Reliability Mathematical Model (ARMM),[11,12] developed by North American Aviation, Inc., Los Angeles, Calif., has been demonstrated by Holmes and Narver, Inc.[3] ARMM is a computer program that selects those combinations of component failures which cause a system failure and then derives and solves the reliability mathematical model for computing failure probabilities. The results of an ARMM analysis include (1) the probability of successful system operation, (2) the contribution of each component to the probability of system failure, and (3) the most sensitive combination of system components which are the major causes of system unreliability.

Systems Analysis by Fault Tree Evaluation (SAFTE-1) has also been demonstrated by Holmes and Narver, Inc.[3] Fault-tree analysis gives the various combinations of possible occurrences within a system that can lead to a predetermined undesired event; it also allows evaluation of the significance to the system of a component failure. The SAFTE-1 program uses a Monte Carlo technique for fault-tree simulation.[3] The system or fault tree to be analyzed is viewed as a statistical assembly of components, each characterized by an exponential failure distribution and a normal repair distribution. A time to failure and a time to repair are randomly assigned to each component. The system is then tested to determine the time at which failure occurs at the system level. Estimates of system reliability are obtained by testing a sufficiently large population of systems in this manner.

The Generalized Effectiveness Methodology (GEM), developed by the U. S. Naval Applied Science Laboratory, Brooklyn, N. Y., is an analytical model that incorporates all the advantages of ARMM and in addition can be used to determine the effect of repair

and to compute probable system repair time. By means of a modification command language, the user can append, remove, or replace items in the system configuration. GEM also allows variation of failure-rate values; this is particularly useful for sensitivity analyses when there is an absence of good failure-rate data. The code contains a formula library consisting of computer programs for calculating reliability of various systems configurations. This library is expandable to allow inclusion of any new formulas of interest when developing a design. GEM provides a system library that stores system descriptions; these can be recalled, expanded, or modified as desired by the user.

Qualitative Analysis. It would be highly desirable to predict the absolute reliability of a system. However, as previously discussed, this is not possible for nuclear safety systems owing to the limited failure-rate data available. One must rely more heavily on qualitative methods to augment the quantitative analysis. This discussion of qualitative analyses is limited to analysis of design checklists and failure modes and effects analysis.

Failure Mode and Effects Analysis. A Failure Mode and Effects Analysis (FMEA) is a systematic, organized procedure for determining, evaluating, and analyzing all potential failures in an operating system. All potential failure modes and mechanisms are examined in order to evaluate the reliability of various system design elements and to determine the effect and relative consequence of each failure on the system. The single-failure analysis is a form of the FMEA.

The FMEA usually identifies failure modes, possible causes, symptoms and local effects, compensatory provisions, effect on next higher system element, level of severity, failure probability, and recommended action. It supplements reliability prediction because it points out failure mode/effect relations that might otherwise be overlooked. For example, when a valve is added to a system with the intent of adding redundancy, the designer usually considers failure of the valve in fail-to-open or fail-to-close terms. However, when the gross-leakage mode is considered, the valves should be thought of as series elements. Should this latter mode be more significant than the fail-to-open or fail-to-close mode, redundant valves could reduce system reliability.

Design Checklists. Design checklists for reactor plant subsystems can identify generalized and specific questions regarding the potential reliability of a design, the answers to which cannot be directly formulated in a mathematical relation. Answers to questions itemized in a checklist can be compared for each alternative design. The design checklist also aids in the identification of potential problem areas. The design checklist should be a part of the quality-of-design review of the quality-assurance program. It should be developed not only by the designer but also by other engineers reviewing the system design to assure that all advantages and disadvantages of the alternative designs have been identified. This practice has been in use in the past and does not represent a new technique. This approach, however, formalizes the design review.

Comparative Reliability Analysis

Application of reliability-analysis techniques to a system design proceeds in a sequence of logical steps. In general, the steps apply to any system, such as the scram system, power-control system, high-pressure injection system, containment spray system, etc.

A comparative analysis technique has been demonstrated by NUS Corporation[13] in conjunction with the RDT standards program under the direction of the Oak Ridge National Laboratory. In a comparative analysis the derived values presented do not represent an absolute prediction of system behavior but represent a quantitative assessment of system reliability for comparison with other systems designed to perform the same function. An evaluation of the comparative reliability of two PWR containment cooling systems was selected for demonstration because these systems possess unique characteristics which, in a functional sense, differentiate them from other reactor plant systems. First, unlike other process systems, in most cases they are normally not in operation. They are called upon to operate only when the reactor has experienced a loss-of-coolant accident, and, should they malfunction, the safety of the public could be seriously affected. Second, these systems cannot be fully tested to check their designed ability to function since operation in the design mode on a routine basis causes unwarranted maintenance problems.

The quantitative analysis of system reliabilities using the comparative technique is summarized by the following steps:

1. Based on the FMEA and the system descriptions, the reliability model is developed. For a nuclear safety system it is desirable to consider two modes of operation and therefore two separate models:

- The preaccident mode with the equipment in a condition of normal reactor operation.
- The postaccident mode with the equipment in operation after initiation by the accident signal.

2. Analytical expressions are written for converting block diagrams into subsystem reliability statements for both modes of operation.

3. The subsystem reliability expressions are used to express all acceptable system states for mission success for both modes of operation. These states are then combined by the product rule.

4. A sensitivity analysis is performed by assigning probable numerical values to the lowest level reliability characteristics and then varying individual characteristics over a range of several decades.

5. Finally, it is necessary to establish a proper testing interval to assure that the required system reliability is maintained.

Developing Reliability Block Diagrams and Mathematical Models

The block diagram is developed from the system description and shows the evolution of the design from the major system down to the final subsystem, terminating with the lowest identifiable division of each array. This may be a valve, pipe section, relay assembly, relay contact, amplifier, power supply, etc., depending upon the information available. Figure 1 shows a typical block-diagram array going from the major system down to the parts of the subsystem. Starting with the subsystem level, the reliability of the array for each of the units in the system level is calculated. The reliability of the system level is then determined for each of the units of the major system, and, finally, the reliability of the major system can be determined.

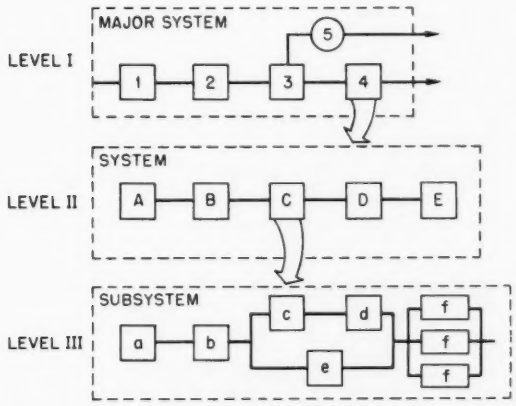

Fig. 1 Reliability block diagram.

For the various combinations of series and parallel paths, it is convenient to use a graph as shown in Fig. 2 for determining the failure probability for various redundant configurations. The abscissa is the failure probability of combinations of identical and functionally redundant components. The ordinate is the failure probability of a single component, F_0. On the same set of coordinates $F_0 = 1 - e^{-\lambda t}$ is plotted as a function of λt (failure rate times operating time). To use the set of curves, enter the abscissa at the selected value of λt and move vertically to the F_0 curve. Then move horizontally to the desired combination curve and read the corresponding value of the combined probability from the abscissa. For example:

1. Starting with a λt of 2×10^{-2}, move vertically to intersect the 1-of-1 curve.

2. At this point, to determine the failure probability for a combination of 3 of 4, move horizontally to the appropriate curve and then vertically back to the abscissa. This results in a failure probability of the combination of 2.3×10^{-3} hr^{-1}.

3. Similarly, for a combination of 2 of 3 and 1 of 2, the failure probabilities for λt of 2×10^{-2} are 1.2×10^{-3} hr^{-1} and 4×10^{-4} hr^{-1}, respectively.

Sensitivity Analysis

Sensitivity analysis is a useful tool for determining which types of components are most critical in the system. Utilizing failure-rate data derived from land-based system data,[14] the failure rates are varied over a range of several orders of magnitude. The range of variation is a function of the range experienced in the data available. In the NUS analysis[13] the range covering the worst to most optimistic case covers plus or minus one and, in some cases, two orders of magnitude. The effect on system reliability is determined by varying component failure rates by generic grouping.

Presentation is by table and graph. The tables list the relative reliabilities, but for graphical presentation it is more convenient to plot the probability of failure. Consequently a higher value represents a lower reliability.

The significance of the sensitivity analysis is shown in Figs. 3 and 4. In the comparative analysis conducted by NUS,[13] sensitivity analyses were performed to determine the effect on system reliability of varying component failure rates by generic grouping. Figure 3 shows the effect on system failure probability of varying the pump failure rate. If the pump failure rate

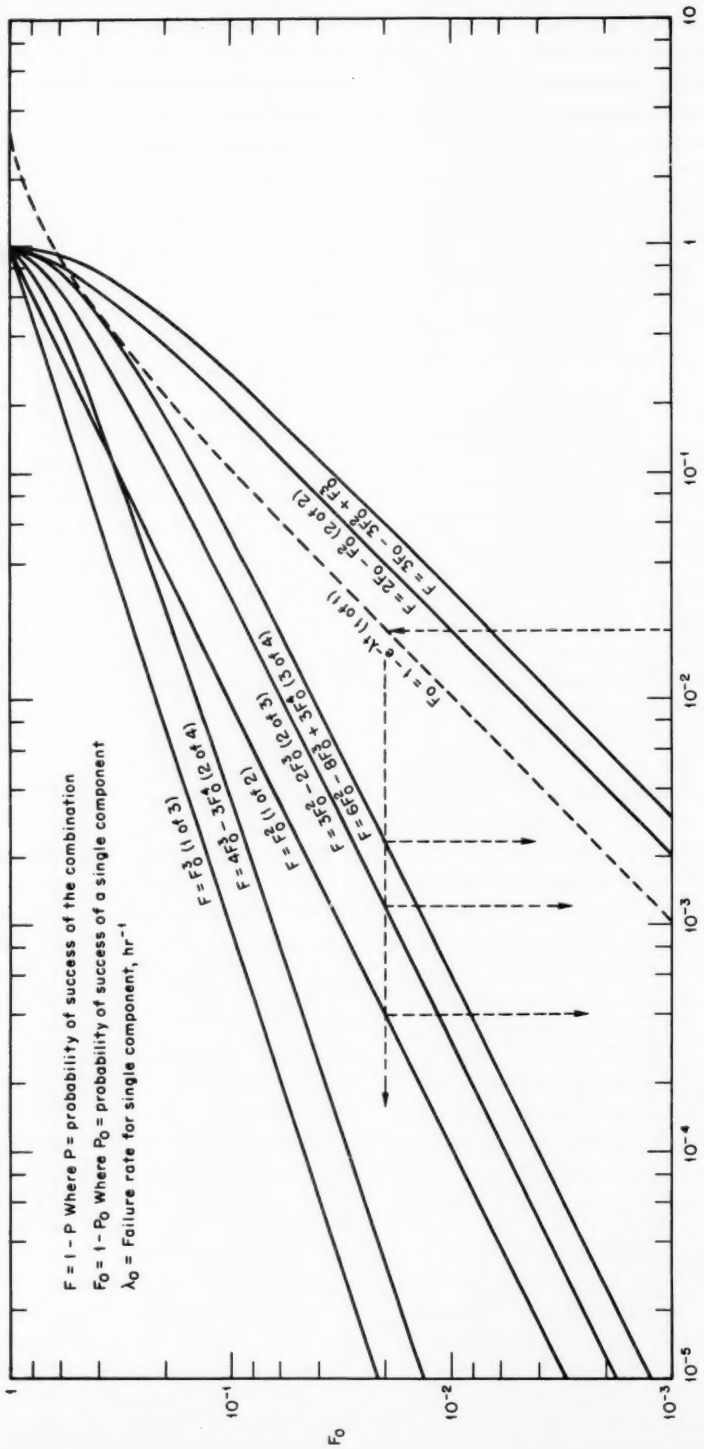
F = 1 - P Where P = probability of success of the combination
F0 = 1 - P0 Where P0 = probability of success of a single component
λ0 = Failure rate for single component, hr⁻¹
F = F0³ (1 of 3)
F = 4F0³ - 3F0⁴ (2 of 4)
F = F0² (1 of 2)
F = 3F0² - 2F0³ (2 of 3)
F = 3F0² - 8F0³ + 3F0⁴ (3 of 4)
F = 6F0² - 8F0³ + 3F0⁴ (2 of 4)
F = 3F0 - 3F0² + F0³ (2 of 2)
F = 2F0 - F0² (2 of 2)
F0 = 1 - e^-λ0t (1 of 1)
F0
F OR λ0t
1
10⁻¹
10⁻²
10⁻³
10⁻⁴
10⁻⁵
10
1
10⁻¹
10⁻²
10⁻³

Fig. 2 Failure probability for various redundant configurations.

is varied by one order of magnitude around the nominal value of 10^2 per 10^6 hr, the total system reliability varies significantly. Therefore it can be concluded that in this particular design the pump is a critical component which requires a larger proportionate share of effort in obtaining a high-quality design. Alternately, the sensitivity of this component may be reduced by considering additional redundancy, should the designer lack confidence in the validity of the failure-rate data available.

Figure 4 shows the effect of varying automatic-valve failure rates on total system reliability. In this case, for failure rates below approximately one failure per 100 cycles, there is no effect on the system failure probability. For valves of failure rate above approximately one failure per 100 cycles, the system failure probability is affected. However, since the nominal value for the failure rate of these particular valves is 10^{-3} per million cycles, it can be concluded that the system failure probability is insensitive to valve failure rate unless the valve failure rate is in error by several orders of magnitude.

Figures 3 and 4 show that the system failure probability for nominal value of failure rates is 10^{-5} Figure 3 shows that varying the pump failure rate around the nominal value changes the system failure

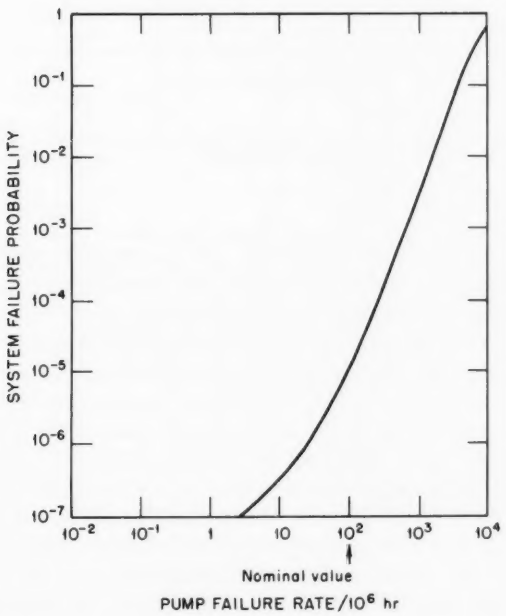

Fig. 3 Effect of varying pump failure rates on system failure probability.

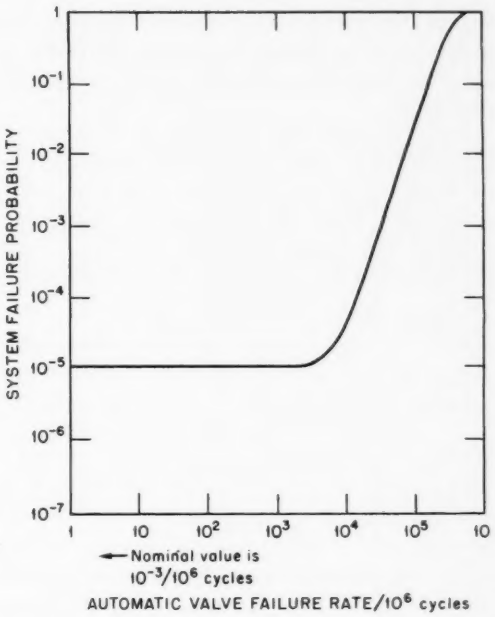

Fig. 4 Effect of varying automatic-valve failure rates on system failure probability.

probability. Varying the valve failure rate around the nominal value in Fig. 4 has no effect on the system failure probability until the failure rate is changed several orders of magnitude. Therefore it may be concluded that in this particular system design the pumps require more attention than the valves.

Sensitivity analysis plays an important role in subsequent engineering decisions. If the probability of system failure is found to be highly sensitive to the conditions of a particular component, it may be necessary to redesign that portion of the system. On the other hand, if the system is relatively insensitive to the failure probability of a particular component, a redesign for cost savings may be possible. The sensitivity analysis influences specifications for procurement or manufacture in that it defines those components which require a low failure rate. It justifies use of established component standards and eliminates unwarranted assignment of rigorous requirements.

Establishment of Testing Frequency

System reliability of redundant configuration can be significantly affected by periodic testing to reveal failed components. Bazovsky[15] shows this in a convenient graph (Fig. 5). This figure demonstrates a

principle: The average failure rate is a function of the test interval. It is important to note that this average failure rate obtained is not usable in further reliability calculations.

Figure 5 shows the curves of the instantaneous failure rate $\lambda(t)$ as a function of the operating time t, and of the average failure rate $\lambda_{av.}(T)$ as a function of the inspection time T. If no testing of the system were performed, the instantaneous failure rate $\lambda(t)$ would approach, in the limit, the value of λ_1, the failure rate of the system's most reliable redundant element which is capable of performing the system function alone. However, if the system were tested every T_1 hr, the instantaneous failure rate $\lambda(t)$ reduces to zero every T_1 hr, as shown in the zigzag curve at the bottom of the graph. The average failure rate $\lambda_{av.}(T_1)$ is shown as the mean line through this curve. Similarly, if the testing time were every T_2 hr, the failure rate would follow the dashed curve and would have the average failure rate $\lambda_{av.}(T_2)$. The $\lambda_{av.}(T)$ curve is the average failure rate of the system as a function of the inspection time T. From Fig. 5 it can be seen that by increasing the testing and repair frequency, the average failure rate can be reduced, thereby enhancing system reliability. There are practical limitations to this approach since too short a testing interval combined with a reasonable time for repair may impose operating restrictions on the plant. It is therefore desirable to maintain as long a test interval as possible without seriously compromising the overall system reliability.

Operating with Failed Components in Parallel Redundant Configurations

The effect of testing frequency of the components on systems reliability is determined as part of the system reliability calculation. For an existing plant the question arises as to the action that should be taken in the event one component of a parallel redundant configuration becomes inoperative. It is highly undesirable, from a plant operation point of view, to have to shut down the plant while the repair is being made. One approach that may be applicable is to increase the testing frequency of the remaining components of the parallel redundant configuration to achieve the same reliability as exists for the normal configuration. The objective is to choose a test interval such that the reliability of the reduced configuration at the end of the shortened test interval is no less than the reliability of the normal configuration at the end of a normal test interval. In practice, if a failure in the reduced configuration were revealed by the test, the system would be considered subminimal; this could require plant shutdown.

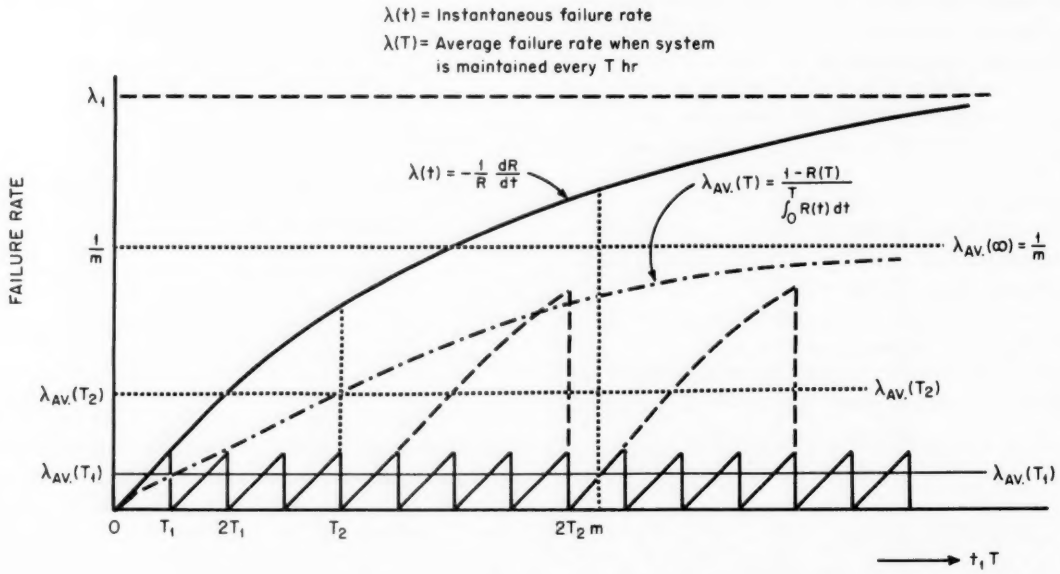

Fig. 5 Failure rate of redundant system without and with preventive maintenance.

This principle can be demonstrated in Fig. 6. A generalized curve has been developed which shows the dependence of the reduced test interval on failure rate for the remaining components of a parallel redundant configuration when one is inoperative, such that the same probability of success is attained as when all components of the parallel redundant configuration are operable. Two cases have been considered for demonstration purposes. Case A is a normal configuration of 1-of-2 dependence that becomes 1 of 1 in an abnormal situation. Case B is a normal 2-of-3 dependence that becomes 2 of 2 in an abnormal situation. The mathematical expressions for calculating these reliabilities are as follows.

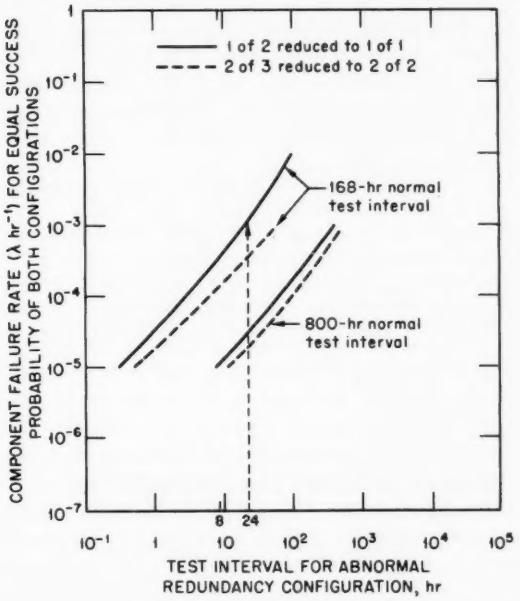

Fig. 6 Operating with failed components in parallel redundant configurations.

Case A: 1 of 2 normal; 1 of 1 abnormal

$$\text{Normal:} \quad R = 2\exp(-\lambda t_1) - \exp(-2\lambda t_1) \quad (1)$$

$$\text{Abnormal:} \quad R = \exp(-\lambda t_2) \quad (2)$$

Case B: 2 of 3 normal; 2 of 2 abnormal

$$\text{Normal:} \quad R = 3\exp(-2\lambda t_1) - 2\exp(-3\lambda t_1) \quad (3)$$

$$\text{Abnormal:} \quad R = \exp(-2\lambda t_2) \quad (4)$$

where λ = failure rate
R = reliability
t_1 = normal test interval
t_2 = shortened test interval

Two test periods for the normal configuration have been considered. They are 168 hr (weekly) and 800 hr (monthly). The curves were developed as follows:

1. For the 168-hr test interval and the 1-of-2 configuration, for t_1 = 168 hr, a value of λ was assumed.

2. The reliability of the 1-of-2 configuration was determined from Eq. 1.

3. Using the same assumed value of λ and the calculated value of R from Eq. 1, Eq. 2 was solved for the shortened test interval, t_2.

4. This process was repeated for several values of λ. As a result, the 168-hr test-interval curve in Fig. 6 represents the locus of points for defining the shortened test interval for a 1-of-1 configuration which will result in the same reliability as the normal test interval for a 1-of-2 configuration.

5. This process was repeated for the case of a 2-of-3 parallel redundance at 168 hr using Eqs. 3 and 4. The 1-of-2 and 2-of-3 parallel redundances at 800 hr were also calculated.

The use of these curves is demonstrated in the following example. For a given 1-of-2 parallel redundant configuration, each component is tested on a weekly (168-hr) basis. If, when performing this weekly test, one component is found to be inoperative, the same reliability can be achieved by increasing the test frequency of the remaining component. If the failure rate of the component is $10^{-3}\,hr^{-1}$, enter the ordinate of the curve of Fig. 6 at this value and move horizontally to the 168-hr curve for the 1-of-2 reduced to 1-of-1 curve. Move vertically to the abscissa and read 24 hr. This says that the reliability at the end of 24 hr for the 1-of-1 configuration is the same as the reliability at the end of 168 hr for the 1-of-2 configuration.

There are limitations in the application of this approach. If the failure rate of the component is $10^{-5}\,hr^{-1}$, it can be seen in Fig. 6 that for the 168-hr normal test interval for a 1-of-2 configuration, the abnormal configuration test interval is approximately 3×10^{-1} hr.

This test frequency is considered impractical in plant operation. However, if the component had a very low failure-rate probability, the normal test interval would probably be higher. This would offset that problem. Figure 6 shows that if the normal test interval

is 800 hr instead of 168 hr for the same failure rate, $10^{-5}\,hr^{-1}$, and the 1-of-2 normal configuration, the test interval for the 1-of-1 configuration to achieve the same reliability is approximately 8 hr. This would be acceptable operating practice.

This technique does not consider the effect of repair time. However, suppose the components being considered are pumps. Pumps must be limited to a finite number of starts or degradation of the pump or its associated circuitry will result. If, for example, nuclear safety-system pumps are tested on a weekly test interval for the normal configuration (1 of 2) and on an 8-hr test interval for the abnormal configuration (1 of 1), it would be advisable to establish the repair time on the basis of allowable starting cycles. Pumps of this type should conservatively be good for 500 starts before the reliability is affected. Therefore, if the repair time is established as 4 days ($\sim\frac{1}{2}$ the normal test time), the operating pumps would receive 12 start cycles during this period. This would not significantly affect the time interval between pump overhauls (~10 years) since it is not expected that this condition would occur very often.

Data

As discussed previously, the amount of failure data on equipment and components used specifically in nuclear reactor safety and protective systems is not adequate. The reason for this is twofold. First, there are not enough large nuclear generating stations in operation to provide data sources. Second, and perhaps most important, there is no organization for collecting, organizing, analyzing, and distributing the data that are being produced.

On the other hand, a number of organizations do accumulate and publish failure data on a variety of components, mostly for military application. Some of these data are applicable to nuclear reactor protection-system analyses.

For electronic components, MIL-HDBK-217A is useful. Also Air Force-sponsored work at the Rome Air Development Center (RADC) reliability bank is a convenient source of data. In particular, the Report RADC-TR-67-108(Vol. 2), Rome Air Development Center Reliability Notebook, Vol. II, provides extensive and useful data.

The Failure-Rate Data (FARADA) program is a joint effort of Army, Navy, Air Force, and NASA to compile and disseminate data to prime contractors and major subcontractors in military and space-systems equipment. The FARADA program is directed by the Naval Ordnance System Command and is administered by the Naval Fleet Missile Systems Analysis and Evaluation Group at Corona, Calif.

The FARADA program lists all types of components, both electronic and nonelectronic. However, participation in the program is, in general, limited to government contractors, and the data are not available for commercial application through normal channels.

For nonelectronic component failure data, the Naval Material Management Maintenance Data Collection System and the Air Force 66-1 Data Program are valuable sources. Also, Report RADC-TR-66-828, RADC Unanalyzed Nonelectronic Part Failure Data, contains data applicable to the nuclear power program. Some other sources of failure data are:

W. H. Dickinson, Report on Reliability of Electric Equipment in Industrial Plants, AIEE paper 62-61, July 1962.

D. R. Earls and M. F. Eddins, Reliability Engineering Data Series Failure Rates, AVCO Corporation, April 1962.

S. N. Greenberg, Reliability Analysis Data for Systems and Component Design Engineers—Handbook, Report TRA-873-74, General Electric Company and MSD, 1965.

Conclusions

A significant amount of work has been done in the field of reliability and applied with great success to nonnuclear systems. The application of formal reliability evaluation methods to all nuclear plant systems will result in higher levels of probability of the system to function when called upon to operate. Unfortunately a standard reliability approach to nuclear safety systems is not in use today. Hence the rationale for designing nuclear safety systems does not always follow a logical sequence. Reliability techniques are useful engineering tools for the designer in selecting the best of alternative approaches in system design, and these techniques can be useful to the evaluation of license applications to determine adequacy of designs in meeting the established functional requirements as defined in the AEC design criteria.[16] System changes that could improve the overall design from a reliability standpoint become apparent. In addition, the most critical components affecting overall reliability and their order of importance can be identified.

Most of the analyses can be performed without a computer. However, when the complexity of the design demands it, computer programs are available to solve the more sophisticated aspects. Nuclear safety system designs, for the most part, can be handled by means of relatively simple mathematical equations or nomographs. The absence of absolute failure-rate data

can be overcome by the performance of comparative analyses using the sensitivity analysis to identify the critical parts of the design. Since the analysis is comparative, the absolute value of the failure rate of a component usually does not significantly affect the determination as to which of the two systems being compared has the highest probability of success.

Another important consideration is the relation between reliability and quality control. It would be highly desirable if a correlation could be made relating the degree of quality control required to achieve a certain failure rate. (This has been accomplished with considerable success in programs such as Minuteman and Apollo.) Until failure-rate data are available for the components of the system being analyzed, this correlation cannot be made. Until better data are available, the components must be designed, fabricated, and inspected to codes and specifications consistent with the highest commercial nuclear standards. A sensitivity analysis showing certain components to be critical would justify, for example, prototype testing under worst-case environmental conditions. As an alternative the designer may add redundant components if economics allow and if the analysis indicates the same system reliability can be achieved. Additional requirements are costly and therefore should not be indiscriminately applied to all components. The reliability analysis provides the rationale for preventing this.

References

1. I. M. Jacobs, Reliability of Engineered Safety Features as a Function of Testing Frequency, *Nucl. Safety*, 9(4): 303-312 (July–August 1968).
2. I. M. Jacobs, Reactor Protection System. A Reliability Analysis, Report APED-5179, General Electric Company, Atomic Power Equipment Department, June 1966.
3. B. J. Garrick et al., Reliability Analysis of Nuclear Power Plant Protective Systems, USAEC Report HN-190, Holmes and Narver, Inc., Nuclear Division, May 1967.
4. A. R. Eames, Reliability Assessment of Protective Equipment for Nuclear Installations, British Report AHSB(s)R-99, 1965.
5. A. E. Green and A. J. Bourne, Safety Assessment with Reference to Automatic Protective Systems for Nuclear Reactors, British Report AHSB(s)R-117, (Pts. 1 to 3), 1966.
6. E. Parker and R. Roughley, AHSB Reporting System for Plant Faults—Plant Fault Code, British Report AHSB(s)R-127, 1967.
7. A. R. Eames, Data Store Requirements Arising Out of Reliability Analyses, British Report AHSB(s)R-138, 1967.
8. E. R. Snaith, D. Scarrott, and P. Burden, Field Data Reporting Experience in the United Kingdom, Euratom Committee on Reactor Safety Technology, meeting of specialists on the reliability of electrical supply systems and related electromechanical components for nuclear reactor safety, Ispra, Italy, June 27–28, 1968; available from E. R. Snaith or D. Scarrott, United Kingdom Atomic Energy Authority, Risley.
9. J. Ehrentreich and H. Maurer, Reliability Considerations for Electro-Mechanical and Hydraulic Control Rod Drive Systems, Euratom Committee on Reactor Safety Technology, meeting of specialists on the reliability of electrical supply systems and related electromechanical components for nuclear reactor safety, Ispra, Italy, June 27–28, 1968; available from J. E. Ehrentreich or H. Maurer, Euratom Bruxelles, rue Belliard 51-53, Brussels, Belgium.
10. G. Mieze and J. Ebmann, Reliability Analysis of an Emergency Power Supply System, Euratom Committee on Reactor Safety Technology, meeting of specialists on the reliability of electrical supply systems and related electromechanical components for nuclear reactor safety, Ispra, Italy, June 27–28, 1968; available from G. Mieze or J. Ebmann, Institut für Reaktorsicherheit der Technischen Überwachungs-Vereine E. V. Köln, Germany.
11. C. W. McKnight et al., Automatic Reliability Mathematical Model, Report NA-66-838, North American Aviation, Inc.
12. C. W. McKnight et al., An Automatic Reliability Mathematical Model, in *Reliability and Quality Control*, Symposium Proceedings, Miami Beach, Fla., Jan. 12–14, 1965, Institute of Electrical and Electronic Engineers, New York, 1965.
13. C. A. Negin, J. R. Lennon, and E. A. Saltarelli, Comparative Reliability Analysis of Two Pressurized Water Reactor Containment Cooling Systems, USAEC Report NUS-449, NUS Corporation, June 1968.
14. Rome Air Development Center, RADC Unanalyzed Nonelectronic Part Failure-Rate Data Interim Report NED CO 1, Report RADC-TR-66-828, December 1966.
15. I. Bazovsky, *Reliability Theory and Practice*, International Series in Engineering, Prentice-Hall, Inc., Englewood Cliffs, N. J., 1961.
16. General Design Criteria for Nuclear Power Plant Construction Permits, Appendix A of 10 CFR 50 and *Federal Register*, July 11, 1967.

Radiolytic Decomposition of Water in Water-Moderated Reactors Under Accident Conditions

By Stanley E. Turner*

Over the years, radiolytic decomposition of water has been the subject of extensive investigation, primarily in connection with the operation of water-moderated power reactors. Although sufficient information of an engineering nature is available to predict decomposition effects during reactor operation, little information is available for conditions more nearly representative of those expected after a major loss-of-coolant accident. The purpose of this review is to provide a practical evaluation of the potential concentrations of radiolytic gases (hydrogen and oxygen) which may accumulate in the containment atmosphere following a loss-of-coolant accident. Results of the evaluation indicate a reasonable probability that hydrogen and oxygen will accumulate in amounts exceeding the minimum combustible concentration (combustible, or flammable, limit).

Theoretical considerations based on radiolysis data obtained with highly purified water indicate a hydrogen concentration at saturation (equilibrium) of ~1 to 3.9%. However, in practice, the impurities that would be present in the water under postulated conditions are expected to increase the saturation concentration of hydrogen by a significant factor. An estimate of the increase due to even trace quantities of impurities is largely a matter of judgment. At present, if one considers the various contributing factors, a value of 6 to 8 vol.% hydrogen appears to be a reasonable estimate of the limiting or saturation concentration of hydrogen in the containment atmosphere under accident conditions. The limited experimental evidence that is available tends to support the stated saturation value of 6 to 8%.

The saturation concentration of hydrogen in the containment will be the same for pressurized- and boiling-water reactors, although the rate of hydrogen accumulation will be different for the two reactor types. For reactors of the same power, the containment for a boiling-water plant will be smaller than that for a pressurized-water plant; consequently, the rate of hydrogen accumulation (in terms of %/time) will be higher in the boiling-water reactor (BWR) than in the pressurized-water reactor (PWR). To illustrate this point, it can be said that typical values of the time required (under the same set of conservative assumptions) to reach a combustible concentration of hydrogen (assumed to be ~4 vol.%) might be of the order of 16 hr for large BWR's of modern design and perhaps 15 days for current large PWR's. There appears to be more than enough shutdown or decay energy in the reactor fuel to produce a hydrogen concentration in excess of the combustible limit, provided conservative assumptions are made regarding the factors affecting the net rate of hydrogen production.

The net *rate* of hydrogen production is affected principally by two factors: (1) the fraction of the shutdown or decay energy absorbed by the water and (2) the effective rate of hydrogen-gas production per unit of energy absorbed by the water. The greatest uncertainty is attached to the second of these two factors, with experimental values ranging from very low values for stagnant water (where considerable recombination can occur) to an upper limit when hydrogen is swept out by boiling and violent agitation

*Southern Nuclear Engineering, Inc., Dunedin, Fla.

before significant recombination occurs. Following a loss-of-coolant accident, boiling and violent agitation can be expected with an attendant high net rate of hydrogen production. At some later time the coolant will become relatively quiescent, agitated by the recirculation flow. For the latter condition a lower net yield of hydrogen gas would seem reasonable, but experimental justification for a lower value is not available. Consequently, until further experimental information is available, and until a description of the history of events following the accident is developed, a conservative approach (i.e., assuming the upper limit for the hydrogen production rate) appears necessary in arriving at an estimate of the time dependence for hydrogen accumulation.

In view of the possibility of accumulating combustible amounts of radiolytic gases following a loss-of-coolant accident, it seems necessary to (1) obtain additional experimental information to establish the validity of lower values for the hydrogen yield factors under accident conditions, (2) consider means of controlling the hydrogen concentration, or (3) develop convincing arguments that ignition of the flammable mixture of gases will not cause unacceptable damage to the containment or equipment within it.

Theoretical Considerations

The radiolytic decomposition of water is a complex process involving the formation of numerous intermediate products; these products may react in various ways, including combination to re-form water. Because of the very low concentrations of the intermediate, highly reactive decomposition products present at any given time in water under irradiation, even small quantities of impurities can affect significantly the net decomposition observed. Consequently, considerable uncertainty exists in the quantitative description of the radiolytic-decomposition process, and only those data obtained under very carefully controlled experimental conditions can be considered sufficiently reliable for use in theoretical interpretation of the process. The same uncertainty must, of course, be reflected in any final estimate of the level of radiolytic gases that may accumulate in the containment building of a reactor in the event of a major accident.

An excellent summary of the understanding of the radiolytic-decomposition processes in water has been given by Allen,[1] based on information available through 1961. Fundamentally, the radiolytic-decomposition process may be viewed in a simple sense as yielding H_2 and H_2O_2 as the direct decomposition products. It has been observed that the decomposition of water follows the expected mass action law in the presence of excess hydrogen. This behavior accounts principally for the lack of any net decomposition in operating PWR's, for the hydrogen-gas overpressure enhances recombination and effectively suppresses the decomposition. In the absence of other chemical reagents, an excess of oxygen does not appear to suppress decomposition but, in fact, tends to enhance the net yield of hydrogen.

The actual behavior of water under the influence of ionizing radiation is more complex than the simple process mentioned above; i.e., one which yields only H_2 and H_2O_2. Direct products thought[2,3] to occur as a result of the action of radiation on water include molecular hydrogen (H_2), atomic hydrogen (H), the hydroxyl radical (OH), hydrogen peroxide (H_2O_2), and the solvated electron ($e^-_{aq.}$). Evidence supporting the existence of the $e^-_{aq.}$ was discussed by Allen,[1] although he does not completely differentiate between $e^-_{aq.}$ and H as direct products of radiolytic decomposition. To some extent $e^-_{aq.}$ may be considered as one of the ionization products of atomic hydrogen, with the other product being the hydrogen ion (i.e., $H \rightleftharpoons^{H_2O} H^+ + e^-_{aq.}$). Presumably, the immediate products of an ionization rupture of the chemical bond in water would be H or e^- and OH, although these, in part, react within the track (or "spur") on the ionizing radiation to yield the apparent products H_2, H, $e^-_{aq.}$, OH, and H_2O_2.*

Yields from radiolysis of water are usually reported in terms of a *"G"* factor, which is defined as the number of molecules or radicals of the designated product formed per 100 ev of energy absorbed. Generally, subscripts are used to designate primary yield values and a parenthetical designation used to indicate the net or observed yield. Under this convention,† G_{H_2} indicates the yield of molecular hydrogen resulting from the direct action of radiation on water, and $G(H_2)$ represents the net observed hydrogen yield produced by the combination of direct radiation in

*A sixth direct dissociation product, HO_2, apparently can be formed with radiation of high specific ionization (i.e, alpha particles, protons, neutrons, etc.) but does not appear under gamma or beta radiation. Since the present evaluation is concerned only with radiolysis resulting from fission-product decay energy (i.e., gamma and beta radiation), effects associated with radiation of higher linear energy transfer (LET) have not been considered.

†Care should be exercised in reviewing literature articles, since not all authors have adopted or rigorously applied this symbolism for designating yields.

conjunction with all subsequent chemical reactions. The subscripted G values (e.g., G_{H_2}) may be considered as the yield within the ionizing track (or spur) before the products have had an opportunity to diffuse into the water and react chemically with other products or materials. Material-balance considerations impose the requirement that

$$2G_{H_2} + E_{e^-_{aq.}} + G_H = G_{H_2O_2} + G_{OH} \qquad (1)$$

Values of G for the direct yield from gamma radiation, based on the work of numerous investigators, have been derived by Allen[1] and later reviewed by Jenks.[2] These values, shown in Table 1, represent at least reasonable, and probably the "best," values consistent with the current theory. Also shown in Table 1 are the values developed in the Soviet Union (presumably derived independently) and reported by Ershler.[4] Although uncertainty exists in these yield values, the information given by Allen[1] can be used to infer an accuracy of about ±5%, with the exception of the $G_{e^-_{aq.}}$ and G_H derived by Jenks.[2] Values of $G_{e^-_{aq.}}$ ranging from 1.2 to 2.9 have been reported (see discussion in Jenks' report[2]), and the best value would appear to be 2.31, based largely on material-balance requirements.

Table 1 Yields of Primary Products of Gamma Radiolysis of Pure Water

(Direct Yield, G, in Terms of Molecules or Radicals Formed per 100 ev Absorbed)

	G_{H_2}	$G_{e^-_{aq.}}$	G_H	$G_{H_2O_2}$	G_{OH}
Jenks values[2]	0.44	2.31	0.44	0.70	2.34
Allen values[1]	0.45	2.9		0.71	2.34
Ershler values[4]	0.45	2.75		0.70	2.25

Once formed, the direct radiolytic products can undergo a variety of chemical reactions which are generally assumed to occur uniformly throughout the irradiated water. The most recent listing of contributing chemical reactions has been compiled by Jenks[2,3] and is reproduced here as Table 2. Of the 20 reactions

Table 2 Interactions of Radiolytic Products of Water Including Rate Constants and Assumed Activation Energies[2,3]

Reaction No.	Reaction	Rate constants at or near 25°C (sec^{-1}, M^{-1}, liter)	Assumed activation energy, kcal/mole
8	$e^-_{aq.} + O_2 \rightarrow O_2^-$	1.9×10^{10}	3
9	$e^-_{aq.} + H_2O_2 \rightarrow OH + OH^-$	1.2×10^{10}	3
11	$H + O_2 \rightarrow HO_2$	2×10^{10}	3
12	$H_2 + OH \rightarrow H + H_2O$	4.5×10^7	7
14	$H_2O_2 + OH \rightarrow HO_2 + H_2O$	4.5×10^7	4.5
15	$HO_2 + H_2O_2 \rightarrow OH + H_2O + O_2$	3.7	20
16	$2HO_2 \rightarrow H_2O_2 + O_2$	2.7×10^6	5
16*b*	$O_2^- + O_2^- \xrightarrow{2\,H_2O} H_2O_2 + O_2 + 2OH^-$	1.7×10^7	5
18	$OH + HO_2 \rightarrow H_2O + O_2$	4×10^9	3
18*b*	$OH + HO_2 \rightarrow H_2O_3$	1.1×10^{10}	3
20	$OH + OH \rightarrow H_2O_2$	4×10^9	3
21	$H + H_2O_2 \rightarrow H_2O + OH$	4.4×10^7	4.5
22	$e^-_{aq.} + H^+ \rightarrow H$	2.3×10^{10}	3
23*a*	$e^-_{aq.} + HO_2 \rightarrow H_2O_2$	2×10^{10}	3
23	$H + HO_2 \rightarrow H_2O_2$	2×10^{10}	3
26	$e^-_{aq.} + e^-_{aq.} \xrightarrow{2\,H_2O} H_2 + 2OH^-$	5×10^9	3
27	$e^-_{aq.} + OH \rightarrow OH^-$	3×10^{10}	3
28	$H + H \rightarrow H_2$	1.3×10^{10}	3
29	$H + OH \rightarrow H_2O$	2.5×10^{10}	3
30	$e^-_{aq.} + H \xrightarrow{H_2O} H_2 + OH^-$	3×10^{10}	3

listed in Table 2, seven were considered to define the principal reaction route, and these are listed below to facilitate easy reference.

Reaction No.	Reaction
8	$e^-_{aq.} + O_2 \rightarrow O_2^-$
9	$e^-_{aq.} + H_2O_2 \rightarrow OH + OH^-$
11	$H + O_2 \rightarrow HO_2$
12	$H_2 + OH \rightarrow H + H_2O$
14	$H_2O_2 + OH \rightarrow HO_2 + H_2O$
16	$2HO_2 \rightarrow H_2O_2 + O_2$
18	$OH + HO_2 \rightarrow H_2O + O_2$

Earlier, Allen[1] had postulated a series of six reactions which (allowing for the fact that he did not completely distinguish between $e^-_{aq.}$ and H) are identical to the first six reactions shown above. These reactions are applicable to those dissociation products present *in solution,* and recombination reactions apparently do not occur to any significant extent in the vapor phase.* The presence of a free volume into which some of the net dissociation products (i.e., H_2 and O_2) may escape as gases must be taken into account in evaluating the effects of radiolysis of water. Apparently, most of the experimental work referred to by Allen[1] and Jenks[2] was performed in closed systems, without free gas spaces, to investigate the basic chemical behavior in solution.

If a closed, or single-phase, system is used, escape of radiolytic gases is not permitted and equilibrium concentrations of radiolytic products are rapidly established. Under equilibrium conditions the net rate of change in concentration of the various radiolytic products becomes zero (i.e., the rate of formation equals the rate of consumption), and the chemical reactions postulated by Jenks (see Table 2) may be described by a series of seven simultaneous equations involving the direct radiolysis yields, the equilibrium concentrations, and the reaction rates. These equations, along with an eighth equation derived from material-balance considerations, are shown in Table 3, which has been extracted from Jenks' report.[2] By limiting the chemical reactions considered to the seven principal ones, and by making certain simplifying assumptions (i.e., G_H and G_{HO_2} are taken as zero† and HO_2, H, $e^-_{aq.}$, and OH concentrations are neglected in the material balance), the system of simultaneous equations may be considerably simplified and analytical expressions derived. The simplified equations and the analytical expressions developed by Jenks are shown in Table 4. These equations, which are similar to those developed earlier by Allen, are presumably valid under fairly low-intensity gamma radiation where radical concentrations are sufficiently low to justify neglecting many of their possible interactions. In his report,[2] Jenks states that "These analytic expressions are approximately valid under some of the conditions

*Apparently, large G value for recombination in the vapor phase has been observed,[5] but the low density of the gas reduces the net overall gaseous-phase recombination to a low level; this effect has been neglected for the purposes of the present review.

†In the approximation $G_H = 0$, the direct yield of $G_{e^-_{aq.}}$ must be increased to 2.86 to maintain the proper material balance and to account for the actual G_H which has been neglected.

Table 3 Simultaneous Equations‡ at Steady State[2]

1. $0 = B + k_9(e^-_{aq.})(H_2O_2) - k_{12}(H_2)(OH) - k_{14}(OH)(H_2O_2) - k_{18}(OH)(HO_2) - 2k_{20}(OH)^2 + k_{21}(H_2O_2)(H) + k_{15}(H_2O_2)(HO_2) - k_{27}(OH)(e^-_{aq.}) - k_{29}(OH)(H)$
2. $0 = C + k_{16b}(HO_2)^2 + k_{23}(e^-_{aq.})(HO_2) + k_{20}(OH)^2 - k_9(H_2O_2)(e^-_{aq.}) - k_{14}(OH)(H_2O_2) - k_{15}(HO_2)(H_2O_2) - k_{21}(H_2O_2)(H) + k_{23}(H)(HO_2)$
3. $0 = k_{15}(H_2O_2)(HO_2) + k_{16b}(HO_2)^2 + k_{18}(OH)(HO_2) - k_8(e^-_{aq.})(O_2) - k_{11}(H)(O_2)$
4. $0 = L + k_8(e^-_{aq.})(O_2) + k_{11}(H)(O_2) + k_{14}(OH)(H_2O_2) - k_{15}(H_2O_2)(HO_2) - 2k_{16b}(HO_2)^2 - k_{18}(OH)(HO_2) - k_{23}(H)(HO_2) - k_{23}(e^-_{aq.})(HO_2)$
5. $0 = F - k_8(e^-_{aq.})(O_2) - k_9(H_2O_2)(e^-_{aq.}) - k_{22}(H^+)(e^-_{aq.}) - 2k_{26}(e^-_{aq.})^2 - k_{27}(OH)(e^-_{aq.}) - k_{30}(H)(e^-_{aq.}) - k_{23}(e^-_{aq.})(HO_2)$
6. $0 = A - k_{12}(H_2)(OH) + k_{28}(H)^2 + k_{26}(e^-_{aq.})^2 + k_{30}(H)(e^-_{aq.})$
7. $0 = 2(H_2) + (e^-_{aq.}) + (H) + 2\alpha - [2(H_2O_2) + 4(O_2) + 3(HO_2) + (OH)]$
8. $0 = M + k_{12}(OH)(H_2) + k_{22}(H^+)(e^-_{aq.}) - k_{11}(H)(O_2) - k_{23}(H)(HO_2) - k_{21}(H)(H_2O_2) - 2k_{28}(H)^2 - k_{29}(H)(OH) - k_{30}(H)(e^-_{aq.})$

‡A, B, C, F, M, and L are rates of formation of H_2, OH, H_2O_2, $e^-_{aq.}$, H, and HO_2, respectively. Parenthetical expressions designate molar concentrations of the species.

Table 4 Simultaneous Equations and Derived Analytic Expressions[2]

(Reactions 8, 9, 11, 12, 14, 16, and 18)

Simultaneous Equations

1*a*. $0 = B - A + k_9(e^-_{aq.})(H_2O_2) - k_{14}(OH)(H_2O_2) - k_{18}(OH)(HO_2)$

2*a*. $0 = C + k_{16}(HO_2)^2 - k_9(e^-_{aq.})(H_2O_2) - k_{14}(OH)(H_2O_2)$

3*a*. $0 = k_{16b}(HO_2)^2 + k_{18}(OH)(HO_2) - k_8(e^-_{aq.})(O_2) - A$

4*a*. $0 = A + k_8(e^-_{aq.})(O_2) + k_{14}(OH)(H_2O_2) - k_{18}(OH)(HO_2) - 2k_{16b}(HO_2)^2$

5*a*. $0 = F - k_8(O_2)(e^-_{aq.}) - k_9(H_2O_2)(e^-_{aq.})$

6*a*. $0 = A - k_{12}(H_2)(OH)$

7*a*. $0 = (H_2) + \alpha - (H_2O_2) - 2(O_2)$

Analytic Expressions

9. $$\frac{k_{14}\,C\,\alpha(OH)}{T\,k_9} + \frac{k_{18}\,(OH)}{\sqrt{T\,k_{12}}}\sqrt{A + \alpha k_{12}(OH)}\sqrt{\frac{k_{14}\,C}{k_{16}\,k_9}} = C - A + B - \frac{k_{14}\,CA}{T\,k_9\,k_{12}}$$

9*a*. $$T = C/k_9 + \frac{2(F - C)}{k_8}$$

10. $$(H_2) = \frac{A}{k_{12}(OH)}$$

11. $$(e^-_{aq.}) = \frac{T\,k_{12}(OH)}{A + \alpha k_{12}(OH)}$$

12. $$(H_2O_2) = C/k_9\,(e^-_{aq.})$$

13. $$(O_2) = \frac{F - C}{k_8(e^-_{aq.})}$$

14. $$(HO_2)^2 = \frac{k_{14}}{k_{16}}\frac{C}{k_9}\frac{(OH)}{(e^-_{aq.})}$$

which were considered, ..." Although no information has been found to substantiate the range or conditions of validity of these approximations, it is expected that they will apply with acceptable accuracy under the relatively low-intensity shutdown gamma radiation considered in this evaluation. It should be emphasized, however, that the analytical expressions in Table 4 were developed on the basis of a material-balance equation (Eq. 7*a* of Table 4) which is valid only in solution and does not include provision for free exchange of gases with a vapor space above the water.

In earlier work, Allen developed equations similar to those of Jenks (reaction 18 is omitted in Allen's work) and gave[1] a comparison of the theoretical concentrations with experimentally determined values. The comparison is shown here as Fig. 1. Allen's curves (Fig. 1) were developed largely on the basis of the experimental data of Hochanadel[6] which were obtained for solutions in a closed system without a vapor space and (with but one exception) used added hydrogen peroxide to establish the initial level of "excess oxidant." These data are applicable to highly purified water and are in apparent conflict with experimental data obtained by Dolin and Ershler[7] and by Zittel[8] at Oak Ridge.

In developing the Soviet theory of radiolytic decomposition, Ershler[4] has postulated a series of reactions which he considers to be the essential processes. These reactions and the corresponding reactions from Jenks[2] (Table 2) are:

Reactions postulated by Ershler	Jenks' reaction numbers
(1) $H_2O_2 + H \rightarrow H_2O + OH$	9 and 21
(2) $H_2 + OH \rightarrow H_2O + H$	12
(3) $H_2O_2 + OH \rightarrow H_2O + HO_2$	14
(4) $HO_2 + H \rightarrow H_2O_2$	23
(5) $2\,HO_2 \rightarrow H_2O_2 + O_2$	16
(6) $H + O_2 \rightarrow HO_2$	11 and 8
(7) $HO_2 + H_2O_2 \rightarrow H_2O + O_2 + OH$	15
(8) $H + H \rightarrow H_2$	28

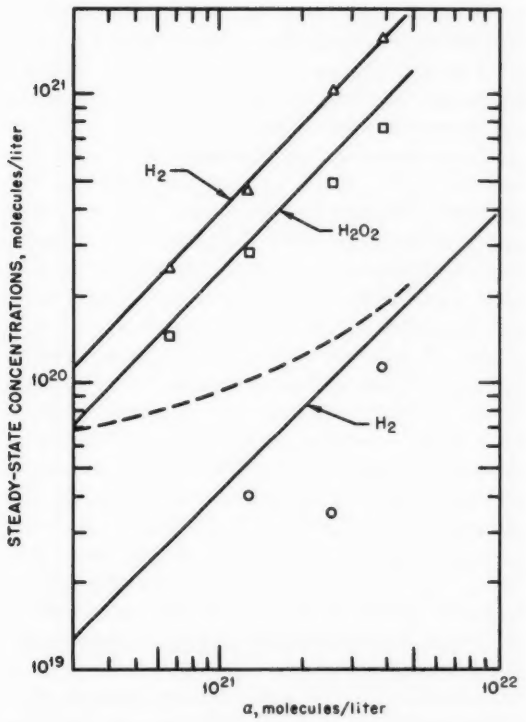

Fig. 1 Theoretical and experimental concentrations of H_2, H_2O_2, and O_2 under equilibrium conditions. The dashed curve is from the Dolin and Ershler[7] data for H_2. (Reproduced from A. O. Allen, *The Radiation Chemistry of Water and Aqueous Solutions,* by permission of Van Nostrand–Reinhold, a division of Litton Industries, Princeton, N. J., 1961.)

The simultaneous equations describing equilibrium concentration, based on the reactions postulated by Ershler, have not been solved for this review. The reactions are all included among those proposed by Jenks, so there is no reason to anticipate that the resulting equilibrium concentrations would differ materially from those predicted by Jenks and Allen.

Superimposed in Fig. 1 is a curve representing concentrations calculated from Russian data given by Dolin and Ershler.[7] In this case the irradiation cell contained a gas space that could conceivably be a contributing factor in the appreciably higher hydrogen concentrations shown in the figure. Allen[9] has discounted the results of Dolin and Ershler,[7] noting that the measured total gas pressures were those to be expected from the observed peroxide concentrations, and has concluded that "their gas analysis was subject to some unsuspected systematic error." However, the Dolin and Ershler data also indicate a higher peroxide concentration than would be predicted theoretically. Allen further concludes[5] that, at the time the Dolin and Ershler[7] data were taken, the sensitivity to small amounts of impurities was not fully appreciated and that this factor could account for significant discrepancies between actual radiolytic yields and theoretical predictions. It may be significant that Ershler, in a later publication,[4] does not utilize or refer to his own earlier data in developing a theoretical explanation of the radiolytic-decomposition process.

In an effort to investigate the importance of the gas-to-liquid ratio on the equilibrium concentrations, the simultaneous equations (Table 4) describing the steady-state conditions were solved using a different material-balance equation. The total quantity (Q) of gaseous components (H_2 and O_2) in the system can be represented by the following relations:

$$\frac{Q_{H_2}}{V_{liq.}} = [H_2]\left(1 + \frac{V_{gas}}{V_{liq.}} \cdot \frac{1}{S_{H_2}}\right) \qquad (2)$$

and

$$\frac{Q_{O_2}}{V_{liq.}} = [O_2]\left(1 + \frac{V_{gas}}{V_{liq.}} \cdot \frac{1}{S_{O_2}}\right) \qquad (3)$$

where $V_{gas}/V_{liq.}$ is the gas-to-liquid volume ratio and S is the solubility coefficient in liters of gas per liter of solution at standard conditions. (The terms in brackets designate the concentrations of these species in solution, usually expressed in moles per liter.) The material-balance equation then becomes

$$[H_2]\left(1 + \frac{V_{gas}}{V_{liq.}} \cdot \frac{1}{S_{H_2}}\right) + \alpha - [H_2O_2] \times \left(1 + \frac{V_{gas}}{V_{liq.}} \cdot \frac{1}{S_{O_2}}\right) = 0 \qquad (4)$$

or, alternatively,

$$a[H_2] + \alpha - [H_2O_2] - b[O_2] = 0 \qquad (5)$$

where a and b are the large parenthetical expressions in Eq. 4. Utilizing this relation in lieu of Eq. 7*a* in Table 4, the revised analytical expressions become

$$\frac{k_{14} C \alpha [OH]}{T k_9} + \frac{k_{18}[OH]}{\sqrt{T k_{12}}} \sqrt{a A + \alpha k_{12}[OH]} \times \sqrt{\frac{k_{14} C}{k_{16} k_9}} = C - A + B - \frac{k_{14} C a A}{k_9 T k_{12}} \qquad (6)$$

$$T = \frac{C}{k_9} + \frac{2b(F - C)}{k_8} \tag{7}$$

and

$$[e^-_{aq.}] = \frac{Tk_{12}\ [OH]}{aA + \alpha k_{12}\ [OH]} \tag{8}$$

with the remaining expressions identical to those obtained by Jenks.

Calculations made with the revised set of analytical expressions have indicated that, for water initially saturated with air, the gas-to-liquid ratio has a rather minor effect on the equilibrium concentrations. (For a $V_{gas}/V_{liq.}$ of 25, hydrogen-gas concentration was increased by about 30% over the calculated values for no gas space.) In a crude sense the effect of a gas space—initially air containing ~20% oxygen—may be viewed as tending to replenish oxygen initially consumed in solution by HO_2 and H_2O_2 formation (Jenks' reactions 8, 11, and 16). Therefore equilibrium conditions will be attained at a slightly higher oxygen concentration (or effective excess oxidant—see Fig. 1), and the hydrogen yield will also be proportionately higher.

The analytical expressions developed in this review (and by Jenks and Allen) may be used to formulate an expression for the ratio of the equilibrium concentrations of H_2 and O_2, independent of the material-balance equation, as follows:*

$$\frac{[H_2]}{[O_2]} = 2\frac{k_8 k_{14}}{k_9 k_{12}} \frac{AC}{(F - C)(F + B)} \tag{9}$$

*In this derivation, the quantity $k_8\ [HO_2]$ was assumed to be negligibly small compared to $k_{14}\ [H_2O_2]$. In view of the short lifetime and low concentration of the HO_2 radical, this approximation should be valid for gamma radiation.

The ratios of partial pressures at equilibrium conditions were calculated on the basis of the gas-solubility data given in Ref. 10, the yield data in Table 1, and the assumption that Henry's law is valid. Results of the calculations are given in Table 5.

From the preceding discussion, the equilibrium ratio of hydrogen to oxygen concentration in the liquid or vapor space should be approximately constant for a given temperature, independent of material-balance requirements or radiation intensity.† Both of these latter factors enter into determining the absolute concentrations but do not alter the ratio. If it is assumed that the gas space is sufficiently large and the radiation intensity sufficiently low that the equilibrium partial pressure of oxygen is not materially different from that in ordinary air (i.e., p_{O_2} = 0.2 atm at atmospheric pressure), then the limiting pressure of the hydrogen generated by radiolytic decomposition will be approximately as shown in Table 5. The lower hydrogen concentrations at elevated temperatures may be qualitatively attributed to two factors: (1) the increased rate of the recombination reactions and (2) the reduced oxygen solubility, which allows equilibrium hydrogen to be attained at a lower concentration. A counteracting effect is the reduced hydrogen solubility, although the solubility of hydrogen does not decrease as rapidly as that of oxygen between 25 and 80°C. Under postaccident conditions in a nuclear plant, the calculated saturation pressure may range

†Both theory and experiment indicate that the concentrations are roughly proportional to the square root of the radiation intensity. The shutdown decay radiation intensity is relatively low—at most a few tenths 1 watt/cm^3—and the calculated $[O_2]$ is not greatly different from that of air-saturated water.

Table 5 Hydrogen-to-Oxygen Ratios at Equilibrium Conditions

	Jenks yields		Allen yields	Ershler yields
	25°C	80°C	25°C	25°C
$[H_2]/[O_2]$ in solution	0.087	0.043	0.106	0.120
p_{H_2}/p_{O_2}	0.140	0.047	0.171	0.194
$p_{H_2}/(p_{O_2}$ = 0.2 atm)	0.028	0.009	0.034	0.039

	25°C	80°C
Solubility constants (Ref. 10)		
Hydrogen (S_{H_2}),‡ or liter-atm/mole	0.01754 1.27×10^3	0.0160 1.40×10^3
Oxygen (S_{O_2}),‡ or liter-atm/mole	0.02831 0.7912×10^3	0.0170 1.272×10^3

‡Solubility coefficient is the volume of gas reduced to standard conditions dissolved in 1 volume of water when the pressure of the gas is 1 atm.

from 0.009 atm (~1%), using Jenks' data at 80°C, to as much as 0.039 atm (~3.9%), using the Ershler data at 25°C.

Although theoretical considerations of the radiolytic decomposition of pure water indicate accumulated hydrogen concentrations somewhat lower than the combustible limit, in a practical case, trace quantities of impurities can react with the intermediate radiolytically produced radicals and upset the chemical balance. These intermediate reaction products exist in concentrations of the order of 10^{-8} to $10^{-10}M$, and only minute quantities of an impurity could easily result in comparable concentration levels. As a consequence, even small amounts of impurities can be very important. It follows that theoretical calculations of hydrogen-gas accumulation in the containment atmosphere of either a BWR or PWR must be increased by some factor to account for the effect of impurities on hydrogen yield. Allen[5] is of the opinion that impurities which would be expected in the recirculating water of an emergency cooling system after a major accident could easily increase the hydrogen concentration by a factor of 2 to 4. If one is conservative and assumes the higher value, the calculated hydrogen accumulation at equilibrium could be as much as about 16% (based on Ershler data at 25°C). In view of the unknown amount of impurities that may be present, and the uncertainty in temperatures and yield values, a level of perhaps 8%—well above the combustible limit—would not be unreasonable to expect. It should be realized that the actual value of the saturation hydrogen accumulation is not, in itself, as significant as the conclusion that the concentration may quite reasonably be anticipated to exceed the combustible limit.

Experimental Information

The principal experimental information (applicable to accident conditions) found consists of the early Russian work (1952) of Dolin and Ershler[7] and the more recent work of Zittel at Oak Ridge.[8,11]

Dolin and Ershler[7] obtained data on the saturation pressures of H_2 and O_2 under X radiation, for various initial concentrations of oxygen, using a system containing a small vapor space. These data, shown in Fig. 2, show clearly the tendency for the hydrogen concentration to saturate and for the saturation concentration to increase with increasing oxygen overpressure. Other data, reported by Dolin and Ershler,[7] for an initial oxygen concentration approximating that in an ordinary air atmosphere, indicates a saturation hydrogen-

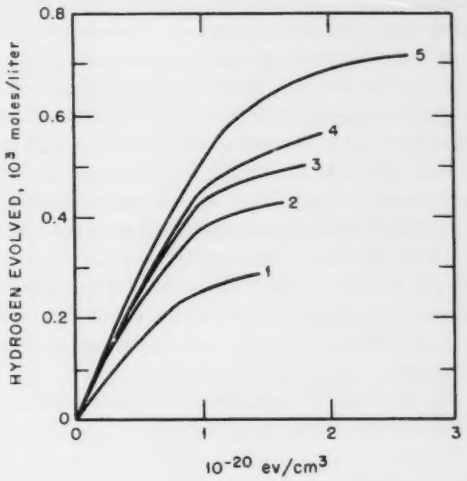

Curve	10^{-3} mole/liter oxygen
1	0.23
2	0.53
3	0.98
4	1.34
5	1.88

Fig. 2 Data of Dolin and Ershler[7] for radiolytic decomposition of water at various initial oxygen concentrations.

gas pressure of 138 mm* (0.181 atm) and a H_2O_2 concentration of 0.28×10^{-3} mole/liter. Allen,[9] however, has questioned the reliability of their gas analysis. Theoretical analysis (for the reported H_2O_2 concentration) predicts a total pressure of H_2 plus O_2 of 0.4 atm, which is in good agreement with the observed pressure of 0.381 atm; however, the theoretical hydrogen content, or partial pressure, is only 0.06 atm, leaving 0.34 of the 0.4 atm to be accounted for by oxygen. The observed peroxide concentration is about twice the calculated concentration, but this conceivably could be attributed to the presence of impurities. If one assumes that the observed peroxide concentration is correct, and also accepts Allen's theoretical explanation of the total gas pressure, then the data of Dolin and Ershler (i.e., total pressure and

*These data, taken at face value, would indicate that the hydrogen-gas accumulation in a containment atmosphere under accident conditions could reach nearly 18 vol.% hydrogen at saturation.

peroxide concentration) indicate that the hydrogen concentration would saturate at about 6 vol.% in a containment atmosphere under accident conditions.

Zittel has reported[8] a saturation pressure of ~0.35 atm for the irradiation of water or boric acid solution* in the presence of a vapor space at a gas-to-liquid ratio of ~0.2. The results of this work are shown in Fig. 3. Unfortunately, only the total pressure was measured,[13] and neither gas analyses nor peroxide concentration measurements were reported. The total saturation gas pressure (~0.35 atm) agrees reasonably well with that observed earlier by Dolin and Ershler† (0.38 atm). In theory, the observed gas pressure should correspond to about 8 vol.% hydrogen.

On the basis of the discussion given above, the available experimental data on hydrogen-gas accumulation in a closed system may be interpreted (in part by theoretical considerations) to infer a saturation value between 6 and 8 vol.%. Since there is some evidence[4] that the hydrogen yield is slightly greater under gamma radiation than under the X radiation used by Dolin and Ershler, the higher value of 8% hydrogen is probably more realistic for cases involving shutdown decay radiation. Allowing for the effects of small amounts of impurities, the 8% value is reasonably consistent with the theoretically derived saturation concentration value.

*Boric acid has previously been found[12] to have little or no effect on the radiolysis of water.

†Dolin and Ershler observed saturation at a considerably smaller total radiation dose, thus implying a smaller gas-to-liquid ratio.

Rates of Radiolytic Hydrogen Generation

In estimating the rate of hydrogen accumulation in the containment atmosphere following a loss-of-coolant accident, the two principal items to consider are (1) the macroscopic, or *net* effective radiolytic yield factor, $G(H_2)$ and (2) the fraction of the shutdown decay radiation absorbed by the water. Although the microscopic yield of radiolytic hydrogen, G_{H_2}, seems to be fairly well established, the macro-

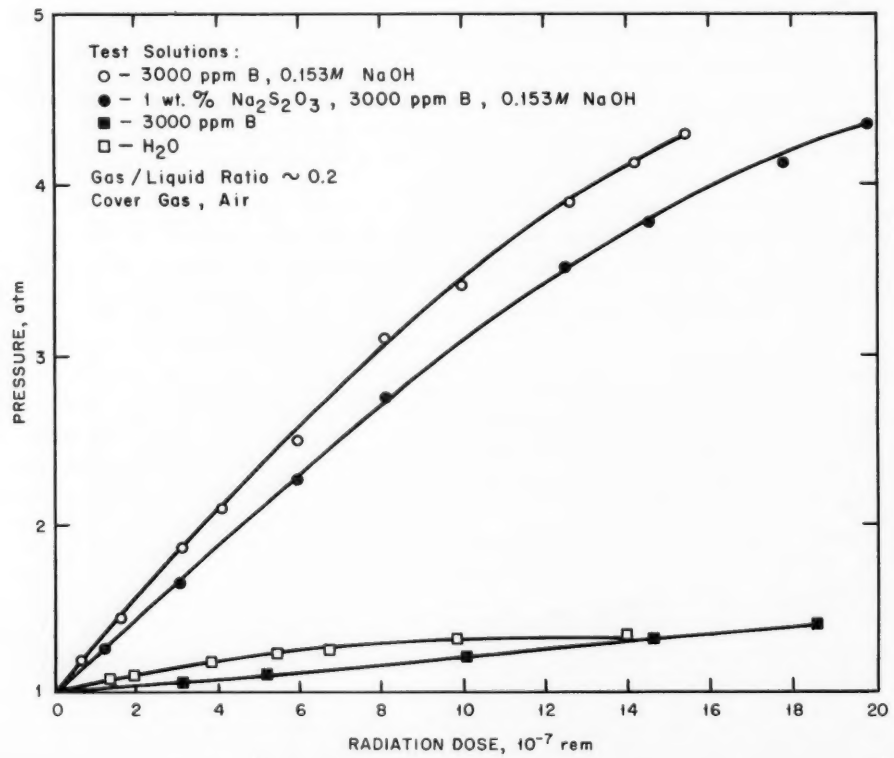

Fig. 3 Radiolytic decomposition of water measured by Zittel.[8]

scopic yield factor, $G(H_2)$, is subject to considerable uncertainty. As the theoretical considerations illustrate, the saturation concentration of hydrogen in a closed system is dependent on the value of G_{H_2}, whereas $G(H_2)$ enters principally in determining the *rate of approach* to saturation. Following reactor shutdown, the decay energy rate decreases with time, so the overall hydrogen production rate [at a constant $G(H_2)$] will decrease correspondingly. In addition, $G(H_2)$ does not remain constant; as equilibrium conditions are approached, the effective $G(H_2)$ will decrease and approach zero.

Various measurements of the effective $G(H_2)$ have been reported, and the spread in values is large. Quite low values (as low as ~0.012) have been obtained[14] for quiescent water where considerable recombination can occur before the hydrogen gas can escape to the atmosphere, whereas high values have resulted[1] where strong reducing agents are present (e.g., values as great as 4.1 have been observed in $FeSO_4$ solutions). Zittel[8,11] has observed an apparent $G(H_2)$ as high as 1.0 in the irradiation of alkaline thiosulfate solutions under certain conditions (i.e., very low ratios of gas-to-liquid volumes in his experimental arrangement). Unfortunately, these data* are not readily amenable to theoretical interpretation because of the absence of information on the concentrations of other products of radiolysis. For the irradiation of water, Gordon and Hart[14] (data given here as Table 6) have observed a $G(H_2)$ of 0.40 ± 0.04, independent of temperature (25 to 96°C), under simulated boiling conditions where CO_2 gas was bubbled through the water to sweep out

*The data are extremely interesting, and it is hoped that additional information will be forthcoming.

Table 6 Data of Gordon and Hart[8] for Radiolytic Decomposition of Bubbling Water

Radiation-Induced Decomposition of Bubbling Water

Composition of solution	Volume polution, ml	Type of radiation	CO_2 rate, cm^3/min	Temp., °C	Intensity, ev/(liter)(min)	Thermal-neutron flux	pH	$G(H_2)$
3X H_2O	102	Gamma ray	20	25 ± 2	7.5×10^{20}		~6.0	0.35
3X H_2O	69.2	Gamma ray	20	25 ± 2	7.5×10^{20}		~6.0	0.37
3X H_2O	50 ± 2	Gamma ray	20	25 ± 2	7.5×10^{20}		~6.0	0.40
3X H_2O	27.4	Gamma ray	20	25 ± 2	7.5×10^{20}		~6.0	0.42
3X H_2O	56	Gamma ray	0	25 ± 2	7.5×10^{20}		~6.0	0.012
3X H_2O	50	Gamma ray	20	25 ± 2	7.5×10^{20}		0.4	0.48
3X H_2O	50	Gamma ray	20	25 ± 2	7.5×10^{20}		3.3	0.48
3X H_2O	50	Gamma ray	20	25 ± 2	7.5×10^{20}		7.3	0.45
3X H_2O	50	Gamma ray	6	25 ± 2	2.2×10^{20}		~6.0	0.44
3X H_2O	50	Gamma ray	6	25 ± 2	1.3×10^{20}		~6.0	0.32
3X H_2O	107	Gamma rays + neutrons	190	~60	1.25×10^{22}	1.33×10^{13}	~6.0	0.31
1 m*N* KI	110	Gamma rays + neutrons	190	~60	1.25×10^{22}	1.33×10^{13}	~6.0	0.34
0.03*M* H_3BO_3	106	$^{10}B(n,a)^7Li$	190	~60	1.25×10^{22}	1.33×10^{13}		1.34†

Effect of Temperature on the Gamma-Ray-Induced Decomposition of Bubbling Water‡

Temp., °C	$G(H_2)$	$G(O_2)$
8 ± 2	0.37	0.09
25 ± 2	0.40 ± 0.04	0.20 ± 0.02
43 ± 6	0.43	0.18
68 ± 2	0.37	
88 ± 2	0.30	
96 ± 1	0.37 ± 0.04	0.15 ± 0.02

†$^{10}B(n,a)^7Li$ yield only.

‡50 ml 3X H_2O; 7.5×10^{20} ev/(liter)(min).

radiolytic gases before recombination could occur to a significant extent. In a summary report on boiling-water technology,[12] Breden has inferred from operating data that the effective $G(H_2)$ in BWR's may be as low as 0.15–0.2 molecule/100 ev. These values, however, were derived from data at BWR operating temperatures (~545°F), and a higher value of $G(H_2)$ would probably be more applicable under accident conditions.

The liquid used to cool the reactor core following an accident can be expected to experience boiling, with steam sweeping out the radiolytic gases as they are formed. Thus, at least initially, it seems reasonable to assume that conditions approximating those investigated by Gordon and Hart[14] will exist and that a probable upper limit for radiolytic hydrogen production would occur when the value for $G(H_2)$ is equal to the theoretical limit of 0.44 (i.e., when $G(H_2) = G_{H_2} =$ 0.44 molecule/100 ev, for the irradiation of water). Although boiling and violent agitation may occur for some period of time following the loss-of-coolant accident, the coolant may later become relatively quiescent, agitated only by the recirculation flow. Under these conditions, a lower value of $G(H_2)$ may be appropriate, although a definitive description of the course of events later in the history of the accident has not been developed. Consequently, the use of a $G(H_2)$ of 0.44 should be conservative if significant amounts of strong reducing agents are not leached by the coolant during its recirculation flow over various components, including concrete surfaces, within the reactor building.

In assessing the overall rate of hydrogen accumulation, it has proved convenient to use an additional variable, f, defined as the fraction of the decay radiation absorbed by the water and therefore effective in causing radiolytic decomposition. Selection of a value of f to use under accident conditions introduces considerable uncertainty in the estimate of radiolytic hydrogen release. For normal shutdown, or under accident conditions in which the fuel-cladding remains intact, the beta particles emitted by decay of the fission products would be captured within the fuel and cladding and would not contribute to radiolysis. The gamma rays from the fission products constitute approximately 50% of the total decay energy[15] and would be captured in approximate proportion to the effective masses of the various materials present in the core. In modern reactors, at a water density of 1.0, the water will absorb about 14% of the gamma decay energy, or approximately (0.5 × 14) = 7% of the total core decay energy, giving an effective f of 0.07.

For an accident in which fission products are released from the fuel rods, the fraction of the radiation energy absorbed by the water will be larger than the fraction absorbed in the shutdown case considered above. This is because some of the fission products will emit radiation directly to the water, permitting both gamma *and* beta radiation to be effective in causing radiolytic decomposition. Report TID-14844 indicates that initially ~20% of the decay energy is derived from the iodine isotopes, 7.7% from the rare gases (Kr and Xe), and the remaining 72.2% from "solid" nonvolatile fission products.[16] Following the fission-product releases postulated in Report TID-14844, it can be assumed that 50% of the iodine escapes from all the fuel elements and is totally absorbed in the water (alternatively, all the iodine escapes from 50% of the fuel elements); all of the rare gases escape and distribute throughout the containment building; and 1% of the solid fission products is released and absorbed in the water. The released iodine will then contribute 10% of the total decay energy as radiation captured by the water, whereas the remaining iodine will contribute only (10 × 0.07) = 0.7%. Since the rare gases are not in intimate contact with the water, they have been assumed to be only one half as effective as they would be were they absorbed in the water. Consequently, the rare gases contribute 3.9% of the total decay energy to the water. Of the solid fission products, 1% is assumed to contribute (1% × 0.722) = 0.7% of the total decay energy to the water. The solid fission products remaining in the fuel and cladding will contribute only 7% of their energy to the water, or (7 × 0.722) = 5% of the total decay energy. Distributed as described above, the decay radiation energy directly absorbed by the water is 20% of the total (i.e., $f = 0.2$). With time and the differing rates of decay of the various fission products, the f value may change, although this represents a refinement that does not warrant consideration in view of the uncertainty in estimating f values.

Application to Specific Reactor Types

Disregarding consideration of the equilibrium or saturation hydrogen concentrations for the moment, calculations have been made of the rate and net quantity of hydrogen which could be produced as a function of time following reactor shutdown. Results of these calculations, generalized to a $G(H_2)$ of 1.0 molecule/100 ev absorbed and an f of 1.0, are shown in Fig. 4. From these general curves the hydrogen yield

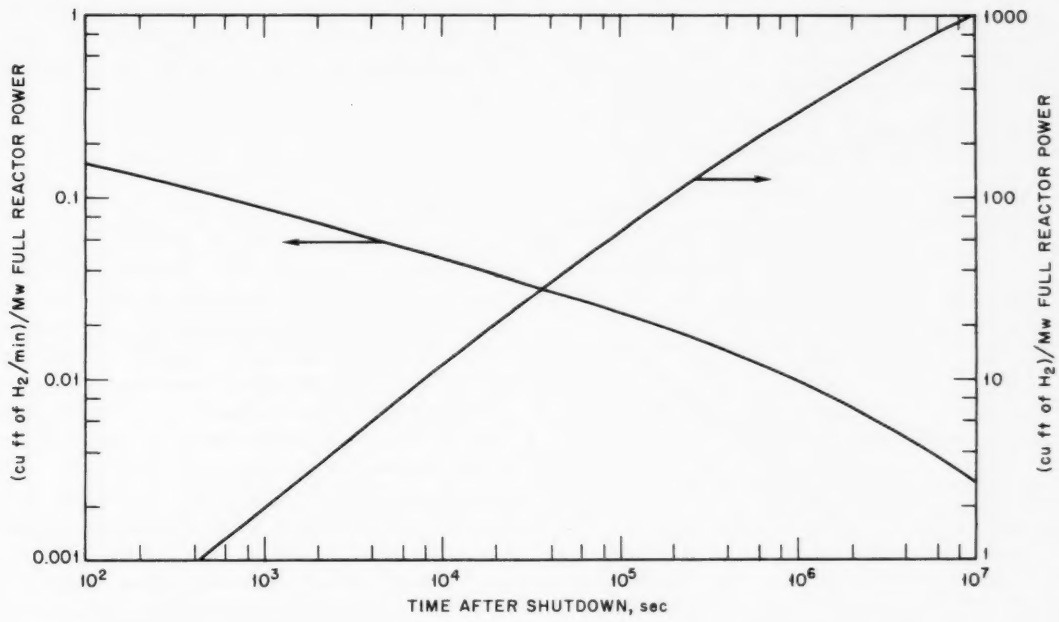

Fig. 4 Hydrogen production during shutdown per unit full reactor power (Mw) at $f = 1.0$ and $G(H_2) = 1.0$ (after 2 years' reactor operation).

of any reactor system may be determined by multiplying values read from the curves by the reactor power, by a specific value of $G(H_2)$, and by an appropriate value for f, the fraction of decay energy absorbed in the water. For the purpose of these calculations, values of heat-generation rate following reactor shutdown were based on information given in the Containment Handbook;[15] the values used are given in Fig. 5 and are for a reactor operating period of 2 years.

Using the general H_2 production curves shown in Fig. 4, a minimum time for the accumulation of combustible concentrations of hydrogen can be determined. On the basis of a flammability limit of 4% H_2 in the containment atmosphere, a $G(H_2)$ of 0.44, and an f of 0.2, a typical large BWR* could accumulate a flammable concentration of hydrogen in $\sim 5.5 \times 10^4$ sec, or ~15 hr. Further irradiation [if the $G(H_2)$ remained constant rather than saturating] could result in the accumulation of ~18% hydrogen in 6 days. Although lower values of $G(H_2)$ or f would give slower rates of hydrogen accumulation, it appears that flammable concentrations of hydrogen could accumulate in a BWR containment structure within a relatively short period of time following an accident.

A similar calculation has been made for PWR's, assuming, for illustrative purposes, a typical reactor of 3250 Mw(t) housed in a containment building of 2.6×10^6 cu ft free air volume. For a constant $G(H_2)$ value of 0.44 and an f of 0.2, a hydrogen concentration of 4% could accumulate in approximately 1.4×10^6 sec, or about 16 days; the limiting or saturation concentration could be reached in about 2 months.

A comparison of the results given above [based on a constant $G(H_2)$] with the evaluation of saturation concentrations given in the previous section shows that there is sufficient decay energy available for the hydrogen to reach the saturation level. At this point, $G(H_2)$ becomes zero and, in practice, the equilibrium concentrations become the more important consideration in evaluating the maximum or limiting concentration of radiolytic hydrogen gas in the containment structure.

The estimated times to reach combustible concentrations are based on conservative assumptions for $G(H_2)$ and f, i.e., 0.44 and 0.2, respectively. In view of the uncertainty attached to these values, it seems necessary to examine the sensitivity of the critical times to the assumptions made. For a given reactor

*For illustrative purposes, a "typical" large BWR was assumed to operate at 3300 Mw(t) and to be designed with a containment free air volume of 300,000 cu ft.

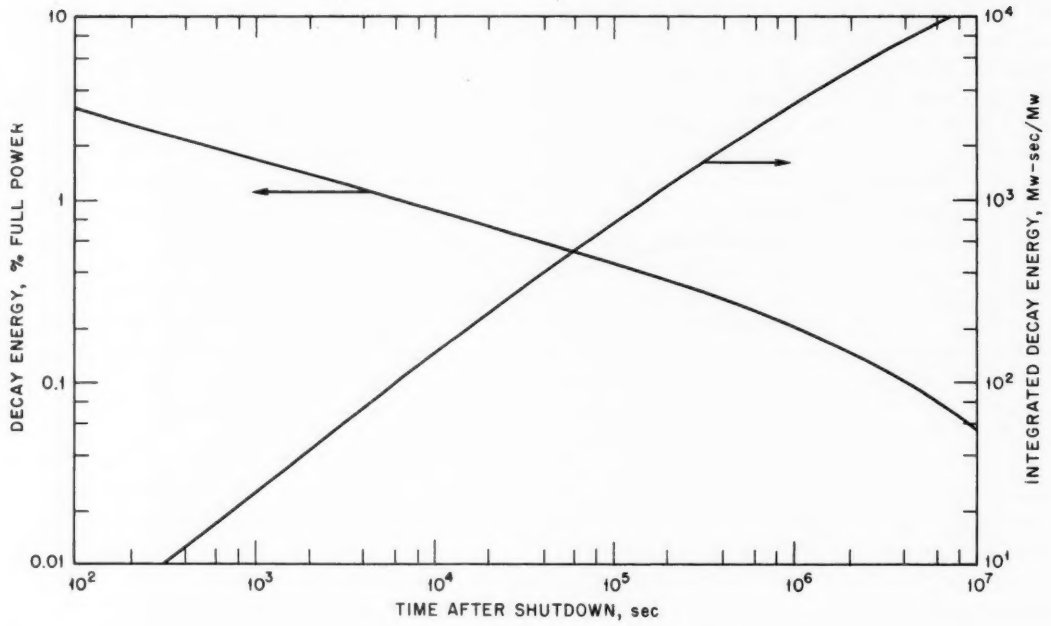

Fig. 5 Decay energy following 2 years' reactor operation.

design (i.e., power level and containment building free air volume), the product of $G(H_2)$ and f is the paramount factor in estimating the time required to reach a combustible concentration.* For the two cases considered above, decreasing the product of $G(H_2)$ and f by a factor of only 2—which may be either a decrease in $G(H_2)$ alone, or in f, or some combination—would increase the time from ~15 hr to ~40 hr for the BWR and from ~16 days to ~60 days for the PWR. Obviously, the calculated accumulation of hydrogen is very sensitive to the two parameters mentioned above, and it should be emphasized that the values of $G(H_2)$ and f used here are considered to be quite conservative.

As a matter of interest, the hydrogen generation rate in a fuel-storage pool was estimated. In the pool, f would be about 0.07 (intact fuel elements), and the value of $G(H_2)$ of ~0.012 reported by Gordon and Hart[14] for stagnant conditions would be applicable. Furthermore, the radiolytic dissociation would be highly localized (i.e., in the immediate vicinity of the core) without steam evolution, and the local equilibrium concentration values should be attained fairly rapidly. Even at 10^5 sec (slightly over 1 day) following shutdown, the maximum hydrogen generation rate would be the equivalent of 0.06 cu ft/min from an entire core loading. This amount of gas production would not be expected to result in observable gas bubbling; rather, the gas would remain in solution, slowly diffusing to the surface, where some of the hydrogen which had not recombined could escape into the atmosphere.

*Here, as elsewhere in this review, contributions to the hydrogen concentration from sources other than radiolytic decomposition (e.g., metal–water reactions) have not been considered, but would reduce the minimum time required to reach combustible limits.

Effect of Chemical Additives

Little applicable information has been found in the literature on the effect of various additives in neutral or alkaline solutions on the radiolytic yield of hydrogen. Allen[1] and Hochanadel[6] have referred to some early work under X radiation on solutions of NO_2, SeO_3^{2-}, and $Fe(CN)_6^{4-}$, in which the solute was oxidized in an amount equivalent to the hydrogen produced. Breden[12] indicates that numerous investigations have shown that boric acid has little or no effect on radiolysis under gamma radiation.

At Oak Ridge, Zittel's measurements[8,11] with boric acid–thiosulfate solutions and low gas-to-liquid

ratios have shown markedly enhanced hydrogen yields compared to pure water. As a first approximation, thiosulfate may be considered to be oxidized in an amount equivalent to the hydrogen produced by a simple overall reaction

$$2H^+ + 2S_2O_3 = \xrightarrow{\gamma} H_2 + S_4O_6^{2-}$$

in which 1 mole of H_2 is produced for every 2 moles of thiosulfate consumed. This simplified approach does not take into consideration the complex chain of reactions which probably occurs, but serves to approximate the net amount of hydrogen produced. If one assumes that a typical containment spray system in a PWR design gives a thiosulfate concentration of 0.15 mole/liter, then complete oxidation would yield 0.075 mole of hydrogen per liter of solution. For a gas-to-liquid volume ratio of ~25, the hydrogen gas accumulated in the gas space would be about 6 vol.%. At this overpressure of hydrogen, further radiolytic decomposition of the water would probably be suppressed, and the saturation hydrogen concentration would remain at about 6%.

For Zittel's experiments at Oak Ridge, using a 1 wt.% thiosulfate solution, the calculated saturation pressure of hydrogen would be ~4.5 atm at a gas-to-liquid ratio of 0.2. The Oak Ridge data, although not based on irradiation to saturation, show that at 10^8 r dose 43.2% of the thiosulfate has been destroyed (reported as iodine equivalent). This quantity of thiosulfate destruction, by the simple analysis above, would yield ~43% of the final hydrogen production. At the experimental[8] gas-to-liquid ratio of 0.2, this hydrogen production should yield a partial pressure of ~2 atm, which is in reasonable agreement with the 3 atm total gas pressure observed.* On the basis of this calculation, the simple approach would appear reasonably valid, although a direct comparison is not possible in the absence of an analysis of the gases produced in the Oak Ridge experiments. It can be inferred that the presence of thiosulfate in a spray system does not necessarily have an adverse effect on the equilibrium pressure of hydrogen in the containment atmosphere, at a gas-to-liquid ratio of ~25, since the final pressures, arrived at via different reaction routes, are approximately equal for thiosulfate solutions or for water.

*It is known[13] that oxidation of the thiosulfate proceeds somewhat farther (i.e., higher order polythionates and perhaps free sulfur) than indicated by the simple reaction given above.

References

1. A. O. Allen, *The Radiation Chemistry of Water and Aqueous Solutions*, Van Nostrand–Reinhold, New York, 1961.
2. G. H. Jenks, Effects of Reactor Operation on HFIR Coolant, USAEC Report ORNL-3848, Oak Ridge National Laboratory, October 1965.
3. G. H. Jenks and J. C. Griess, Water Chemistry in Pressurized and Boiling Water Power Reactors, USAEC Report ORNL-4173, Oak Ridge National Laboratory, November 1967.
4. B. V. Ershler and G. G. Myasishcheva, Mechanism of the Radiolysis of an Aqueous Solution of H_2, O_2, and H_2O_2, in Proceedings of the Second All-Union Conference on Radiation Chemistry, Akademiya Nauk, USSR, page 116, Translation for the USAEC by the Israel Program for Scientific Translations, 1964.
5. A. O. Allen, Brookhaven National Laboratory, personal communication, 1968.
6. C. J. Hochanadel, Effects of Cobalt γ-Radiation on Water and Aqueous Solutions, *J. Phys. Chem.*, **56**: 587 (1952).
7. P. I. Dolin and B. V. Ershler, Radiolysis of Water in the Presence of H_2 and O_2 Due to Reactor Radiation, Fission Fragments and X Radiation, in *Proceedings of the International Conference on the Peaceful Uses of Atomic Energy, Geneva, 1955*, Vol. 7, p. 564, United Nations, New York, 1956.
8. H. E. Zittel, Radiolysis Studies, in ORNL Nuclear Safety Research and Development Program Bimonthly Report for March–April 1968, USAEC Report ORNL-TM-2230, Oak Ridge National Laboratory, May 30, 1968.
9. A. O. Allen and H. A. Schwarz, Decomposition of Water Under High Energy Radiation, in *Proceedings of the Second United Nations International Conference on the Peaceful Uses of Atomic Energy, Geneva, 1958*, Vol. 29, p. 30, United Nations, New York, 1958.
10. H. A. Lange, *Handbook of Chemistry*, 9th ed., McGraw-Hill Book Company, Inc., New York, 1956.
11. H. E. Zittel, Radiation Stability of Spray Solutions, in Nuclear Safety Program Annual Progress Report for Period Ending Dec. 31, 1967, USAEC Report ORNL-4228, Oak Ridge National Laboratory, April 1968.
12. C. R. Breden, Boiling Water Reactor Technology Status of the Art Report, Vol. II, Water Chemistry and Corrosion, USAEC Report ANL-6562, Argonne National Laboratory, February 1963.
13. T. H. Row, Oak Ridge National Laboratory, personal communication, 1968.
14. S. Gordon and E. J. Hart, Radiation Decomposition of Water Under Static and Bubbling Conditions, in *Proceedings of the Second United Nations International Conference on the Peaceful Uses of Atomic Energy, Geneva, 1958*, Vol. 29, p. 13, United Nations, New York, 1958.
15. Wm. B. Cottrell and A. W. Savolainen (Eds.), U. S. Reactor Containment Technology, USAEC Report ORNL-NSIC-5, Volume II, Oak Ridge National Laboratory, August 1965.
16. J. J. DiNunno, F. D. Anderson, R. E. Baker and R. L. Waterfield, Calculation of Distance Factors for Power and Test Reactor Sites, USAEC Report TID-14844, Mar. 23, 1962.

Brine-Heater Leakage-Control Problems in Large Power-Desalting Plants

By W. H. Kelley, Jr.*

Abstract: *A study was made of brine-heater leakage problems in large nuclear dual-purpose power–desalting plants utilizing light-water reactors and multistage flash evaporators. Leakage of reactor condensate into the water plant was found to have an inconsequential effect on product-water purity. Leakage of brine into the reactor presents a considerable problem in demineralization or blowdown-and-makeup cost. The best presently available solution to the demineralization problem appears to be the use of a coated-filter ion-exchange unit, with immediate shutdown of a leaking brine heater. An installed spare brine heater was found to be economically attractive in preventing loss of power and product-water revenues. The use of vertical tube evaporators (VTE's) in place of or in conjunction with the conventional brine heaters would ensure against leakage of brine into the reactor plant. Several schemes utilizing VTE's appear economically attractive.*

The growth in world production of desalted seawater is shown in Fig. 1. The curve shows a fairly uniform exponential increase over the years to the present output of over 50 million gallons per day (Mgd), or about 56,000 acre-ft per year. Estimated future world-population trends compared to similar estimates of available natural freshwater supplies indicate that the trend of Fig. 1 may continue for several decades. This is the background for the present world interest in, and programs of, desalination. The current world-production rate represents only about 5% of the requirement of the Metropolitan Water District (MWD) of Southern California, which distributed over 1 million acre-ft in fiscal year 1966. Present-generation desalting plants are characterized by module sizes on the order of 1-Mgd capacity, product-water cost of about $1.25 per 1000 gal, and application only to areas of extreme demand. Plants in short-term planning have

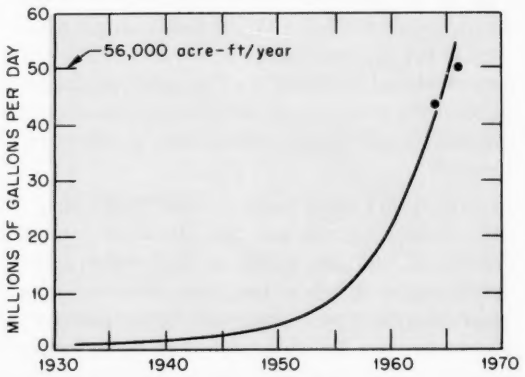

Fig. 1 Growth in world production of desalted seawater.

module capacities on the order of 50 Mgd, product costs of about 25¢ per 1000 gal, and are applicable to municipal and industrial supplies. Long-term plans include plants with a capacity of 1 billion gallons per day (Bgd) producing water at even lower cost and applicable to even agricultural use. The necessary extrapolation of plant sizes is seen in comparing the capacity of the proposed 150-Mgd MWD plant with the current world production. If built, this plant's output would be several times the present world production and would supply less than 15% of the MWD's present total demand.

The large size and economic requirements of next-generation desalting plants dictate the use of nuclear energy sources. Since current power reactors inherently produce steam at a temperature too high for utilization by desalting plants (due to scaling problems), it is convenient to combine the desalting

*Oak Ridge National Laboratory, Oak Ridge, Tenn.

plants with electric power plants. The first large (~100 Mgd) dual-purpose plants will therefore utilize light-water reactors supplying prime steam to turbogenerators, the back-pressure turbine's exhaust being condensed in the brine heaters of the water plants. The water plants will utilize the multistage flash (MSF) process, which is at present the most widely used and highly developed. A temperature profile for this process and the overall plant is shown in Fig. 2.

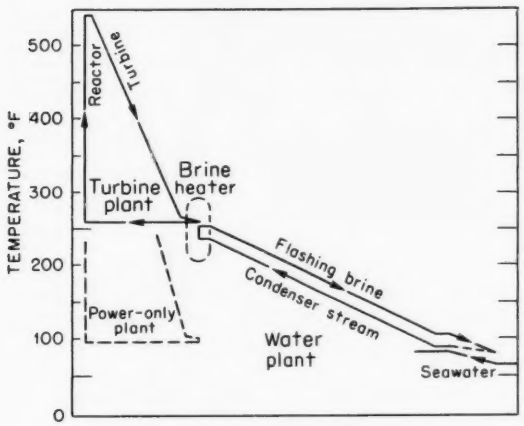

Fig. 2 Typical plant temperature profile.

The MSF evaporator consists of a series or train of pressure vessels (stages), each operating at successively lower temperature and pressure. The flashing brine stream flows in the bottom of these vessels through interconnecting orifices, a portion of the brine flashing into steam in each vessel and the stream being cooled through evaporation. At the lower-temperature end of the train, a portion of the stream is removed as blowdown and is replaced by fresh treated seawater. The stream is cooled and recirculated through condenser tubes in the top of the evaporator, the tubes serving to condense the flashed brine that is withdrawn as product water. The condenser stream is heated regeneratively by the condensing process in the evaporator and is further heated in the brine heater to a temperature compatible with flashing in the first stage.

The related pressure profile is shown in Fig. 3. The important point in the leakage problem is that the steam pressure from the back-pressure turbine is intermediate between the inlet and outlet brine pressures in the brine heater. This is due: (1) to the necessity that the steam be at a higher temperature

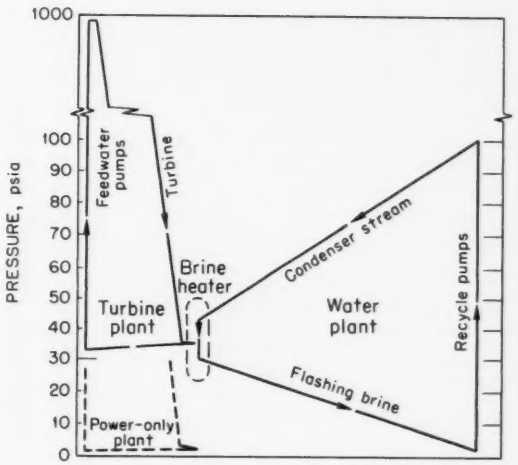

Fig. 3 Typical plant pressure profile.

than the outlet brine for proper heat transfer, (2) to the brine-side pressure drop through the heater, and (3) to the considerable pressure differential from top to bottom of the heater due to its physical size (see Fig. 4). It is impractical either to overpressurize the brine, due to pumping cost, or to overpressurize the steam, due to the danger of brine boiling and scaling. Thus, depending on the location of the leak, it will be possible to have leakage in either direction in event of brine-heater tube leaks. In a power-only plant, the condenser coolant would be at atmospheric pressure or above, and the condensing steam at perhaps 0.5 psia, ensuring against leakage of reactor coolant into the tube-side stream. This fact has been mentioned as a safety feature in hazards analyses but is not applicable to dual-purpose plants.

The purposes of the brine-heater leakage-control study[1] were to investigate the problem and then develop design criteria and operational procedures for preventing leakage from affecting the safe and economical operation of the overall plant. The study is general in nature but is referenced particularly to the proposed 150-Mgd MWD plant design by Bechtel Corporation.[2] Table 1 shows some major features of this plant, of the Israel plant,[3] and of two power-only plants[4,5] which were used as references for certain detailed reactor features. The thermal power rating shown for the MWD plant reactor is approximately that required for the listed electric and water outputs. The MWD plant is actually designed for electric power output aside from the dual-purpose portion of the plant.

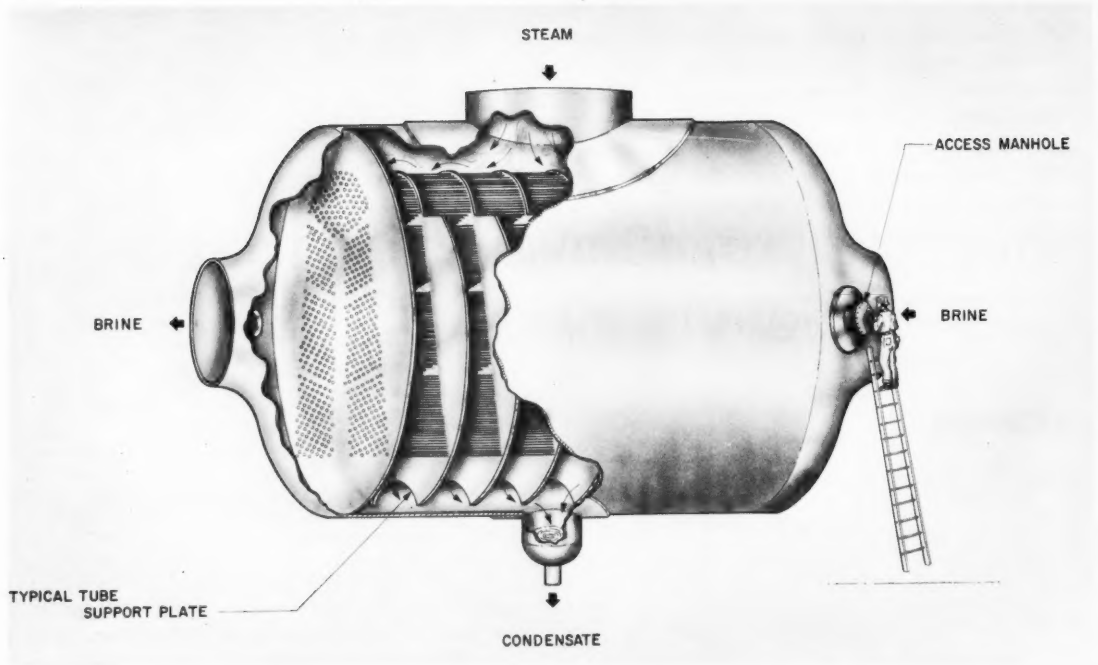

Fig. 4 Brine heater typical of MSF plants in the 200-Mgd class.

Table 1 Major Features of Some Dual-Purpose and Power-Only Plants

	MWD plant[2]	Israel plant[3]	Vermont Yankee[4] BWR	Haddam Neck[5] PWR
Reactor power, Mw(t)	1750*	1250	1590	1473
Reactor power, Mw(e)	355	250	530	490
Product water, Mgd	150	100		
Evaporator ground area, acres	6	8.5		
Evaporator trains	3	4		
Evaporator stages	53	31		
Brine heaters	6	4		
Brine-heater size, ft	27 X 22 X 15	17.5 X 32 X 7		
Steam flow rate, lb/hr	5.28×10^6	3.42×10^6	6.43×10^6	6.2×10^6
Primary coolant cleanup system flow rate, lb/hr			80,000†	48,000†
Brine recycle flow rate, lb/hr	360×10^6	290×10^6		

*The Mw(t) figure for the MWD plant is estimated to be appropriate for a normal dual-purpose plant producing 355 Mw(e) and 150 Mgd. The MWD plant will actually have a great electrical capacity aside from the dual-purpose portion of the plant.

†Flow rates for the Vermont Yankee and Haddam Neck plants have been used in certain calculations because detailed design information is available. Specific reactors have not been selected for the MWD and Israel plants.

Leakage from a BWR into the Water Plant

Dual-purpose plants utilizing BWR's would appear to be more sensitive to brine-heater leakage problems than would PWR plants, due to the fundamental design differences between the two types of reactors. In the BWR the reactor coolant boils directly in the core, and the steam produced circulates through a direct cycle to the turbine and brine heater. In a PWR the primary coolant is pressurized to prevent boiling, and steam is produced in a steam generator in a secondary circuit resembling the single circuit of the BWR. Thus the PWR enjoys an additional degree of isolation between the reactor and the water plant, compared to the BWR plant. Leakage problems in the BWR dual-purpose plant are discussed first, and in this subsection the leakage from the reactor to the water plant is considered. This analysis is similar to that in an earlier General Electric Company report,[6] with one additional factor—concentration buildup in the recycle brine—being considered here. The factors affecting contamination of the product water by reactor coolant are listed and discussed briefly below:

1. *Radioactivity Level in the Reactor Core Coolant.* The radioactivity in the core coolant water results from induced activity in corrosion products and in the water itself and from the leakage of solid and gaseous fission products through holes that develop in the fuel cladding.

2. *Reactor Boiling Decontamination Factor.* The radioactivity level in the condensate is due to moisture entrained in the steam and condensate in the boiling process and therefore depends on the efficiency of the separators and dryers employed. General Electric Company reports[6] a factor of 10,000 reduction in the condensate, based on power-reactor experience. Table 2 shows a tabulation[7] of radioisotopes in BWR condensate at the end of a normal core life with a substantial number of cladding failures. The resulting activity for all isotopes is 2.2×10^{-3} $\mu c/cm^3$ at 1-hr decay. This is equivalent to 2.7 times the maximum permissible concentration (MPC) level allowed by the *Code of Federal Regulations* (10 CFR 20) for the particular combination of isotopes for normal continuous use. The MPC fraction is used here to permit comparison of the level at any point in the plant with the allowable MPC level.

3. *Brine-Heater Leak-Size Factor.* Owing to the great amount of heat-transfer surface utilized in typical brine heaters, large leaks must be postulated to show significant results in calculations. One completely severed tube in each of the six MWD plant heaters, with a 10 psi pressure differential, resulted in a calculated leakage of only $\frac{1}{6}$ of 1% of the steam flow rate. Leakage of 1% of the steam (53,000 lb/hr) was used in the calculation that follows.

4. *Dilution in Recycling Brine Stream.* The radioactivity level in the steam will be attenuated by dilution in the recycle brine stream. The attenuation factor will be equal to the ratio of the steam leakage (in lb/hr) to the recycle flow rate, assuming that the former is small compared to the latter. The MWD plant recycle flow rate is 360 million lb/hr.

5. *Concentration Buildup in Recycling Brine.* The contamination level in the recycling brine in the evaporator will increase due to recirculation of the brine past the point of inleakage. The increase will be a factor greater than the single-pass dilution level (item 4 above), depending on the fraction of the recycle stream which is removed as blowdown and product and which is made up. In the MWD plant case, this factor is $\frac{1}{7}$.

6. *Water Plant Evaporation Factor.* This factor is similar to that at the reactor steam–water interface (item 2 above). A factor of $\frac{1}{1000}$ is used here, although much higher efficiencies are possible, depending on the desired product-solids content and the cost and pressure drop of moisture separators.

The above factors are summarized and a calculation of the resulting product-water radioactivity level as a fraction of the allowable MPC is shown in Table 3. The product-water-activity level is seen to be only 0.28×10^{-5}, or 0.00028% of MPC. The level would have to be increased by a factor of about 3.5×10^{5} to reach the allowable MPC. Any mishap catastrophic enough to cause an increase of this magnitude would surely precipitate a plant shutdown for reasons aside from the product-activity level. It is therefore concluded that contamination of the product water by BWR coolant is not a significant potential hazard to the safe and economical operation of the overall plant.

Leakage of Brine into a BWR

In a boiling-water reactor, about $\frac{1}{8}$ of the total core coolant flow rate circulates through the steam-condensate circuit. The remainder of the coolant is recirculated, some within the reactor pressure vessel and some through external circuits. The solids content of the coolant, about 0.5 to 1.0 ppm, is maintained by bypassing about $\frac{1}{600}$ of the total core flow through a small bypass demineralizer. The bypass stream is cooled for demineralization at conventional tempera-

Table 2 Radioisotopes in Normal BWR Condensate[7]

(Modern Zirconium-Clad Core Near End of Fuel Life, with Substantial Number of Cladding Defects)

Half-life	Isotope	No decay, $\mu c/cm^3$	1 hr, $\mu c/cm^3$	1 day, $\mu c/cm^3$	MPC,* $\mu c/cm^3$	1-hr fraction of MPC
		Products of Neutron Bombardment of Water				
112 min	^{18}F	1×10^{-3}	8×10^{-4}	1×10^{-7}	8×10^{-4}	1.0
10 min	^{13}N	3×10^{-3}	5×10^{-5}			
		Corrosion Products from Moisture Carry-Over				
5 years	^{60}Co	2×10^{-6}	2×10^{-6}	2×10^{-6}	5×10^{-5}	0.04
72 days	^{58}Co	2×10^{-6}	2×10^{-6}	2×10^{-6}	1×10^{-4}	0.02
13 hr	^{64}Cu	9×10^{-6}	9×10^{-6}	2×10^{-6}	3×10^{-4}	0.03
		Fission Products from Moisture Carry-Over				
8 days	^{131}I	2×10^{-7}	2×10^{-7}	2×10^{-7}	2×10^{-6}	0.1
21 hr	^{133}I	1×10^{-6}	1×10^{-6}	4×10^{-7}	7×10^{-6}	0.143
		In-Transit Decay of Noble-Gas Fission Products				
28 years	^{137}Cs	4×10^{-9}	4×10^{-9}	4×10^{-9}	2×10^{-5}	0.0002
28 years	^{90}Sr	6×10^{-9}	6×10^{-9}	6×10^{-9}	1×10^{-7}	0.06
54 days	^{89}Sr	1×10^{-6}	1×10^{-6}	1×10^{-6}	1×10^{-5}	0.1
13 days	^{140}Ba	3×10^{-6}	3×10^{-6}	3×10^{-6}	3×10^{-5}	0.1
10 hr	^{91}Sr	6×10^{-5}	6×10^{-5}	1×10^{-5}	7×10^{-5}	0.857
3 hr	^{92}Sr	2×10^{-5}	2×10^{-5}	1×10^{-7}	7×10^{-5}	0.286
85 min	^{139}Ba	1×10^{-3}	6×10^{-4}			
32 min	^{138}Cs	1×10^{-3}	2×10^{-4}			2.7362
17 min	^{88}Rb	2×10^{-4}	3×10^{-5}			
15 min	^{89}Rb	2×10^{-3}	2×10^{-4}		Radioactivity level	
14 min	^{91}Rb	2×10^{-3}	2×10^{-4}		is 2.7 times or	
9 min	^{139}Cs	6×10^{-3}	6×10^{-5}		270% of MPC	
3 min	^{90}Rb	1×10^{-2}			(1-hr decay).	
1 min	^{92}Rb	3×10^{-4}			Level is 0.63 of MPC	
1 min	^{140}Cs	5×10^{-3}			at 1-day decay;	
		2.7×10^{-2}	2.2×10^{-3}	2×10^{-5}	3.0 at no decay (calculation not shown).	

*Maximum permissible contamination levels for the short-lived isotopes are not listed in 10 CFR 20, and the omission here in the summation is not considered important. Although fluid cycle times in the reactor and water plant are on the order of several minutes, product-water transportation and distribution are expected to require hours.

ture (about 140°F max.) and is reheated for return to the core. In power-only plants the steam-circuit corrosion and erosion products picked up in the turbine, condenser, and piping are removed by a much larger full-flow condensate demineralizer. The condensate temperature (about 95°F in a normal power-only plant) is well under the maximum temperature limit for ion-exchange resins. The cleanup duty is about 40 ppb entering and 1 ppb leaving. The very low solids content in the core is necessary to minimize induced radioactivity in the steam and to minimize the danger of chloride-induced stress-corrosion cracking in austenitic stainless steels in the reactor. Two types of demineralizers are currently in use for full-flow condensate demineralization: the conventional mixed-bed (deep bed) type and the coated-filter type. The coated-filter unit utilizes filter elements with a ¼-in.-thick coating of finely ground conventional ion-exchange resins. The coating is flushed off and replaced frequently due to pressure-drop increase.

The coated-filter demineralizer is adaptable to dual-purpose plants because the frequent replacement of the

Table 3 Factors Affecting Leakage of BWR Coolant to the Product Water

BWR condensate activity	2.7 X MPC
Brine-heater leak size factor, lb/hr	53,000
Dilution in recycle brine, lb/hr	1/360,000,000
Concentration due to water plant recycle	7
Water plant evaporation factor	1000
Radioactivity level in product water*	0.28×10^{-5} X MPC

* $\frac{2.7 \times 53{,}000 \times 7.0}{360{,}000{,}000 \times 1000} = 0.28 \times 10^{-5}$

small resin inventory eliminates the problem of anion-resin deterioration due to high temperature. The capacity of the unit is extremely limited, however, in the event of salt inleakage. It will presumably be necessary to shut down a leaking brine heater immediately upon detection of a significant leak. The analysis to follow of the effect of salt inleakage to the reactor is based on failure of the full-flow condensate demineralizer, with only the small bypass demineralizer on stream.

The postulated leak in this case is a single ⅛-in.-diameter hole with a 10 psi pressure differential. The quantity of inleakage is 1.1 gal/min, or 503 lb/hr. The analysis is similar to that for steam leakage and will not be discussed in detail. Table 4 shows the pertinent factors and calculated increase in the core-coolant solids level, which is seen to be 426 ppm. A relatively small brine leak, as compared to that postulated for steam leakage, is thus seen to drastically affect the solids level in the reactor core in the absence of the full-flow condensate demineralizer.

Table 4 Factors Affecting Leakage of Brine into a BWR Plant Based on Vermont Yankee Plant[4] Flow Rates

(Condensate Demineralizer Assumed Inoperative)

Contamination level assumed in brine, ppm	68,000
Quantity of inleakage, lb/hr	503
Condensate flow rate, lb/hr	6,430,000
Reactor core-coolant flow rate, lb/hr	48,000,000
Concentration factor due to core recycle	600
Contamination level in core coolant,* ppm	426

* $\frac{68{,}000 \times 503 \times 6{,}430{,}000 \times 600}{6{,}430{,}000 \times 48{,}000{,}000} = 426$. (The 6,430,000 factor divides out and could be omitted: the contaminant could have been considered to leak directly into the core.)

Brine-Heater Leakage from and into a PWR

In PWR's the reactor primary coolant is pressurized to prevent boiling and is circulated from the core through the primary side of a steam generator. Steam is produced in a secondary circuit that includes the turbine and condenser or brine heater. Two types of steam generators are used: one in which a portion of the secondary-side throughput is recirculated, and one in which the secondary-side stream flows through in a single pass. In PWR's of the first (recirculating) type, a high solids content, 500 to 600 ppm, is permissible in the boiling water in the steam generator. Cleanup is by blowdown and makeup of about $\frac{1}{130}$ of the steam-condensate flow rate. In PWR's utilizing once-through steam generators, the secondary-side stream entering the steam generator must be of extremely high purity. Full-flow condensate demineralization is used, as in the single BWR circuit.

In dual-purpose plants using PWR's of either type, the hazards associated with brine-heater leakage in either direction are less than in the BWR plant. This is because of the intermediate coolant circuit in the PWR plant which provides an additional tube-wall barrier and an additional dilution factor compared to the BWR plant. The problem of salt leakage into the PWR secondary circuit will, however, affect the economics of the cleanup blowdown-or-demineralization. The effect of the leak postulated in the BWR analysis (⅛-in.-diameter hole, 503 lb/hr) on a PWR intermediate coolant-loop blowdown rate is shown in Table 5. This single relatively small leak is shown to increase the blowdown rate by a factor of 2.3. The cost of the normal 48,000 lb/hr makeup for the four coolant loops is about $12,000/year, based on the use of MSF plant product water at 22¢ per 1000 gal. The 2.3 factor would thus represent a cost increase of about $16,000 per year based on the very small postulated leak. Actual inleakage might be much greater if leaks were not repaired immediately upon detection. The effect of a salt leak on a PWR system with once-through steam generators and a demineralizer would be even more serious in the cost of ion-exchange-resin regeneration or replacement. Salt leaks into PWR plants can be expected to precipitate shutdowns at the same frequency as in BWR plants, although, from the strictly hazards standpoint, the leaks cannot be considered as serious in the PWR case.

Some confusion may arise in connection with Tables 3 to 5 regarding contaminant concentration factors and the use of hourly flow rates rather than cycle circulation times. The concentration factors are

Table 5 Factors Affecting Leakage of Brine into PWR Intermediate Coolant Circuit Based on Haddam Neck Plant[5] Flow Rates

Normal (background) TDS level in loop, ppm	550
Coolant-loop flow rate, lb/hr	1,551,000
Blowdown-and-makeup flow rate, lb/hr	12,000
Contamination level assumed in brine, ppm	68,000
Volume of inleakage ($\frac{1}{8}$-in.-diameter hole, 10 psia ΔP), lb/hr	503
Concentration factor due to recycle	130
Loop TDS added per cycle, normal (background), ppm	4.2
Loop TDS added per cycle due to leak, ppm	5.5
Total loop TDS with assumed leak, ppm	9.7
Increase in blowdown and makeup,* factor	2.3

$$\frac{\text{*Normal contamination added per cycle} + \text{leakage contamination added per cycle}}{\text{Normal contamination added per cycle}} = \text{ratio of blowdown, or demineralization with inleakage, to normal}$$

$$\frac{\dfrac{550}{\dfrac{1{,}551{,}000}{12{,}000}} + \dfrac{68{,}000 \times 503}{1{,}551{,}000 \times 4\dagger}}{\dfrac{550}{\dfrac{1{,}551{,}000}{12{,}000}}} = \frac{\dfrac{550}{130} + 5.5}{\dfrac{550}{130}} = \frac{4.2 + 5.5}{4.2} = \frac{9.7}{4.2} = 2.3$$

†The specified flow rates are for each of four coolant loops; the quantity of brine inleakage must therefore be divided by 4.

based on the simple fact that, if $\frac{1}{2}$ of a recycling stream having contaminant inleakage is blown down and made up, the ultimate concentration of contaminant will be twice the first-pass level. Similarly, if $\frac{1}{3}$ is blown down, the final concentration will be three times that of the initial pass, etc. For the purpose of determining final concentrations, hourly flow rates may be used rather than per-cycle quantities, although this would be erroneous if the time to reach maximum concentration were in question. This latter factor is of little interest here because the cycle times being considered are on the order of a few minutes, and maximum concentrations will be reached in about an hour.

Possible Solutions to the Leakage Problem

Fairly detailed cost-estimate studies of many possible brine-heater leakage-control schemes were made. For BWR and once-through-type PWR reactors, the most practicable presently available condensate clean-up scheme would utilize the coated-filter demineralizer for normal corrosion and erosion products. In the event of salt inleakage, condensate from the leaking heater would be diverted to a drain or holdup tank during the time required for shutdown. A spare installed brine heater to be valved on stream to replace a leaking heater would permit the related section of the evaporator to remain on stream during repair of the leaking heater. The loss of power and product revenues was found to amount to $17,000 per shutdown. This amount applied to several heaters, and about two leaks per heater per year would easily justify the cost of the spare heater in the 30-year life of the plant. (The above figures are based on the MWD plant.[2])

Several schemes utilizing VTE's in place of or in conjunction with the brine heater of the MSF plant appear economically attractive. The VTE's would assure a steam pressure higher at all points in the heater than the pressure of the brine. The VTE's need only operating experience and general-industry acceptance to be practicable.

Acknowledgments

The work reported here was sponsored by the USAEC under contract with Union Carbide Corporation. The author gratefully acknowledges the contribu-

tions of many members of the Oak Ridge National Laboratory and Oak Ridge Gaseous Diffusion Plant staffs to all phases of the Ref. 1 report preparation.

References

1. W. H. Kelley, Jr., Studies on Control of Brine Heater Leakage in Large Dual-Purpose Nuclear Desalting Plants, USAEC Report ORNL-TM-2049, Oak Ridge National Laboratory, May 1968.
2. Bechtel Corporation, Engineering and Economic Feasibility Study for a Combination Nuclear Power-Desalting Plant, USAEC Report TID-22330 (Vols. 1–3), December 1965.
3. Kaiser Engineers and Catalytic Construction Company, Engineering Feasibility and Economic Study for Dual-Purpose Electric Power–Water Desalting Plant for Israel, USAEC Report 66-1-RE, January 1966.
4. Vermont Yankee Nuclear Power Corporation, Plant Design and Analysis, Vermont Yankee Nuclear Power Station, Docket 50-271, Vols. 1–3, 1966.
5. Connecticut Yankee Atomic Power Company, Facility Description and Safety Analysis, Haddam Neck Plant, USAEC Report NYO-3250-5 (Vols. 1 and 2), May 1966.
6. F. E. Crever et al., Representative Design of Nuclear Power/Desalting Plants Now Available, General Electric Company and Chicago Bridge and Iron Company (unpublished report).
7. L. H. McEwen and J. M. Smith, Application of BWR's in Water Desalting Service, General Electric Company, 1964 (unpublished report).

Thermal Bowing in Pin-Type Fuel Rods

By C. Anderson, R. Anderson, R. Baer, F. Lobbin, and R. Riggs*

Abstract: *An iterative process was formulated and utilized to determine the complex interaction between bowed fuel rods and the channel thermal hydraulics of a water reactor. The methods used and the results are described in detail within the body of the paper.*

Asymmetrical temperature distribution in the fuel-rod cladding may result in bowing of the fuel pin and a potential thermal instability. Temperature asymmetry occurs as a result of skewed power generation within the fuel rod, local flux perturbations within the reactor core, and circumferential variations in the coolant temperature. The thermal instability may occur in the following manner: An initial bowing of the fuel rod may constrict the coolant-flow area in the hot channel while simultaneously increasing the flow area in the other coolant channels adjacent to the fuel rod. The resultant effect is an accentuation of the initial temperature asymmetry which leads to increased bowing and constriction of the hot channel. This process may continue until actual point contact between the rods is made and hot-channel coolant flow is stopped.

The article discusses how this instability can be circumvented by proper specification of the tolerances between the fuel rod and its end supports or by the use of intermediate supports. Typical results for the case of end supports are presented. It was found that tight tolerances must be employed at the end of the fuel rod experiencing the largest temperature asymmetry (i.e., the coolant outlet end). This precaution greatly reduces the magnitude of the initial bow of the rod and precludes the possibility of a channel thermal instability occurring.

Bowing of fuel rods in a nuclear core can occur if the circumferential temperature of the fuel-rod cladding is asymmetrical; i.e., the temperature is greater on one side of the rod than the other. The temperature gradient, which causes bowing of the fuel rod, can result from the combination of asymmetrical power generation and circumferential variations in the coolant-temperature distribution. Asymmetrical power generation in the rod can occur due to the overall radial thermal-flux distribution in the core and local perturbations in the flux caused by control rods and burnable poison elements or curtains. Circumferential variations in the coolant temperature can occur as a result of varying amounts of heat transfer to the surrounding coolant channels due to both the location of burnable poison elements and the amount of power generated in the individual fuel rods.

The bowing of a fuel rod affects the surrounding flow channels. The result can be a constriction of the coolant-flow area in the thermally limiting coolant (hot) channels and a simultaneous increase in the flow area in the other flow channels. If this condition occurs, the flow constriction increases the magnitude of the friction pressure drop in the hot channel relative to the other components (e.g., elevation and acceleration) of the total pressure drop. Since the total pressure drop of the hot channel must remain equal to the pressure drop of the other channels, the coolant mass flow rate is reduced and the enthalpy rise is increased within the hot channels.

The reduced coolant flow in the hot channel and increased coolant flow in the surrounding channels can lead to greater circumferential temperature asymmetry in the cladding of the fuel rods surrounding the constricted hot channel. This, in turn, may lead to increased channel constriction.

This article describes an iterative process to determine the interaction of fuel-rod bow and the thermal hydraulics of the affected coolant channels. The method is particularly applicable to conventional light-water-reactor pellet-in-tube type of fuel rods. The basic method of analysis is discussed in general terms. The method is then described in more detail, and the various equations utilized in the analysis are presented for the case where the fuel rod is supported only at its ends. An extension of the method to the analysis of

*Hittman Associates, Inc., Columbia, Md.

the case where intermediate spacers are used is described. The results for various degrees of end restraint for simply supported fuel rods are presented and discussed.

General Description of Method

The magnitude and direction of the fuel-rod bow are determined by an iterative process. Bowing of a fuel rod affects the thermal hydraulics of the adjacent coolant channels and, in turn, affects the cladding-temperature distribution of the fuel rod. It is this temperature distribution, together with the constraints provided at the ends and intermediate points along the fuel rod (by grid plates and spacers), which establishes the magnitude and direction of fuel-rod bow.

The basic analytical procedure is as follows:

1. A direction and magnitude of fuel-rod bow along its length are assumed.

2. The effect of the fuel-rod bow on the flow rates in the adjacent channels is determined. For the purposes of the detailed analysis presented below, the conservative assumption is made that no mixing occurs between coolant channels. If appreciable mixing can be shown to occur by either analytical or experimental techniques, the actual magnitude of bowing could be significantly less than the predicted bowing.

3. The axial variation of coolant-temperature distribution in each of the coolant channels adjacent to the fuel rod is calculated based on flow rates determined in step 2 and the local heat-generation rates in the fuel rods forming each coolant channel. In the particular core analyzed using this method, the burnable poison rods, which generate a negligible quantity of heat relative to the fuel rods, were a significant cause of coolant-temperature variations between adjacent channels.

4. A two-dimensional heat-transfer analysis of the fuel rod is performed at various axial locations using the channel coolant temperatures calculated in step 3. This heat-transfer analysis establishes the cladding-temperature distribution and the circumferential variation of heat flux into the coolant channels.

5. The magnitude and direction of fuel-element bow are calculated based on the axial and circumferential variations of the cladding temperature calculated in step 4.

6. The process is repeated iteratively until convergence is achieved. The bow calculated in step 5 replaces the assumed bow of step 1. The heat fluxes calculated in step 4 are utilized in step 3 of the next iteration.

Detailed Description of Method

The details of the method of analysis, including the appropriate equations, are presented below. The coolant-channel thermal-hydraulic analysis, the two-dimensional temperature-distribution calculations, the fuel-rod bowing analysis for end supports only, and the fuel-rod bowing analysis with intermediate supports are discussed individually.

Coolant-Channel Thermal-Hydraulic Analysis

To perform the coolant-channel thermal-hydraulic analysis, the coolant channel is divided into a number of axial sections. The coolant pressure drop in an average unbowed coolant channel is calculated. This calculation includes the pressure drop due to coolant acceleration, elevation, friction, and flow path changes at the entrance and exit of the channel. The pressure drop calculated for the average channel is considered the core pressure drop.

The flow rate in the coolant channels affected by bowed fuel rods (designated the hot channels) is then calculated by an iterative procedure. Again, the coolant channels are divided into a number of axial sections. The hot-channel flow rate and pressure-drop calculations consider the effects of fuel-rod bow, plenum effects, and heat input. The coolant enthalpy at each axial section is calculated, and single- or two-phase friction pressure-drop correlations are used, as appropriate.

To accurately compute the hot-channel flow where the flow vs. pressure-drop curve may contain inflections, a table of hot-channel flow vs. pressure drop is constructed by a stepwise reduction of flow from 100% (times some optional input multiplier) of the average channel value to a flow resulting in a pressure drop below that of the average channel. The flow vs. pressure-drop table is then searched and interpolated for a pressure-drop value equal to that calculated for the average channel. Once the hot-channel flows are determined, enthalpy, temperature, and steam quality values are calculated and printed.

Because of the large number of calculations involved, a computer code called PINCH (Pin-Channel) is utilized to perform the thermal-hydraulic analysis. This code is based on the STDY-3 computer code (Ref. 1).

The total channel pressure drop is given by the equation

$$\Delta P_{\text{tot.}} = \Delta P_{\text{acc.}} + \Delta P_{\text{elev.}} + \Delta P_{\text{frict.}} + \Delta P_{\text{entrance + exit}} \qquad (1)$$

The acceleration, elevation, entrance, and exit pressure losses are calculated based on a mass velocity corresponding to the inlet flow, $G_{\text{in.}}$. The friction pressure drop, $\Delta P_{\text{frict.}}$, is given by the equation

$$\Delta P_{\text{frict.}} = \frac{1}{2g_c} \sum_i \frac{G_i^2}{D_i} \times \left(\frac{f/f_{\text{iso.}}}{\rho} \right) f_{\text{iso.}} \Delta Z \quad \text{Nonbulk boiling}$$

$$+ \frac{1}{2g_c} \sum_i \frac{G_i^2}{D_i} (\Phi_{LO})^2 \Delta Z f_{\text{iso.}} \quad \text{Bulk boiling} \qquad (2)$$

since

$$\frac{G_i^2}{D_i} = \frac{G_{\text{in.}}^2}{D_{\text{in.}}} \times \left(\frac{A_{\text{in.}}}{A_i} \right)^3 \qquad (3)$$

The friction pressure drop may be rewritten in the form

$$\Delta P_{\text{frict.}} = \frac{1}{2g_c} \frac{G_{\text{in.}}^2}{D_{\text{in.}}} \times \sum_i \left(\frac{f/f_{\text{iso.}}}{\rho} \right) f_{\text{iso.}} \Delta Z \times F \quad \text{Nonbulk boiling}$$

$$+ \frac{1}{2g_c} \frac{G_{\text{in.}}^2}{D_{\text{in.}}} \sum_i (\Phi_{LO})^2 \times \Delta Z \times F f_{\text{iso.}} \quad \text{Bulk boiling} \qquad (4)$$

where

$$F = \left(\frac{A_{\text{in.}}}{A_i} \right) \quad \text{Constricted channel} \qquad (5)$$

Once the flow rate in each of the coolant channels is determined, the coolant temperature at every axial section of each channel is calculated by a simple heat balance. The heat-balance calculations account for all the heat input into the channel from the surrounding fuel rods and assume that there is no exchange of coolant between channels.

Two-Dimensional Fuel-Rod Heat-Transfer Model

A two-dimensional heat-transfer model of the cross section of the fuel rod is used to calculate the circumferential variation of centerline cladding temperature and heat flux. The model accounts for the asymmetric power generation in the fuel rod due to the gross core radial power distribution and local perturbations resulting from control rods and burnable poison rods. The model includes a calculation to determine whether or not a particular segment of the coolant channel is in nucleate boiling. This enables the use of a boiling or nonboiling coolant film coefficient correlation, as appropriate.

The fuel pellet and cladding are divided into radial and circumferential regions. A nodal point in each region represents the mean temperature of that region. Coolant temperatures are obtained from the thermal-hydraulic analysis code. Thermal admittances connect each nodal point to the four surrounding nodal points and are used to determine the heat flow through the element. The admittances are calculated according to the following general equation:

$$Y = \frac{kA}{\Delta X} \qquad (6)$$

The TAP-4 (Thermal Analyzer Program) computer code[2] is utilized to iteratively calculate the temperature at each nodal point. This code solves the basic conduction heat-transfer equation by means of relaxation techniques according to the following equation:

$$T_i = \frac{Q_i + \sum_j Y_{i,j} T_j}{\sum_j Y_{i,j}} \qquad (7)$$

The specific formulas for the radial and circumferential admittances are

$$Y_R = \frac{2\pi kH}{\ln \dfrac{r_n}{r_{n-1}}} \left(\frac{\Delta\theta}{360} \right) \qquad (8)$$

$$Y_\theta = \frac{(r_{n+1} - r_{n-1})kA}{\pi r_n} \left(\frac{360}{\Delta\theta} \right) \qquad (9)$$

The fuel pellet was assumed to be concentrically located within the fuel rod. A gap admittance of 1000 Btu/(hr)(sq ft)(°F) was used to evaluate the heat flow between the fuel pellet and cladding surfaces.

The nodal heat generation is calculated by the equation

$$Q_i = q_i''' V_i \qquad (10)$$

$$V_i = \left(\frac{r_{n+1} - r_{n-1}}{2} \right) (r_n A) \left(\frac{\Delta\theta}{360} \right) \qquad (11)$$

There was a significant asymmetry in the power generation within the fuel rods analyzed. This was caused by control rods and burnable poison elements in proximity to the channel. For this reason it was necessary to formulate individual heat-generation rates for each node. The pointwise power edits of the PDQ-6 code, used for the core nuclear analysis, were employed to determine the local power distribution in the fuel rod.

Both forced-convective nonboiling and subcooled boiling regions are considered in the model. The nonboiling coolant film temperature difference is calculated using the Dittus–Boelter film coefficient correlation

$$h = 0.023(\mathrm{Re})^{0.8}(\mathrm{Pr})^{0.4}\frac{k}{D} \qquad (12)$$

The cladding temperature associated with nonboiling is calculated by

$$t_c = t_{\text{cool.}} + q''/h \qquad (13)$$

A subroutine is included in the TAP-4 program which calculates the film temperature gradient using the Jens–Lottes correlation for nucleate boiling.

$$t_c = t_{\text{sat.}} + 60\left(\frac{q''}{10^6}\right)^{0.25} \exp(-P/900), \,^{\circ}\mathrm{F} \qquad (14)$$

Bowing Model—End Supports Only

A model was developed to allow the calculation of temperature induced deflection in fuel elements under steady-state conditions. The effects of finite clearances between the fuel-element support pins and the restraint points at the ends of the fuel rod are included in the model. The fuel rod is treated as a simply supported beam which deflects as a result of an asymmetrical temperature distribution and is restrained by forces imposed by the surroundings. Assumptions implicit in the model are:

1. The fuel-rod cross section is constant along its length.
2. The fuel-rod cross section is symmetric about the plane of bowing.
3. Fuel-rod support pins and surroundings are essentially rigid.
4. The deflections are small compared to the length.

The various deflections that result in fuel-rod bowing may be categorized as follows:

1. Thermal or resultant deflection
   - Free deflection.
   - Forced deflection.
2. Mechanical deflection
   - Straightness deflection.
   - Alignment deflection.
   - Grid-plate slope deflection.

The above terms are defined as follows:

Free deflection: Free deflection results from the asymmetrical temperature distribution where the effect of end restraints is neglected.

Forced deflection: The forced deflection is caused by the end moments that result from the interaction of the thermally distorted fuel rod with its end supports. An allowance is made for the finite clearances at each end of the rod.

Thermal deflection: Resultant of the free and forced deflections.

Straightness deflection: The straightness deflection is due to an initial nonstraightness of the fuel element.

Alignment deflection: This deflection is a result of fuel-element grid-plate hole misalignment. This misalignment is a function of the grid-plate hole perpendicularity and fuel-element parallelism.

Grid-plate slope deflection: The grid-plate slope deflection is due to nonparallelism between the upper and lower grid plates. The grid-plate slope deflection within a single fuel bundle is the same for each fuel rod and does not contribute to the channel construction for those channels within a bundle.

Mechanical deflection: Sum of the straightness, alignment, and grid-plate slope deflections.

The total deflection is obtained by superimposing the thermal or resultant deflection and the mechanical deflection.

The free-deflection curve is obtained by double integration. The fuel rod is treated as a simply supported beam under a fictitious load. The fictitious load is the external moment distribution required to exactly counteract the thermal gradients in the fuel-element cladding such that the cladding is not bowed.

The free-deflection curve is obtained by a numerical solution of the following equation:

$$\frac{d^2y}{dx^2} = \frac{M}{EI} \qquad (15)$$

where the boundary conditions are

$$y_{(x=0)} = 0 \qquad (15a)$$

$$y_{(x=L)} = 0 \qquad (15b)$$

The acceleration, elevation, entrance, and exit pressure losses are calculated based on a mass velocity corresponding to the inlet flow, $G_{\text{in.}}$. The friction pressure drop, $\Delta P_{\text{frict.}}$, is given by the equation

$$\Delta P_{\text{frict.}} = \frac{1}{2g_c}\sum_i \frac{G_i^2}{D_i} \times \left(\frac{f/f_{\text{iso.}}}{\rho}\right) f_{\text{iso.}}\Delta Z \quad \text{Nonbulk boiling}$$

$$+ \frac{1}{2g_c}\sum_i \frac{G_i^2}{D_i}(\Phi_{LO})^2 \Delta Z f_{\text{iso.}} \quad \text{Bulk boiling} \qquad (2)$$

since

$$\frac{G_i^2}{D_i} = \frac{G_{\text{in.}}^2}{D_{\text{in.}}} \times \left(\frac{A_{\text{in.}}}{A_i}\right)^3 \qquad (3)$$

The friction pressure drop may be rewritten in the form

$$\Delta P_{\text{frict.}} = \frac{1}{2g_c}\frac{G_{\text{in.}}^2}{D_{\text{in.}}} \times \sum_i \left(\frac{f/f_{\text{iso.}}}{\rho}\right) f_{\text{iso}}\Delta Z \times F \quad \text{Nonbulk boiling}$$

$$+ \frac{1}{2g_c}\frac{G_{\text{in.}}^2}{D_{\text{in.}}} \sum_i (\Phi_{LO})^2 \times \Delta Z \times F f_{\text{iso.}} \quad \text{Bulk boiling} \qquad (4)$$

where

$$F = \left(\frac{A_{\text{in.}}}{A_i}\right) \quad \text{Constricted channel} \qquad (5)$$

Once the flow rate in each of the coolant channels is determined, the coolant temperature at every axial section of each channel is calculated by a simple heat balance. The heat-balance calculations account for all the heat input into the channel from the surrounding fuel rods and assume that there is no exchange of coolant between channels.

Two-Dimensional Fuel-Rod Heat-Transfer Model

A two-dimensional heat-transfer model of the cross section of the fuel rod is used to calculate the circumferential variation of centerline cladding temperature and heat flux. The model accounts for the asymmetric power generation in the fuel rod due to the gross core radial power distribution and local perturbations resulting from control rods and burnable poison rods. The model includes a calculation to determine whether or not a particular segment of the coolant channel is in nucleate boiling. This enables the use of a boiling or nonboiling coolant film coefficient correlation, as appropriate.

The fuel pellet and cladding are divided into radial and circumferential regions. A nodal point in each region represents the mean temperature of that region. Coolant temperatures are obtained from the thermal-hydraulic analysis code. Thermal admittances connect each nodal point to the four surrounding nodal points and are used to determine the heat flow through the element. The admittances are calculated according to the following general equation:

$$Y = \frac{kA}{\Delta X} \qquad (6)$$

The TAP-4 (Thermal Analyzer Program) computer code[2] is utilized to iteratively calculate the temperature at each nodal point. This code solves the basic conduction heat-transfer equation by means of relaxation techniques according to the following equation:

$$T_i = \frac{Q_i + \sum_j Y_{i,j}T_j}{\sum_j Y_{i,j}} \qquad (7)$$

The specific formulas for the radial and circumferential admittances are

$$Y_R = \frac{2\pi kH}{\ln \dfrac{r_n}{r_{n-1}}}\left(\frac{\Delta\theta}{360}\right) \qquad (8)$$

$$Y_\theta = \frac{(r_{n+1} - r_{n-1})kA}{\pi r_n}\left(\frac{360}{\Delta\theta}\right) \qquad (9)$$

The fuel pellet was assumed to be concentrically located within the fuel rod. A gap admittance of 1000 Btu/(hr)(sq ft)(°F) was used to evaluate the heat flow between the fuel pellet and cladding surfaces.

The nodal heat generation is calculated by the equation

$$Q_i = q_i''' V_i \qquad (10)$$

$$V_i = \left(\frac{r_{n+1} - r_{n-1}}{2}\right)(r_n A)\left(\frac{\Delta\theta}{360}\right) \qquad (11)$$

There was a significant asymmetry in the power generation within the fuel rods analyzed. This was caused by control rods and burnable poison elements in proximity to the channel. For this reason it was necessary to formulate individual heat-generation rates for each node. The pointwise power edits of the PDQ-6 code, used for the core nuclear analysis, were employed to determine the local power distribution in the fuel rod.

Both forced-convective nonboiling and subcooled boiling regions are considered in the model. The nonboiling coolant film temperature difference is calculated using the Dittus–Boelter film coefficient correlation

$$h = 0.023(\mathrm{Re})^{0.8}(\mathrm{Pr})^{0.4}\frac{k}{D} \tag{12}$$

The cladding temperature associated with nonboiling is calculated by

$$t_c = t_{\mathrm{cool.}} + q''/h \tag{13}$$

A subroutine is included in the TAP-4 program which calculates the film temperature gradient using the Jens–Lottes correlation for nucleate boiling.

$$t_c = t_{\mathrm{sat.}} + 60\left(\frac{q''}{10^6}\right)^{0.25} \exp(-P/900), \,^{\circ}\mathrm{F} \tag{14}$$

Bowing Model—End Supports Only

A model was developed to allow the calculation of temperature induced deflection in fuel elements under steady-state conditions. The effects of finite clearances between the fuel-element support pins and the restraint points at the ends of the fuel rod are included in the model. The fuel rod is treated as a simply supported beam which deflects as a result of an asymmetrical temperature distribution and is restrained by forces imposed by the surroundings. Assumptions implicit in the model are:

1. The fuel-rod cross section is constant along its length.
2. The fuel-rod cross section is symmetric about the plane of bowing.
3. Fuel-rod support pins and surroundings are essentially rigid.
4. The deflections are small compared to the length.

The various deflections that result in fuel-rod bowing may be categorized as follows:

1. Thermal or resultant deflection
   - Free deflection.
   - Forced deflection.
2. Mechanical deflection
   - Straightness deflection.
   - Alignment deflection.
   - Grid-plate slope deflection.

The above terms are defined as follows:

Free deflection: Free deflection results from the asymmetrical temperature distribution where the effect of end restraints is neglected.

Forced deflection: The forced deflection is caused by the end moments that result from the interaction of the thermally distorted fuel rod with its end supports. An allowance is made for the finite clearances at each end of the rod.

Thermal deflection: Resultant of the free and forced deflections.

Straightness deflection: The straightness deflection is due to an initial nonstraightness of the fuel element.

Alignment deflection: This deflection is a result of fuel-element grid-plate hole misalignment. This misalignment is a function of the grid-plate hole perpendicularity and fuel-element parallelism.

Grid-plate slope deflection: The grid-plate slope deflection is due to nonparallelism between the upper and lower grid plates. The grid-plate slope deflection within a single fuel bundle is the same for each fuel rod and does not contribute to the channel construction for those channels within a bundle.

Mechanical deflection: Sum of the straightness, alignment, and grid-plate slope deflections.

The total deflection is obtained by superimposing the thermal or resultant deflection and the mechanical deflection.

The free-deflection curve is obtained by double integration. The fuel rod is treated as a simply supported beam under a fictitious load. The fictitious load is the external moment distribution required to exactly counteract the thermal gradients in the fuel-element cladding such that the cladding is not bowed.

The free-deflection curve is obtained by a numerical solution of the following equation:

$$\frac{d^2y}{dx^2} = \frac{M}{EI} \tag{15}$$

where the boundary conditions are

$$y_{(x=0)} = 0 \tag{15a}$$

$$y_{(x=L)} = 0 \tag{15b}$$

The free-deflection moment diagram is calculated by dividing the fuel rod into an arbitrary number of axial sections. At each axial section the rod is further subdivided into a number of equal angular segments, and the internal thermal moment about the assumed plane of bending is calculated. The thermal bending moment at each axial section is calculated by the equation

$$M = \sum_{i=1}^{N} M_i \tag{16}$$

where

$$M_i = F_i l_i \quad \text{(see Fig. 1)} \tag{17}$$

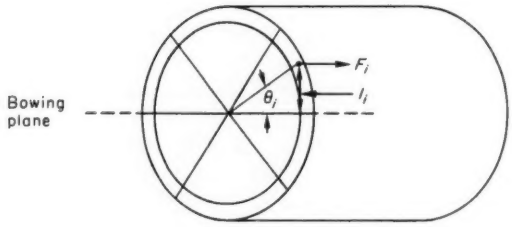

Fig. 1 View of an axial segment of a fuel element.

The perpendicular distance from the center of the angular segment to the plane of bending is $l_i = [(d_o + d_i)/4] \sin \theta_i$. The thermal forces are given by the equation

$$F_i = \alpha E \frac{A_c}{N} \Delta T_i \tag{18}$$

where

$$T_i = T_i - \overline{T} \tag{19}$$

and

$$\overline{T} = \frac{\sum_{i}^{N} T_i}{N} \tag{20}$$

The value of $\overline{T}$ calculated from Eq. 20 sets the sum of the internal forces equal to zero.

The final form for the total thermal moment at each axial section is given by the equation

$$M = \frac{\alpha E \pi}{16N}(d_o^2 - d_i^2)(d_o + d_i) \sum_{i=1}^{N} \Delta T_i \sin \theta_i \tag{21}$$

The forced-deflection curve resulting from the element end restraints is calculated directly from the moment equation where, for the case of a moment applied to the fuel rod by the support structure at $x = L$,

$$M = \frac{xM'}{L} \tag{22}$$

with the boundary conditions

$$y_{(x=0)} = 0 \tag{23}$$

and

$$y_{(x=L)} = 0 \tag{24}$$

The equation for this deflection is

$$y = -\frac{M'Lx}{6EI}\left(1 - \frac{x^2}{L^2}\right) \tag{25}$$

The slope at each end of the forced-deflection curve is

$$\left(\frac{dy}{dx}\right)_{x=0} = \frac{M'L}{6EI} \tag{26}$$

and

$$\left(\frac{dy}{dx}\right)_{x=L} = \frac{M'L}{3EI} \tag{27}$$

Similar equations may be derived for the forced-deflection curve with end fixity at $x = 0$.

The end moment M' is determined from the slope of the forced-deflection curve by the equation

$$M' = \frac{3EI}{L}\left(\frac{dy}{dx}\right)_{x=L} \tag{28}$$

forced-deflection-curve slope

The forced-deflection slope is determined from the slope of the free-deflection curve and the slope of the resultant deflection curve using the equation

$$\left(\frac{dy}{dx}\right)_{\substack{\text{forced-}\\\text{deflection}\\\text{curve}}} = \left(\frac{dy}{dx}\right)_{\substack{\text{free-}\\\text{deflection}\\\text{curve}}} - \left(\frac{dy}{dx}\right)_{\substack{\text{resultant}\\\text{deflection}\\\text{curve}}} \tag{29}$$

The amount of end fixity is determined by the clearances between the ends of the fuel rod and the support structure. The slope of the resultant deflection

curve at the ends of the fuel rod is therefore established by the clearance. The free- and forced-deflection curves are then superimposed to give the resultant deflection curve.

Resultant deflection curves are obtained for two mutually perpendicular planes of bending. The resultant deflection curves for each plane of bending are added vectorially to determine the actual resultant bow magnitude and direction.

A digital computer code called BOW was written to perform the numerical computations required by the above equations, particularly the determination of the free-deflection curve. The results were compared with hand calculations of the moment equation using the area-moments method and the conjugate-beam method. The solutions using each of the methods were essentially equivalent.

Partial mechanical bow of the fuel elements can arise from misalignment of the supporting pins on the fuel-rod end caps and the receptacle holes in the grid plate. The equation for the deflection resulting from this type of bow is

$$y = y_m \frac{x}{L}\left[1 - \frac{x}{2L^2}(3L - x)\right] \qquad (30)$$

where y_m is the deflection that would arise from the support misalignment if the element were supported at one end and free at the other end (see Fig. 2).

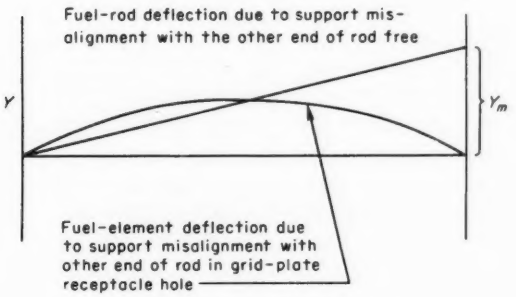
Fuel-rod deflection due to support misalignment with the other end of rod free
Y
Y_m
Fuel-element deflection due to support misalignment with other end of rod in grid-plate receptacle hole

Fig. 2 Mechanical bow from element misalignment.

Bowing Model—Intermediate Supports

The basic bowing model described above can be extended to treat the case where the fuel rod is supported at intermediate points along its length as well as at its ends. This is the usual situation for long fuel rods.

The method of treating intermediate supports is outlined below as a series of steps required for each iteration. The equations for the case where there are two intermediate support points are presented.

The steps in the calculational procedure are:

1. Assume an initial bow configuration.
2. Calculate the thermal hydraulics of the surrounding coolant channels and the cladding-temperature distribution at various axial locations in the same manner as that described for the fuel rod supported only at its ends.
3. Calculate the thermal moment and the free-deflection curve in the same manner used for the case where the fuel rod was supported only at its ends.

The supports at the ends of the fuel rods and at the intermediate locations along the length of the fuel rod impose loads that alter the deflection calculated in step 3. These loads, in fact, result in a deflection of zero (plus or minus the manufacturing tolerances, clearances, and deflection of the support structure) at these axial locations.

4. Calculate the loads at the ends of the fuel rods and at the intermediate support points which yield a deflection equal in magnitude and opposite in direction to the free deflection calculated in step 3. These loads can be determined from basic beam theory. The effect of tolerances and clearances should be included in the selected deflections.
5. Algebraically add the deflections calculated in steps 3 and 4 to determine the resultant deflection.
6. Algebraically add the deflection resulting from misalignment in the same manner used for a fuel rod supported only at its ends.

Step 4 is illustrated below for the case of two intermediate supports located so as to form three equal unsupported spans, as shown in Fig. 3.

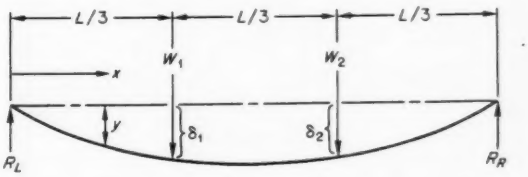

Fig. 3 Fuel-rod deflection with two intermediate supports.

The general equation for the deflection due to loads W_1 and W_2 and the reactions R_L and R_R can be obtained by adding solutions,[3] yielding the following equations:

$$y = \frac{-x}{9EI}\left[W_1\left(\frac{5}{9}L^2 - x^2\right) + 0.5W_2\left(\frac{8}{9}L^2 - x^2\right)\right] \quad \text{for } 0 \le x \le L/3 \quad (31a)$$

$$y = \frac{-1}{18EI}\left[W_1(L-x)\left(\frac{-L^2}{9} - x^2 + 2Lx\right) + W_2 x\left(\frac{8}{9}L^2 - x^2\right)\right] \quad \text{for } \frac{L}{3} \le x \le \frac{2L}{3} \quad (31b)$$

$$y = -\frac{(L-x)}{9EI}\left[0.5W_1\left(\frac{-L^2}{9} - x^2 + 2Lx\right) + W_2\left(\frac{-4L^2}{9} - x^2 + 2Lx\right)\right] \quad \text{for } \frac{2L}{3} \le x \le L \quad (31c)$$

To determine the loads W_1 and W_2, assume the free deflections calculated in step 3 are δ_1 and δ_2. Using deflections of equal magnitude but opposite direction of these deflections in Eqs. 31*a* to 31*c* yields

$$-\delta_1 = \frac{-L^3}{486EI}(8W_1 + 7W_2) \quad (32a)$$

and

$$-\delta_2 = \frac{-L^3}{486EI}(7W_1 + 8W_2) \quad (32b)$$

Solving Eqs. 32*a* and 32*b* simultaneously yields

$$W_1 = \frac{162}{5}\frac{EI}{L^3}(8\delta_1 - 7\delta_2) \quad (33a)$$

and

$$W_2 = \frac{162}{5}\frac{EI}{L^3}(8\delta_2 - 7\delta_1) \quad (33b)$$

Results

The coolant-channel thermal-hydraulic, fuel-rod heat-transfer, and fuel-rod-bowing models and methods described above were applied to the PM type 4 core. This core, which will be used in the PM-3A power plant in Antarctica, has fuel rods 33 in. long with a 0.373-in. OD, 0.015-in. thick, 348 stainless-steel cladding. The fuel rods are arranged in a triangular array; therefore each fuel rod has six adjacent coolant channels.

The initial portion of the effort was directed toward determining the combination of power level, coolant inlet temperature, and operating pressure which caused the most severe thermal limitations. Since subcooled nucleate boiling over a portion of the element surface reduced the cladding temperature asymmetry, and therefore the potential bowing problem, it was not apparent which values of these parameters were most limiting. Therefore a preliminary parametric study was performed.

It was found that the maximum free deflection occurred when the reactor pressure, inlet temperature, and power level were simultaneously at their maximum operating values.

The deflection of the fuel rod was then studied considering three sets of cases:

1. No end restraints.
2. Bottom (inlet end) restraint.
3. Top (outlet end) restraint.

The thermal-hydraulic analysis was performed assuming the worst combination (from a bowing viewpoint) of mechanical tolerances and hot-channel factors. That is, the fuel rod was assumed to be displaced and mechanically bowed so as to restrict the flow in the adjacent coolant channel having the greatest heat input and increase the flow in the other five coolant channels. The uncertainties in the predictions of power generation were also assumed so as to result in a greater heat input into the thermally limiting channel and a lesser heat input into the other five channels.

The thermal-hydraulic analysis yielded values of coolant temperature at a number of axial locations for each of the six coolant channels. These served as input to the two-dimensional heat-transfer model that was used to calculate the circumferential temperature distribution of the cladding at a number of axial locations. This cladding-temperature distribution was then used to calculate the axial distribution of the thermal moment along the length of the fuel rod.

The results for the case of no end restraints are shown in Fig. 4*a* and are designated as having a moment multiplier of 1.0. The gross effect of thermal bow on the coolant-channel thermal-hydraulics and cladding temperature was studied parametrically. The thermal moment was arbitrarily multiplied by factors of 1.73 and 3.0. These results are also presented in Fig. 4*a* and show that an increase in the thermal moment results in an increase in fuel-rod bow; therefore, for the unrestrained case, it can be concluded that thermal bow will further restrict the hot-channel flow rate, thereby adversely affecting the cladding-temperature

distribution. This will, in turn, result in a greater bow, etc.

The results for the case where an inlet end restraint was assumed are presented in Fig. 4*b*. Again, moment multipliers of 1.0, 1.73, and 3.0 were considered. The inlet end constraint was assumed to limit the slope at the bottom of the fuel rod to 0.006. This degree of end restraint provided no benefit for moment multipliers of 1.0 and 1.73 since the slope of the unrestrained deflection curves was less than 0.006 for these cases. There was a very small reduction in the fuel-rod bowing for the moment multiplier of 3.0. The reduction in bowing with an inlet fixity is small since the maximum asymmetrical cladding-temperature distribution occurs in the upper (outlet) region of the element.

There is a significant effect on fuel-element bow resulting from a restraint on the outlet end of the fuel rod, as shown in Fig. 4*c*. Again, the restraint was assumed to limit the slope to 0.006. Figure 4*c* shows a decrease in the resultant thermal bowing into the hot channel with increasing temperature asymmetry (which corresponds to a greater thermal moment). This is very important since this leads to a negative feedback rather than the positive feedback shown for the unrestrained case. The outlet restraint is very effective because the maximum temperature difference (and consequently the maximum thermal moment and fuel-rod slope) occurs at this end of the fuel rod. The mechanical restraint at this end introduces a large forced deflection in a direction opposite to the free deflection in the region of the fuel rod where the free deflection is greatest. As the free deflection is increased (increased moment multiplier in the case illustrated), the forced deflection needed to limit the slope to 0.006 increases more than the free deflection, resulting in a lesser total deflection into the hot channel.

Although increasing the end fixity results in a decrease in the maximum resultant thermal bowing, it also results in an increase in the maximum mechanical bow resulting from misalignment of the ends of the fuel rod in the grid plate. If large circumferential temperature variations exist, and rod misalignment is minimized, outlet end fixity will have a far greater effect in reducing the resultant thermal bow than the increase in the accompanying mechanical bow.

On the basis of these results, it was decided to provide constraint at the outlet end of the fuel rod. Both the minimum and maximum clearances at the upper end of the fuel rod were analyzed. The minimum clearance was found to yield a greater mechanical bow from element misalignment and a lesser amount of resultant thermal bow relative to the maximum clearance. The total bow was nearly the same for both cases but slightly more severe for the maximum clearance case.

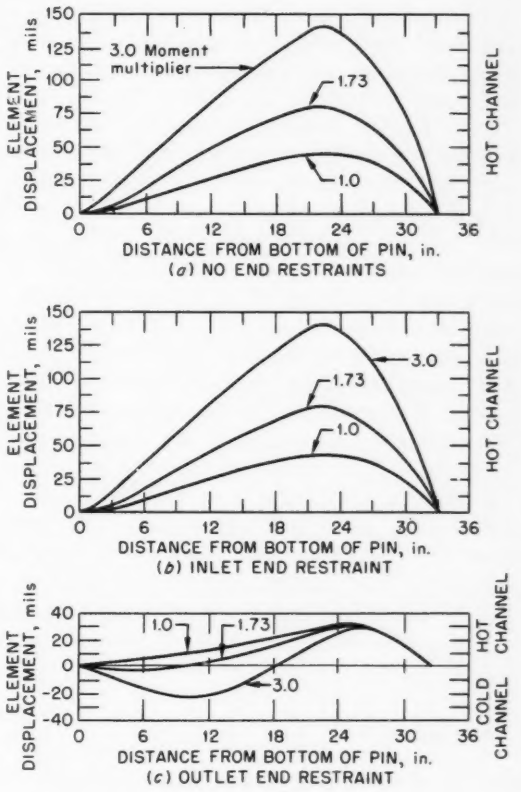

Fig. 4 Resultant thermal bowing characteristics of a fuel rod.

The total thermal and mechanical bow for the fuel rod is shown in Fig. 5 for three iterations. Since each complete iteration requires a considerable amount of computer and hand calculations, the problem was not

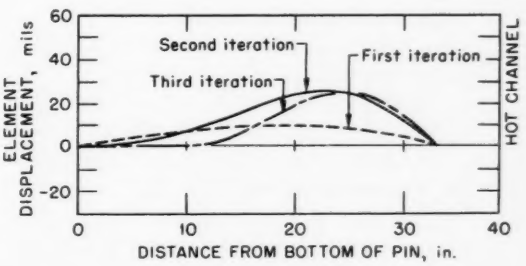

Fig. 5 Total bowing (resultant thermal and mechanical) of fuel rod.

run to close convergence. However, the three iterations performed were sufficient to establish the maximum bow and the corresponding maximum coolant-enthalpy rise in the hot channel.

For the first iteration, only a 10-mil mechanical bow into the hot channel was assumed. This bow was used as input data to the PINCH code, and the coolant-temperature rise in all the channels adjacent to the fuel rod was determined. The corresponding cladding-temperature distribution was then used in the BOW code to determine the magnitude of the fuel-rod resultant thermal bow. The maximum mechanical bow was added to the thermal bow, and the resulting total bow is designated as the second iteration in Fig. 5. This amount of bow was used as input in the PINCH code and the calculation procedure was repeated. These results are designated as the third iteration in Fig. 5. As Fig. 5 shows, a reduction in the total bow occurred between the second and third iterations. The actual bow curves fall somewhere between the results of the second and third iterations. Since the second-iteration PINCH calculations contained the second-iteration maximum-bow calculations, this case yields an upper limit on the flow restriction in the hot channel.

Nomenclature

A = area perpendicular to heat flow, sq ft
A_c = total cross section area of cladding
A_i = flow area of channel in section i
$A_{\text{in.}}$ = inlet flow area of channel
d_o = outside cladding diameter
d_i = inside cladding diameter
D = hydraulic diameter
D_i = hydraulic diameter of the channel in section i
$D_{\text{in.}}$ = hydraulic diameter at the inlet of the channel
E = modulus of elasticity of the fuel-rod cladding
$f_{\text{iso.}}$ = nonboiling friction factor
$f/f_{\text{iso.}}$ = friction factor ratio for heating and local boiling
F = term in the friction pressure-drop calculation which accounts for the variable flow area of the coolant channel resulting from bowed fuel rods
F_i = force in the ith segment from circumferential temperature asymmetry
g_c = acceleration of gravity
G_i = mass velocity (mass flow rate per unit area) in the channel in section i
$G_{\text{in.}}$ = mass velocity (mass flow rate per unit area) at the channel inlet
h = film coefficient
H = height
I = moment of inertia of the fuel-rod cladding
k = thermal conductivity
L = length of fuel rod
l_i = perpendicular distance from the middle of the ith segment to the bowing plane
M = thermal bending moment
M' = applied end moment at L
n = node number
N = number of equal angular segments
P = reactor operating pressure
$\Delta P_{\text{acc.}}$ = acceleration pressure drop
$\Delta P_{\text{elev.}}$ = elevation pressure drop
$\Delta P_{\text{entrance and exit}}$ = pressure drop due to coolant-channel geometry at the entrance and exit of the channel
$\Delta P_{\text{frict.}}$ = friction pressure drop
$\Delta P_{\text{tot.}}$ = total channel pressure drop
Pr = Prandtl number
q'' = heat flux to coolant from local segment of fuel rod of cladding
q''' = nodal region volumetric heat-generation rate
Q = nodal heat generation
r = radial distance
Re = Reynolds number
T = temperature
t_c = cladding-OD surface temperature
$t_{\text{cool.}}$ = coolant temperature
$t_{\text{sat.}}$ = coolant saturation temperature
T_i = cladding temperature at the ith segment
$\overline{T}$ = average temperature of an axial section
V_i = volume of nodal region i
W_1 = load exerted by intermediate spacer at $X = L/3$
W_2 = load exerted by intermediate space at $X = 2L/3$
x = axial distance measured from the bottom or inlet end of the element
ΔX = distance between adjacent nodal points
y = displacement of the element from the unbowed position
Y = thermal admittance
Y_R = thermal admittance in radial direction
Y_θ = thermal admittance in the circumferential direction
ΔZ = axial increment length
α = thermal coefficient of expansion

δ_1 = free deflection of fuel rod at $X = L/3$
δ_2 = free deflection of fuel rod at $X = 2L/3$
$(\Phi_{LO})^2$ = ratio of two-phase frictional pressure-drop gradient to corresponding isothermal liquid gradient
ρ = density of the fluid
θ_i = angle measured from the bending plane to the middle of the ith segment
$\Delta\theta$ = angular increment, degrees

References

1. R. S. Pyle, STDY-3, A Program for the Thermal Analysis of a Pressurized Water Nuclear Reactor During Steady-State Operation, USAEC Report WAPD-TM-213, Westinghouse Electric Corp., Bettis Atomic Power Laboratory, June 1960.
2. Hittman Associates, Inc., The TAP-4 Program, Report HIT-162(Rev.), Sept. 26, 1966.
3. R. J. Roark, *Formulas for Stress and Strain*, (4th ed.), McGraw-Hill Book Company, Inc., New York, 1965.

Higher Power Densities in Water Reactors– Economic and Technical Bases

By William J. Gallagher and N. Barrie McLeod*

Abstract: *The relation between design criteria of no fuel damage and design practices is described. Design limits, including burnout and fuel center melting, and design margins are discussed and examined from the viewpoint of potential for further improvement in power density. A target of 10% increase in power density is used for purposes of illustration. It is demonstrated, in the case of the heat-transfer limitation (the usual limit), that most factors require an approximate 20% improvement in order to yield a 10% average power-density improvement. In the case of the center-melting limit, a 10% improvement in the factors yields a 10% power-density improvement.*

With regard to economic incentives, it is concluded that the major incentive for improvements is at the initial plant design stage, where potential capital-cost savings of $1.30/kw(e) (0.02 mill/kw-hr) and $2.40/kw(e) (0.04 mill/kw-hr) in the BWR and PWR can be realized with a 10% power-density improvement based on a comparison of stretch ratings with stretch ratings. Where specific power of an existing reactor is to be increased, the benefits of reduced fuel-inventory charges are offset by the higher enrichment needed to maintain burnup with the required annual refueling. Under these circumstances a 10% improvement in specific power (equivalent to a 10% improvement in power density) yields a saving of 0.010 mill/kw(e)-hr in the BWR and 0.007 mill/kw(e)-hr in the PWR at current equilibrium-core target burnup levels. A 30% increase in these target burnup levels would give not only direct savings but also a significant increase in potential benefits of specific power increases. However, current burnups and specific powers have exploited most of the potential economic benefits in fuel cost, and successful large-scale demonstration approaching these fuel-performance levels must be the ultimate base from which further improvements are made. In the meantime the incentives for demonstrated increases in power density justify continued efforts in:

1. Critical heat-flux testing to improve the understanding and predictability of this phenomenon.

2. Irradiation testing and measurements to improve the understanding of material and fuel properties in the case of fuel melting.

3. Long-term irradiation tests and measurements to improve the understanding of fuel swelling rates and fission-gas release at both high burnups and high specific power.

Nuclear energy costs, specifically fuel-inventory charges and a part of the reactor plant cost, are inversely related to average core power density. In addition, plant operational flexibility can be influenced by the margin between normal and maximum permissible operating levels. Hence there are continuing incentives to increase core power capability through prudent increases in average core power density. The magnitude of the incentive is, of course, related to the ability to exploit power-density increases. Maximum incentive exists at the initial reactor design stage, at which both fuel-inventory cost and capital cost can be reduced. At the stage of fuel design for an existing reactor, the fuel-inventory cost can be lowered by first designing to produce increased power up to the "stretch" rating of the plant and thereafter designing to produce the same power with fewer fuel assemblies. Where neither of the above is attempted, operational flexibility can be increased by widening the margin between maximum capability and rated capability.

The principal criterion for a power-capability evaluation in a water reactor is that no core damage that would preclude future power operation is to occur during steady-state operations, during operational power transients, or during plausible overpower or underflow transients. In this article the design limits set by each of the four U. S. light-water reactor suppliers

*NUS Corporation, Rockville, Md.

to ensure that this criterion is met are analyzed in depth with respect to fuel-cycle economic incentives and instrumentation and control capabilities.

In the operation of water reactors, the limits on reactor power are determined primarily by maximum cladding temperature, maximum fuel temperature, flow stability, nuclear stability, and instrument accuracies. An acceptable cladding temperature is generally maintained by preventing thermal burnout by not exceeding the critical heat flux [also termed "departure from nucleate boiling" (DNB)]. An acceptable maximum fuel temperature can be best achieved by limiting maximum rod power output as expressed by the linear heat rate. Cladding failure resulting from high temperatures caused by a flow instability can be avoided by limiting the maximum void fraction. Nuclear instabilities such as xenon oscillations may produce axial or radial power tilts which, if they are not or cannot be corrected or damped, will ultimately force a power-level reduction in order to stay within acceptable design limits. Instrument uncertainties in indicating reactor power level have, in some cases, limited the maximum safe power output.

Each of these factors impacts on attainable maximum power level or power density. Reactor plant economics are proportional to reactor power capability; this gives the reactor supplier and the utility a strong incentive to operate the reactor at the maximum safe power level. Deciding what level is safe requires in-depth analysis—summarized in some detail here—of the various interrelations among these factors.

At least one (probably more than one) of the above factors determines the maximum power capability of any reactor. But even within these limits the core designer has flexibility in his quest to achieve lowest energy costs. Burnup can be increased almost independently of heat-transfer limits simply by increasing fuel enrichment. Ultimately some limit is reached, possibly an economic one, beyond which additional savings from further burnup are less than the cost of carrying the additional inventory; or possibly the available reactivity-control methods become unable to handle additional enrichment and still maintain the shutdown reactivity margin with one stuck control rod; or possibly accumulated fission-gas pressure imposes a burnup limit beyond which increased cladding strain and probability of cladding failure makes it imprudent to operate. The core designer also has the option, infrequently exercised, of varying fuel-rod diameter. An attempt to reduce the effects of a limiting surface heat flux (or linear heat rate) by reducing fuel-rod diameter runs into the economic limit of rapidly increasing fuel-fabrication costs coupled with some required increase in fuel enrichment.

In the final analysis, it is the surface heat-flux limit (or linear heat-rate limit) that imposes a finite fuel-inventory cost, and this inventory cost imposes an economic limit on burnup. Attempts to reduce inventory costs mandate an economically dictated fuel-rod diameter, a diameter surprisingly insensitive to most other design parameters. In summary, the heat-transfer (or linear heat-rate) limits, through the normal design process of cost minimization, influence optimum fuel burnups and attainable fuel cost.

In this article the various design limits and their current status are discussed. These limits are related to core average specific power and power density. Plant- and fuel-cost incentives for improvements are identified.

Design Criteria in Water Reactors

Criterion 6, Reactor Core Design (category A), of the AEC's "General Design Criteria for Nuclear Power Plant Construction Permits"[1] is as follows:

> The reactor core shall be designed to function throughout its design lifetime, without exceeding acceptable fuel damage limits which have been stipulated and justified. The core design, together with reliable process and decay heat removal systems, shall provide for this capability under all expected conditions of normal operation with appropriate margins for uncertainties and for transient situations which can be anticipated, including the effects of the loss of power to recirculation pumps, tripping out of the turbine generator set, isolation of the reactor from its primary heat sink, and loss of all off-site power.

Criterion 6 has generally led to reactor design limits that provide a high degree of confidence that no fuel-element damage will occur during normal operation or anticipated transients. (These design limits also apply to replacement fuel.)

Interpretation of AEC Criteria

"Fuel-element damage," "normal operation," and "anticipated transients" are key terms in Criterion 6. The U. S. reactor vendors have interpreted them as follows:

Fuel-element damage is defined by General Electric Company, for example, as perforation of the cladding which would permit release of fission products to the coolant. This definition is accepted by all reactor manufacturers, although the design limits by which

damage is prevented are not yet uniquely defined. The control-element ejection accident (caused, for example, by drive-mechanism failure) and the loss-of-coolant accident (caused by a break in a primary-system pipe) are examples of hazards during which fuel-element damage may occur.

Normal operation of the reactor is defined as steady operation up to and including rated power as well as transients occurring during startup and turbine-generator load swing other than a loss-of-load transient. Thus fuel must be designed to withstand at least the power transients associated with loading and unloading the generator at design rates.

Anticipated transients are transients other than those described above. The anticipated transient is one which "may have a reasonable probability of occurrence but yet is considered to be out of the range of normal operator-controlled maneuvering."[1] Examples include (1) loss of flow to the reactor caused by failure of power to the main coolant pumps, (2) reactivity-addition transients caused by improper operation or malfunction of control-rod-drive mechanisms at design withdrawal rates, (3) loss of turbine load, and (4) cold-water-addition transients. Other transients that transgress primary-system pressure boundaries are considered in evaluation of hazards which may involve release of radioactivity to the containment.

Design Limits for Power-Capability Analyses

Design limits generally imposed to meet the reactor design criterion of "normal operation with appropriate margins for uncertainties and for transient conditions which can be anticipated"[1] are:

1. Specification of a minimum departure from nucleate boiling ratio (DNBR) or a critical heat-flux ratio (CHFR) in conjunction with a suitable correlation.
2. Specification that cladding strains will not exceed a design value, usually 1% plastic strain from all causes such as fuel growth, fission-gas generation, or pellet ratcheting at any time during fuel lifetime.
3. Specification that fuel temperatures will not exceed a fixed value, usually the melting temperature.
4. Specification that hydraulic-flow instabilities such as parallel channel or coupled nuclear-hydraulic oscillations will not occur.

These are the limits. Margins for uncertainties and for anticipated transients are introduced by hot-channel factors, by flow factors, and by selection of the power level and reactor conditions under which the limits are to be respected. That these conditions are not exceeded is guaranteed by the mode of operation of the reactor and the reactor protection system.

Reactor Manufacturers' Design Limits. Table 1 summarizes the design limits set by each of the four U. S. light-water reactor suppliers. The design limits set by each supplier are similar. Note that in Table 1 the fuel-temperature limit, in practice, is to prevent fuel melting at design overpower. This limit is stated for the pressurized-water reactor (PWR) design. In the boiling-water reactor (BWR) design, General Electric states a fuel-damage limit in terms of a rod power of 28 kw/ft; this is equivalent to 1% plastic strain in the cladding. At 28 kw/ft, fuel center-line melting has occurred since the onset of melting typically occurs at approximately 22 kw/ft. Boiling-water reactor fuel has also been designed so that fuel temperatures do not exceed melting temperature at possible overpower operating transients. Establishing the higher limit, however, may be significant in exploiting economics of the light-water reactors.

Either of two philosophies can be applied: (1) the design limit can be set as a stringent or tight design limit and the reactor designed right up to the limit or (2) the design limit can be set very loosely but a wide margin established between operating parameters and the design limit. Thus, in evaluation of reactor performance, it is necessary to verify the significance of the design limit and to establish the margin to the design limit.

Application of Design Limits. Thermal-hydraulic design of nuclear fuel is considered acceptable if design limits are not exceeded at the maximum steady-state and overpower conditions and during anticipated transients. The relations of power, flow, and pressure must be considered for each transient to ensure that the design limits are met for transient conditions.

Although the ultimate acceptability of a given thermal-hydraulic design depends on detailed analyses of the various reactor transients, the following two design analyses provide important information for evaluation of the design for water reactors. The thermal-hydraulic design limits are evaluated for two conditions:

- A steady-state condition in which a transient power factor is applied to account for power excursions or overshoot due to reactivity-insertion transients: Westinghouse Electric Corp. and Combustion Engineering, Inc., allow for 12% overpower above the steady-state power. Babcock & Wilcox designs for an overpower of 114% of rated power. Current General Electric philosophy is not to design the core for

Table 1 Thermal-Hydraulic Design-Limit Values Specified for Water Reactors

Design limit	General Electric	Westinghouse	Babcock & Wilcox	Combustion Engineering
Minimum DNBR or CHFR at rated power	Minimum CHFR >1.9	No limit	No limit	No limit
Minimum DNBR or CHFR at design overpower	Minimum CHFR >1.0	DNBR >1.3	DNBR >1.38	DNBR >1.3
DNB critical heat-flux correlation	Hench–Levy	Westinghouse W-3	Wilson–Ferrell	Westinghouse W-3
Maximum cladding strain	1% plastic strain*	1% plastic strain	1% plastic strain	0.75% plastic strain
Cladding stress limit	Cladding stress less than yield strength	Cladding stress less than yield strength	Cladding stress less than yield strength	Cladding stresses less than two-thirds of yield under normal operations
Fuel-temperature limit	No central melting during steady-state normal operation	No central melting at design overpower	No central melting at design overpower	No central melting at design overpower
Flow stability	No flow instability	No flow instability	No flow instability	No flow instability
Reference	Browns Ferry design and analysis report	Zion facility description and safety-analysis report	Oconee preliminary safety-analysis report	Calvert Cliffs preliminary safety-analysis report

*Linear rod power <28 kw/ft at any time.

overpower conditions but to size the core for rated conditions and then to demonstrate that suitable margins for operating transients exist. In practice this has meant for General Electric an equivalent design overpower of 115%.

- The loss-of-flow accident resulting from loss of pumping power: In the loss-of-flow transient analysis, power and flow are calculated as a function of time after initiation of the transient from the steady-state power level. Cognizance is taken of the influence on power resulting from the reactivity temperature coefficient, increased void generation, and control-rod insertion.

In each of these conditions, factors must be included for uncertainties in power and flow distribution.

Consideration of Lifetime Effects and Design Limits. The design limits that guarantee that reactor core design criteria are met do not vary with time. Therefore it is necessary to demonstrate for an initial core or for replacement fuel that the design limits will not be violated throughout the projected lifetime of the fuel. The reactor manufacturer will have analyzed the lifetime effects on fuel burnup and power distributions. As a result he will be able to demonstrate DNBR's or minimum CHFR's as a function of time for the warranted power. Replacement fuel, of course, must be subjected to the same rigorous treatment.

In general, the thermal-hydraulic heat-removal design limits can be considered as a function only of conditions existing at the instant under examination. Thus, given reactor power distributions for specific times in fuel lifetime, the proximity to DNBR's or CHFR's can be determined for that time alone. This is in contrast with the time-dependent limits due to irradiation—such as fuel-rod cladding strain, creep collapse, fission-gas pressures, or fuel temperature—for which past events influence present margins.

Extending Design Limits

Status Today. Both BWR and PWR plants currently being licensed for construction permits are rated at higher power densities (50 kw/liter in a BWR and 100 kw/liter in a PWR) than ever before and generally at plant ratings exceeding 500 Mw(e) and as high as 1125 Mw(e). In addition, design burnup in fuel approaches a peak of 50,000 Mwd/metric ton U and an average of 32,000 Mwd/metric ton U at power ratings required for the high power densities. Questions may be asked as to how these developments have come about. Were design limits of the past too conservative? How well established are the design limits now used? Where have the improvements been made? What reactor operating experience supports the designs? What further improvements can be expected?

Limits imposed in reactor design have remained relatively the same throughout water-reactor develop-

ment. Avoidance of DNB and prevention of fuel melting have guided design almost universally. Higher power density or higher fuel specific power have been attained through improvements in:

- Knowledge of physical properties of materials.
- Empirical heat-transfer correlations.
- Power-distribution control.

To illustrate the development leading to today's reactors, Table 2 summarizes the evolution of design parameters from the Yankee Nuclear Power Station at Rowe, Mass., to current PWR and BWR designs.

Improvements in power distributions are reflected in Fq, the hot-channel factors for heat flux. For Yankee Rowe, $Fq = 5.17$; that is, peak rod power and local power densities are 5.17 times the average value. The peaking factor has an important influence on core design: the size and economics of the core are determined largely through core average values.

In the Diablo Canyon class of reactor, starting up 11 years after Yankee, the peak-to-average power density has fallen to 2.82. If the peak rod power as a limit had remained constant, average specific power [kw(t)/kg U] could have been increased by a factor of 1.8. In fact, the average specific power has been increased by a factor of 2.9. This reflects gains in other areas, mainly increased knowledge of physical properties and operating experience in both test and power reactors.

Physical properties, including thermal conductivity and predictive methods for fuel-cladding contact conductance, are areas in which improvement has been made. The result is that, with respect to a design limit of no fuel melting at overpower, the design parameter values have also been increased. Therefore, today, fuel melting can be said to occur at linear rod power values of about 22 kw/ft, a value nearly independent of rod diameter.

Table 2 also shows that reactor control has improved. Design overpower has been reduced in BWR's from 127% in Big Rock Point (startup 1962) to between 115 and 120% in the 3293-Mw(t)[1064 Mw(e)] Browns Ferry station (startup 1970). In PWR's the design overpower has been decreased from 135% in Indian Point (startup 1962) to 112% in Diablo Canyon (startup 1971).

Average power density of the core is influenced by each of the above and also by the critical heat-flux limits. General Electric has described the improvements in correlation of the heat-transfer data on critical heat flux which led to the power-density increase to 51 kw/liter in its Browns Ferry-class BWR. Improvement yielding the current Hench–Levy critical heat-flux correlation depended on investment in research and development in critical heat-flux testing of multirod electrically heated tests. The same has been true in PWR technology on critical heat flux which has led to improved correlations based on multirod electrically heated tests by various manufacturers.

Thus, by improving operating control, power measurement, and prediction of reactor conditions and reactor parameters, it has been possible to increase reactor power density from ~29 kw/liter in Dresden 1 to 51 kw/liter in Browns Ferry and from 68 kw/liter in Yankee to ~100 kw/liter in Diablo Canyon.

Potential Improvement Areas. Three principal design limits have been discussed to this point: critical heat flux, fuel temperature, and cladding strain under irradiation. Other limits on clad corrosion, hydraulic stability, and freestanding cladding must also be respected. These three limits are discussed below with respect to influence of improvements on the limit. We take improvements to mean a closer approach to or a raising of the limits imposed until now.

We have examined the potential effect on core power density of arbitrary improvements in the critical heat flux for typical PWR and BWR conditions. Figure 1 shows the results of the calculations normalized to the current class of reactors, which we take to be defined by the Diablo Canyon PWR and the Browns Ferry BWR. Flow and channel dimensions are held constant in the evaluation, and we have required that the CHFR also be held constant.

For a 10% increase in the critical heat flux, PWR core power density could be increased by 5.3%, and BWR core power density, by 5.8%. For a 20% increase in critical heat flux, core power density can be increased by 9.8 and 11.4% for the PWR and BWR, respectively. To exploit the Fig. 1 result requires that the predicted value of critical heat flux be increased. What is the potential for such an improvement? This is of course difficult to say. However, directions that may lead to improvement are as follows:

1. More precise measurement of the conditions at which the critical heat flux is reached.
2. Improved representation of reactor heat-generation profiles in the electrically heated tests used for critical heat-flux determination.
3. Emphasis in development of empirical correlations covering the ranged variables anticipated in normal and off-design operation.
4. Testing to and beyond the critical heat flux to evaluate the consequences of exceeding the "limit."

5. Development of methods which improve the critical heat flux.

The power level at which the critical heat flux is reached is also a function of the enthalpy of the coolant. It is possible therefore to increase the core power density at which the critical heat flux is reached by improving coolant mixing and thereby lowering the coolant enthalpy.

The effect of mixing on the proximity to the critical heat flux depends on the ratio of hot-channel flow to nominal channel flow as determined by their relative areas. In addition, mixing becomes more important with larger local (rod) variations in power which result in different amounts of heat addition to channels in the same region of the core. In general, core power density can be increased as mixing is increased.

Application of relevant heat-transfer correlations to three-dimensional fluid heat-transfer calculations for reactor fuel can demonstrate the effects of various amounts of mixing. This can be done by using a mixing flow rate with the appropriate average enthalpy of adjacent channels expressed as a fraction of total channel flow. The effect of mixing on the CHFR and on the subsequent allowable core power density varies with the above factors. The maximum allowable increase in core power density between no mixing and the maximum effect of mixing is in the range 10 to 20% for a typical PWR. Furthermore, above a value of 40 to 50% mixing, there is little to be gained by further mixing since mixing also leads to greater pressure drops.

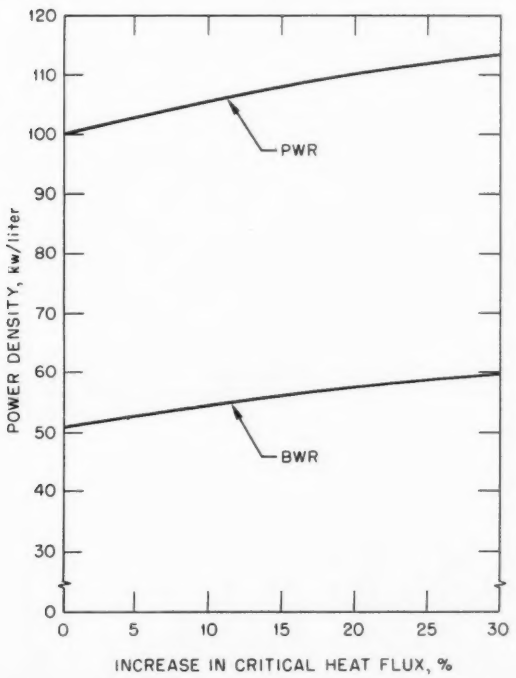

Fig. 1 Allowable power-density increase as a function of increase in critical heat flux.[1]

Mechanical Integrity of Cladding and Fuel. There are certain limits, sometimes appropriately called "soft limits," which may become important only over a long period or are currently important because their consequences are not fully understood. In the former category are cladding rupture due to internal fission-gas pressure or pellet swelling. In the latter category is center melting of UO_2. These tend to be interrelated.

Design methods that cope with these problems are fairly straightforward: enough plenum volume is designed into the top of the fuel rod to keep fission-gas pressure within predetermined limits; the density of the UO_2 pellet and the cladding-to-pellet gap are chosen so that pellet swelling does not exceed predetermined limits; and the UO_2 center temperature (as dictated by the parameter kw/ft) is kept below melting so that the incompletely understood consequences of fuel melting need be of no concern.

In general, fission-gas pressure is proportional to burnup; but, because fission-gas diffusion and escape are strongly fuel-temperature dependent, fission-gas pressure is related to time–average temperature, i.e., time–average kw/ft. Swelling of UO_2 also occurs, but, if UO_2 density is low enough, external pellet dimensions do not change until a predictable fraction of fission-product pairs have been produced. Finally, if fuel temperatures are high, the rate of the swelling is reduced through escape of fission gases from the pellet. Figure 2 shows the pellet density required to reach various burnups as a function of time–average fuel rating, kw/ft, without exceeding 1% cladding strain. Curves of this type are necessary at the fuel design stage but are also useful for operational decisions with existing fuel: one of the inputs to a decision to continue irradiation of fuel when it is near its target burnup would be the likelihood of cladding failure as determined from the type of information in Fig. 2.

Summary

Target fuel performance can safely be increased only through demonstrated improvements in fuel design limits, particularly heat-transfer and linear heat-

Table 2 Evolution of Principal Thermal-Hydraulic-Mechanical Parameters for PWR and BWR Core Designs

	Yankee Rowe	Indian Point 1	San Onofre	Haddam Neck	Ginna	Turkey Point	Indian Point 2	Kewaunee	Surry	Burlington	Diablo Canyon
Designer	**W**	**B&W**	**W**	**W**	**W**	**W**	**W**	**W**	**W**	**W**	**W**
Average Ratings at 100%											
Thermal output, Mw(t)	392.0	585.0	1347.0	1473.0	1300.0	2097.0	2758.0	1650.0	2441.0	3083.0	3250.0
Total coolant flow, 10^6 lb/hr	37.8	52.8	78.0	1003.0	67.1	100.6	136.2	67.5	100.6	133.9	135.7
Power density, kw/liter	58.3	76.4	70.9	65.8	75.3	79.2	83.2	95.6	91.9	93.1	98.1
Lineal heat rate, kw/ft	2.3	3.0	4.6	4.4	4.9	5.3	5.7	6.2	6.2	6.5	6.7
Surface heat flux, 10^3 Btu/(hr)(sq ft)	86.3	128.0	143.3	136.4	151.8	164.2	175.6	191.0	191.0	196.3	207.0
Flow/power, lb/(hr)(kw)	96.5	90.5	58.0	68.8	51.7	47.9	49.5	40.8	41.3	43.4	41.7
Flow velocity, ft/sec	14.0	21.5	13.3	14.3	15.1	13.9	16.1	14.9	14.5	15.8	15.8
Mass velocity, 10^6 lb/(hr)(sq ft)	2.2		2.02	2.21	2.43	2.35	2.56	2.43	2.35	2.54	2.54
Maximum Ratings at 100%											
Lineal heat rate, kw/ft	11.6	12.9	15.0	14.3	16.7	17.3	18.5	17.4	17.5	17.9	18.9
Surface heat flux, 10^3 Btu/(hr)(sq ft)	446.3	540.0	463.0	443.5	517.5	533.6	570.8	539.0	538.7	553.7	583.0
Fuel temperature, °F			3900.0	3800.0	3920.0	4070.0	4200.0	4000.0	4100.0	4100.0	4100.0
Hot-channel factor (heat flux), F_q	5.17	4.21	3.23	3.25	3.41	3.25	3.25	2.82	2.82	2.82	2.82
Minimum CHFR or DNBR	2.2		2.07	2.82	1.9	1.85	1.81	1.85	1.86	1.86	1.61
Rated Overpower		135.0	118.0	118.0	112.0	112.0	112.0	112.0	112.0	112.0	112.0
Fuel temperature at overpower	4330.0	4850.0	4100.0		4150.0	4270.0	4400.0	4250.0	4350.0	4400.0	4450.0
Fuel Rod											
Pellet diameter, in.	0.294	0.260	0.3835	0.3835	←			0.0369			→
Diametral cap, in.	0.004	0.004	0.0055	0.0055	←			0.0065			→
Cladding O.D., in.	0.340	0.304	←					0.422			→
Cladding thickness, in.	0.021	0.020	0.0165	0.0165	←			0.0243			→
Cladding t/D	0.062	0.067	0.039	0.039	←			0.058			→
Cladding material	s.s.	s.s.	s.s.	s.s.	←			Zircaloy 4			→
Fuel Assembly											
Total number	76.0	120.0	157.0	157.0	120.0	167.0	193.0	121.0	157.0	193.0	193.0
Array	18 X 18	14 X 14	14 X 14	15 X 15	14 X 14	15 X 15	15 X 15	14 X 14	15 X 15	15 X 15	15 X 15
Rods per assembly	304.0	195.0	180.0	204.0	179.0	204.0	204.0	179.0	204.0	204.0	204.0
Active length, in.	75.4	98.5	120.0	121.8	←			144.			→
Core equivalent diameter, in.	91.9	77.7	110.9	119.5	96.5	119.5	133.7	96.5	119.5	133.7	133.7

	Fort Calhoun	Oconee, Crystal River, Three Mile Island	Calvert Cliffs	Elk River	Big Rock Point	Dresden 1	Oyster Creek	Nine Mile Point	Easton	Browns Ferry
Designer	**CE**	**B&W**	**CE**	**AC**	**GE**	**GE**	**GE**	**GE**	**GE**	**GE**
Average Ratings at 100%										
Thermal output, Mw(t)	1420.0	2468.0	2440.0	58.0	157.0	626.0	1600.0	1538.0	2381.0	3293.0
Total coolant flow, 10^6 lb/hr	71.7	131.3	122.0	2.7	12.0	25.7	66.8	67.5	74.0	99.6
Power density, kw/liter	76.0	80.1	75.2	25.6	45.0	22.2	33.6	34.1	51.15	50.8
Lineal heat rate, kw/ft	5.7	5.4	5.5	3.1	3.3	4.0	4.7	4.8	7.1	7.0
Surface heat flux, 10^3 Btu/(hr)(sq ft)	164.0	167.6	162.0	90.7	110.0	91.8	107.5	108.7	164.5	163.2
Flow/power, lb/(hr)(kw)	50.5	53.2	50.0	46.1	76.4	41.1	41.8	43.9	31.3	30.2
Flow velocity, ft/sec	13.3	15.7	13.8							
Mass velocity, 10^6 lb/(hr)(sq ft)	2.15	2.53	2.23							
Maximum Ratings at 100%										
Linear heat rate, kw/ft	17.6	17.5	16.9	10.8	10.5	12.2	14.5	14.6	18.4	18.3
Surface heat flux, 10^3 Btu/(hr)(sq ft)	509.0	543.0	501.0	313.0	352.0	280.0	331.4	335.0	427.8	425.0
Fuel temperature, °F	4320.0	4160.0	3775.0	3700.0	2800.0		3550.0	3600.0	4400.0	4380.0
Hot-channel factor (heat flux), F_q	3.10	3.24	3.10	3.46	3.22	3.06	3.14	3.08	2.6	2.6
Minimum CHFR or DNPR	1.97	2.27	2.15	2.2			2.47	2.51	1.9	1.9
Rated Overpower	112.0	114.0	112.0	125.0	127.0	125.0	120.0	120.0		
Fuel temperature at overpower	4640.0	4400.0	4155.0	3350.0			4325.0	4400.0		
Fuel Rod										
Pellet diameter, in.	0.382	0.362	0.382	0.4075	0.345	0.496	0.488	0.488	0.488	0.488
Diametral cap, in.	0.006	0.006	0.006	0.0022	0.005	0.005	0.011	0.011	0.010	0.010
Cladding OD, in.	0.440	0.420	0.440	0.450	0.388	0.567	0.570	0.570	0.562	0.562
Cladding thickness, in.	0.026	0.026	0.026	0.020	0.019	0.033	0.035	0.035	0.032	0.032
Cladding t/D	0.059	0.062	0.059	0.044	0.049	0.058	0.062	0.062	0.057	0.057
Cladding material	←	Zircaloy 4	→	s.s.	s.s.	←		Zircaloy 2	→	
Fuel Assembly										
Total number	133.0	177.0	217.0	148.0	56.0	488.0	560.0	532.0	548.0	764.0
Array	14 X 14	15 X 15	14 X 14	5 X 5	12 X 12	6 X 6	←		7 X 7	→
Rods per assembly	176.0	208.0	176.0	25.0	144.0	36.0	←		49.0	→
Active length, in.	128.0	144.0	137.0	60.0	70.0	134.0	←		144.0	→
Core equivalent diameter, in.	105.5	128.9	145.4	60.0	62.5	128.0	160.2	156.1	158.5	187.1

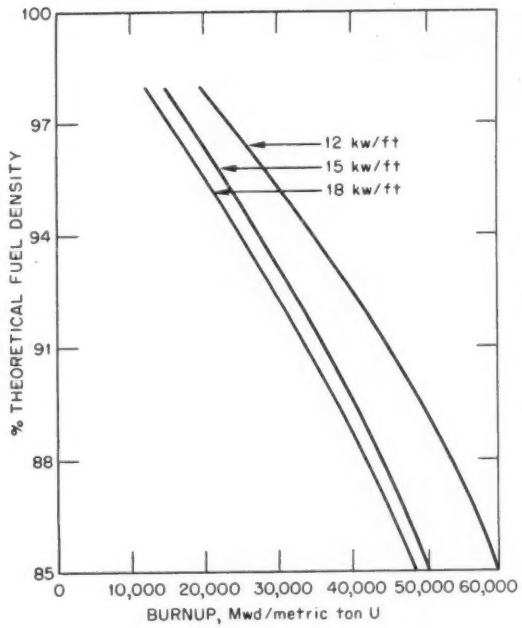

Fig. 2 Burnup capability vs. fuel-pellet density. (Typical PWR fuel rod with most limiting tolerances at various linear heat ratings; burnup capabilities based on design limit of 1% cladding strain.)

rate limits, and in improved knowledge of the mechanisms of long-term fuel swelling, fission-gas release, and melting. As is demonstrated in the following section, design limits impose the ultimate limit on economic performance.

Economic Dependence on Design Limits

With the basic design criterion in mind that no fuel-cladding damage is to occur under normal operation or anticipated transients, and with the design limits clearly defined which meet this criterion, the question can be raised as to the actual power capability and the economics of the reactor. The reactor operator can utilize knowledge of the design limits and of how the core margins are determined to examine whether the reactor, as built and functioning, is capable of increased power. An alternative method of increasing fuel utilization in operating reactors is to increase specific power in the fuel by refueling with a reduced number of fuel assemblies. In this way, advances in reactor technology on which new reactor design are to be based can also be used to upgrade the performance of earlier-generation reactors.

The approach to defining (1) the magnitudes of the incentives and (2) the most advantageous modes of economically exploiting further improvements is as follows: The design limits are first related to the core averages upon which the core is sized; unit fuel costs are then developed parametrically to clearly show basic economic dependences, particularly on burnup and specific power. The economic optimum burnup is then examined, and its important dependences are noted. The incentives for increased specific power are then defined, first without and then with fuel-rod-diameter changes. Finally the potential for plant capital-cost savings is developed.

Relation Between Limiting and Average Conditions

To this point, the economic figure-of-merit of power density (kw/liter) has been loosely used. Actually only plant size (and hence cost) is directly related to power density; fuel costs are directly related to fuel specific power (kw/kg U). However, because of both safety considerations (minimum reactivity coefficients) and economic considerations (minimum enrichment), all water reactors have similar water-to-fuel ratios. Hence there is only a uniform conversion factor separating the power density and specific power of water reactors, and the looseness of usage is not without justification.

In the following the permissible core average specific power is related to the surface heat-flux limit and the linear heat-rate limit. As will be seen, the development is general; however, a *very key point* in applying the following is: where there are several possible limiting conditions, it is essential that the location and nature of the most limiting limit be known and that its characteristics (such as heat flux and peaking factor) be appropriately used in the equations.

A corollary of this is that, when improving one limit, it is prudent to assure oneself that another limit does not become governing.

Using the following definitions:

Heat-flux limit

$$\left(\frac{Q}{A}\right)_{\text{av.}} = \left(\frac{Q}{A}\right)_{\text{lim}} \times \frac{1}{R_h(\text{CHFR})} \quad \text{Btu/(hr)(sq ft)}$$

Linear heat-rate limit

$$\left(\frac{P}{l}\right)_{\text{av.}} = \left(\frac{P}{l}\right)_{\text{lim}} \times \frac{1}{R_l} \quad \text{kw/ft}$$

the permissible average specific power, S, can be shown to be:

Heat-flux limit

$$S = \frac{(Q/A)_{\text{lim}} \pi Dr/D_p}{0.1361 \rho D_p \times 3413 \times 12 X k R_h \text{ (CHFR)}} \quad \text{kw(t)/kg U}$$

Linear heat-rate limit

$$S = \frac{(P/l)_{\text{lim}}}{0.1361 \rho D_p^2 k R_l} \quad \text{kw(t)/kg U}$$

where Q/A = surface heat flux, Btu/(hr)(sq ft)
P/l = linear heat rate, kw(t)/ft
R_h = composite hot-channel and overpower factor for heat-transfer limit
R_l = composite hot-channel and overpower factor for linear heat-rate limit
CHFR = critical heat-flux ratio
S = permissible average specific power, kw(t)/kg U
D_r = fuel-rod outside diameter, in.
D_p = pellet outside diameter, in.
ρ = UO_2 density, g/cm^3
k = fraction of power transferred through cladding

$$0.1361 = \frac{12 \times 2.54^3 \times (\pi/4) \times (238/270)}{1000}$$

3413 = Btu/kw(t)-hr

As implied by the above, the composite hot-channel factors include all relevant factors such as gross nuclear, local nuclear, engineering, flow, instrument, and overpower. Also, in applying the above, the standard cautionary word on the CHFR should be given: the CHFR is the heat-flux margin ratio at the limiting point; it is *not* a power margin ratio. The power margin ratio should be determined from the appropriate heat-transfer correlation. Typically it will be roughly the square root of the CHFR, as demonstrated above.

Since fuel-inventory (and certain plant capital) costs have an inverse dependence on specific power, it is apparent that fuel costs will go down if the limits can be increased and/or if the peaking factors and CHFR can be reduced. Note also that decreased fuel-pellet diameter has the potential for reducing fuel-inventory costs, although care must be taken that rod diameter changes do not adversely affect the heat-transfer limit.

In applying the above equations, it should be self-evident that the most limiting (i.e., the lowest specific power) of the two conditions is to be used.

Fuel-Cost Dependence on Design Parameters

A parametric representation of fuel costs is a key step in defining incentives. Because of the normal design process of cost minimization, certain cost components tend to influence other components. For an understanding of economic pressures on design, and the impact of improved design limits, there is no substitute for a parametric representation of unit fuel costs (with a clear identification of unit fuel costs), independent variables, dependent variables, and the constants and constraints of nature. It is the present purpose to define the effect of specific-power variation on water-reactor fuel cost under all conceivable combinations of fuel performance.

The following is a detailed but straightforward parametric representation of total fuel cost, both direct and indirect (costs due to unrecovered fuel investment). Costs are discussed first in terms of $/kg U and then converted to mills/kw(e)-hr.

Direct Costs. 1. *Fabrication (F), $/kg U.* The cost of fabrication can have a fuel-rod-diameter dependence expressed as:

$$F = K \left[1 + \left(\frac{0.4}{D_p}\right)^2\right] \quad \$/\text{kg U}$$

where K is an appropriate constant and D_p is fuel-pellet diameter in inches. Furthermore, the cost of fabrication is strongly sensitive to fabrication-plant throughout. Hence, as nuclear power develops, fabrication costs, in constant dollars, are expected to decrease substantially.

2. *Recovery of Spent Fuel (R), $/kg U.* This direct cost includes the costs of shipping, reprocessing, and reconversion which are necessary expenditures in the recovery of the residual values of uranium and plutonium in spent fuel.

3. *Net Cost of Fissile Material Destroyed (N), $/kg U.* The net cost of fissile material is the initial enriched-uranium cost, U_i, less the credits for recovered uranium, U_f, and plutonium, Pu. The initial and final uranium costs are a function of enrichment, and, having an enrichment–attainable burnup relation, can be related to burnup. The plutonium credit is simply the product of the price of fissile plutonium in $/g and the plutonium content, g fissile Pu/kg U. The latter has some sensitivity to burnup.

Indirect Costs. Indirect costs are those incurred to pay carrying charges on all unrecovered fuel investment. These include prereactor investment charges for fabrication and uranium, in-core charges for fabrication, uranium, plutonium, and recovery (a credit since revenues are received prior to expenditures) and postreactor charges for uranium, plutonium, and recovery. The prereactor charges can be handled by use of a factor, $1 + iT_{pr}$, on the direct initial uranium and fabrication costs; and the postreactor charges can be handled by use of a factor, $1/(1 + iT_{po})$, on the recovery and final uranium and plutonium credits. In the above, i is the appropriate interest rate per annum, and T_{pr} or T_{po} are, respectively, the appropriate average prepayment times (years) and postreactor times to payment or value recovery. The in-core charges are based on the time–average in-core investment, taken in this case to be half the initial plus half the final investment.

Total Fuel Costs. As outlined above, a direct cost per mass ($/kg U) is determined for each direct-cost component and appropriately increased or discounted for prereactor and postreactor investment charges. The unit energy cost for these direct costs, plus the out-of-core indirects, is then obtained from:

$$\text{Mills/kw(e)-hr} = \frac{1000}{24\eta B} \quad (\$/\text{kg U})$$

where η is net efficiency in kw(e)/kw(t) and B is burnup in Mwd/metric ton U.

The in-core investment charges are obtained from the average unrecovered investment:

$$\text{Mills/kw(e)-hr} = \frac{1000i}{24 \times 365 \times \eta \cdot L \cdot S} \quad (\$/\text{kg U})_{av.}$$

where i is the per annum interest rate in fractions/year, L is the average capacity factor, and S is the average specific power in kw(t)/kg U.

Then total unit fuel costs (C) are:

$$C = \frac{1000}{24\eta B}\left[F(1+iT_f) + U_i(1+iT_u) + \frac{R}{1+iT_r} - \frac{(U_f + \text{Pu})}{1+iT_{po}}\right] + \frac{1}{2}\frac{i}{8.76\eta LS}\left[F(1+iT_f) + U_i(1+T_u) - \frac{R}{1+iT_r} + \frac{U_f + \text{Pu}}{1+iT_{po}}\right] \text{ mills/kw(e)-hr}$$

The prereactor and postreactor T subscripts are defined by their association. The problem with the above equation is that it does not parametrically express the quantities U_i, U_f, and Pu in terms of burnup or specific power.

The cost of enriched uranium can be represented by the sum of a natural-uranium cost and an enriching cost component. For a constant diffusion-plant tails composition of 0.20% ^{235}U, and enrichments in the range 2.6 to 4% ^{235}U, a close approximation for U_i in $/kg U is:

$$U_i = C_n\left(\frac{e - 0.2}{0.511}\right) + C_E(2.219e - 2.342)$$

where e = ^{235}U enrichment, %
C_n = cost of natural uranium as UF_6, $/kg U
C_E = separative work cost, $/kg U

[Note: C_n = 2.613 × ($/lb U_3O_8) + 2.20 ($/lb U conversion); and 2.613 = kg U/lb U_3O_8 × 1.005 conversion loss.]

$$U_i = (1.957C_n + 2.219C_E)e - 0.391C_n - 2.342C_F$$

or, in general, $U_i = U_1 e - U_2$, where U_1 and U_2 are constants. At prices of C_n = $23.46/kg U and C_E = $26.00/kg U, then:

$$U_i = 103.60e - 70.06$$

(Maximum approximation error in the above is $0.36/kg U in the range 2.6 to 4% enrichment.)

It is evident that, if enrichment can be expressed as a function of burnup, the dependence of U_i on attainable burnup can be defined. This is now demonstrated.

A useful equilibrium-cycle relation between fuel burnup, B, and refueling fraction, f, for large power reactors with fairly uniform power distributions, *at constant initial enrichment* is:

$$B(f) = \left(\frac{1+f_0}{1+f}\right) B(f_0)$$

where the zero subscript refers to a convenient reference point of burnup B_0 and corresponding refueling fraction f_0.

Since these reactors are designed for approximately annual refueling, the annual core average burnup per year is equal to the product of discharge burnup B and the refueling fraction f. On the basis of an energy balance, $fB = 365SL$.

The above defines a very important constraint on this analysis: refueling fraction must be compatible

with burnup, specific power, and capacity factor if the desired annual refueling is to occur.

The relation between attainable burnup and required enrichment is an inherent nuclear characteristic of any particular design. Significant design work, using nuclear data and neutron behavior models carefully normalized to experiment, indicates a surprisingly linear relation between initial enrichment and attainable burnup *at constant refueling fraction*. This has the form:

$$e = e_0 + \alpha_0 \, [B(f_0) - B_0]$$

where α_0 is a nuclear characteristic slope typically 0.07 to 0.08% enrichment increase per 1000 Mwd/metric ton U burnup increase.

The above equation can be combined with the previous two equations, eliminating the refueling fraction f with the constraint imposed by the 1-year cycle. The resulting equation, below, gives the enrichment required to achieve a given burnup, subject to a 1-year refueling interval at whatever refueling fraction the capacity factor–specific power characteristic dictates:

$$e = e_0 + \alpha_0 \left(\frac{B + 365SL}{1 + f_0} \right) - B_0$$

Strictly speaking, an additional enrichment term related to specific power is required. This is, in effect, the enrichment equivalent of the reactivity tied up in the power coefficient. The relation is not linear over the whole range from zero to full power, but, in the vicinity of full power, the incremental enrichment can be given by

$$\Delta e = k(S - S_0)$$

where k is a nuclear characteristic of a particular fuel design; or, in general, redefining constants:

$$e = \epsilon + \beta(B + 365SL) + kS$$

where ϵ and β are nuclear characteristics of any given reactor design.

Finally, to complete the parametric representation, the values of final uranium and plutonium must be defined in terms of burnup. It turns out that, for fractionally fueled water reactors, an excellent assumption is that final uranium enrichment is close to being independent of initial enrichment and burnup: it is typically in the range 0.9 to 1% initial enrichment and burnup *at constant SL*. When specific power and/or capacity factors change, a change in enrichment is necessary to offset changes in the refueling fraction and power coefficient. It turns out that a reasonable assumption is that any initial enrichment increment will result in the same final enrichment increment if the burnup is constant. Hence final uranium values, having the correct value vs. enrichment slope at normal discharge enrichment, have the form:

$$U_f = V_1 S(365\beta L + k) - V_2$$

where V_1 is chosen for the correct value vs. enrichment slope at a reference-design discharge enrichment and V_2 is chosen to fit the correct actual value at the discharge enrichment. In this way, changes in final enrichment are correctly reflected in the vicinity of the reference-design discharge enrichment.

A reasonable approximation for net fissile recognizes that fissile plutonium is close to its saturation concentration for the burnups of interest in water reactors. Hence plutonium content of spent fuel can be adequately represented parametrically by:

$$G_p = G_{po} + \gamma B \qquad \text{g/kg U}$$

where G_{po} and γ are nuclear characteristics of any given reactor design.

Parametric Representation. Rewriting the original total cost equation but, for the sake of algebraic simplicity, ignoring the prereactor and postreactor factors (they can be readily reinserted):

$$240\eta C = \frac{10{,}000}{B}(F + U_i + R - U_f - \mathrm{Pu}) + \frac{i}{2}\frac{10{,}000}{365SL}(F + U_i - R + U_f + \mathrm{Pu})$$

Substituting:

$$U_i = U_1 e - U_2$$
$$= U_1 \, [\epsilon + \beta \, (B + 365SL) + kS] - U_2$$

$$= U_3 \frac{B + 365S \, (L + k')}{10{,}000} - U_4$$

$$\mathrm{Pu} = PG_p = P\left(G_{po} + \gamma' \frac{B}{10{,}000}\right)$$

$$b = \frac{B}{10{,}000} \quad \text{and} \quad s = \frac{365S}{10{,}000}$$

$$U_f = V_3 s(L + k') - V_2$$

Table 3 Nuclear and Cost Data for 800-Mw(e) Boiling- and Pressurized-Water Reactors with Equilibrium Fuel Cycles

	BWR	PWR
Nuclear Factors		
Design S, kw(t)/kg U	22.3	34.4
Design D_p, in.	0.488	0.367
ϵ, %	0.47	0.63
β	0.59×10^{-4}	0.59×10^{-4}
k	0.0090	0.0058
k'	0.42	0.27
Final enrichment, $\%^{235}$U	0.75	0.95
G_{po}, g/kg U_i	3.60	3.77
γ'	0.56	0.91
Cost Factors and Derived Cost Factors		
$F = 1.15 \times 40\,[1 + (0.4/D_p)^2]$, \$/kg U	77	101
$R = (32 + 5 + 6)/1.10$, \$/kg U_i	39	39
P, \$8.00/g discounted	7.27	7.27
$U_3 \times 1.15$, \$/kg U	70.30	70.30
$U_4 \times 1.15$, \$/kg U	24.60	5.50
$V_3/1.10$, \$/kg U	40.80	44.50
$V_2/1.10$, \$/kg U	16.50	21.30
i, per annum	0.12	0.12
L	0.80	0.80

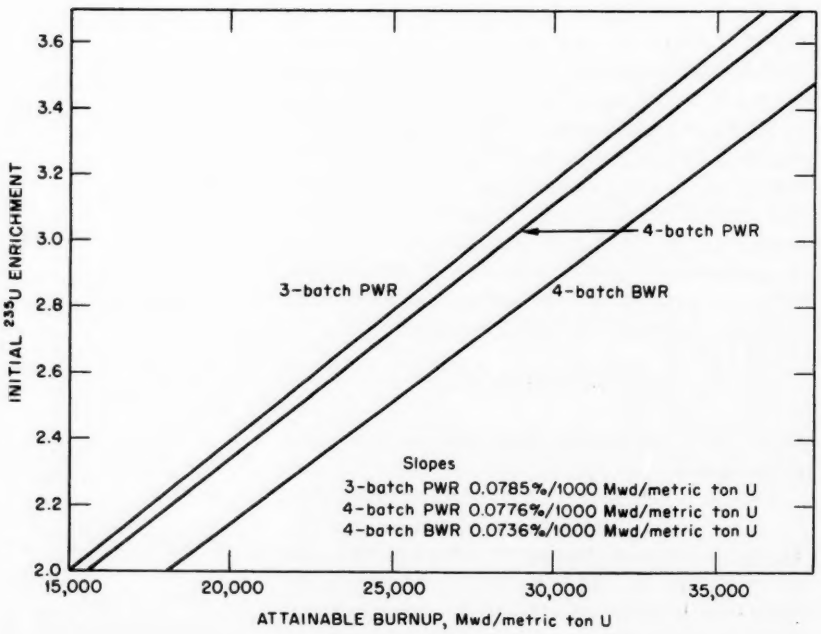

Fig. 3 Attainable burnup vs. initial feed enrichment for equilibrium-cycle reactors with a fixed discharge fraction.

where $U_3 = 10{,}000\beta U_1$
$U_4 = U_2 - U_1\epsilon$
$k' = k/(365\beta)$
$V_3 = 10{,}000\beta V_1$

Rearranging yields:

$$240\eta C = \frac{1}{b}[F + R + V_2 + (U_3 - V_3)s(L + k') - U_4 - PG_{po}] + b\left[(U_3 + P\gamma')\frac{i}{2sL}\right] + \frac{i}{2sL}(F - R - V_2 - U_4 + PG_{po}) + U_3 + (U_3 + V_3)\frac{i}{2}\left(1 + \frac{k'}{L}\right) - P\gamma'$$

Lest one lose the physical significance of the above, it is worth reviewing the significance of each term. There are four terms:

First term: Of the six subterms the first two (fabrication and recovery) will dominate. The remainder are out-of-core uranium and plutonium investment costs plus correction terms on the net fissile-material consumption. This first term is inversely proportional to burnup.

Second term: Of the two subterms the first (uranium) will dominate. This second term represents the carrying cost of the variable portion of fissile-material investment and is proportional to burnup and inversely proportional to specific power.

Third term: Of the five subterms the first (fabrication) will dominate. This third term represents the carrying charges for process costs and the fixed portion of fissile-material investment. It is inversely proportional to specific power.

Fourth term: Of the two subterms the first (uranium) will dominate. These two subterms are the net cost of fissile material destroyed, except that the first subterm has an investment charge associated with it.

The above equation is the required parametric equation of nuclear fuel costs and is very powerful and useful in understanding fuel-cost behavior. Examination shows that the first two terms can be used to optimize burnup; the minimum cost occurs when these two terms are equal. However, if one examines the nature of the minimum, one discovers it to be very broad. If $c_{opt.}$ is the sum of the two first terms, corresponding to an optimum burnup, $b_{opt.}$, the following sensitivities to off-optimum burnup, $b = b_{opt.} \pm \delta b$, apply:

$$\frac{\delta c}{c_{opt.}} = \frac{1}{2}\left(\frac{\delta b^2}{b_{opt.} \times b}\right)$$

For example, at 20% less than optimum burnup, there is only a 2.5% increase in $c_{opt.}$, and that term includes only two of the four terms in the total fuel cost.

The key point in the above discussion is: at optimum burnup the sensitivity of fuel costs to specific power is a maximum. However, because there is so little incentive to go to the full optimum burnup, it is likely that burnups in the range 80 to 90% of optimum will prevail. This means that the second term in the parametric equation will yield only 80 to 90% of its maximum incentive to go to higher specific powers.

Application to Current Water Reactors

In order to define specific incentives for increased specific power, nuclear and cost data will now be presented. Table 3 has been developed based on typical 800-Mw(e) boiling- and pressurized-water reactors. The enrichment–burnup characteristics were developed from Fig. 3 plus the equations in this section. Figure 3 shows the enrichment–burnup characteristic at constant refueling fraction and from this is derived the characteristic for annual refueling.

The cost factors given in the lower half of Table 3 reflect current commercial data. The dependence of fabrication cost on fuel-pellet diameter is recognized. Each of the costs has been appropriately increased by a factor of 1.15 or discounted by a factor of 1.1 to reflect prereactor and postreactor fuel-investment charges, respectively. Enriched-uranium valuations are based on 0.2% diffusion-plant tails, \$8/lb U_3O_8 and \$26/kg U separative work.

Substitution of the appropriate terms, plus use of a reference burnup of 27,000 Mwd/metric ton U ($b = 2.70$) for the BWR and 31,500 Mwd/metric ton U ($b = 3.15$) for the PWR, yields the following fuel-cost dependences, including that of fabrication cost, F.

For the BWR:

$$C = \frac{B_0}{B}\left(0.371\frac{F}{F_0} + 0.142\frac{S}{S_0} + 0.022\right) + \frac{B}{B_0}\frac{S_0}{S}(0.241) + \frac{S_0}{S}\left(0.092\frac{F}{F_0} - 0.064\right) + 0.992 \text{ mill/kw(e)-hr}$$

$= 1.796$ mills/kw(e)-hr at reference of $B_0 = 27{,}000$ Mwd/metric ton U; $S_0 = 22.3$ kw(t)/kg U

For the PWR:

$$C = \frac{B_0}{B}\left(0.418\frac{F}{F_0} + 0.145\frac{S}{S_0} + 0.113\right) + \frac{B}{B_0}\frac{S_0}{S}(0.189) + \frac{S_0}{S}\left(0.079\frac{F}{F_0} - 0.030\right) + 0.947 \text{ mill/kw-hr}$$

= 1.861 mills/kw(e)-hr at reference of B_0 = 31,500 Mwd/metric ton U; S_0 = 34.4 kw(t)/kg U

The above equations give a result that includes an S-dependent term usually ignored in fuel-cost sensitivity analyses; this term arises from applying the annual refueling constraint, plus the power-coefficient correction, to the analysis. Physically, increased specific power at constant burnup and annual refueling increases the refueling fraction, which must be compensated by an enrichment increase.

The existence of this term implies a dramatic upper limit to further fuel-cost savings from increased specific power at current target burnups and fuel-rod dimensions, as can be seen from:

C = sum of the two S-dependent terms

$$= a\frac{S}{S_0} + b\frac{S_0}{S}$$

$$C_{min.} = 2\sqrt{a \times b}$$

$$S_{opt.} = \sqrt{\frac{b}{a}}\,S_0$$

The following summarizes the fuel-cost incentives:

	BWR	PWR
a	0.142	0.145
b	0.269	0.238
$S_{opt.}/S_0$	1.38	1.28
$2\sqrt{a \times b}$, mills/kw-hr	0.391	0.371
$a + b$, mills/kw-hr	0.411	0.383
Maximum incentive, mills/kw-hr	0.020	0.012
Incentive for S/S_0 = 1.10 mills/kw-hr	0.010	0.007

A repeat of the above analysis, with burnups increased by a factor of 1.3, shows a maximum incentive of 0.068 mill/kw(e)-hr for the BWR and 0.050 mill/kw(e)-hr for the PWR (achieved at a specific-power increase of 70%, a dubious prospect). This clearly demonstrates that the incentive for higher burnup includes the increased potential to benefit from increases in average specific power.

An extension of the above analysis to include analysis of conditions at higher burnups and reduced fuel-rod diameters would require careful reevaluation of the cost coefficients, since the coefficients in the present analysis are most valid at current reference-design conditions. Qualitatively, however, one might anticipate smaller fuel-pellet diameters; their increased cost would offset the future benefits of economies of scale, keeping fabrication costs similar to those used here. Thus optimum burnups would tend to remain higher than current target levels. As previously shown under the subheading "Relation Between Limiting and Average Conditions," a decreased fuel-pellet diameter yields, ipso facto, an increased specific-power capability and gives the potential of realizing some of the remaining benefits from combined higher power–higher burnup operation. However, the extent to which fabrication-cost compromises at reduced pellet diameter can be allowed to offset benefits of increased specific power must include consideration of the potential capital-cost benefits of increased power density.

Sensitivity of Plant Cost to Power Density

The principal source of plant-cost savings from increased power density is from (1) reduced pressure-vessel size and hence direct and indirect cost reductions and (2) reduced coolant volume and hence reduced containment costs, both direct and indirect. Report WASH-1082 (Ref. 2) indicates that a 10% increase in power density will save the following:

	BWR	PWR
Pressure vessel, $/kw(e)	0.48	0.76
Containment, $/kw(e)	0.84	1.68
Total, $/kw(e)	1.32	2.44
Total, mills/kw-hr	0.023	0.042

The above savings have been converted to unit cost basis by the conversion factor

$$\text{Mills/kw(e)-hr} = \frac{i}{8.76L} \times [\$/\text{kw(e)}]$$

where i is the per annum interest rate, L is the capacity factor, and 8.76 is the number of hours per year/1000. At $i = 0.12$ and $L = 0.80$, this factor is 0.0171.

Summary

In the previous section ("Design Criteria in Water Reactors"), it was shown that a given percentage increase in permissible heat flux could be exploited by increasing power density by about half of that percentage. In this section, increases in power density have been shown to be directly related to increases in specific power, and the effects of specific power increases on fuel cost have been examined. It is concluded that, for current water-reactor designs at target performance levels, the incentive for increased specific power is surprisingly small, about 0.01 mill/kw-hr for the BWR and 0.007 mill/kw-hr for the PWR for a 10% increase in specific power. This surprising lack of sensitivity is due to the fact that the reduction in carrying charges at higher specific powers is significantly offset by the additional enrichment required to maintain burnup levels with (1) the larger refueling fraction and (2) the larger reactivity tied up in power coefficient at the higher specific powers. The sensitivity of fuel costs to specific power is significantly less at current target burnups than it would be at closer to economic optimum burnups, but other design factors, such as excess reactivity control and operational flexibility, are becoming more restrictive on both specific-power and fuel-burnup increases.

The clearest incentive for power-density increases is in the initial design stage, where plant costs can be influenced. Here the incentive for a 10% power-density increase is 0.02 mill/kw-hr for the BWR and 0.04 mill/kw-hr for the PWR.

Acknowledgment

The authors wish to thank Lowell Tripp for his helpful discussions and assistance with some of the calculations for this work.

References

1. General Design Criteria for Nuclear Power Plant Construction Permits, *Federal Register* (July 11, 1967) and 10 CFR 50, Appendix A.
2. Jackson and Moreland–S. M. Stoller Associates, Current Status and Future Technical and Economic Potential of Light Water Reactors, USAEC Report WASH-1082, March 1968.

LEGAL NOTICE

This journal was prepared under the sponsorship of the U. S. Atomic Energy Commission. Neither the United States, nor the Commission, nor any person acting on behalf of the Commission:

A. Makes any warranty or representation, expressed or implied, with respect to the accuracy, completeness, or usefulness of the information contained in this journal, or that the use of any information, apparatus, method, or process disclosed in this journal may not infringe privately owned rights; or

B. Assumes any liabilities with respect to the use of, or for damages resulting from the use of any information, apparatus, method, or process disclosed in this journal.

As used in the above, "person acting on behalf of the Commission" includes any employee or contractor of the Commission, or employee of such contractor, to the extent that such employee or contractor of the Commission, or employee of such contractor prepares, disseminates, or provides access to, any information pursuant to his employment or contract with the Commission, or his employment with such contractor.

Nuclear Science Abstracts

The U. S. Atomic Energy Commission, Division of Technical Information, publishes *Nuclear Science Abstracts (NSA)*, a semimonthly journal containing abstracts of the literature of nuclear science and engineering.

NSA covers (1) research reports of the U. S. Atomic Energy Commission and its contractors; (2) research reports of government agencies, universities, and industrial research organizations on a worldwide basis; and (3) translations, patents, books, and articles appearing in technical and scientific journals.

Complete indexes covering subject, author, source, and report number are included in each issue. These indexes are cumulated and sold separately.

Availability of NSA

SALE *NSA* is available on subscription from the Superintendent of Documents, U. S. Government Printing Office, Washington, D. C. 20402, at $42.00 per year for the semimonthly abstract issues and $38.00 per year for the cumulated-index issues. Subscriptions are postpaid within the United States, Canada, Mexico, and all Central and South American countries, except Argentina, Brazil, Guyana, French Guiana, Surinam, and British Honduras. Subscribers in these Central and South American countries, and in all other countries throughout the world, should remit $52.50 per year for subscriptions to semimonthly abstract issues and $47.50 per year for the cumulated-index issues. The single-copy price for the abstract issues is $1.75 postpaid, with this exception: Add one-fourth of $1.75 for mailing to the countries to which the $52.50 subscription rate applies.

EXCHANGE *NSA* is also available on an exchange basis to universities, research institutions, industrial firms, and publishers of scientific information. Inquiries should be directed to the Division of Technical Information Extension, U. S. Atomic Energy Commission, P. O. Box 62, Oak Ridge, Tennessee 37830.

TECHNICAL PROGRESS REVIEWS may be purchased from Superintendent of Documents, U. S. Government Printing Office, Washington, D. C. 20402. *Nuclear Safety* at $3.50 per year (six issues) for each subscription or $0.60 per issue; each of the other journals at $2.50 per year (four issues) or $0.70 per issue. The use of the order form below will facilitate the handling of your order.

POSTAGE AND REMITTANCE: Postpaid within the United States, Canada, Mexico, and all Central and South American countries except Argentina, Brazil, Guyana, French Guiana, Surinam, and British Honduras. For these Central and South American countries and all other countries: add, for each annual subscription, $1.00 for *Nuclear Safety* and $0.75 for each of the other journals; for single issues, add one-fourth of the single-issue price. Payment should be by check, money order, or document coupons, and MUST accompany order. Remittances from foreign countries should be made by international money order or draft on an American bank payable to the Superintendent of Documents or by UNESCO book coupons.

order form

SUPERINTENDENT OF DOCUMENTS
U. S. GOVERNMENT PRINTING OFFICE
WASHINGTON, D. C. 20402

Please send — 1, 2, or 3 years

- ☐ Isotopes and Radiation Technology ____
- ☐ Nuclear Safety ____
- ☐ Reactor and Fuel-Processing Technology ____
- ☐ Reactor Materials ____

Enclosed: document coupons ☐ check ☐ money order ☐

Charge: Superintendent of Documents No._____

SUPERINTENDENT OF DOCUMENTS
U. S. GOVERNMENT PRINTING OFFICE
WASHINGTON, D. C. 20402

(Print clearly)

_____
Name

_____
Street

_____
City, State, ZIP Code